UNIVERSIDAD AUTÓNOMA DE MADRID
FACULTAD DE CIENCIAS
DEPARTAMENTO DE BIOLOGÍA MOLECULAR

TESIS DOCTORAL

REDOX SIGNALING RESPONSES TO LAMINAR SHEAR STRESS IN VASCULAR ENDOTHELIAL CELLS

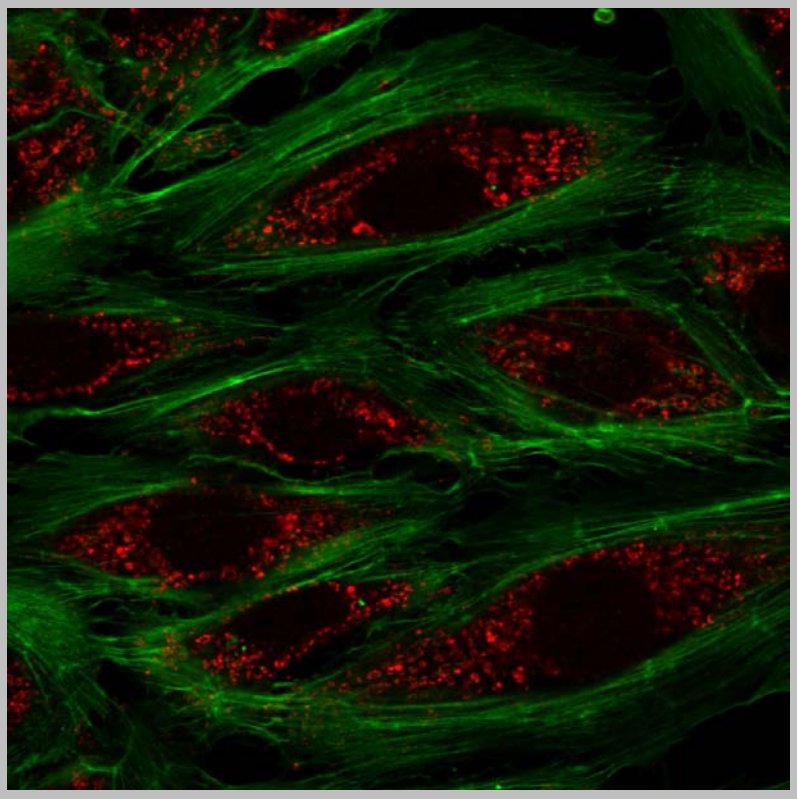

Rosa M. Bretón Romero
Madrid 2013

UNIVERSIDAD AUTÓNOMA DE MADRID

FACULTAD DE CIENCIAS

Departamento de Biología Molecular

Memoria de Investigación presentada por

ROSA M. BRETÓN ROMERO

Licenciada en Farmacia

Para optar al grado de
Doctorado en bioquímica, biología molecular, biomedicina y biotecnología.

Dirigida por

SANTIAGO LAMAS PELÁEZ

Profesor de Investigación

La presente tesis ha sido realizada en el Centro de Biología Molecular "Severo Ochoa", CSIC

Santiago Lamas Peláez, Doctor en Medicina (Fisiología), Profesor de Investigación del CSIC en el Centro de Biología Molecular "Severo Ochoa"

CERTIFICA:

> Que la presente Tesis Doctoral, titulada *"Redox signaling responses to laminar shear stress in vascular endotelial cells"* ha sido realizada bajo su dirección por **ROSA M. BRETÓN ROMERO**, estimando que se encuentra concluida y en condiciones de ser presentada y defendida públicamente para optar al grado de Doctor.

Y para que conste a todos los efectos firmo la presente autorización en Madrid a 30 de Abril de 2013.

Fdo: Prof. Santiago Lamas Peláez

SUMMARY

Endothelial cells (EC) in the vascular system are constantly subjected to the frictional force of shear stress (SS) due to the pulsatile nature of blood flow. Laminar shear stress (LSS) is a protective hemodynamic regulator of endothelial function, and limits the development of different inflammatory diseases related to increased cardiovascular risk. Although high levels of ROS have been described to be toxic, substantial evidence suggests that a transient production of hydrogen peroxide (H_2O_2) behaves as an intracellular messenger. Our studies explored the mechanisms whereby LSS-promoted ROS generation activates key endothelial signaling pathways. We found that LSS rapidly promotes a transient production of superoxide radical anion ($O_2^{\cdot-}$) and H_2O_2 which mediate the sequential activation of p38 MAPK, an increase in the activity of eNOS and the subsequent nitric oxide production. LSS is able to regulate the expression of antioxidant defence systems; however the early response to SS in the vascular endothelium is still unclear. We focused our attention on peroxiredoxins (PRX), which are highly sensitive enzymatic sensors of H_2O_2 and demonstrated that PRX3 (located in the mitochondria) is potentially regulated by flow. Our data suggested that mitochondriae behave as mechanosensor organelles in EC since LSS is able to induce mitochondrial fission mediated by Drp1, which correlates with an increase in mitochondrial membrane potential and a decrease in mitochondrial respiration. It is well known that SS induces platelet activation and the release of purine nucleotides such as ADP which interacts with endothelial receptors. Our studies have identified p38 MAPK as an upstream kinase critically involved in ADP-mediated eNOS activation, demonstrating a key role for PTEN inactivation by ADP in the sequential activation of p38 MAPK and eNOS. Our data support a model in which ADP promotes the transient inactivation of PTEN, leading to an increase in PIP3 levels, which then triggers the activation of PI3K/Akt, Rac1 and p38 MAPK, and enhanced eNOS activity.

This work adds new insights into the response to fluid flow providing data for undescribed pathways on the regulation of $NO^{\cdot}$ signaling and mitochondrial function in the vascular endothelium.

RESUMEN

El flujo laminar, *LSS*, se considera un mecanismo homeostático al que se ven sometidas las células endoteliales debido al carácter pulsátil del flujo sanguíneo. Se ha relacionado con una función protectora que impide el desarrollo de diferentes enfermedades inflamatorias relacionadas con aumento de riesgo cardio-vascular. El incremento sostenido de especies reactivas de oxígeno (ROS) se considera tóxico para células y tejidos. Sin embargo, cada vez parece más aceptado el concepto de un papel señalizador fisiológico mediado por concentraciones bajas de ROS y más concretamente de H_2O_2 en el endotelio vascular. En este estudio, nos hemos centrado en conocer la respuesta endotelial y la activación de rutas de señalización en respuesta a la generación de ROS por LSS. Observamos un incremento de ROS como una respuesta temprana en el endotelio que es necesaria para la activación secuencial de la proteína p38 MAPK y de eNOS, y la consiguiente producción de óxido nítrico. LSS regula la expresión de enzimas antioxidantes con el fin de contrarrestar la producción excesiva de ROS a largo plazo; sin embargo no se conoce en profundidad como responde el endotelio ante producciones rápidas de ROS. Hemos detectado la activación de la enzima antioxidante peroxirredoxina 3 (PRX3), localizada en la mitocondria, a tiempos tempranos de LSS. Nuestros resultados proponen un papel activo para las mitocondrias como sensores del flujo laminar tras comprobar que LSS se asocia con fisión mitocondrial mediada por Drp1, un incremento en el potencial de la membrana mitocondrial y una disminución en la tasa de respiración mitocondrial. Es conocido que LSS induce asimismo la activación de las plaquetas y la liberación de nucleótidos purínicos (como el ADP), que interacciona con receptores endoteliales. Hemos identificado p38 MAPK como una proteína moduladora de la activación de eNOS por ADP, demostrando la implicación que tiene la fosfatasa PTEN en esta ruta de activación. Nuestros datos sugieren un modelo en el que ADP promueve la inactivación de PTEN, originando unincremento en los niveles de PIP3 y la activación de p38 MAPK, que a su vez conduce a la activación de eNOS.

Nuestros resultados identifican nuevos mecanismos de la respuesta endotelial al flujo sanguíneo, identificando rutas no descritas previamente de regulación de la síntesis de $NO^{\cdot}$ y función mitocondrial en el endotelio vascular.

LIST OF ABBREVIATIONS

BAEC	Bovine aortic endothelial cells
BCA	Bicinchoninic Acid Assay
bFGF	Basic fibroblast growth factor
BH4	Tetrahydrobiopterin
BSA	Bovine serum albumin
Cys	Cysteine
DAPI	4',6-diamidine-2-phenylidone
EC	Endothelial cells
ECGF	Endothelial cell growth factor
EGF	Epidermal growth factor
eNOS	Endothelial nitric oxide synthase
FAD	Flavin adenie dinucleotide
FBS	Fetal bovine serum
FCCP	Carbonyl cyanide 4-(trifluoromethoxy)phenylhydrazone
FMN	Flavin mononucleotide
GAPDH	Glyceraldehyde 3-phosphate dehydrogenase
GO	Glucose oxidase
GRX	Glutaredoxin
HBSS	Hank's buffered saline solution
HRP	Horseradish peroxidase
HUVEC	Human umbilical vein endothelial cells
H_2O_2	Hydrogen peroxide
ICAM-1	Intercellular cell adhesion molecule 1
LSS	Laminar shear stress
MEF	Murine embryonic fibroblast
MLEC	Murine lung endothelial cells
NADPH	Nicotinamide adenine dinucleotide phosphate-oxidase

NO•	Nitric oxide
Opti-MEM	Optimal-Minimum Essential Medium
O2-•	Superoxide radical anion
MAPK	Mitogen activated protein kinase
PBS	Phosphate-buffered saline
PDGF	Platelet-derived growth factor
PH	Pleckstrin homology domain
PI3K	Phosphoinositide 3-kinase
PIP_2	Phosphatidylinositol-4,5-phosphate
PIP_3	Phosphatidylinositol-3,4,5-phosphate
PBS	Phosphate-buffered saline
PCR	Polymerase chain reaction
PRX	Peroxiredoxin
PTK	Protein tyrosine kinase
PTEN	Phosphatase and tensin homolog
PTP	Protein tyrosine phosphatases
PVDF	Polyvinylidene difluoride
qPCR	Quantitative PCR
RIPA	Radio-Immunoprecipitation Assay
RNS	Reactive nitrogen species
ROS	Reactive oxygen species
rpm	Revolutions per minutes
SDS-PAGE	Sodium Dodecyl Sulfate-Polyacrylamide Gel Electrophoresis
siRNA	Short interfering Ribonucleic acid
SOD	Superoxide dismutase
Srx	Sulfiredoxin
TBS	Tris buffered saline
TGFβ	Transforming growth factor-β
TMRM	Tetramethylrhodamine methyl ester

TRX	Thioredoxin
Tyr	Tyrosine
WB	Western blot

TABLE OF CONTENTS

LIST OF ILLUSTRATIONS

LIST OF FIGURES

LIST OF TABLES

LISTA DE ILUSTRACIONES

LISTA DE TABLAS

1. INTRODUCTION

1. INTRODUCTION

1.1 ENDOTHELIUM

A single monolayer of endothelial cells (ECs) lines the inner surface of the entire vascular system. This continuous organ consists of 10^{13} cells, covers an area around 1-7 m^2, and weighs approximately 1kg in an adult human (Khazaei et al., 2008) . Because of its location, the endothelium acts as a natural and selective barrier between the blood and others organs and tissues. As a barrier, the endothelium is semipermeable and regulates the transfer of small and large molecules and fluid between the blood and the interstitial space. Its structure is important for the integrity and maintenance of vessel wall, and also for the circulatory function. However, it does not mean endothelium is just an inert barrier. In addition, it is a metabolically active monolayer, constantly exposed to both biochemical and biomechanical stimuli. The endothelial layer is a dynamic and active tissue, and endothelial cells are able to control many important functions in vascular homeostasis (Galley and Webster, 2004). The ability of the vascular endothelium to sense and respond to the flow of blood was observed more than 150 years ago by the pathologist Virchow, who pointed to the heterogeneous morphology of the endothelium along the arterial tree, which correlated with the patterns of flow to which the cells were exposed. This observation leads to an array of studies both *in vivo* and *in vitro* in an attempt to characterize the multiple effects of blood flow on the endothelium (Resnick et al., 2003).

Endothelial dysfunction, condition in which the endothelium loses its physiological tendence to promote vasodilation and inhibit platelet aggregation and leukocyte adhesion (Galley and Webster, 2004), is a marker of vascular disease and plays an important role in the initiation and progression of many vascular disorders such as atherosclerosis, hypertension or diabetes (Khazaei et al., 2008).

1.2 HEMODYNAMIC FORCES IN THE VASCULATURE

Vascular endothelial cells are key players in the homeostasis of vascular function. They are constantly exposed to the pulsatile flow of blood through the vasculature due to its pump-driven nature. Blood flow generates three different hemodynamic forces which are sensed by endothelial cells:

- COMPRESSIVE STRESS (also known as hydrostatic pressure): this is the normal force exerted on the vessel wall due to the pressure of the blood. It is created by the hydrostatic forces of blood.
- CIRCUMFERENTIAL STRESS: is caused by changes in the vessel diameter due to pulsatility of blood flow. Changes in pressure during the cardiac cycle cause the vessel wall to stretch, which results in cyclic circumferential stress on the wall, specifically the basement membrane. It is created as a result of intercellular connections among endothelial cells.
- SHEAR STRESS: is the tractive tangential force produced by the blood passing along the luminal surface of the endothelium. It is the frictional force per unit area produced by a moving viscous fluid on a solid surface and its magnitude increases with fluid velocity and viscosity (Papadaki et al., 1999).

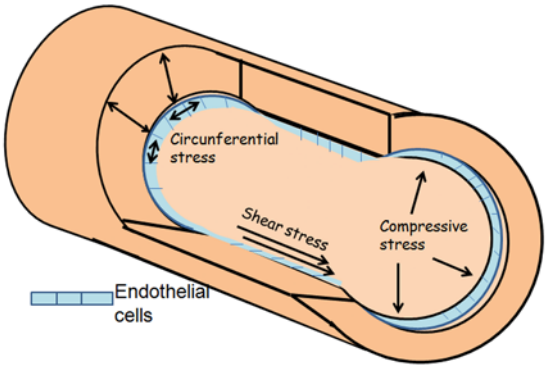

Illustration 1. Forces acting on the vessel wall. *Pulsatile flow of blood results in three types of hemodynamic on the vessel wall: compressive stress, circumferential stress and fluid shear (Papadaki and Eskin, 1997). Modified from (Hahn and Schwartz, 2009).*

Among these hemodynamic forces, shear stress appears to be a particularly important force because it stimulates the release of vasoactive substances and changes gene

expression, cell metabolism, and cell morphology (Davies, 1995). The magnitude of the shear stress can be estimated in the major part of the vasculature as a simple laminar flow in a circular tube, assuming blood as an incompressible Newtonian fluid. Newtonian fluids are those that possess a linear relationship between stress and strain rate and their flow is governed by the Navier-Stokes equations. Blood shear stress (τ_s) is proportional to blood flow viscosity (μ), and the shear rate or gradient of the velocity perpendicular to the direction of the shear ($\frac{du}{dy}$), according to the following equation (Nerem et al., 1998):

$$\tau = \mu \frac{du}{dy}$$

Blood flow can be modeled as a simple laminar flow in a circular cylindrical tube where vessel diameter is much larger than individual cells. From this conditions wall shear stress (Ƭ) can be described by Poiseuille formula (Nerem et al., 1998) :

$$\tau\, wall = \frac{32\mu Q}{\pi D^3} = \frac{4\mu Q}{\pi r^3}$$

where Q is the flow rate, μ the blood viscosity, D the diameter and r the internal radius of the vessel (Ku, 1997).

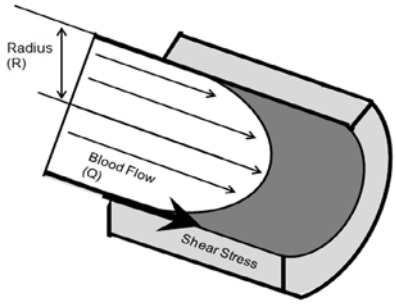

Illustration 2..Hemodynamic shear stress. Hagen-Poiseuille velocity profile in a circular cylinder. *Model depicts the conceptual relationship between blood flow, properties of blood and vessel size in the unbranched portions of medium-sized arteries (Malek et al., 1999).*

Changes in blood flow, thus generating altered hemodynamic forces, are responsible for acute vessel tone regulation, the development of blood vessels structure during embryogenesis and early growth, as well as chronic remodeling and generation of adult blood vessels (Resnick et al., 2003). Measurement using different modalities show that

shear stress ranges from 2 to 20 dyn/cm^2 (Dewey et al., 1981) in the major human arteries, and between 1 to 6 dyn/cm^2 in the venous system (Malek et al., 1999).

1.3 ENDOTHELIAL CELL BIOLOGY AND SHEAR STRESS

Endothelial shear stress, as described above, is the tangential stress derived from the friction of the blood on the endothelium. It is expressed in units of force/ unit area (N/m^2 or Pascal [Pa] or dyn/cm^2; 1N/m^2 = 1 Pa = 10 dyn/cm^2) (Nichols et al., 1991). In endothelium it is also dependent on the viscosity and velocity of the fluid and on the presence of geometric irregularities or obstructions along the vascular tree. Fluid flow can be either laminar or turbulent.

- LAMINAR SHEAR STRESS (LSS): blood flows in an ordered laminar pattern in "linear" areas of the vasculature and endothelial cells suffer a pulsatile shear stress dependent on the cardiac cycle. It is a unidirectional flow characteristic of healthy and relatively straight vessels segments, and it is considered to be atheroprotective. It promotes the release of factors from endothelial cells that favor endothelial cell survival and prevent coagulation, migration of leukocytes, and smooth muscle and endothelial cell proliferation (Yoshizumi et al., 2003, Traub and Berk, 1998). Cells exposed to laminar flow undergo elongation and reorientation with their longitudinal axis parallel to the direction of the flow (Dewey et al., 1981, Flaherty et al., 1972), a phenomenon that has been demonstrated both *in vivo* and *in vitro* (Helmlinger et al., 1991, Levesque and Nerem, 1985). This reorientation produces a decrease in the endothelial resistance and shear stress (Barbee et al., 1995).

- TURBULENT FLOW: it is also known as oscillatory or disturbed shear stress and it is closely associated with atherogenesis. This kind of flow occurs at areas of abrupt curvatures, in geometrically irregular regions in the vasculature or upstream and downstream of stenoses, where the laminar flow is disrupted and the velocity at any given point varies continuously over time (Chatzizisis et al., 2007). The endothelial cells exposed to oscillatory shear stress are unable to become reoriented and are exposed to high shear stress gradients. Either turbulent flow or

very low shear stress promotes the secretion of different factors such as angiotensin II (Ang II), platelet-derived growth factor (PDGF), endothelin 1 (ET-1), monocyte chemoattractant protein-1 (MCP-1) or vascular cell adhesion molecule-1 (VCAM-1); which contribute to the development of atherosclerosis. The release of these products and the expression of cell adhesion molecules, including VCAM-1 and ICAM-1 by endothelial cells, promote pro-thombotic, pro-migratory, and pro-apoptotic signals.

The nature and the magnitude of shear stress are essential for the long-term maintenance of the structure and function of vascular vessels.

Shear stress is capable of eliciting multiple responses in endothelial cells, and the identification of mechanotransducer molecules is a matter of active research. Several endothelial components located at the surfaces (luminal, junctional and basal) of the cells have been established as “mechanosensors”, as they may directly sense and transduce the mechanical force from the membrane to the intracellular compartment. Glycocalix, integrins, platelet cell adhesion molecule-1 (PECAM-1), vascular endothelial-cadherin, tyrosine kinase receptors, G proteins, primary cilium, caveolae and ion channels among others, have been established as mechanosensor molecules. They are able to transmit the signals via the cytoskeleton or by a biochemical cascade through the generation of second messengers and transcription factors activation, which bind to positive or negative shear stress responsive elements (SSREs) inducing or suppressing mechanosensitive genes (Papadaki and Eskin, 1997, Tzima et al., 2005, Davies, 1995). Several intracellular pathways are activated simultaneously, and the great majority of them converge into MAP kinases cascades suggesting their role in mechanotransduction (Li et al., 2005).

In the last decade, several publications have implicated reactive oxygen species (ROS) in the maintenance of steady vessel wall conditions, and in the vascular response to fluid flow. Both LSS and disturbed flow are associated with the generation of ROS and redox-induced signaling responses (Lehoux, 2006). While LSS is believed to generate low levels of ROS triggering redox-sensitive physiological signaling pathways and antioxidant responses, disturbed flow increase ROS giving way to enhanced expression of inflammatory mediators (De Keulenaer et al., 1998).

1.4 REACTIVE OXYGEN SPECIES: NATURE, SOURCES AND DETECTION

ROS is a collective term which includes different chemical species formed upon an incomplete reduction of oxygen.

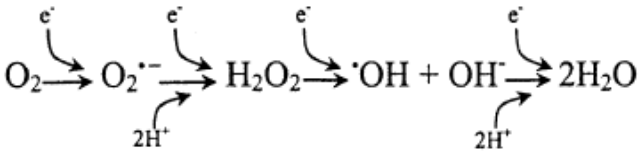

Illustration 3. ROS produced upon an incomplete reduction of oxygen

Reduction of molecular oxygen by an electron, mediates the initiation of ROS production. The first ROS produced after molecular oxygen reduction is superoxide radical anion ($O_2^{-\cdot}$), a very reactive but extremely unstable ROS that dismutates into the next ROS, hydrogen peroxide (H_2O_2). This reaction is either spontaneous or catalyzed by the enzyme superoxide dismutase (SOD). H_2O_2 is further reduced by an electron capture to lead to the formation of hydroxyl radical ($HO^{\cdot}$) via the Fenton reaction in the presence of Cu^{2+} of Fe^{2+} ions. Different ROS exhibit different chemical properties.

ROS molecule	*Main properties*
$O_2^{-\cdot}$	free radical highly reactive relatively short biological half-life unsuitable for crossing biological mebranes enzymatic defense systems: superoxide dismutase (SOD)
H_2O_2	non free radical two electron oxidant not highly reactive longer half-life able to penetrate biological membranes important role in the production of $HO^{\cdot}$ via oxidation of transition metals role as an intracellular signaling molecule

	enzymatic defense systems: catalase, glutathione peroxidase, thioredoxins, peroxiredoxins
$HO^{\cdot}$	free radical one electron oxidant high reactivity with biomolecules

Table 1. Chemical properties of ROS

ROS generation occurs under physiological, as well as pathophysiological conditions. Many cell types are able to produce low levels of $O_2^{-\cdot}$ and H_2O_2 in response to different extracellular stimuli, including:

- cytokines such as transforming growth factor β (TGF-β1) (Thannickal et al., 1998), Interleukin-1 (Krieger-Brauer and Kather, 1995), Interleukin-3 (Sattler et al., 1999), interferon-γ (Krieger-Brauer and Kather, 1995), and tumor necrosis factor -α (TNF-α) (Lo and Cruz, 1995);

- peptide growth factors such as platelet-derived growth factor (PDGF) (Sundaresan et al., 1995), epidermal growth factor (EGF) (Bae et al., 1997), basic fibroblast growth factor (bFGF) (Lo and Cruz, 1995) and insulin) (May and de Haen, 1979);

- agonist of heterotrimeric G protein-coupled receptors such as angiotensin II (Zafari et al., 1998, Ushio-Fukai et al., 1999), thrombin (Holland et al., 1998), thyrotropin (Krieger-Brauer and Kather, 1995), endothelin and bradykinin (Greene et al., 2000);

- shear stress (Rhee et al., 2000).

Endothelial cells are able to generate ROS which in low concentrations exert physiological roles. However, an excess of endothelial ROS is pathological due to their cytotoxic and mutagenic properties, being involved in endothelial dysfunction, inflammatory activation or tissue injury. ROS production in conjunction with endothelial activation and inflammatory cell recruitment leads to an equilibrium between oxidizing agents and antioxidant responses mediated by SODs, catalase and glutathione peroxidase (GPx), peroxiredoxins (Prx), thioredoxin (Trx) and heme oxygenase (HO-1) among others (Lehoux, 2006).The imbalance between ROS and oxidants and the capability of the cell to mount an effective

antioxidant response is known as "*oxidative stress*" (Ray et al., 2012). Oxidative stress results in nucleic acid, proteins or lipids damage, and it is implicated in several diseases such as atherosclerosis (Stocker and Keaney, 2004, Harrison et al., 2003), aging (Haigis and Yankner, 2010), diabetes or neurodegeneration (Andersen, 2004) among others. However, since ROS have been established as important signaling molecules, *oxidative stress* also refers as "*a disruption of redox signaling and control*" (Jones, 2006)

ROS SOURCES:

In endothelial cells, intracellular generation of ROS may arise from NADPH oxidases (NOX), mitochondrial respiration, uncoupled eNOS and xanthine oxidoreductase, although other sources have been also described such as cyclooxygenases, lipooxygenases or cytochrome P450. I will briefly review the main ROS sources in the endothelium:

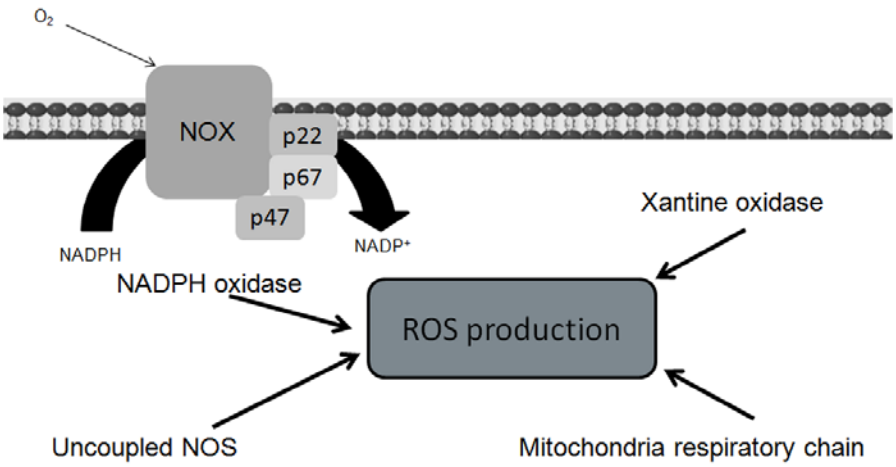

Illustration 4 ROS sources in endothelium. *ROS generation arises mainly from NADPH oxidases, mitochondrial respiratory chain, uncoupled eNOS and xanthine oxidase.*

NADPH OXIDASES:

In contrast to other oxidases, NOX family enzymes have no known biosynthetic or catabolic function but catalyze ROS as their primary function (Brieger et al., 2012, Burgoyne et al., 2012). NOX family enzymes are transmembrane electron transporters.

They transport electrons across biological membranes from the electron donor NADPH to molecular oxygen, leading to generation of $O_2^{-\cdot}$ (Bedard and Krause, 2007). Until the end of the 20th century, just the "phagocyte NADPH oxidase" NOX enzyme had been discovered (Rossi and Zatti, 1964). However, seven family members with a wide tissue distribution have been identified (NOX1-5 and dual oxidase 1-2) (Cheng et al., 2001). All NOX isoforms have six trans-membrane alpha helices with cytosolic N- and C-termini. They are differentially expressed and regulated in several tissues being their subcellular topology also distinct. In addition they show preference for yielding either $O_2^{-\cdot}$ or H_2O_2. For example NOX1, NOX2 and NOX5 produce mainly $O_2^{-\cdot}$, while NOX4 generates mainly H_2O_2 (Altenhofer et al., 2012, Takac et al., 2011). NOX4, the major catalytic component of endothelial NADPH oxidase (Ago et al., 2004, Schroder et al., 2012) is the more distantly related NOX enzyme. While its activity is dependent on p22phox, it does not require any cytosolic subunits such as p47phox, p67phox, p40phox or Rac as others NOX isoforms do.

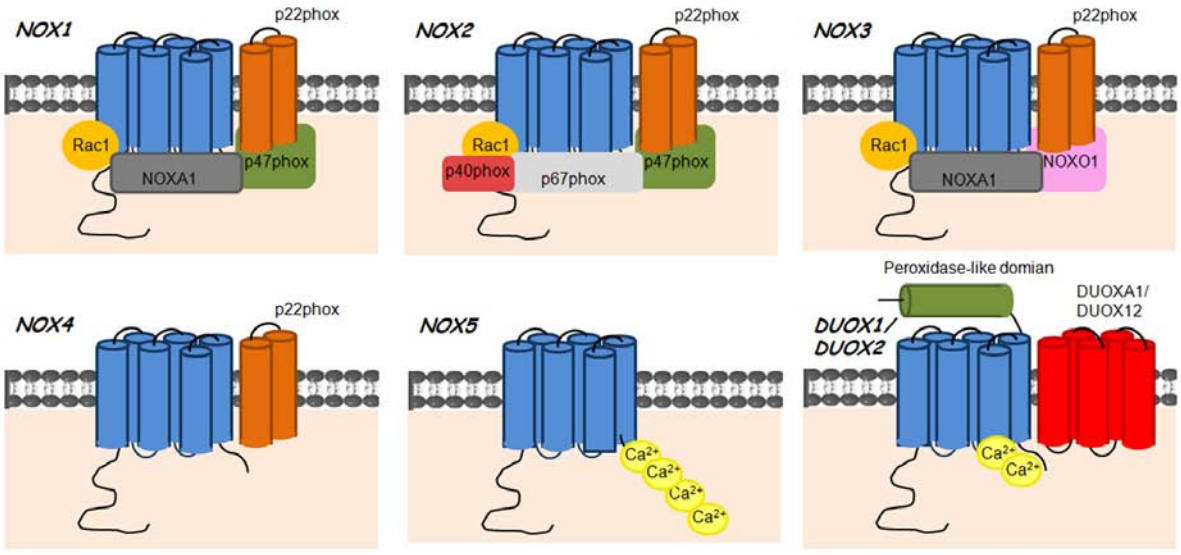

Illustration 5. NADPH oxidase isoforms. *Seven members of the NADPH oxidases have been described (NOX1-5, DOUX1-2) Modified from (Drummond et al., 2011).*

MITOCHONDRIA:

Mitochondriae represent the main intracellular source of ROS under physiological conditions. Notwithstanding, ROS production by mitochondriae can also be enhanced by several intracellular stimuli. The generation of mitochondrial ROS is a consequence of oxidative phosphorylation linked to aerobic respiration occurring within the mitochondrial electron transport chain (ETC).This machinery is situated in the inner mitochondrial membrane and it is able to catalyze electron transfer using more than 80 peptides organized in four complexes (Finkel and Holbrook, 2000). The transfer of electrons usually leads to the formation of ATP by the fifth complex; however, at several sites along the respiratory chain, electrons derived from NADH or FADH can directly react with oxygen or other electro acceptors and generate free radicals. Electron leakage from the ETC causes partial reduction of molecular oxygen (1-electron reduction of O_2) to $O_2^{-\cdot}$ instead of reduction to H_2O. Thus 1-2% of the O_2 consumed is converted into ROS (Chance et al., 1979). It has recently been proposed that mitochondrial ROS play an essential role in several redox-dependent signaling processes (Nemoto et al., 2000, Werner and Werb, 2002). The discovery of superoxide dismutase enzyme isoform MnSOD located in the matrix of the organelle was the main step in establishing the generation of H_2O_2 inside the mitochondria.

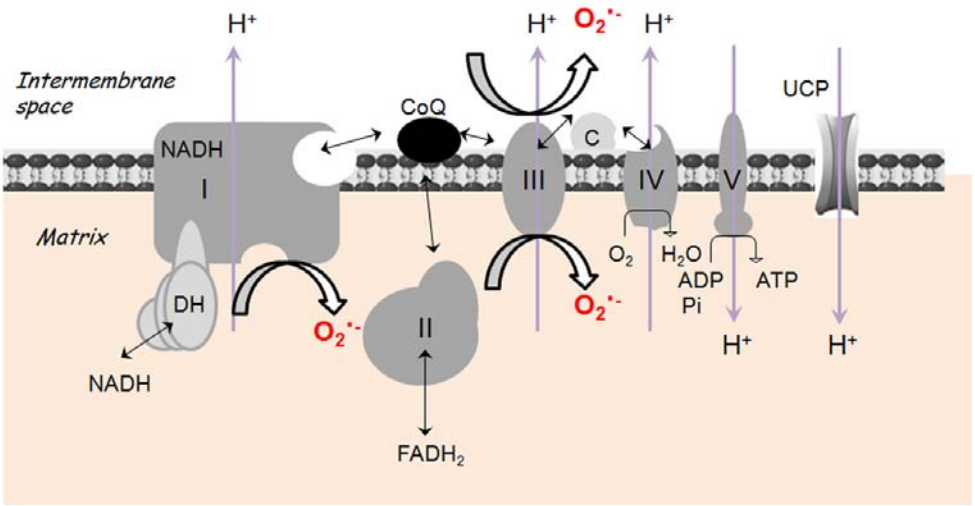

Illustration 6. Model of ROS generation in the mitochondria. *Electron leakage from Complex I and Complex III causes partial reduction of O_2 and $O_2^{-\cdot}$ production. Modified from (Balaban et al., 2005).*

NITRIC OXIDE SYNTHASE(S):

At the mid-1980 it was found a new gaseous free radical molecule previously defined as *"endothelial-derived relaxing factor (EDRF)".* This molecule was nitric oxide ($NO^{\cdot}$) (Hancock, 2008).

In mammals $NO^{\cdot}$ is produced by a family of nitric oxide synthase (NOS) enzymes. There are three different isoforms, two of them constitutively present (the endothelial nitric oxide synthase, eNOS or NOS3, and the neuronal nitric oxide synthase, nNOS or NOS1), and one which is inducible (iNOS or NOS2). They are all flavin-and heme- containing enzymes that act as homodimers shuttling electrons from the NADPH bound at the C-terminal (reductase domain) to the N-terminal heme (oxidase domain), reducing O_2 and incorporating into the guanidine group of L-arginine to produce L-citrulline and $NO^{\cdot}$. However, those enzymes can become a source of $O_2^{-\cdot}$ in endothelium exposed to oxidant or hemodynamic stresses when exposure to oxidative stress, particularly to peroxynitrite, or in the absence of cofactors (L-arginine or the reducing cofactor tetrahydrobiopterin (BH4)) occurs (Vasquez-Vivar et al., 1998), eNOS uncouples to a monomeric form, and generates $O_2^{-\cdot}$ instead of $NO^{\cdot}$ (Landmesser et al., 2003). This process is known as "uncoupling". Recently, it has been reported that S-glutathionylation of eNOS can also induce a reversible uncoupling of eNOS providing a new molecular understanding of how oxidant stress alter endothelial function (Chen et al., 2010). eNOS uncoupling has been recognized in human patients with endothelial dysfunction due to vascular diseases such as hypercholesterolemia, diabetes or hypertension (Stroes et al., 1997, Heitzer et al., 2000, Higashi et al., 2002).

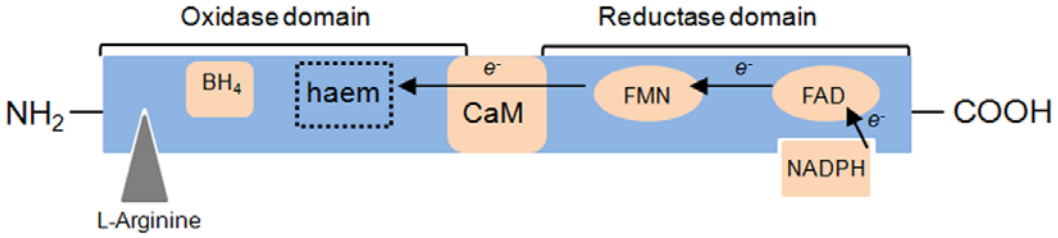

Illustration 7. Schematic representation of NOS. *The oxigenase domain consists of a haem centre and binbing sites for L-arginine and BH4. The reductase contains binding sites for FAD, FMN and NADPH. CaM binding domain lies between oxidase and reductase domain.*

$NO^{\cdot}$ is generated in biological tissues and is an important regulator of a broad range of functions (Zweier et al., 1995, Moncada et al., 1991) . It is known to regulate blood pressure, vascular tone, neural signaling and immunological function (Moncada et al., 1989, Garthwaite, 1991, Langrehr et al., 1993), but it also cause cellular injury via formation of high levels of reactive nitrogen species (RNS). RNS are various nitric-oxide-derived compounds that play a crucial role in the physiologic role of many cells (Martinez and Andriantsitohaina, 2009). Each of these compounds has got different properties attending to their reactivity, half-life, lipid solubility or biological activity (Nathan, 2003). They can induce posttranslational modifications on different cellular targets and interact with ROS, including its high reactivity with $O_2^{-\cdot}$ by an enzyme-independent mechanism to form peroxinitrite ($ONOO^-$), (a higly reactive oxidant that mainly nitrates tyrosine residues in nonenzymatic reactions).

RNS molecule	*Formula*	*Formation*
Dinitrogen trioxide	N_2O_3	From $NO^{\cdot}$ andO2
Nitric oxide or nitrogen monoxide	$NO^{\cdot}$	From NOS
Nitrite	NO_2^-	From $NO^{\cdot}$
Nitrogen dioxide	$NO_2^{\cdot}$	From $ONOO^-$ decomposition
Nitronium cation	NO_2^+	From $ONOOCO_2^-$ decomposition
Nitrosonium cation	NO^+	From NO.
Nitrosoperoxycarbonate anion	$ONOOCO_2^-$	$ONOO^-$ and CO_2
Nitroxyl	HNO	From one-electron reduction of $NO^{\cdot}$
Nitryl chloride	Cl-NO_2	From NO_2^- and HOCl
Peroxynitrite	$ONOO^-$	From $NO^{\cdot}$ and $O_2^{-\cdot}$
S-Nitrosothiols	RSNOs	From covalent addition of an NO. group to a cysteine thiol/sulfydyl

Table 2. Main Reactive Nitrogen Species

Three main posttranslational modifications can be induced by RNS:

- S-nitrosylation: the covalent addition of an $NO^{\cdot}$ group to a cysteine thiol/sulfhydryl to form an S-nitrosothiol derivative (RSNO). S-nitrosothiols can be reduced by Trx or Grx (Holmgren et al., 2005).

- Glutathionylation: the addition of glutathione (GSH), or other low-molecular-weight thiols, to the cysteine sulfhydryl residues of proteins
- Tyrosine nitration: a two-step process in which the first reaction is the generation of tyrosyl radical by oxidation of tyrosine by reactive species generated from $ONOO^{\cdot}$ and a second step in which tyrosyl radical reacts with NO_2 to form 3-NO_2^- Tyr (3-nitrotyrosine).

As it has been described above in the case of ROS, when the generation of RNS in a system exceeds its ability to neutralize and eliminate them, nitrosative stress occurs (Ogino and Wang, 2007) inducing cell damage and death.

XANTHINE OXIDASE:

Xanthine oxidoreductase, termed as xanthine oxidase (XOR), is an iron-sulfur molybdenum flavoprotein enzyme that catalyzes the last steps of purine metabolism: the transformation of hypoxanthine and xanthine to uric acid, with $O_2^{-\cdot}$ or H_2O_2 generation as by-products (Jarasch et al., 1981). It exists in two forms, as xanthine dehydrogenase (XDH) and as xanthine oxidase (XO) (Harrison, 2002). The XDH activity present in the vascular endothelium is converted into XO by processes including thiol oxidation and/or proteolysis. The ratio between XO and XDH in the cells is critical to determine the amount of ROS produced by these enzymes (Granger, 1988). Increases both in the expression and activity of XO have been related to vascular diseases (Guzik et al., 2006, Spiekermann et al., 2003). In the last decade, XOR has been discovered to produce $NO^{\cdot}$ itself (Godber et al., 2000, Li et al., 2001) adding a new essential vascular role for this enzyme in biological tissues (Harrison, 2002).

In the following table main sources for each ROS molecule is described:

ROS molecule	*Main sources*
$O_2^{-\cdot}$	"Leakage" of electrons from the ETC NADPH oxidase Xanthine oxidase uncoupled nitric oxide synthase
H_2O_2	From $O_2^{-\cdot}$ spontaneously or catalyzed by SODs NADPH oxidase Glucose oxidase Xanthine oxidase
$OH^{\cdot}$	From $O_2^{-\cdot}$ via SOD and H_2O_2 via transition metals (Cu, Fe)

Table 3. Main ROS sources.

The precise understanding of the physiological relevance of ROS and redox signal transduction, and even the nature and source of the reactive species after physiological stimuli have not always been clearly described. This is in part due to the relative difficulty in the study of ROS generation and detection, based on the scarcity of specific and reliable techniques.

ROS AND RNS DETECTION:

$O_2^{\cdot -}$:

- CYTOCHROME C REDUCTION:

$$Fe^{3+} + \text{cit}\,c + O_2^{\cdot -} \longrightarrow Fe^{2+} + \text{cit}\,c + O_2$$

BASIS OF THE DETECTION: ferricytochrome c is reduced to ferrocytochrome c in the presence of $O_2^{-\cdot}$. This reaction can be followed spectrophotometrically at 550 nm.

0 **ADVANTAGES:**

- Can measure $O_2^{-\cdot}$ production by numerous enzymes, whole cells and vascular tissues

- **DISADVANTAGES:**
  - Non specific $O_2^{\cdot-}$. There is need to demonstrate specificity for superoxide radical anion by exogenous SOD
  - Cytochrome c has restricted intracellular access
  - Insensitive to detect low rates of $O_2^{\cdot-}$
  - Interferences with several endogenous reductants

➢ ACONITASE:

BASIS OF THE DETECTION: aconitase catalyzes the interconversion of citrate to isocitrate. Aconitase is a member of [4Fe-4S] containing (de)-hydratases particularly susceptible to be inactivated by $O_2^{\cdot-}$ due to the oxidation followed by reversible loss of Fe.

- **ADVANTAGES:**
  - Useful for cytosolic and mitochondrial $O_2^{\cdot-}$ production
  - Specificity for $O_2^{\cdot-}$ detection
- **DISADVANTAGES:**
  - In basal conditions a fraction of aconitase is inactive
  - $ONOO^-$ can oxidize aconitase Fe clusters

➢ HYDROETHIDINE:

BASIS OF THE DETECTION: Hydroethidine (dihydroethidium, HE) can undergo a two-electron oxidation to form the DNA-binding fluorophore ethidium bromide.

- **ADVANTAGES:**
  - Cell permeable
  - HE derivatives can specifically detect mitochondrial $O_2^{\cdot-}$ production
  - The fluorescence can be detected by flow cytometry, or fluorescence microscopy
- **DISADVANTAGES:**
  - Reacts with many other oxidants. It is considered a redox indicator
  - Highly susceptible to photooxidation and photobleaching
  - High concentration of the probe results in artifactual oxidation falsely attributed to ROS generation

➢ LUCIGENIN ASSAY:

BASIS OF THE DETECTION: $O_2^{-\cdot}$ can be measured by chemiluminiscence reaction in the presence of the chemiluminogenic probe lucigenin.

- **ADVANTAGES:**
  - Cell permeable
  - High specificity
  - High sensitivity
  - Minimal cellular toxicity
- **DISADVANTAGES:**
  - Artifactual generation of $O_2^{-\cdot}$ due to lucigenin potential for redox cycling
  - Limitation in estimating quantitative $O_2^{-\cdot}$ rate production

➢ ELECTON SPIN RESONANCE AND SPIN TRAPPING:

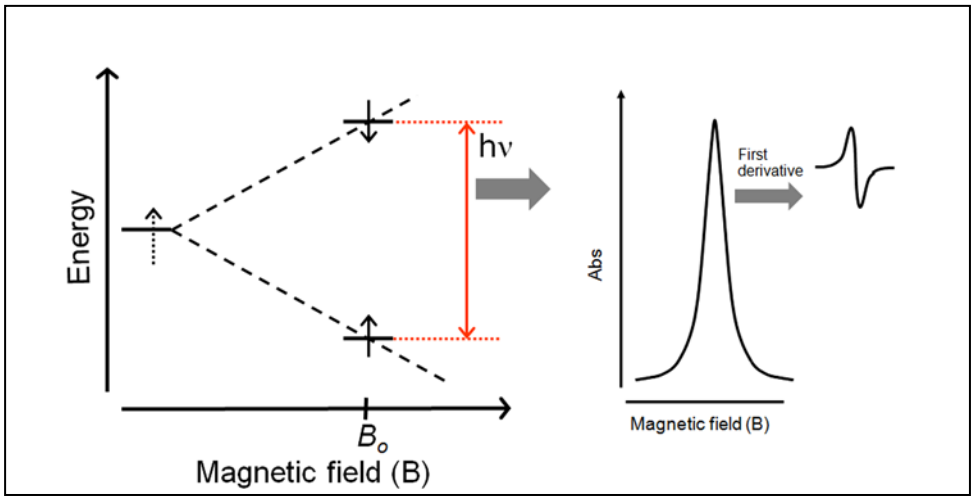

Illustration 8. EPR principles

BASIS OF THE DETECTION: this technique is also known as electron paramagnetic resonance (EPR). It is based on the magnetic properties of unpaired electrons and their molecular environment. Unpaired electrons can exist in two orientations, either parallel or antiparallel with respect to an applied magnetic field. The energy differences of these states correspond to the microwave region of the electromagnetic spectrum. Unpaired

electrons are too low in concentration and exhibit too short half-life to be directly detected in biological systems This can be avoided by employing more stable secondary radical species which form carbon adducts, the so called “spin traps” as DMPO and DEPMPO.

- **ADVANTAGES:**
  - Direct detection of free radicals
  - Stabilization of captured ROS
- **DISADVANTAGES:**
  - In the presence of tissue reductants, such as ascorbate, the ESR-active adducts can be reduced leading to an underestimation of ROS formation
  - Light sensitivity

H_2O_2:

- AMPLEX RED:

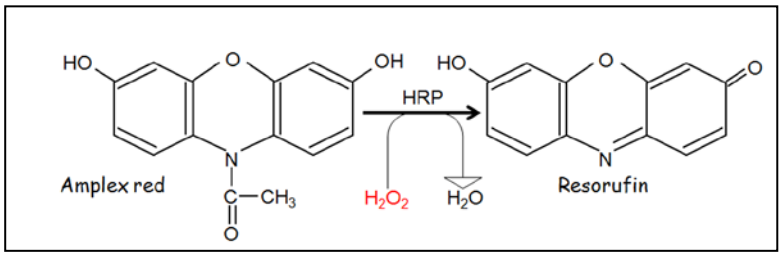

Illustration 9. Detection of H_2O_2 with Amplex red

BASIS OF THE DETECTION: H_2O_2 reacts with Amplex Red [N-acetyl-3,7,dihydroxyphenoxazine] in a reaction catalyzed by horseradish peroxidase (HRP; stoichiometry 1:1). Resorufin exhibits a maximum of fluorescence emission and excitation of 587 and 563 nm respectively.

- **ADVANTAGES:**
  - Highly sensitive allowing measurement of concentrations of H_2O_2 as low as 50 nM
  - HRP is active over a wide pH range

- **DISADVANTAGES:**
  - Light oxidation of the reagent: high oxidation in controls
  - Extracellular buffer may interfere in measurements. It is necessary to check the positive controls in the buffer of interest.

➢ DCFH-DA [5-(AND 6-)CHLOROMETHYL-2',7'-DICHLORODIHYDROFLUORESCEIN DIACETATE] (CMDFM-DA):

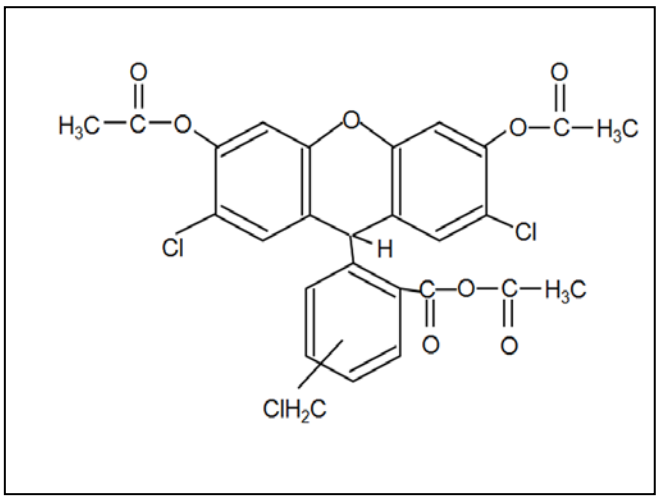

Illustration 10. CMDCFH-DA

BASIS OF THE DETECTION*:* CMDCFH-DA diffuses into cells and becomes trapped as a result of its deacetylation by esterases. The probe is then oxidized by oxidants like H_2O_2 to yield the highly fluorescent product CMDCF. Accumulation of the probe in cells can be measured on the basis of an increase in fluorescence at 530 nm on excitation at 488 nm. The fluorescence is proportional to the concentration of ROS cells.

- **ADVANTAGES:**
  - Cell permeable
  - Highly sensitive to changes in cellular redox state
  - Suitable for monitoring changes in ROS concentration over time
  - The fluorescence can be detected by flow cytometry, or fluorescence microscopy.
- **DISADVANTAGES:**
  - Reacts with many other oxidants. It is considered as a redox indicator
  - The probe undergoes oxidation in solution, hence working solutions should be prepared fresh

- High concentrations of the probe are cytotoxic and could result in artifactual oxidation attributed to ROS generation
- Highly susceptible to photooxidation and photobleaching.

➢ HYPER VECTORS:

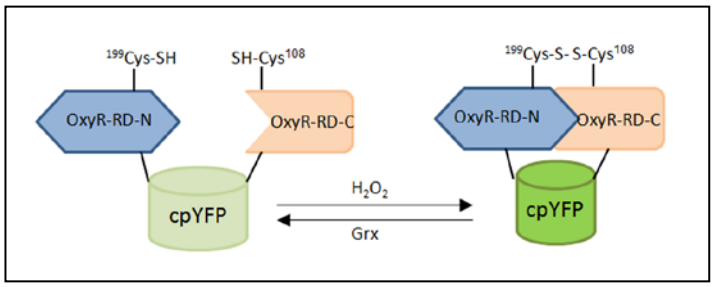

Illustration 11. Domain structure of HyPer

BASIS OF THE DETECTION: This probe consist of the circularly permuted yellow fluorescent protein (cpYFP) inserted into the regulatory domain of the prokaryotic H_2O_2-sensing protein, OxyR. H_2O_2 induces the formation of a disulfide bond between Cys^{199} and Cys^{208} located in the N- and C-terminal of OxyR respectively. This conformational change drives a ratiometric fluorescence change of cpYFP. The fluorescence spectrum of HyPer has two excitation maxima at 420 and 500 nm and an emission maximum at 516 nm.

0 **ADVANTAGES:**

- Highly specific fluorescent probe for detecting H_2O_2 inside living cells
- High sensitivity toward H_2O_2. It is insensitive to $O_2^{-\cdot}$, oxidized glutathione, $ONOO^-$ and $NO^\cdot$
- Ratiometric sensor: on exposure to H_2O_2, the excitation peak at 420 nm decreases while the peak at 500 nm increases
- Targeting specific subcellular compartments
- The fluorescence can be detected by flow cytometry, microplate reading or fluorescence microscopy

0 **DISADVANTAGES:**

- Reverse reaction with H_2O_2 catalyzed by glutaredoxin (Grx)

- Dependent on transfection efficiency
- Susceptible to photobleaching

➢ HRP-BASED SPECTROPHOTOMETRIC ASSAY WITH 3,5,3' 5' TETRAMETHYLBENZIDINE:

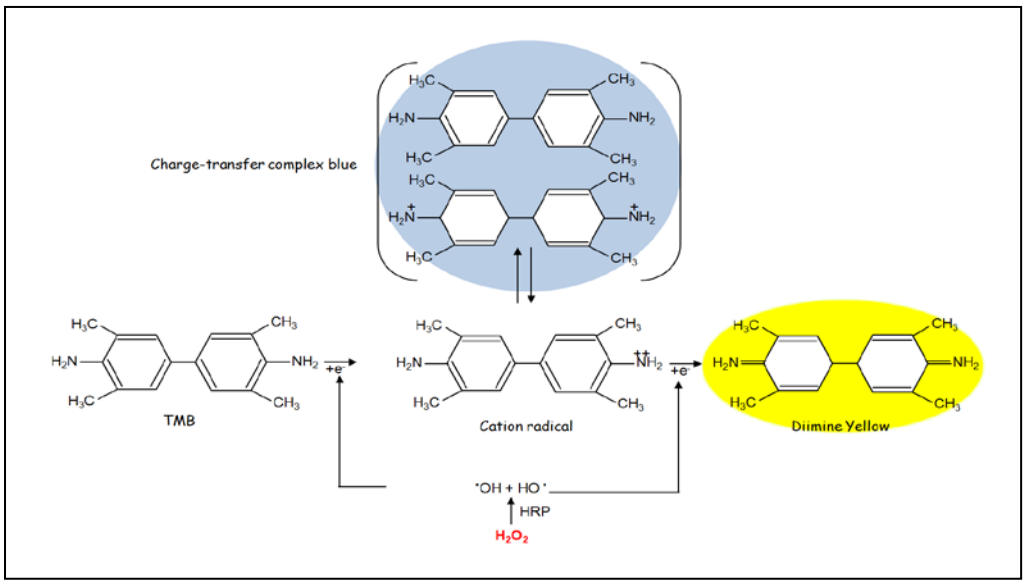

Illustration 12.Chemical structure of TMB and its oxidation products

BASIS OF THE DETECTION: exposure of TMB to H_2O_2 in the presence of HRP results in the formation of an intermediate product in equilibrium with a charge-transfer complex responsible for the blue color of the reaction (Abs at 653 nm). Further oxidation yields a yellow product (diimine, abs at 450 nm).

0 **ADVANTAGES:**

- Highly sensitive to H_2O_2
- High stability of the oxidation products

0 **DISADVANTAGES:**

- Photosensitive

➢ PICO GREEN + SNAP TAGGED TECHNOLOGY:

BASIS OF THE DETECTION: SNAP–tagR is a 20-kDa mutant of DO6-alkylguanine-DNA alkyltransferase (AGT) that reacts rapidly with benzylguanine and benzylchloropyrimidine derivatives. By conjugating the deprotection-based H_2O_2 probe PG1 to benzyl 2-chloro-6-aminopyrimidine, a SNAP-tag substrate probe selective for H_2O_2 detection was synthesized.

0 **ADVANTAGES:**

- Cell permeable
- Selective for H_2O_2
- High sensitivity
- Organelle targeted

0 **DISADVANTAGES:**

- Non reversible reaction: cannot be used for measuring transient changes in H_2O_2 production
- Very little published data

$NO^{\cdot}$:

➢ GRIESS REACTION:

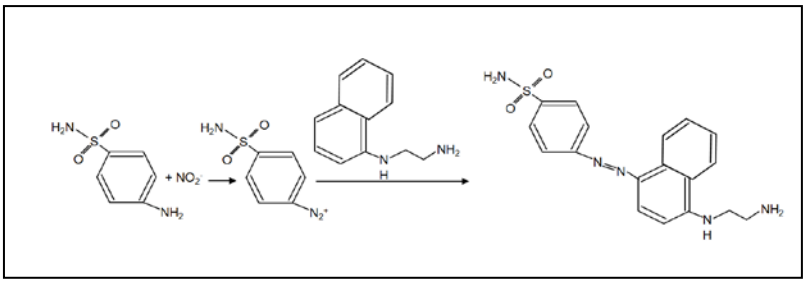

Illustration 13. ***Griess reaction***

BASIS OF THE DETECTION: The nitrosating agent dinitrogen trioxide (N_2O_3) generated from the autoxidation of $NO^{\cdot}$ or from the acidification of nitrite (NO_2^-) reacts with sulfanilamide to yield a diazonium derivative. This reactive intermediate will interact with N-1-naphthylethylene diamine to yield a colored diazo product that absorbs strongly at 540 nm.

- **ADVANTAGES:**
  - Quantify NO_2^- in extracellular fluids such as plasma, urine and lymph
  - Simple, rapid and inexpensive assay
- **DISADVANTAGES:**
  - Indirect determination of NO
  - Sensitivity limit: 2-3 µM
  - Presence of heparin in the sample may produce Griess reagent precipitation

➢ FLUORESCENCE SPECTROSCOPY:

BASIS OF THE DETECTION: Fluorometric detection of $NO^{\cdot}$ can be performed by the use of either diaminonaphtalene (DAN) or diaminofluoroscein-2-diacetate (DAF-2DA). DAN reacts with NO_2- yielding the highly fluorescent product naphthotriazole (NAT). DAF-DA difusses into cells and tissues, it is hydrolyzed by esterases trapping DAF-2 intracellularly where it is able to react with NO-derived nitrosating agents to yield the fluorescent product DAF-2 triazole (DAF-2 T)

- **ADVANTAGES:**
  - Enhanced sensitivity of measuring NO_2^- and $NO^{\cdot}$
  - High specificity
  - Minimal interference by nitrite decomposition
  - Useful in vitro and in vivo
- **DISADVANTAGES:**
  - DAF-2 can react with nitroxyl (HNO)
  - Photosensitive, leading possible false positives

➢ CHEMILUMINESCENCE ANALYSIS:

BASIS OF THE DETECTION*:* NO gas combines with ozone to produce NO in the excited state (NO_2^*), which upon decay emits light detected by a photomultiplier.

- **ADVANTAGES:**
  - Detects $NO^{\cdot}$ and its oxidation products nitrite (NO_2^-) and nitrite (NO_3^-)

- High sensitivity (1 pM NO)
- Small volume of sample is required
- Low artifactual effects

0 **DISADVANTAGES:**

- Liquid or gaseous samples are required
- Specialized equipment
- Does not anayze $NO^{\cdot}$ release over brief intervals
-

➢ ELECTON SPIN RESONANCE AND SPIN TRAPPING:

BASIS OF THE DETECTION: technique described above. For $NO^{\cdot}$ detection colloid iron diethyldithiocarbamate, $Fe(DETC)_2$ is a reliable spin trap.

0 **ADVANTAGES:**

- Specific for bioactive $NO^{\cdot}$ detection
- Does not react with nitrite or nitrate
- High stability of the adduct allows measurement of cumulative amount of $NO^{\cdot}$ produced over time

0 **DISADVANTAGES:**

- $Fe(DETC)_2$ can be oxidized by H_2O_2 or $O_2^{-\cdot}$
- Light sensitivity

➢ ELECTROCHEMICAL DETECTION OF NO.:

BASIS OF THE DETECTION: in this technique the voltage of the electrode is controlled to catalyze $NO^{\cdot}$ oxidation on the electrode surface. Electrods are typically filaments made of carbon or platinum.

0 **ADVANTAGES:**

- Sensitivity sufficient for biological samples
- Quantitative methodology

There are several assays that indirectly reflect the presence of NO. in biological samples. Briefly:

- measurement of cGMP. This method estimates NO production by measuring cGMP changes in reporter cells since activation of guanylate cyclase by NO leads to increased production of cGMP (Ros et al., 1995).
- measument of citrulline as a coproduct of the action of NOS on L-arginine. This assay detects the conversion of radio-labelled [^{3}H]L-arginine to radio-labelled [^{3}H]L-citrulline. Since L-arginine conversion leads to equimolar amounts of NO as well as L-citrulline, the amount of [^{3}H]L-citrulline can be used indirectly to reflect NO production and eNOS activity (Hecker et al., 1990).
- Hemoglobin assay: two different approaches are possible. NO oxidizes reduced hemoglobin to methemoglobin which can be detected spectrophotometrically (Ignarro et al., 1987) of by electron paramagnetic resonance assay (EPR) with hemoglobin traps by measuring nytrosyl-hemoglobin adduct (Arroyo and Kohno, 1991).

1.5 REDOX SIGNALING

For many years ROS were described as unwanted toxic products of cellular metabolism, assuming that the faster the elimination of them, the better for the cell (Rhee, 2006). However, substantial evidences in the last two decades, have established ROS and RNS as important signaling molecules. Different redox- active species have distinct biological properties, which include reactivity, half-life and lipid solubility among others. While $HO^{\cdot}$ presents indiscriminate reactivity towards biological molecules, $O_2^{-\cdot}$ presents a very short lifespan allowing it to react with very few molecules. It reacts specifically with iron-sulfur clusters of key cellular proteins altering their activity (Gardner et al., 1995). H_2O_2 has been described by the end of the 90s as an *important signaling molecule* in different cells. Its intrinsic nature makes H_2O_2 a small, diffusible and ubiquitous molecule able to reach and react with different cellular subcomponents acting as an intracellular second messenger (D'Autreaux and Toledano, 2007, Rhee et al., 2003). It induces reversible and covalent

modifications on specific cysteine thiols residues located in active and allosteric sites of the proteins resulting in alterations on their activities. Despite H_2O_2 is a mild oxidant and hence relatively inert to most biomolecules, it can oxidize cysteine residues in proteins to produce disulfide (R-S-S-R), via formation an intermediate cysteine sulfenic acid (R-S-OH) (Claiborne et al., 1993, Denu and Tanner, 1998). Disulfide bonds can occur between cysteines within the same protein (intramolecular disulfide bond (Lee et al., 2002b)) or between cysteines located in two different molecules producing an homo- or hetero-dimer ((intermolecular disulfide bond (van der Wijk et al., 2004)). They can also form a mixed-disulfide between glutathione and the thiol of another protein (S-glutathionylation). Proteins thiols can undergo further two-electron oxidations by H_2O_2 to form sulfinic (R-SO_2H) or sulfonic acid (R-SO_3H). Because the ionization constant (pKa) of the sulfhydril group of most cysteines residues (Cys-SH) is around 8.5, few proteins might be expected to possess a cysteine residue that is susceptible to oxidation by H_2O_2 in cells. However, certain protein cysteine residues exist as thiolate anions at neutral pH as a result of the lowering of their pKa values by charge interactions between the negatively charged thiolate and nearby positively charged amino acid residues (Rhee et al., 2003). The pKa of a cysteine is dependent on the charge of the adjacent amino acids within its quaternary structure. Once a cysteine thiol has been oxidized, it needs to be re-reduced if the signal has to be ended. Several enzymatic and non-enzymatic systems are responsible for this process. Disulfides and sulfenic groups can be reduced by TRXs and PRXs), while GRXs catalyzes S-glutathionylated cysteine reduction (Holmgren et al., 2005). Sulfinic acid groups can be reduced back to sulfenic by a family of ATP-dependent enzymes termed sulfiredoxins (Srx) (Biteau et al., 2003). Overoxidation to sulfonic acid is considered to be biologically irreversible. Not only cysteine residues are susceptible to oxidation; in addition, methionine, tryptophan and tyrosine residues can be also modified by oxidation. However, the functional impact of those events in physiological signal transduction is still incompletely described (Janssen-Heininger et al., 2008).

Even when several ROS and RNS have been demonstrated to act as signaling molecules with important regulatory functions, I will focus on H_2O_2 effects on redox signaling.

In order to characterize the importance of H_2O_2 redox signaling in cellular functions it is essential to identify the cellular targets able to sense and transduce the signal induced.

MOLECULAR TARGETS OF H_2O_2 REDOX SIGNALING:

- TYROSINE PHOSPHATASES: The protein tyrosine phosphatase family (PTP) share a catalytic mechanism that requires a reduced cysteine, making them potentially sensitive to inactivation by redox stimuli. These essential cysteines have a pKa between 4.7 to 5.4 in the catalytic domain (His-Cys-X-X-Gly-X-X-Arg-Ser/Thr, where X is any amino acid), and exist as a thiolate anion at neutral pH (Denu and Dixon, 1998). This active site is therefore a target for various mild oxidants such as H_2O_2 resulting in enzyme inactivation. The net effect on protein phosphorylation is a result of the equilibrium with protein tyrosine kinases (PTKs). Hence, oxidative inactivation of phosphatases may enhance MAPK activation (Kamata et al., 2005, Seth and Rudolph, 2006). The ability of physiologically H_2O_2–production to inhibit PTP has been described after the exposure to peptide growth factors; for example, EGF leads to the production of H_2O_2 and the concomitant inhibition of PTP1B (Bae et al., 1997) or PDGF which induces the oxidation and inhibition of SHP-2 (Meng et al., 2002) and PTEN (Kwon et al., 2004).

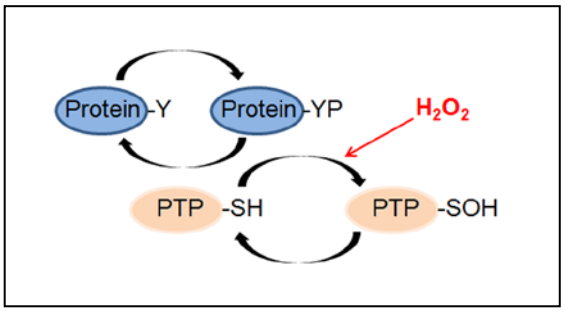

Illustration 14. Proposed model for H_2O_2 as modulator of protein tyrosin phosphorylation

- PROTEASES: proteases such as caspases and matrix metalloproteinases (MMPs) are regulated by oxidative stress. While in the specific case of caspases, H_2O_2 inhibits its activation *in vivo* (Lee and Shacter, 2000) some studies suggest that MMPs can be either activated or inhibited by ROS (Zhang et al., 2001, Okamoto et al., 2004).
- MOLECULAR ADAPTORS AND CHAPERONES: These protein systems include the family of heat shock proteins (Hsp) and protein disulfide isomerases (PDI) (Winter and Jakob, 2004). In 1999, the heat shock protein Hsp33 was shown to be regulated by oxidative stress (Jakob et al., 1999). Hsp33 in its inactive conformation has four

cysteine residues in the thiolate anion state that bind Zn^{2+}. Oxidative stress leads to the oxidation of these cysteine residues forming two intramolecular disulfide bonds, which cause Zn release and Hsp33 activation (Graumann et al., 2001). Mammalian Hsp25, 60, 70 and 90 also present redox-active cysteine residues, and their oxidation induces changes in chaperone functions (Diaz-Latoud et al., 2005, Hoppe et al., 2004, Nardai et al., 2000). PDI is a multifunctional member of the TRX superfamily (Janssen-Heininger et al., 2008). It is able to bind to its substrate only in its reduced state, releasing the substrate protein after being oxidized (Sitia and Molteni, 2004, Tsai et al., 2001). Apart from this function, oxidized PDI, with its active thiols in the disulfide form, can act as an electrophile forming disulfide bonds in sulfhydryl-containing substrate proteins (Gruber et al., 2006).

- TRANSCRIPTION FACTORS: Apart from being subjected to redox control through the oxidation of kinases, phosphatases or chaperones, transcription factors are also well known targets of oxidative stress (Na and Surh, 2006). NF-κB was the first eukaryotic transcription factor shown to respond directly to oxidative stress (Schreck et al., 1991). Since then several families of transcription factos, such as AP-1, p53 or Hif-1α, have been described to be modulated directly by oxidative changes (Semenza, 2001, Haddad and Land, 2000, Duan and Nilsson, 2006). This modulation can be translated either into activation or inhibition.
- REDOX ENZYMES: In the following table I have summarized different redox enzymes able to react with H_2O_2 and the reactions rates with H_2O_2 for selected cysteines located in their active site. As it is shown, Prxs are the ones with the highest rate constant and therefore affinity for H_2O_2 (Winterbourn and Hampton, 2008).

Thiol	*Rate constant (M^{-1} s^{-1})*
GSH	0.89
Cysteine	2.9
N-Acetylcysteine	0.16
Thioredoxin	1.05
Peroxiredoxins	1-4 x 10^7

Table 4. Reaction rates with H_2O_2 for selected low molecular weight thiols and thiol protein.

1.6 PEROXIREDOXINS

Prxs are a ubiquitous family of antioxidant enzymes that exert their protective antioxidant role through their peroxidase activity by reducing peroxides. In mammals, this family of proteins presents six different isoforms (Seo et al., 2000, Knoops et al., 1999) (Prx 1-6), divided in three distinct classes: typical 2-Cys Prxs (Prx 1-4), atypical 2-Cys Prxs (Prx 5) and 1-Cys Prxs (Prx6). All Prxs share the same basic catalytic mechanism. The active cysteine residue (also known as peroxidatic cysteine) is oxidized to a sulfenic acid by the peroxide substrate. The recycling of the sulfenic acid back to a thiol is what distinguishes the three Prx classes (Wood et al., 2003).

- TYPICAL 2-CYS PRXS (PRX 1-4): in the second step of the peroxidase reaction, the peroxidatic cysteine sulfenic acid is attacked by the resolving cysteine located in the C-terminus of another molecule of Prx forming an intermolecular disulfide bond. This intermediate product is then reduced by different oxidoreductases (mainly TRX).

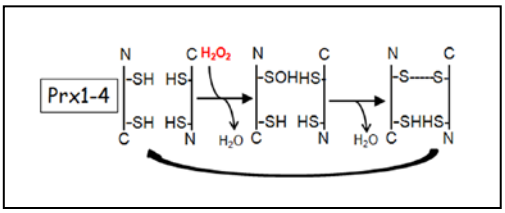

Illustration 15. Typical 2-cys PRX catalytic cycle

- ATYPICAL 2-CYS PRXS (PRX5): in this kind of Prxs, both the peroxidatic, and the resolving cysteines are located in the same molecule. Therefore, an intramolecular disulfide bond is formed before being recycled by an electron donor.

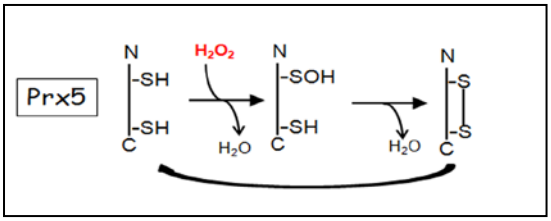

Illustration 16. Atypical 2-Cys PRX catalytic cycle

- 1-CYS PRXS (PRX6): They do not contain a resolving cysteine. Their cysteine sulfenic acid generated by the reaction with peroxides is reduced by a thiol-containing electron donor.

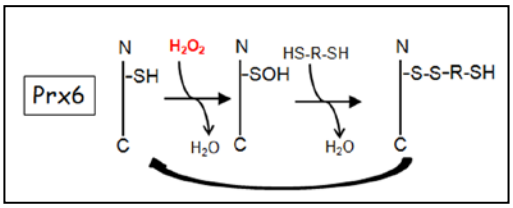

Illustration 17. 1-Cys PRX catalytic cycle

2. AIMS

2. AIMS

2.1 PROJECT OBJECTIVE

The general aim of the research presented in this thesis was to elucidate the redox-induced signaling responses of endothelial cells to laminar shear stress. We sought to increase our understanding on how H_2O_2 is produced by endothelial cells by fluid flow and what physiological role does it play in the accepted protective role of laminar shear stress on vascular function.

More specifically:

2.2 PROJECT AIMS

2.2.1 SPECIFIC AIM 1: IDENTIFICATION OF REACTIVE OXYGEN SPECIES (ROS) IN ENDOTHELIAL CELLS DURING THE EARLY RESPONSE PHASE OF LAMINAR SHEAR STRESS (LSS).

Hypothesis: LSS promotes the generation of controlled ROS production.

Experimental layout: To study ROS production during laminar flow, we used an *in vitro* shear system, the cone-and-plate viscometer and different approaches to specifically measure superoxide radical anion and hydrogen peroxide production.

2.2.2 SPECIFIC AIM 2: INVESTIGATE THE REDOX INDUCED SIGNALING RESPONSES MEDIATED BY LSS.

Hypothesis: LSS-induced ROS could act as important signaling molecules with regulatory function during laminar flow, mediating the activation of different signaling pathways.

Experimental layout: To study the redox induced signaling responses mediated by LSS, we focused our interest in those described in the literature known to be activated both by exogenous treatment of H_2O_2 and by laminar flow.

2.2.3 SPECIFIC AIM 3: IDENTIFICATION OF ENDOTHELIAL EARLY SENSORS OF H_2O_2 INDUCED BY LSS.

Hypothesis: Very few proteins are susceptible of oxidation by H_2O_2 in the range of endogenous cellular concentrations. A common feature among them is the existence of less a low-pKa cysteine residue in the form of thiolate at neutral pH. Since different kinetics studies have identified the antioxidant enzymes peroxiredoxins as the most favored H_2O_2 targets, they could play an important role in LSS signaling.

Experimental layout: To determine the involvement of the different PRX isoforms in LSS-induced signaling pathways, we examined their activation by the study of their oxidation state in response to LSS.

2.2.4 SPECIFIC AIM 4: IDENTIFICATION OF ENDOTHELIAL SOURCES OF ROS PRODUCTION.

Hypothesis: ROS generation during laminar flow may arise from the transient activation of NADPH oxidase isoforms, enzymes that do not produce ROS as a metabolic substrate but as their primary function.

Experimental layout: We studied the basal expression of the different NOXs isoforms in our model of endothelial cells and their implication in LSS-induced signaling pathways by different molecular knockdown or chemical inhibition approaches.

2.2.5 SPECIFIC AIM 4: STUDY OF MITOCHONDRIAL FUNCTION DURING LAMINAR FLOW.

Hypothesis: The mechanical force promoted by LSS is sensed by mitochondriae altering their functionality and metabolic behaviour.

Experimental layout: To establish the physiological importance of LSS on mitochondrial function, we examined mitochondrial morphology and bioernergetic profiles upon LSS stimulation.

2.2.6 SPECIFIC AIM 5: STUDY OF p38 MAPK AND eNOS SEQUENTIAL ACTIVATION IN A REDOX INDEPENDENT MANNER. ROLE OF PTEN IN THE RESPONSE TO ADP

Hypothesis: Aside from its role in mechanotransduction, LSS has been described to directly activate platelets inducing the release of different agonists which interact with endothelial receptors. Among these factors, extracellular nucleotides such as ADP have been defined as vasoactive substances able to interact through endothelial receptors and activate endothelial nitric oxide synthase (eNOS). This led us to investigate whether p38 MAPK might regulate eNOS activation mediated by ADP. Given the role of the redox sensitive phosphatase PTEN in crucial signaling pathways we sought to establish its participation in ADP-mediated endothelial responses.

Experimental layout: We studied the sequential activation of p38 MAPK and eNOS upon ADP stimulation and $NO^{\cdot}$ production after knocking down p38 MAPK by the use of different strategies. We then attempted to establish the potential interactions among PTEN, p38 MAPK and eNOS in the endothelial response to ADP.

3. EXPERIMENTAL PROCEDURES

3. EXPERIMENTAL PROCEDURES

3.1 ENDOTHELIAL CELLS

Cells were maintained in a standard incubator (37°C, 5% CO_2). Studies were all done after maintaining cells under starvation overnight.

PRIMARY CELLS

BOVINE AORTIC ENDOTHELIAL CELLS (BAEC): Aortas were obtained from an authorized slaughterhouse and transported to the laboratory in cold Phosphate Buffered Saline (PBS) supplemented with antibiotics (100 µg/ml penicillin, 100 U/ml streptomycin, and 50 µg/ml Fungizone). Aortas were cleaned from adipose and connective tissues, and stumps of intercostal vessels were tightly closed. After cleaning aortas with PBS, a sterile solution of 0.03% collagenase (Sigma) in Hank's Balanced Salt Solution (HBSS, Gibco) was dripped onto the luminal surface of the aorta and incubated at 37ºC for 15 minutes. Aortas were washed with RPMI medium supplemented with 10% Fetal Bovine Serum (FBS, Gibco) and the digest was centrifuged, resuspended in the same medium and grown on plates coated with 0.2% gelatin (Sigma) in PBS. BAEC were utilized at passages 3-7 and maintained in medium RPMI (Gibco), supplemented with 10% FBS and 1% penicillin-streptomycin (Gibco).

MOUSE LUNG ENDOTHELIAL CELLS (MLEC): MLEC were isolated from lungs of wild type and null mice 3-4 weeks-old. Animals were sacrificed by cervical dislocation, and lungs were collected in ice-cold HBSS. Lung tissue was minced and digested for 1 h at 37ºC in 0.1% collagenase type I (Sigma). The digest was passed through a blunt 19.5 gauge needle and filtered through a 70 µm cell strainer. Cells were plated into coated plates with MLEC medium containing 50% DMEM (Gibco), 50% F-12 (Invitrogen), 20% FBS, 10 mg/ml Heparin (Sigma), 2 mM L-glutamine (Gibco), 1% penicillin-streptomycin, 50 µg/ml Endothelial Cell Growth Factor (ECGF). Cells were subjected to negative and positive sorting with magnetic beads coated with CD16/CD32 or ICAM-2, to obtain a pure

population of endothelial cells. MLEC were characterized by their morphology as polygonal cells forming a tight-fitting monolayer as well as by positive immunofluorescent staining with an antibody against factor VIII (von Willebrand factor). MLEC were used at passages 2-4.

HUMAN UMBILICAL VEIN ENDOTHELIAL CELLS (HUVEC): The umbilical vein was carefully dilated with a cannula and one end of the cord was clamped with a hemostat. Using a syringe, a solution of 0.1% collagenase type I (Sigma) in HBSS was flushed through the vein. The cord was clamped on the other end with a second hemostat and collagenase solution was spread by inverting the cord 2-3 times. After incubation for 30 minutes at 37ºC, one end of the cord was opened and the digest effluent from the vein was collected into complete medium supplemented with serum. Detached endothelial cells were centrifuged, resuspended in Endothelial Basal Medium-2 (EBM-2, Lonza) supplemented with endothelial growth medium 2 (EGM-2) and grown on plates coated with 0.2% gelatin in PBS. HUVEC were used from passage 2-5.

MOUSE EMBRYONIC FIBROBLASTS (MEF): Mouse embryonic fibroblasts from p38 MAPK α were kindly provided by Drs. Angel Nebreda and Almudena Porras, and cultured in medium DMEM supplemented with 10% FBS and 1% penicillin-streptomycin.

3.2 SHEAR STRESS EXPERIMENTS

Endothelial cells were grown to confluent monolayers and two different methodologies were employed to investigate the effects of shear stress on the endothelium. Endothelial cells were exposed in both systems to physiologic levels of steady laminar shear stress (12 dyn/cm^2) along various times.

CONE-AND-PLATE SYSTEM: This is essentially a rotational viscometer. It consists of a stationary plate (60 mm tissue culture dish) coated with gelatin (0.2 % in PBS), and a rotating inverted cone in near contact with a lower plate. The cone is usually designed with an angle of less than 4°. Endothelial cells were grown to confluence and stimulated by rotating the cone unidirectionally into the culture medium to produce steady, laminar shear stress (LSS). The flow induced by the cone-and-plate model is well characterized. It was first described and applied to biological systems in the early 1980's (Dewey et al., 1981).

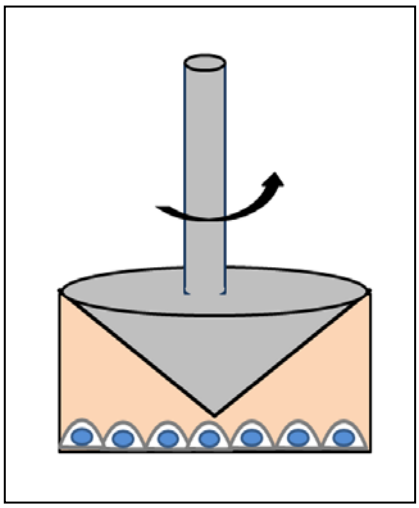

Illustration 18. Cone and plate system

This methodology has been chosen along this work to analyze shear stress effects on endothelium in protein activation or expression by immunoblot or qPCR techniques, or reactive oxygen species studies by flow cytrometry measurements

IBIDI PUMP SYSTEM: This is a perfusion system which consists of two different pieces: a portable fluidic unit (two syringes connected by a µ–slide were the endothelial cells are grown), and the pump. The pump generates a constant pressure which pumps de medium from one syringe to the other and back. Endothelial cells were cultured on the inner surface of µ-slide VI$^{0.4}$ and µ-slide I Luer, previously coated with 0.2% gelatin in PBS always taking care that the cells are just reaching confluence when starting a new experiment. The perfusion set on the fluidic unit was filled with 12 ml of equilibrated medium (without any slide). The level of both reservoirs was equilibrated at around 5 ml each after removing all air from the tubes for at least a couple of hours before starting the flow experiment. To get out the air bubbles from the tubes a flow cycle without any slide was begun. Once no bubbles were present along the system, the slide was adapted.

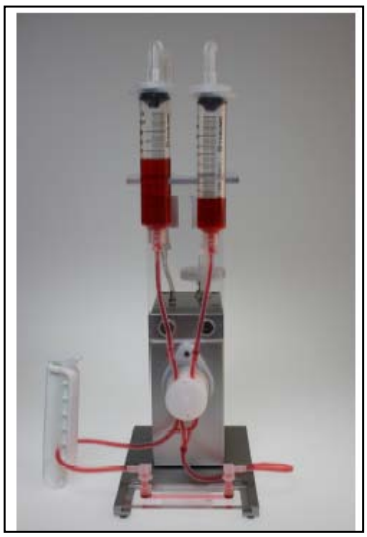

Illustration 19. Ibidi pump system

The Ibidi pump system was used for immunofluorescence protocols and for analyzing the shear stress response with live cell imaging.

3.3 HYDROGEN PEROXIDE AND SUPEROXIDE ANION MEASUREMENTS. REACTIVE OXYGEN SPECIES DETECTION.

SUPEROXIDE RADICAL ANION DETECTION ($O_2^{-\cdot}$).

After exposure to either static or laminar flow conditions endothelial cells were incubated for 20 minutes at 37ºC in humidified air and 5% CO_2 with 5 µM DHE or Mitosox probes (Invitrogen). After incubation, ROS production was analyzed by flow cytometry using an FL3 channel. DHE fluorescence was also analyzed by fluorescence microscopy. After exposure to either static or laminar flow conditions, endothelial cells were incubated with 2 µM DHE and fixed for 15 minutes with 3% paraformaldehyde in PBS. The fluorescence intensity of each experiment was expressed in arbitrary units and calculated by measuring the intensity of at least 50 cells per condition with a fluorescent microscope Nikon Eclipse T2000U (Nikon, Amstelveen, The Netherlands).

Aconitase is a member of [4Fe-4S] containing (de)-hydratases particularly susceptible to be inactivated by $O_2^{-\cdot}$. To determine aconitase activity cells were grown in 60 mm-diameter culture dishes and exposed to different time of LSS. After treatment, cells were rinsed with PBS and scraped in ice-cold PBS. Cells were centrifuged for 5 min at 1500 rpm and resuspended in lysis buffer (50 mM Tris-HCl, 2 mM sodium citrate and 0.6 mM MnCl2, pH 7.4) and lysates were frozen at -80ºC. On the day of processing they were defrost and centrifuged for 20 seconds at 14000 rpm. 30-50 µg of lysate were diluted into 50 nM Tris-HCl, 5 mM sodium citrate, 0.6 mM $MnCl_2$, 0.2 mM NADPH+, 2U isocitrate dehydrogenase and then aconitase activity was determined spectrophotometrically at 340 nM by monitoring NADPH formation.

HYDROGEN PEROXIDE DETECTION (H_2O_2)

Endothelial cells were transfected with the cytosol-targeted *HyPer* vector (Hyper-cyto, Evrogen) and exposed to laminar shear stress. Fluorescence was measured using an Axiovert200 (Zeiss) microscope. Image intensities were quantified using Metamorph and ImageJ software.

Vector type	*Mammalian expression vector*
Reporter	HyPer
Reporter codon usage	mammalian /E. coli
Promoter for Hyper	$P_{CMV\ IE}$
Host cells	mammalian
Selection	prokaryotic- kanamycin eukaryotic- neomycin
Replication	prokaryotic - pUC ori eukaryotic - SV40 ori

Table 5. HyPer vector characteristics.

Intracellular H_2O_2 production was also measured via extracellular leakage of H_2O_2 from endothelial cells using peroxide-linked Amplex Red fluorescence assay. Cells were exposed to either static or shear stress conditions and after treatment they were incubated with 5 µM Amplex red reagent (Molecular Probes) and 0.1 U/ml horseradish peroxidase (HRP) for 30 minutes. Supernatant fluorescence was detected via plate reader at excitation and emission of 571 nm and 585 nm, respectively. H_2O_2 production was estimated using a standard curve.

3.4 ENZYMATIC GENERATION OF HYDROGEN PEROXIDE FLUXES. HYDROGEN PEROXIDE AND GLUCOSE/GLUCOSE OXIDASE TREATMENTS

To generate a continuous flux of H_2O_2, endothelial cells were cultured in Dulbecco´s PBS buffer supplemented with 5.6 mM glucose and 1 mM L-arginine. Different quantities of glucose oxidase (GO) were added to the extracellular medium. The rate of H_2O_2 production by GO was previously calculated spectrophotometrically using the coupled reaction with HRP and 2,2′-Azino-bis(3-

ethylbenzothiazoline-6-sulfonic acid) diammonium salt (ABTS) as substrate (ε 415 nm = 3.6 x 10^4 $M^{-1}cm^{-1}$) in the same buffer used for cell assays, covering a wide range of known concentrations of GO.

$$Glucose + O_2 \xrightarrow{GO} Gluconic\ acid + H_2O_2$$

$$H_2O_2 + HRP \longrightarrow Compound\ I + H_2O$$

$$Compound\ I + ABTS \longrightarrow ABTS^{\bullet} + Compound\ II$$

$$Compound\ II + ABTS \longrightarrow ABTS^{\bullet} + HRP$$

The protocol was as follows:

1. The calibration solution was prepared and warmed at 37ºC (Dulbecco´s PBS buffer and supplemented with 5.6 mM glucose and 1 mM L-arginine, 20 µg/ml HRP and 50 µM ABTS).
2. Desired concentrations of GO were prepared in the calibration solution.
3. The absorbance of the mixture was measured at 415 nM using a spectrophotometer for 20-30 minutes.
4. H_2O_2 flux generated by each amount of GO was determined taking into account the slopes of its kinetic reaction (Absorbance vs time), ABTS ε (ABTS ε 415 nm = 3.6 x 10^4 $M^{-1}cm^{-1}$) and the fact that 1 single molecule of hydrogen peroxide per two of ABTS* is produced.

After incubation at 37ºC, cells were scraped and hydrogen peroxides fluxes were followed by western blot.

3.5 CHEMILUMINESCENCE ANALYSIS OF NO· PRODUCTION

The chemiluminescence method detects NO and its oxidation products nitrite (NO_2^-) and nitrate (NO_3^-) in liquid culture medium. 100µL aliquots of the supernatants just before and after different treatments were aspirated into a Hamilton syringe and injected through an air-tight septum into a purge vessel (A) containing a reaction mixture, consisting of 45mM potassium iodide (KI) and 10

mM iodine (I_2) in glacial acetic acid kept at 60ºC and continuously bubbled with nitrogen. Under these conditions NO_2^- and NO_3^- are converted to NO. The sample/carrier gas mixture was passed first through a cooled water jacket (B), bubbles through 1M NaOH (C), followed by passage through an inline filter (D) to prevent acid vapors form reaching the NOA reaction, and is carried toward the NO analyzer (Sievers NOA, Model 280, Boulder, CO) (E). NO gas combines with ozone to produce the excited state NO_2^*, which upon decay emits light that passes though a red filter (F) and is detected at 600 nm by a photomultiplier tube inside the NOA. The emitted light is recorded with the instrument software.

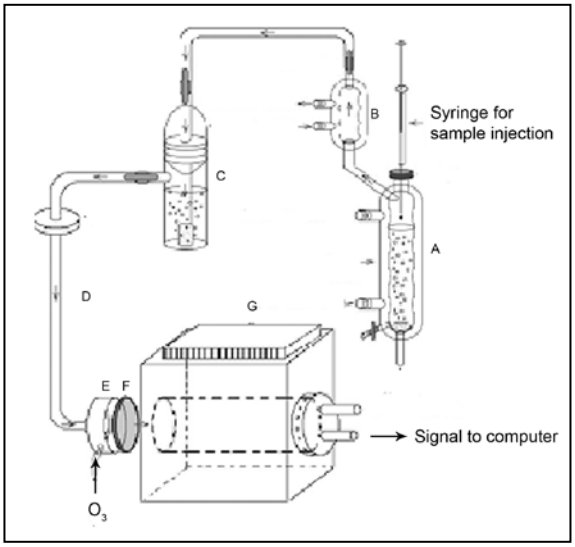

Illustration 20. Analysis of samples by chemiluminiscence Adapted from (Hart et al., 2005).

3.6 SMALL INTERFERING RNA (siRNA)

siRNA transfection assay was performed to down regulate particular genes of interest. We designed small interfering RNA duplex oligonucleotides targeting constructs for the specific knock down of the proteins of our interest. Constructs were purchased from Ambion. Using opti-MEM, lipofectamine 2000 (Invitrogen) and siRNA were diluted separately for 5 minutes, and combined incubating the mix for 25 minutes at room temperature. Endothelial cells were transfected with 30-40 nM siRNA at a confluence around 80%. After 5 hours of transfection, the medium was removed, and replaced by culture medium supplemented with 10% FBS and 1% penicillin-streptomycin. Then they were incubated for 24 or 48 hours in at 37ºC.

The following sense oligonucleotides were used:

Protein	*Sequence*
Akt	5′-GGACGUGUACGAGAAGAAGdTdT-3
NOX4	5’-ACUGAGGUACAGCUGAAUGtt-3’
PTEN	5′- GUAUAGAGCGUGCAGAUAAtt-3´
p38α MAPK	5’-GGUCUCUGGAGGAAUUCAAtt-3’

Table 6. Small interfering RNA sequences.

3.7 RNA EXPRESSION AND RT-PCR

Endothelial cells were washed with PBS and processed for RNA isolation by guanidinium thiocyanate–phenol-chloroform extraction. cDNA was synthesized using an iScript cDNA synthesis kit and mRNA expression was determined by SYBR green-based real-time quantitative PCR reactions. Relative mRNA expression was determined using the GAPDH gene as a housekeeping.

Gene	*Species*	*Sequence (5’ to 3’)*
NOX1	Bovine	F: GCACAAGCATGGCTTCAGTA R: CTGGCGAATACTGCTGTTCA
NOX2	Bovine	F: TGCCTGTCTGtCGAAATCTG R: GCATTCACACACCACTCCAC
NOX4	Bovine	F: CCCTTTGGAAGTCCATTTGA R: TCCAGTCATCCAGCAGAGTG
Glyceraldehyde 3-phosphate dehydrogenase (GAPDH)	Human	F: GCCTGGTCACCAGGGCTGC R: CTCGCTCCTGGAAGATGGTGATGG

Table 7. Primer pairs used for quantitative real-time PCR.

3.8 WESTERN BLOT ANALYSIS

Western blot analysis, here also termed protein blotting or immunoblotting, is a common technique used to identify proteins based on their ability to bind to specific antibodies.

PREPARATION OF CELL LYSATES

WHOLE CELL LYSATE: following experimental treatment, cells were washed once with PBS and lysed with 100-150 µL RIPA lysis buffer [50 mM Tris-HCl, pH 7.4, 150 mM NaCl, 1% Nonidet P-40, 0.25% sodium deoxycholate, 1 mM EDTA, 2 mM Na_3VO_4, 1 mM NaF and protease inhibitor cocktail tablets (Roche, following the instructions provided by the supplier)] using a plastic cell scraper. Lysates were further homogenized by passing cells through an insulin syringe before centrifuging them at 4º for 20 minutes at 12800 rpm. The supernatant was collected and protein content was determined by the bicinchoninic protein assay kit (BCA) assay using bovine serum albumin (BSA) as a protein standard. Samples were mixed with Laemmeli buffer and boiled for 10 minutes at 100ºC prior to use.

SUBCELLULAR FRACTIONATION: following experimental treatment, cells were washed once with PBS, trypsinized and resuspended in buffer A (150 mM KCl, 25 mM Tris-HCl, 2 mM EDTA, 0.1% BSA, 10 mM K-phosphate, 0,1 mM $MgCl_2$, pH 7.4). Samples were treated with digitonine for 1 min, and centrifuged for 1 min at 6000rpm. The resulting pellet is an enriched mitochondrial fraction, while the supernatant is a soluble cytosolic fraction. Both fractions were resuspended and diluted respectively in RIPA lysis buffer buffer (50 mM Tris-HCl, pH 7.4, 150 mM NaCl, 1% Nonidet P-40, 0.25% sodium deoxycholate, 1 mM EDTA, 2 mM Na_3VO_4, 1 mM NaF and protease inhibitor cocktail tablets from Roche). Lysates were further homogenized by passing cells through an insulin syringe before centrifuging them at 4º for 20 minutes at 12800 rpm. The supernatant was collected and protein content was determined by BCA assay using BSA as a protein standard.

SDS-PAGE ELECTROPHORESIS

Aliquots of cell lysate (20-50 µg of protein) were mixed with Laemmli buffer with β-mercaptoethanol and boiled for 10 minutes at 100ºC prior to use. In non-reducing conditions β-mercaptoethanol was not added. Equal amounts of protein were loaded on SDS polyacrylamide gels (from 7.5 to 15% acrylamide) and separated using the Mini-PROTEAN 3 electrophoresis module (Bio-Rad). The molecular weight of proteins was determined by comparison with the pre-stained protein marker (Precision Plus Protein Dual Color, Bio-Rad).

Reagents (ml)	*Resolving gel % Acrylamide*			
	7.5	***10***	***12***	***15***
H_2O	5.43	4.8	4.3	3.55
40% Acrylamide	1.875	2.5	3	3.75
1.5 M Tris (pH 8.8)	2.5	2.5	2.5	2.5
10% SDS	0.1	0.1	0.1	0.1
10% Ammonium persulfate	0.1	0.1	0.1	0.1
TEMED	0.006	0.006	0.006	0.006

Reagents (ml)	*Stacking gel*
H_2O	7.25
40% Acrylamide	1.25
1.5 M Tris (pH 8.8)	1.25
10% SDS	0.1
10% Ammonium persulfate	0.1
TEMED	0.01

Table 8. SDS-Polyacrylamide gel recipes.

ELECTROBLOTTING

After protein separation by SDS-PAGE, proteins were transferred to a nitrocellulose membrane (Whatman) by electroblotting. The protein transfer can be achieved either by placing the gel-membrane sandwich between Whatman paper in transfer buffer (semi-dry transfer) or by complete immersion of a gel-membrane sandwich in a buffer (wet transfer). In this work semi-dry transfer was used for proteins with molecular masses of ≤100 kDa.

SPECIFIC PROTEIN STAINING

After electroblotting, unspecific protein binding sites were blocked by incubating the membrane in 3% non-fat milk or BSA in Tris Buffered Saline (TBS)-Tween for 1 hour at room temperature. The membranes were then probed with primary antibodies at room temperature for a couple of hours or overnight at 4ºC (*Table 9*). Membranes were washed with TBS-Tween for three times (5 minutes each) and then incubated with the secondary antibody for 1 hour at room temperature. After three additional washing steps, proteins were visualized by means of the Li-Cor Odyssey Infrared Imaging System.

Antigen	*Description*	*Specie*	*Provider*	*Catalog n.*	*Dilution*	*Conditions*
Akt	Polyclonal antibody	Rabbit	Cell signaling	9272	(1:1000)	4ºC ON
phospho-Akt (Ser 473)	Polyclonal antibody	Rabbit	Cell signaling	9271	(1:1000)	4ºC ON
β-actin	Monoclonal ntibody	Mouse	Sigma	A1978	(1:15000)	RT 1h
C-myc (E9)			Santa Cruz Biotech	sc-40		RT 1h
CuZnSOD	Polyclonal antibody	Rabbit	Santa Cruz Biotech	sc11407	(1:2000)	RT 1h
DLP1		Mouse	BD Transd. Lab	611116	(1:1000)	4ºC ON
phospho-DRP1 (Ser616)	Polyclonal antibody	Rabbit	Cell signaling	3455	(1:1000)	4ºC ON
phospho-DRP1 (Ser637)	Polyclonal antibody	Rabbit	Cell signaling	4867	(1:1000)	4ºC ON
eNOS	Monoclonal antibody	Mouse	BD Transd Lab	610297	(1:1000)	RT 1h
phospho eNOS (Ser1177)	Polyclonal antibody	Rabbit	Cell signaling	9571	(1:1000)	4ºC ON
phospho eNOS (Ser633)	Polyclonal antibody	Rabbit	Cell signaling	612664	(1:1000)	4ºC ON
phospho eNOS (Thr495)	Polyclonal antibody	Rabbit	Cell signaling	9574	(1:1000)	4ºC ON
GST	Monoclonal antibody	Mouse	GenScript			RT 1h
MnSOD	Monoclonal antibody	Rabbit	Assay design	SOD-110	(1:2000)	RT 1h
p38 MAPK	Polyclonal antibody	Rabbit	Cell signaling	9212	(1:1000)	4ºC ON

phospho p38 MAPK (Thr 180/Tyr 182)	Polyclonal antibody	Rabbit	Cell signaling	9215	(1:1000)	4ºC ON
phospho p38 MAPK (Thr 180/Tyr 182)	Monoclonal antibody	Mouse	Cell signaling	9212	(1:1000)	4ºC ON
p44/42 MAPK	Polyclonal antibody	Rabbit	Cell signaling	137F5	(1:1000)	4ºC ON
phospho p44/42 MAPK (Thr 202/Tyr 204)	Polyclonal antibody	Rabbit	Cell signaling	9101	(1:1000)	4ºC ON
peroxiredoxin 1	Polyclonal antibody	Rabbit	Ab frontier	LF_PA0095	(1:2000)	4ºC ON
peroxiredoxin 2	Polyclonal antibody	Rabbit	Ab frontier	LF_PA0007	(1:2000)	4ºC ON
peroxiredoxin 3	Polyclonal antibody	Rabbit	Ab frontier	LF-PA0030	(1:2000)	4ºC ON
peroxiredoxin 4	Polyclonal antibody	Rabbit	Ab frontier	LF-PA0009	(1:2000)	4ºC ON
peroxiredoxin 5	Polyclonal antibody	Rabbit	Ab frontier	LF-PA0210	(1:2000)	4ºC ON
peroxiredoxin 6	Polyclonal antibody	Rabbit	Ab frontier	LF-PA0211	(1:2000)	4ºC ON
peroxiredoxin SO3	Polyclonal antibody	Rabbit	Ab frontier	LF-PA0004	(1:2000)	4ºC ON
phospho mlc2	Polyclonal antibody	Rabbit	Cell signaling	3674	(1:1000)	4ºC ON
PTEN	Polyclonal antibody	Rabbit	Cell signaling	9552	(1:1000)	4ºC ON
phospho PTEN (Ser 380/Thr 382/383)	Polyclonal antibody	Rabbit	Cell signaling	9552	(1:1000)	4ºC ON

Table 9. Antibodies used for immunoblotting staining.

3.9 MEASUREMENT OF MITOCHONDRIAL MEMBRANE POTENTIAL (Ψ_M)

Different fluorescent probes derives from rhodamine can be used to measure mitochondrial membrane potential, including tetramethylrhodamine methyl ester (TMRM) and tetramethylrhodamine ethyl ester (TMRE). Those indicator dyes are lipophilic cations accumulated by mitochondriae in proportion to Δψ. In this work after exposure to either static or laminar flow conditions, endothelial cells were incubated with 0.5 μM TMRM in the culture medium for 10 minutes at 37ºC. Upon incubation, this cell-permeant, cationic, fluorescent dye is sequestered by viable mitochondria exhibiting a red shift in both its absorption and fluorescence emission spectra.

Cells were washed twice with PBS, trypsinized and centrifuged for 5 minutes at 1200 rpm. Pellets were resuspended in PBS and were kept in-ice until they were analyzed by flow cytometry with Becton Dickinson FACSCanto II flow cytometer. Excitation was performed at 532 nm, and emission was detected at 575 nm. Dissipation of ψ_m causes TMRM to leak out of mitochondria into the cytosol where TMRM became unquenched. FCCP, which dissipates the membrane potential, was used as control.

3.10 MEASUREMENT OF MITOCHONDRIAL OXYGEN CONSUMPTION USING A CLARK ELECTRODE

Illustration 21. Oxygen electrode unit

After experimental treatments, endothelial cells were washed twice with PBS, trypsinized and counted before being centrifuged for 5 minutes at 1200 rpm. Pellets were resuspended in growth medium just before injecting the sample in the electrode. The Clark type electrode uses a silver/platinum-electrode immersed in an electrolyte solution. An oxygen-permeable membrane, which encloses the electrode, enables the measurement of oxygen exchange between the sample and the electrolyte solution. When the platinum electrode is polarized at - 0.6V with respect to the silver electrode, every oxygen molecule that reaches its surface from the sample, via the gas permeable membrane, is reduced to water through thefollowing reaction:

At the cathode:

$$O_2 + 2H_2O + 4e^- \longrightarrow 4OH^-$$

For each reduction there must be an oxidation, and this occurs at the silver anode as follows:

At the anode:

$$4Ag^+ + 4Cl^- \longrightarrow 4AgCl + 4e^-$$

3.11 MEASUREMENT OF MITOCHONDRIAL OXYGEN CONSUMPTION USING A SEAHORSE EQUIPMENT

One day before the experiment, XF24 tissue plates were coated with BD bioscences Cell-Tak ™ Cell Adhesive using a density of 3.5 µg/cm^2 in 0.1 M $NaHCO_3$ making sure that the final pH was between 6.5 and 8.0. This reagent was left at room temperature for 20-30 minutes, and after removing the remaining solution it was rinsed in sterile water to remove bicarbonate. Plates were dried and stored at 4ºC overnight.

Protocol:

1. The day of the experiment , cells were exposed to shear stress, tripsinized and plated in XF24 tissue culture plates previously coated with Cell-Tak TM cell Adhesive warmed up for 20 minutes at room temperature.
2. 100 µl of cell suspension (100000 cells) were seeded in each well and plates were centrifuged slowly stopping as it reached 450 rpm without braking.
3. The orientation of the plates was reversed, they were then centrifuged up to 650 rpm and stopped again with no braking.
4. Plates were transferred to a 37ºC incubator without CO_2 for 25 minutes.
5. After incubation, 400 µl of fresh medium without bicarbonate was added to each well and returned to the incubator for 15 minutes before proceeding with XF assay protocol.
6. All wells were injected sequentially with 2 µM oligomycin, 0.6 µM FCCP, 0.4 µM FCCP and 1 µM antimycin A plus 1 µM rotenone to obtain different respiratory parameters.

3.12 BLUE NATIVE ELECTROPHORESIS

Experiments were conducted in EC permeabilized by digitonine. Briefly, cells were exposed to different time points of LSS and collected after trypzinization. Cells were washed twice with PBS, and pellets (1 million cells approximately) were resuspended in 8 mg/ml digitonine in PBS for 10 minutes in ice. Samples were centrifuged for 5 minutes at 10000 g and pellets were resuspended in 1.5 M aminocaproic acid, 50 mM Bis-Tris/HCl pH 7 and 10% digitonine for 5 min in ice.

Samples were centrifuged once again at maximum speed for 30 min at 4ºC and digitonin-solubilized mitochondrial protein was run through Blue Native (BN) gradient gels (8% to 16%) at 4ºC. After electrophoresis, the gels were electroblotted onto polyvinylidene difluoride (PVDF) membranes and sequentially probed with specific antibodies. The site of the observed oligomeric conformations was determined by their relative migration compared with OXPHOX complex II (70 kDa).

Reagents (ml)	*Resolving gel* *8%*	*(gradient gel)* *16%*	*Stacking gel*
AB (48:1.5)	0,8	1,6	0,6
Gel buffer 3X	1,6	1,6	2
H_2O	2,6	0,8	3,4
Glicerol	-	1	-
10% Ammonium persulfate	0,03	0,012	0,055
TEMED	0,003	0,0012	0.001

Table 10. Native polyacrylamide gel.

AB (48:1.5): Acrilamide 48%; Bis-Acrilamide 1.5%

Gel buffer 3X: Tris 3M, 0.3% SDS, pH 8.45

Cathode buffer: Tricine 50 mM, 0.02% G-250, Bis-Tris 15 mM pH 7,0

Anode buffer: Bis-Tris 150 mM, aminocaproic acid 1.5 M, pH 7,0

3.13 IMMUNOFLUORESCENCE. CONFOCAL FLUORESCENCE MICROSCOPY

Following experimental treatment endothelial cells were washed once with PBS, fixed with 2% paraformaldehyde in PBS and permeabilized in 0.025% Triton-X 100. Prior to antibody incubation, cells were blocked with 3% bovine serum albumin (BSA) or 10% goat serum. Primary antibody in 3% BSA was applied overnight at 4ºC. Cells were washed twice with PBS, and incubated with secondary antibody conjugated to Alexa Fluor 488, 568 or 647 (Molecular Probes) for 1 hour at room temperature. For staining of F-actin, Alexa Fluor 488 phalloidin was incubated together with the secondary antibody. Nuclei were labeled with DAPI (1 µg/ml) in PBS for 5 minutes at room temperature after removing excess secondary antibody twice with PBS. To identify mitochondria, before fixing the cells, they were incubated with 400 nM of Mitotracker Red Deep (Molecular Probes) in growth medium for 20 minutes at 37ºC prior fixation. Cells were mounted on slides, which were examined using an Olympus DSU microscope; images were analyzed using Metamorph software.

Antigen	*Description*	*Species*	*Provider*	*Catalog n.*	*Dilution*	*Conditions*
DLP1	Polyclonal antibody	Mouse	BD Transduc Lab	611112	(1:100)	4ºC ON
Peroxiredoxin 3	Polyclonal antibody	Rabbit	Ab Frontier	LF-PA0030	(1:200)	4ºC ON
Vinculin	Monoclonal antibody	Mouse	Sigma		(1:400)	4ºC ON
Phalloidin	Monoclonal antibody				(1:200)	RT 1h

Table 11. Antibodies used for immunofluorescence staining.

3.14 FLUORESCENT RESONANCE ENERGY TRANSFER (FRET) MEASUREMENT

Monitoring of PIP_3 production and Rac1 activation were performed by the use of specific FRET probes, as described in detail (Aoki et al., 2008). Briefly, the FRET probe for PIP3 consists of CFP, the PIP_3 binding domain and YFP sequences.

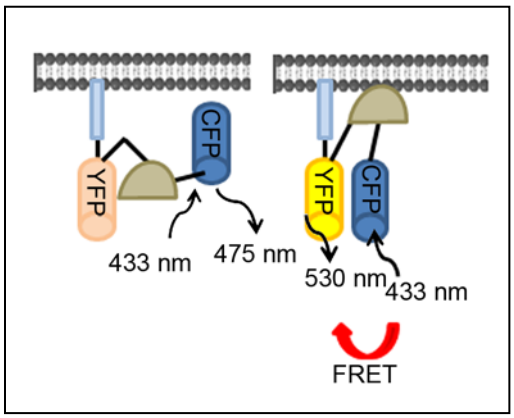

The absence of PIP_3 in the plasma membrane is associated with a large distance between CFP and YFP. When PIP_3 accumulates in the plasma membrane, the probe binds tightly to the latter via PIP_3, resulting in an increase in FRET efficiency.

Illustration 22. Structure of FRET probe for PIP_3

In the case of the Rac1 FRET probe, the increase in FRET efficiency correlates with an activation of the small GTPase Rac1. BAEC were transfected with duplex siRNA targeting constructs specify along with the PIP_3 or Rac1 biosensor plasmids. 48 hours after transfection cells were imaged with an Olympus DSU microscope. Agonists were added after 5 min, and fluorescence images were taken every minute for 1 hour following agonist addition. Analysis was performed using MetaMorph software (Universal Imaging, Downingtown, PA).

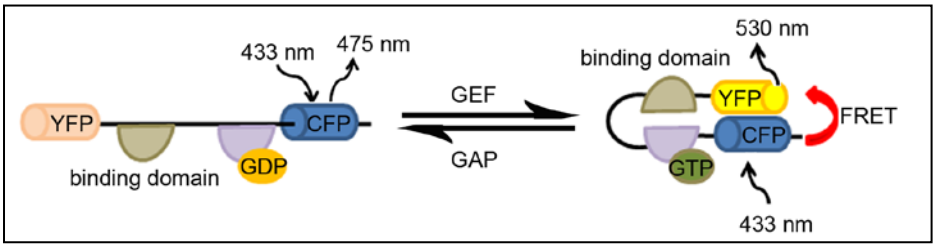

Illustration 23. Structure for FRET probe for Rac1

3.15 MEASUREMENT OF eNOS ACTIVITY. ARGININE-CITRULLINE CONVERSION ASSAY.

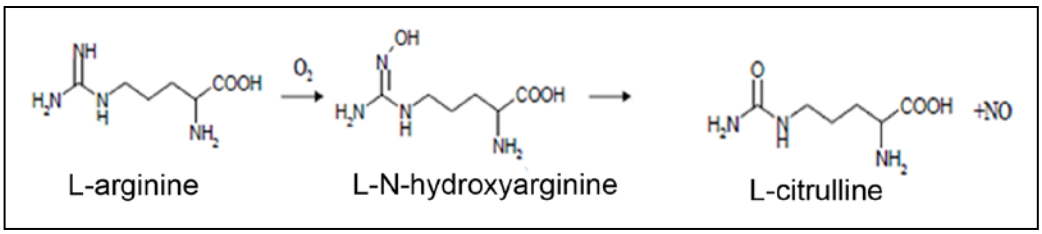

Illustration 24. ***$NO^{\cdot}$ is produced during the conversion of L-arginine to L-citrulline by eNOS***

This assay detects the conversion of radio-labelled [^{3}H]L-arginine to radio-labelled [^{3}H]L-citrulline. Since L-arginine conversion leads to equimolar amounts of NO as well as L-citrulline, the amount of [^{3}H]L-citrulline can be used indirectly as a parameter reflecting NO production. Briefly, the reaction was initiated in cultured BAEC by adding L-[^{3}H]arginine (10 µCi/ml, diluted with unlabeled L-arginine to give a final concentration of 10 µM) plus sufficient amounts of eNOS cofactors FAD, FMN, NADPH, Ca^{2+} CaM and BH_4. Following incubation at 37ºC for 20 minutes, cells were washed with ice-cold PBS and scraped into 2 ml of solution containing 20 mM sodium acetate, 1 mM L-citrulline, 2 mM EDTA, and 2 mM EGTA, pH 5.5, followed by sonication. An aliquot was withdrawn for total protein determination and cellular ^{3}H incorporation, and the remaining sample was applied into a Dowex 50W-X8 400 column to separate [^{3}H]L-citrulline. The flow-through fraction was analyzed by liquid scintillation counting. [^{3}H]L-citrulline formation in the cells is expressed as pmol of [^{3}H]L-citrulline produced / mg of cellular protein / min. Each treatment was performed in triplicate cultures, which were analyzed in duplicate. The detection limit of the arginine-citrulline conversion

assay is in the picomolar range. The basal eNOS activity in these experiments ranged from 0.3 to 0.7 pmol/mg protein/min.

3.16 SCRATCH CELL MIGRATION ASSAY

BAEC were transfected with siRNA-targeting constructs and grown for 24 h to confluence. Cells were trypsinized and added to each chamber of a 8-well cell culture chamber slide (IBIDI, Munich, Germany) allowing it to adhere for 24 h in Dulbecco's modified Eagle's medium with 10% FBS. A linear scratch or wound was made in the confluent cell monolayer with a sterile pipette tip. Cells were washed twice with PBS to remove detached cells and floating cellular debris and maintained with RPMI medium supplemented with 10% FBS. Wound closure was serially recorded using a 10X DIC objective with an inverted Olympus DSU microscope, starting immediately at 0 hours and up to 30 hours after scratch incision. The percentage wound recovery was represented as a function of time.

3.17 PHOSPHOINOSITIDES EXTRACTION

Phosphoinositides are an important component of the cell as they have a variety of roles such as cytoskeleton regulation, generation of second messengers, endosome trafficking, membrane transport, regulation of ion channels, pumps, endocytic and exocytic processes cell survival and replication. Different approaches have been described to isolate lipids in the cells. In this work we have chosen a non-detergent methodology to isolate PIP_3 based on sodium carbonate pH extraction and carbonate resistance. Briefly, after treatment, cells were scraped into 0.3 ml of 0.5 M sodium carbonate, pH 11 and homogenized in a Dounce homogenizer followed by sonication to improve cell disruption. Triplicate 50 µl aliquots were spotted onto a nitrocellulose membrane and dried; the membranes were washed twice with PBS-5% Tween, blocked with PBS-3% BSA for 1 hour at room temperature, incubated with the GST-tagged "PIP_3-Grip" antibody, rinsed extensively, and detected using the GST antibody.

3.18 IMAGE PROCESSING

All image processing was performed with the program ImageJ 1.42 (http://rsb.info.nih.gov/ij).

3.19 STATISTICAL ANALYSIS

Bar graph data are expressed as means ± SEM. For all quantitative data collected, statistical analysis was assessed by an independent *t* test or appropiate non-parametric tests of at least three experiments. The GraphPad Prism software version 5 was used. In experiments involving multiple comparisons, ANOVA was used; a p value of less than 0.05 was considered statistically significant.

4. RESULTS

4. RESULTS

4.1 CRITICAL ROLE OF HYDROGEN PEROXIDE SIGNALING IN THE SEQUENTIAL ACTIVATION OF p38 MAPK AND eNOS IN LAMINAR SHEAR STRESS

4.1.1 LAMINAR SHEAR STRESS INDUCES THE GENERATION OF ROS.

Laminar shear stress (LSS) is a protective hemodynamic regulator of endothelial function and limits the development of atherosclerosis and other vascular wall diseases related to pathophysiological generation of reactive oxygen species. Among the physiological roles of the endothelial cells located in the inner wall of the vascular tree is the transduction of mechanical forces of shear stress into specific biochemical signals (Balligand et al., 2009). Shear stress is associated with the generation of oxidative stress, and our aim was to study the redox-induced signaling responses at early times of laminar shear stress. We first determined the generation of ROS in endothelial cells subjected to physiological conditions of fluid flow. For this purpose we plated endothelial cells until confluence conditions and LSS was simulated *in vitro* by the well-characterized system cone-and-plate model. In these studies, static conditions (cells cultures under no shear stress), were examined as a control of shear stress exposure. First, we detected $O_2^{-\cdot}$ generation by the use of the redox sensitive probe dihydroethidium (DHE) (Navarro-Antolin et al., 2001). As shown in *Figure 1*, LSS induces an increase in superoxide production as it was determined by fluorescence microscopy, with an increase detected as early 5 minutes of shear stress induction and maintained after 1h. DHE oxidation was also determined by flow cytometry in reaching 31.7 ± 6.25 % higher levels compared to static cells after 1 hour shear stress (*Figure 1*).

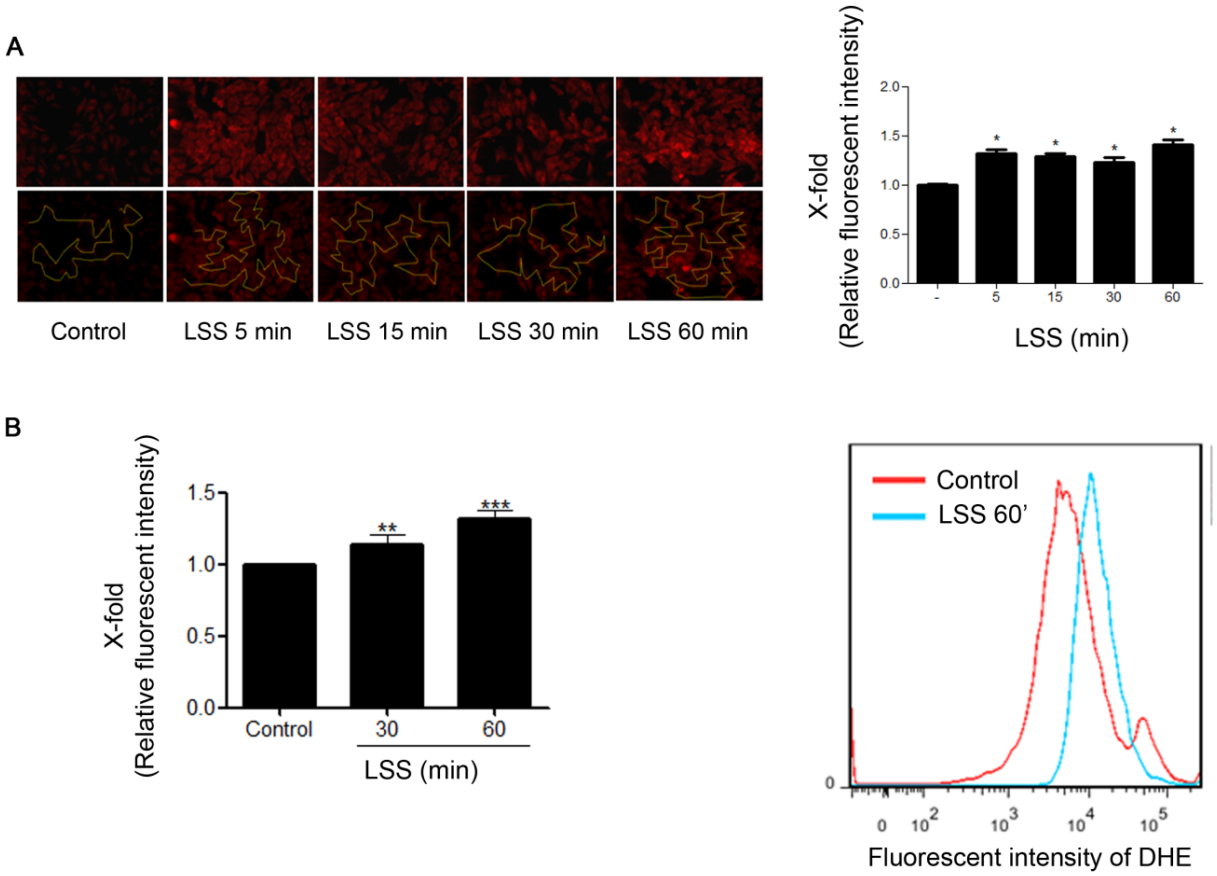

Figure 1. Laminar shear stress increases superoxide radical anion production. *A) DHE fluorescence was analyzed after the indicated times of LSS. Images are duplicated and the lower photographs were used to quantify individual fluorescence of at least 50 cells per time point. Traces join cells randomly selected for quantification. Bar graph represents mean ± SEM of 4 fields, each accounting for the quantification of the individual fluorescence of at least 50 cells. B) BAECs were exposed to LSS and superoxide radical formation was analyzed by flow cytometry in FL3 channel with DHE. A representative histogram is presented in the right panel. *p<0.05, **p<0.01 and ***p<0.0001 vs control.*

Because DHE analysis is not specific for superoxide radical anion (Benov et al., 1998, Fink et al., 2004, Zhao et al., 2003), we used an indirect methodology based on the superoxide chemical reactivity. $O_2^{\cdot -}$ is a very unstable ROS free radical that as a negative charged molecule is unable to diffuse through biological membranes, thus rendering it a poor signalling molecule. Proteins that can react rapidly enough with this ROS include iron-sulfur proteins, and their inactivation is considered as a consequence of superoxide content in cells (Liochev and Fridovich, 1999). Aconitase is a member of [4Fe-4S]

containing enzymes that catalyzes the interconversion of citrate to isocitrate. Superoxide inactivates aconitase due to oxidation followed by reversible loss of Fe from its [4Fe–4S] cluster. The activity of the enzyme can be monitored by following the production of NADPH spectrophotometrically at 340 nm (Tarpey et al., 2004). Thus superoxide concentrations can be estimated by the degree of enzyme inactivation. LSS induced an abrogation of the enzymatic activity of aconitase (***Figure 2***), hence supporting an increase of superoxide radical anion production, in consistence with the results using flow cytometry.

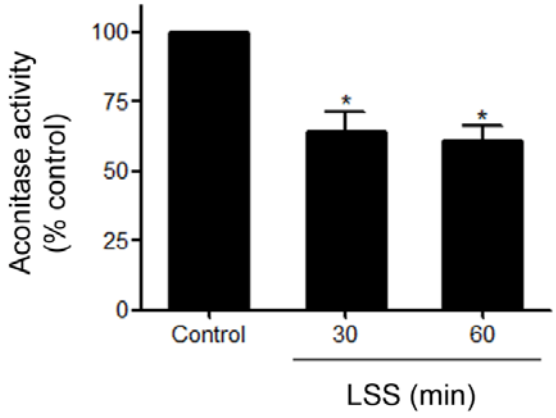

Figure 2. Laminar shear stress decrease aconitase activity. Indirect measurement of superoxide radical anion production. *Aconitase activity was measured by a coupled assay in which the formation of NADPH was followed at 340 nm using isocitrate as a substrate. Bars represent means ± SEM of n=3. *p<0.05, vs control.*

Due to the fact that H_2O_2 represents a much widely accepted ROS able to trigger specific cellular signaling we sought to study its relevance in shear stress responses. Dismutation of $O_2^{-\cdot}$ into H_2O_2 occurs either spontaneoulys or catalyzed by superoxide dismutase and thus concomitant generation of H_2O_2 under LSS can be expected. Due to its high diffusibility, we attempt to detect H_2O_2 generation in both intracellular and extracellular compartments. To detect intracellular H_2O_2 production, we used the H_2O_2 biosensor HyPer (Hyper-cito, Evrogen) (Belousov et al., 2006). Endothelial cells were transfected with the cytosol-targeted HyPer vector using opti-MEM and lipofectamine 2000. We first tested the sensitivity of the methodology by adding exogenous H_2O_2 (***Figure 3***) and

studying the increase in fluorescence. As shown in the figure, 1 µM H_2O_2 added exogenously to endothelial cells was able to induce the reversible oxidation of the HyPer plasmid reflected as an increase of its fluorescence. Endothelial cells transfected with the cyto-HyPer vector were subjected to shear stress and a marked increase in intracellular H_2O_2 generation was detected as early as 5 minutes of fluid flow (***Figure 3***).

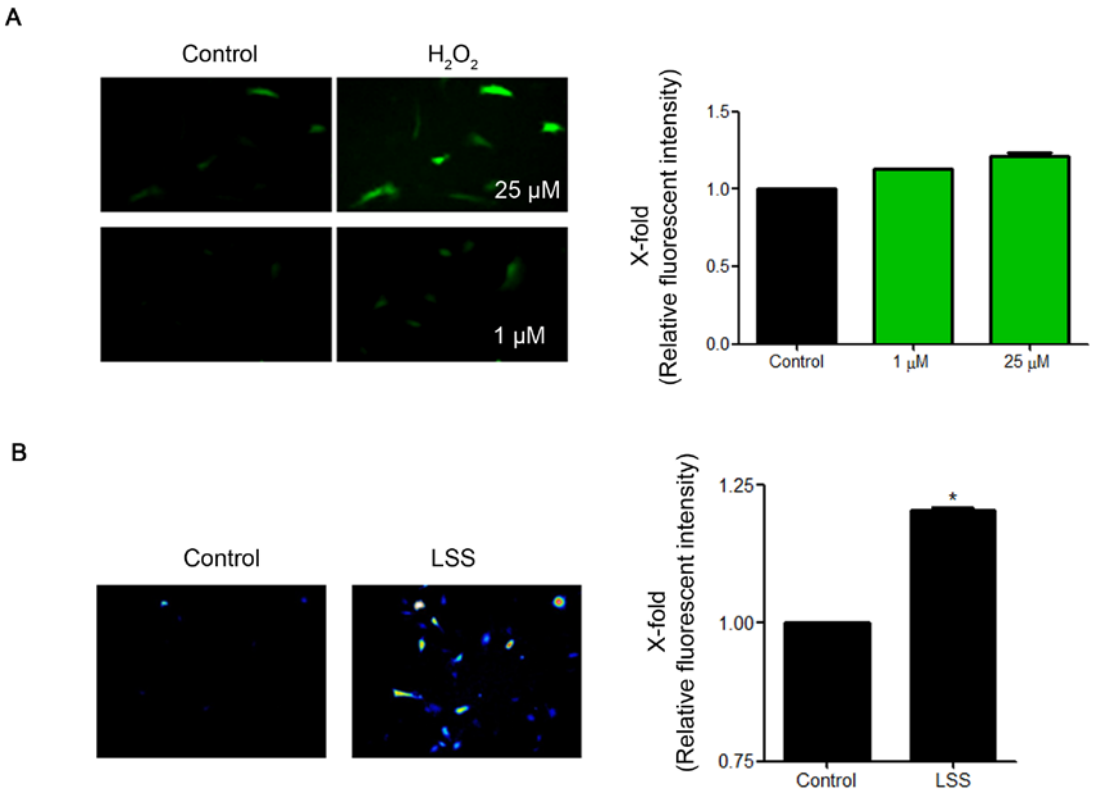

Figure 3. Laminar shear stress increase H2O2 production. Intracellular detection by HyPer fluorescence. *A) BAEC were transfected with the H2O2 biosensor pHyPer-Cyto and YFP fluorescence was detected using confocal microscopy. Note that fluorescence is visible with a concentration of 1 µM H2O2 added extracellularly. Bars represent means ± SEM of n=3. B) Detection of intracellular H2O2 in BAEC transfected with the HyPer-cyto plasmid and exposed to LSS. Image was obtained 5 minutes after the exposure and fluorescence intensity was quantified by Metamorph and ImageJ software. *p<0.05 vs control.*

Intracellular hydrogen peroxide production was also quantified by measuring the extracellular leakage of H_2O_2 with the specific peroxide reagent Amplex Red. We incubated the supernatants of the static- and shear stress-stimulated cells with the Amplex red reagent in combination with horseradish peroxidase (HRP). In the presence of

peroxidase, the Amplex red reagent reacts with H_2O_2 in a 1:1 stoichiometry to produce a red-fluorescent product (resorufin). Results of the fluorescence assay were consistent with a significantly higher accumulation of peroxide in the extracellular medium after fluid flow stimulation compared with static conditions (***Figure 4***).

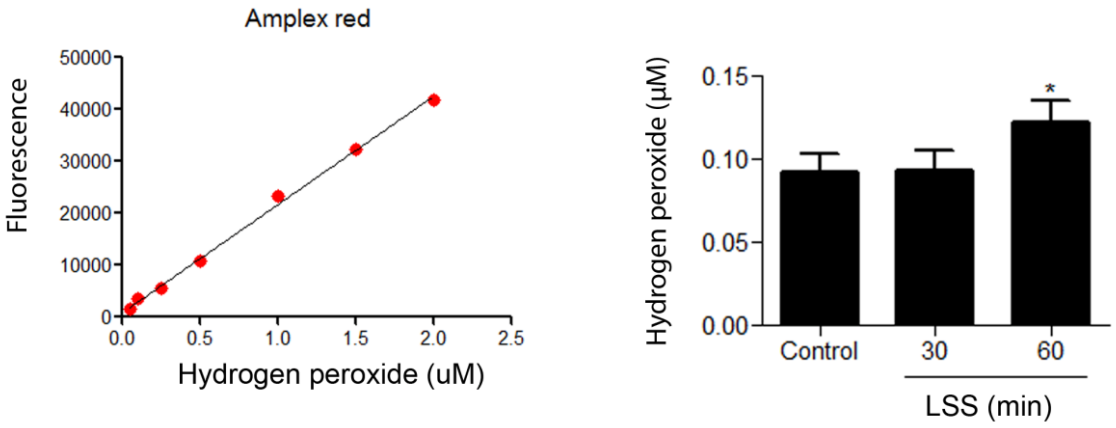

Figure 4.. Laminar shear stress increase H_2O_2 production. Extracellular detection in cells supernatants fluorescence. *A) Reactions containing 5 µM Amplex red reagent, 0.1 U/ml HRP and the indicated amounts of H_2O_2 were incubated for 30 minutes at 37ºC in the dark. Fluorescence was measured (excitation and emission wavelengths of 571 nm and 585 nm respectively). B) Extracellular accumulation of H_2O_2 in BAECs subjected to LSS as determined with Amplex red assay.*

Therefore, our data indicate that LSS at early time points is capable of generating low levels of ROS, and specifically H_2O_2 levels which can be quantitatively considered within signaling concentrations.

4.1.2 LSS AND LOW LEVELS OF HYDROGEN PEROXIDE ACTIVATE p38 MAPK AND eNOS.

LSS is capable of eliciting multiple responses in endothelial cells, activating several intracellular pathways that converge into the activation of different MAPK or stimulate the production of vasoactive molecules such as nitric oxide ($NO^{\cdot}$). In attempting to investigate the redox-induced signaling responses mediated by LSS, we focused our interest on the

study of two different proteins, p38 MAPK and the endothelial nitric oxide synthase (eNOS). Both of them, have been described to become activated by fluid flow (Sumpio et al., 2005, Corson et al., 1996), as well as by exogenous treatments with H_2O_2 (Stone and Yang, 2006, Thomas et al., 2008), even when most reported studies were performed using supraphysiological (i.e. non signaling levels of exogenous H_2O_2). By using western blot methodology and phospho-specific antibodies, we proved p38 MAPK and eNOS were activated at early time points of laminar shear stress, being clearly evident at 15-30 min of fluid flow (***Figure 5***).

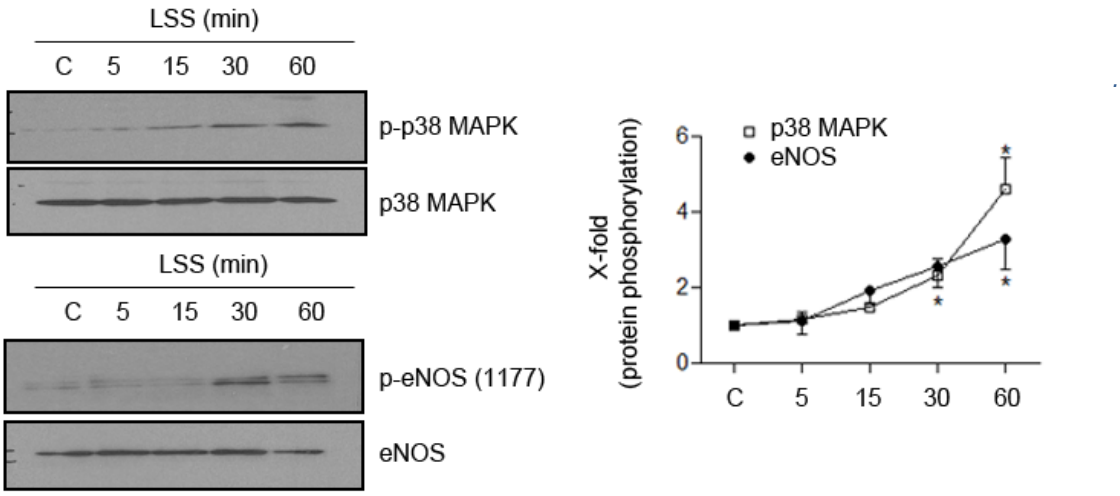

Figure 5. Laminar shear stress induces early activation of p38 MAPK and eNOS in endothelial cells*. BAECs were subjected to various periods of LSS, and activation of p38 MAPK and eNOS was determined using phospho-specific antibodies. Graph represents means ± SEM of at least 3 independent experiments. *p<0.05 vs control.*

Even though the enzymatic activity of eNOS is influenced by different post-translational modifications, such as acylation, S-nitrosylation or phosphorylation and dephosphorylation; phosphorylation has been considered as one of the major post-translational regulatory influences on eNOS activity (Dudzinski and Michel, 2007), being the phosphorylation described along this dissertation at Ser 1177, an activation mark for the enzyme. We next tested concentrations within the low-micromolar range of H_2O_2 effects, observing it elicited a significant increase in eNOS as well as p38 MAPK phosphorylation (***Figure 6***)

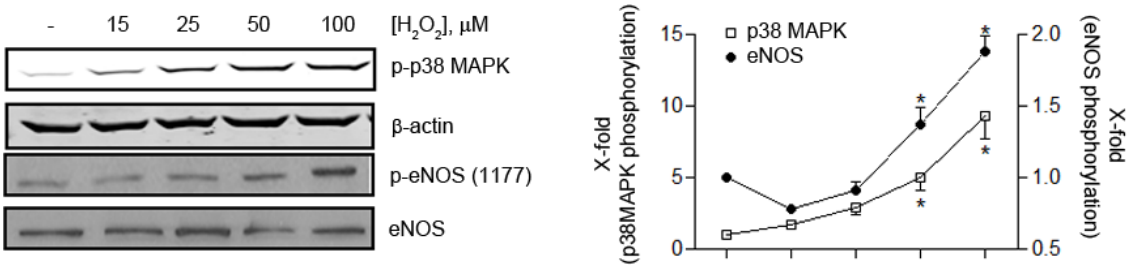

Figure 6. Exogenous treatment of H_2O_2 promotes p38 MAPK and eNOS activation. ***BAECs were stimulated with the indicated concentrations of H_2O_2 for 1 hour and activation of p38 MAPK and eNOS was studied by the use of specific antibodies.***

It is estimated that when exogenous H_2O_2 is added to cells an equilibrium is reached by which the intracellular concentration of H_2O_2 becomes 7-10-fold less than the original one added extracellularly (Antunes and Cadenas, 2000). To circumvent this limitation and to generate peroxide concentrations more closely resembling signaling levels, very low fluxes of H_2O_2 were produced by the physiological enzymatic system of glucose oxidase. First, we calculated the rate of H_2O_2 production by spectrophotometry in PBS buffer, using the coupled reaction with HRP and ABTS as the substrate (***Figure 7***) proving its linearity. Then treatment of endothelial cells with glucose oxidase showed that fluxes as small as 0.1 nM H_2O_2 /min along 40 minutes were enough to produce a robust activation of both proteins (***Figure 7***).

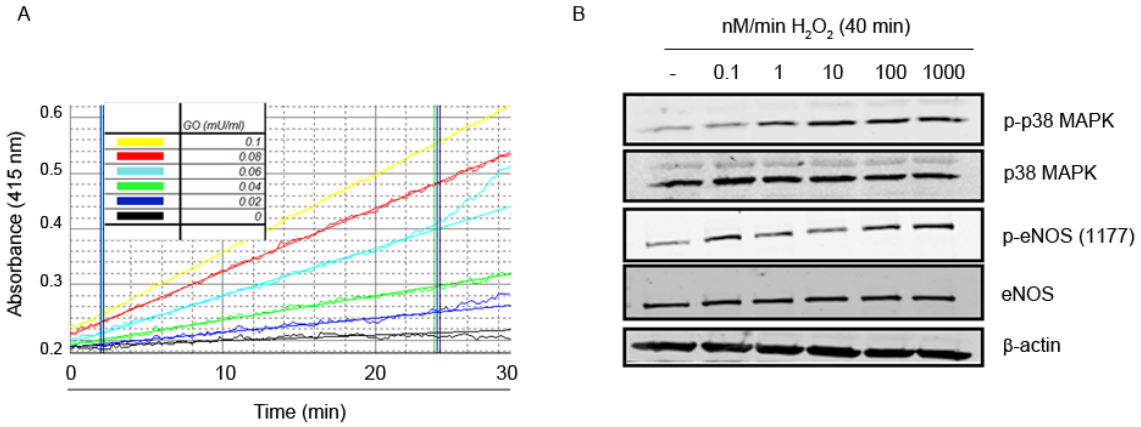

Figure 7. Glucose oxidase generation of H_2O_2 fluxes activates both p38 MAPK and eNOS. *A) The rate of H_2O_2 production by glucose oxidase was calculated spectrophotometrically in Dulbecco´s PBS buffer supplemented with 5.6 mM glucose and 1 mM L-arginine, 20 µg/ml HRP and 50 µM ABTS. The absorbance of*

different amount of glucose oxidase was measured for 20-30 minutes. H_2O_2 flux generated by each amount of glucose oxidase was determined taking into account the slopes of its kinetic reaction. B) BAECs were treated with glucose oxidase concentration to reach the desired H_2O_2 flux during 40 minutes.

We believe it is quite likely that the concentrations of ROS reached during LSS experiments are not far from those obtained after glucose oxidase treatment. To verify the dependence of LSS-induced p38 MAPK and eNOS phosphorylation on the generation of ROS, we evaluated if antioxidant pre-treatment of endothelial cells could affect their activation levels. As shown in (***Figure 8***), preincubation of endothelial cells with PEG-catalase (an enzyme that catalyzes the decomposition of H_2O_2 to water and oxygen), abrogates not only H_2O_2-induced p38 MAPK and eNOS phosphorylation, but also those promoted by LSS.

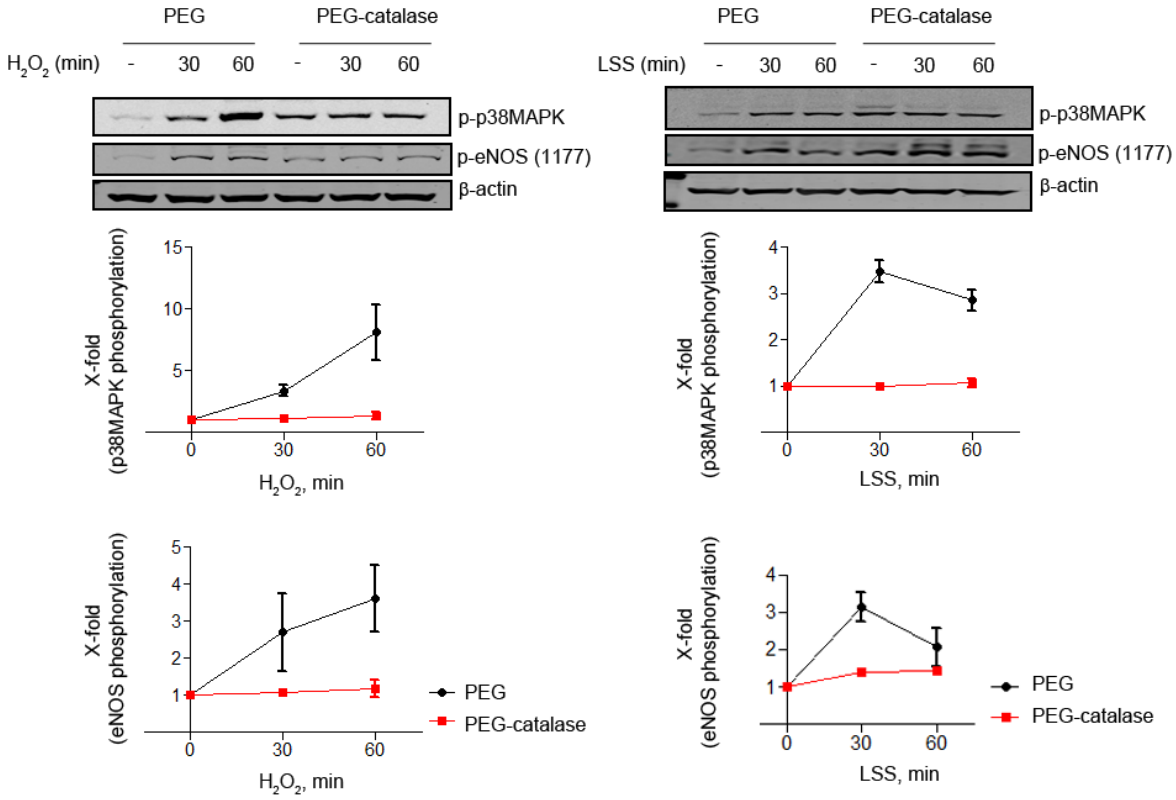

Figure 8. LSS-induced p38 MAPK and eNOS activation is abolished after antioxidant treatment. *A) BAEC were stimulated with 100 μM of H_2O_2 for the indicated time points in the presence or absence of PEG-catalase (100 units/ml overnight). B) Effects of PEG-catalase treatment on LSS-induced p38 MAPK and eNOS phosphorylation. Below each representative immunoblot are shown the results of densitometric analyses from*

pooled data that yielded equivalent results. Each data point represents the mean ± SEM from three independent experiments.

In addition, we treated cells with a general antioxidant reagent (apocynin), and found that it was able to significantly reduce LSS-induced ROS-production, in consistence with lower phosphorylation levels of our proteins of interest (***Figure 9***).

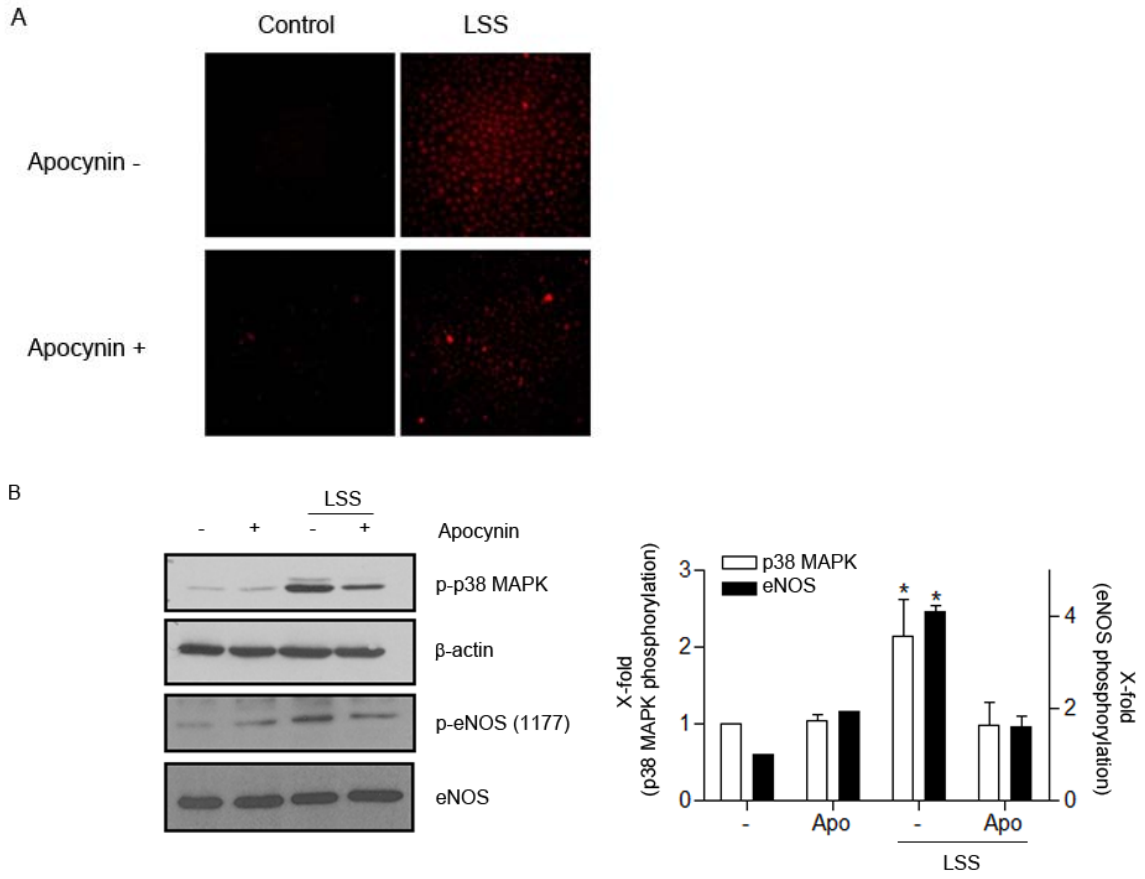

Figure 9. LSS-induced early activation of p38 MAPK and eNOS is dependent upon ROS production. *A) BAECs were incubated with DHE (2 μM) for 2 h and treated with or without apocynin (100 nM, 30min). ROS were determined before and after 1 h LSS. B) p38 MAPK and eNOS activation (immunoblot) were studied under the same conditions. Blots are representative of at least three experiments and each graph depicts the means±SEM derived from three independent experiments. *p<0.05 vs control. Where error bars are not visible they are smaller than the data point.*

Together, these results demonstrate a close correlation between LSS-induced p38 MAPK and eNOS activation and ROS generation during LSS.

4.1.3 NOX4 IS AN IMPORTANT SOURCE OF ENDOTHELIAL HYDROGEN PEROXIDE-MEDIATED ACTIVATION OF p38 MAPK.

Intracellular generation or ROS may arise from different sources including mitochondria respiration, xanthine oxidoreductase, uncoupled eNOS, and NADPH oxidases (NOXs). However, in the context of LSS there is substantial evidence that ROS generation arises from a transient activation of different NOXs isoforms (De Keulenaer et al., 1998, Chatzizisis et al., 2007). Although apocynin was initially described as a selective inhibitor of NADPH oxidase activity and concomitant ROS production (Simons et al., 1990), it is no longer considered an specific NOX inhibitor (Heumuller et al., 2008). Hence, we evaluated the implication of NOXs in the generation of ROS in the vasculature exposed to fluid shear stress with more specific tools. First, we studied the basal expression of the different NOX isoforms in our model of bovine aortic endothelial cells (BAEC). We found that, albeit the expression of NOX1 and NOX2 isoforms was detectable, NOX4 was by far the most abundant isoform in BAEC using quantitative RT-PCR (***Figure 10***).

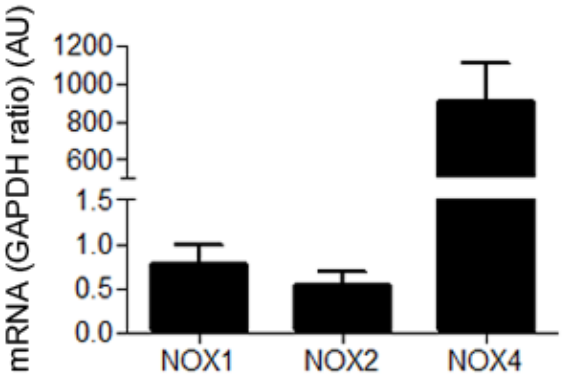

Figure 10. NOX4 is the main NAPDH oxidase isoform expressed in endothelial cells*. Quantitative RT-PCR for NOX1, NOX2, and NOX4 in BAECs.*

In order to study NOX4 involvement, we designed a siRNA to specifically knockdown NOX4 (***Figure 11***), without affecting other NOXs isoforms. Hence, we studied the role of NOX4 in LSS-induced p38 MAPK activation, and we found that both VAS2870 (specific inhibitor of the NOX family (Wind et al., 2010)) and the specific knockdown of NOX4 with siRNA significantly reduced p38 MAPK phosphorylation.

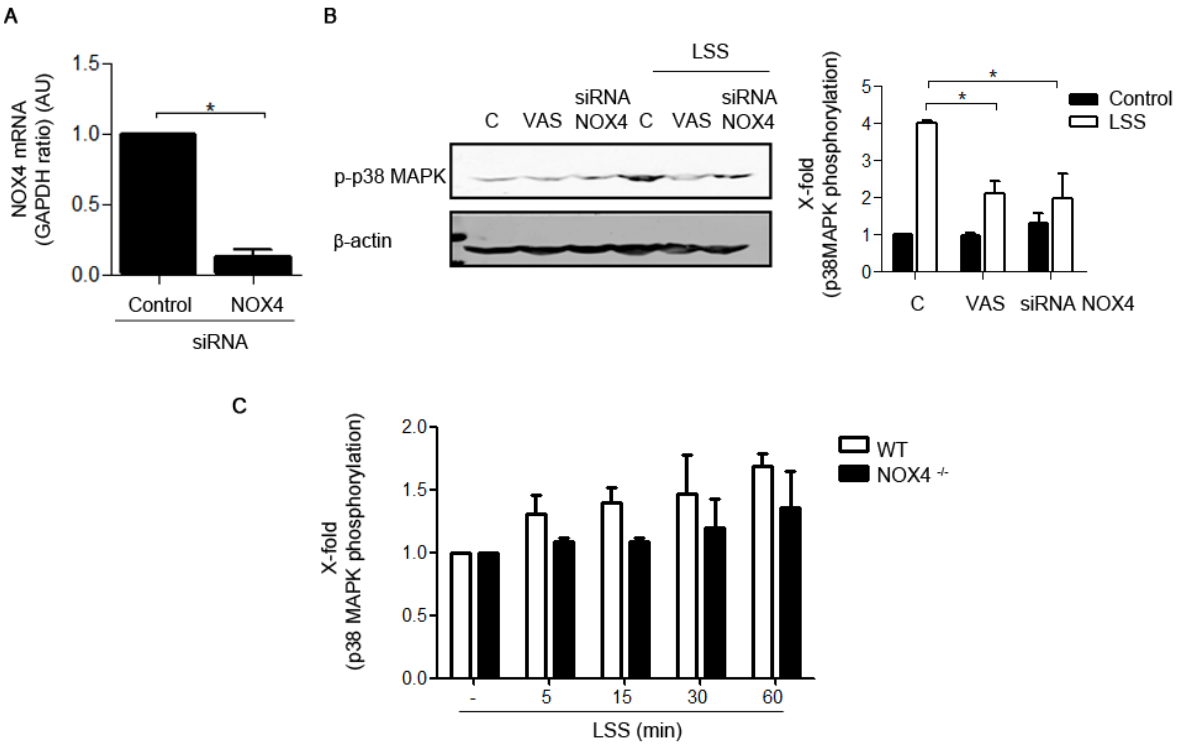

Figure 11. LSS-induced p38 MAPK phosphorylation is NOX4-dependent. *A) siRNA-mediated NOX4 knockdown evaluated by RT-PCR (AU, arbitrary units). B) Immunoblot of phospho-p38 MAPK in BAECs subjected or not to LSS for 60 min and treated with VAS2870 (10 μM, 30 min) or siRNA for NOX4. Blot is representative of at least three experiments and graph depicts the means ± SEM derived from three independent experiments. *p<0.05. C) Experiments were conducted with isolated murine lung endothelial cells (MLEC) from knock-out mice for NOX4 and p38MAPK phosphorylation by laminar shear stress was studied. Bar graph depicts the mean of four independent experiments.*

Furthermore, we isolated murine lung endothelial cells (MLEC) from knock-out animals deficient in different NOX isoforms. Of note, experiments conducted with MLEC from knock-out mice for NOX4, p38 MAPK phosphorylation by LSS was impaired (***Figure 11***). In

order to test if other NADPH oxidases could be involved in p38 MAPK activation, we isolated MLECs from the double NOX1-NOX2 knockout mice. In this case, we did not detect significant differences between MLEC from the double knockout animals and those from wild-type. However, differences in p38 MAPK phosphorylation induced by shear stress became again evident when NOX4 was suppressed in addition to NOX1 and NOX2 in the triple knock-out animals (***Figure 12***).

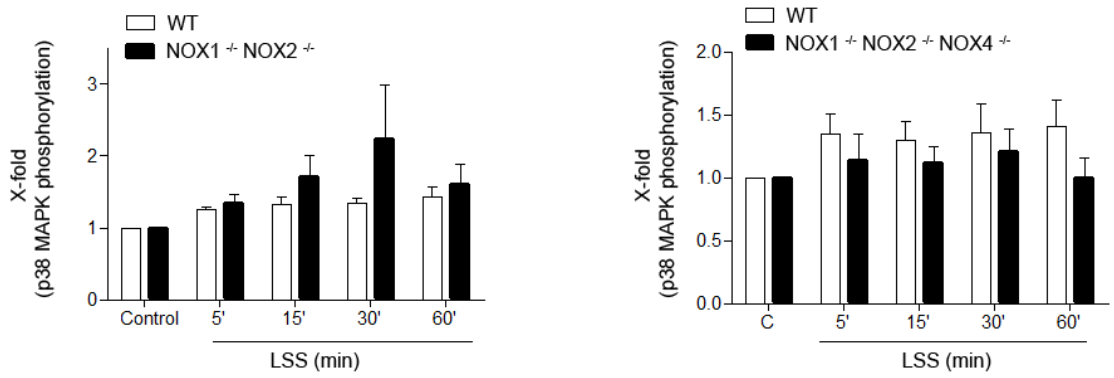

Figure 12. NOX4 is the main NADPH oxidase implied in LSS-induced p38 MAPK activation. *A) p38 MAPK-induced LSS was studied in isolated MLECs from double NOX1/NOX2 knockout and NOX1/NOX2/NOX4 triple knockout mice. Bar graph depicts the mean of four independent experiments*

This set of results support a key role for NOX4 in LSS-mediated generation of peroxide, as its silencing or abolition was associated with a drastic reduction in p38 MAPK phosphorylation.

4.1.4 LSS-DEPENDENT p38MAPK ACTIVATION LIES UPSTREAM OF eNOS PHOSPHORYLATION.

Based on the fast responses of p38 MAPK and eNOS to LSS, and the fact that they share the same activation pattern by ROS, we asked whether there might be a sequential activation between both of them. A cross talk between p38 MAPK and eNOS activation has been already described in several endothelial models. For example, whereas

pharmacological concentrations of exogenous nitric oxide have been reported to increase p38 MAPK phosphorylation (Milkiewicz et al., 2006, Ptasinska et al., 2007), black tea polyphenols activate eNOS by a p38 MAPK-dependent mechanism (Anter et al., 2004). With this in mind, we first examined if eNOS could act upstream of p38 MAPK activation in our model. To his end, MLECs from wild-type of eNOS-deficient mice were exposed to different periods of LSS and p38 MAPK phosphorylation was evaluated. p38 MAPK phosphorylation was still clearly evident in the absence of eNOS (***Figure 13***), supporting that eNOS activation is not necessary for p38 MAPK activation.

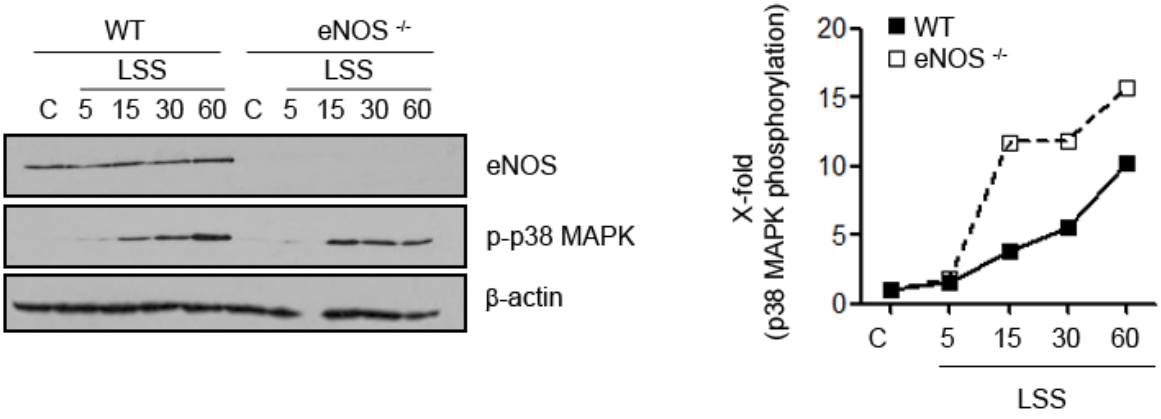

Figure 13. eNOS is dispensable for p38 MAPK activation by LSS. *MLECs from wild-type of eNOS-deficient mice were exposed to different periods of LSS and p38 MAPK phosphorylation was evaluated.*

To further $NO^{\cdot}$ itself does not affect p38 MAPK, we treated endothelial cells with a fast-releasing $NO^{\cdot}$ donor (DEANO) and detected p38 MAPK lack of phosphorylation using anisomycin as a positive control (***Figure 14***).

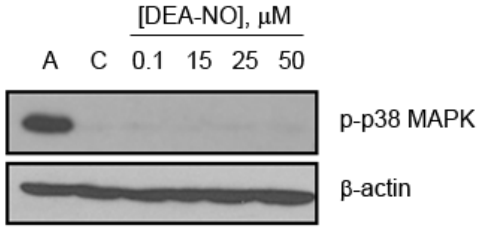

Figure 14. Nitric oxide itself does not promote p38 MAPK activation. *BAECs were treated with a fast-releasing $NO^{\cdot}$ donor (DEANO) and p38 MAPK phosphorylation. Anisomycin was used as a positive control (A, 50 mg/ml for 20 minutes).*

We next evaluated if p38 MAPK behaved as an upstream regulator of eNOS in our cells. We pre-treated the endothelial cells with two different and specific p38 MAPK activity inhibitors (SB203580 and PD169316) before LSS exposure. eNOS phosphorylation induced by LSS was markedly abrogated in the presence of the specific p38 MAPK inhibitors , and this reduction correlated well with a significant decrease in $NO^{\cdot}$ synthesis detected by a chemiluminescence methodology (***Figure 15***).

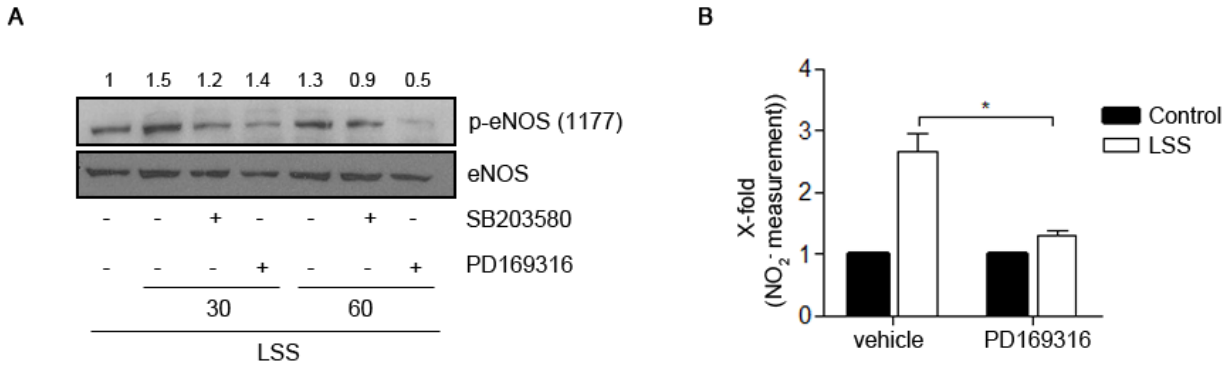

Figure 15. siRNA-mediated p38α-MAPK knockdown significantly reduced eNOS phosphorylation during LSS. *A duplex siRNA targeting construct to knockdown specifically p38 MAPKα was transfected in BAECs and eNOS phosphorylation was detected by using phospho-specific antobodies.*

We developed and validated a duplex siRNA targeting construct to knockdown specifically p38 MAPK in endothelial cells. Although four different isoforms of p38 MAPK have been described in mammals (α, β, γ and δ), the cardiovascular importance of p38α is the best characterized (Denise Martin et al., 2012, Sicard et al., 2010, Kumphune et al., 2010). siRNA-mediated p38α-MAPK knockdown significantly reduced eNOS phosphorylation under LSS induction (***Figure 16***).

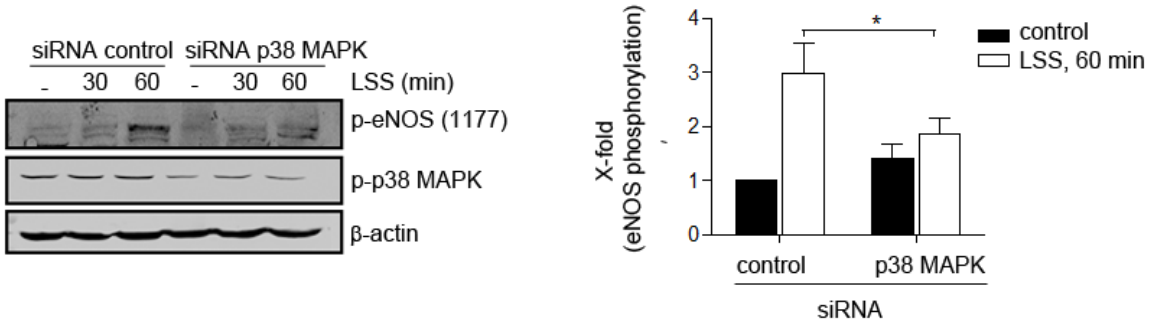

Figure 16. siRNA-mediated p38α-MAPK knockdown significantly reduced eNOS phosphorylation during LSS*. A duplex siRNA targeting construct to knockdown specifically p38α MAPK was transfected in BAECs and eNOS phosphorylation was detected by using phospho-specific antobodies. Blot is representative of at least three experiments and each graph depicts the means±SEM derived from three independent experiments. *p<0.05 vs control.*

These data support that eNOS is dispensable for the response of p38 MAPK to LSS, but in contrast, LSS-dependent p38 MAPK activation is necessary for eNOS phosphorylation and nitric oxide production.

4.1.5 HYDROGEN PEROXIDE ACTIVATION OF eNOS REQUIRES p38α MAPK ACTIVATION.

Keeping in mind p38 MAPK controls eNOS activation by LSS, we sought out to determine whether this effect was also redox-dependent and p38 MAPK was responsible for eNOS phosphorylation by H_2O_2. To test the role of p38 MAPK in mediating the response of eNOS to H_2O_2 we studied the effects of the aforementioned inhibitors in the presence of H_2O_2. Increases in eNOS phosphorylation induced by H_2O_2 were significantly reduced by p38 MAPK inhibition (***Figure 17***). Not only exogenous treatment with H_2O_2 had this effect, but also intracellular production of physiological levels of H_2O_2 by the enzymatic glucose oxidase system were not able to activate eNOS in the presence of p38 MAPK chemical inhibitors (***Figure 17***).

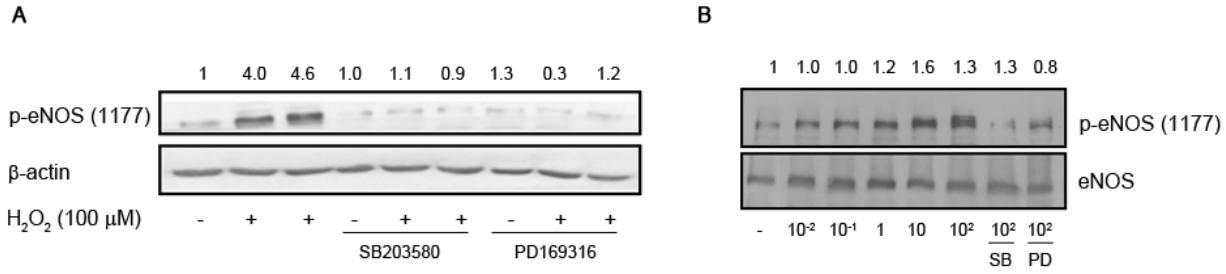

Figure 17. ROS-dependent p38 MAPK activation lies upstream of eNOS phosphorylation. *A) BAECs were treated with H_2O_2 (100 μM, 1 h), and eNOS activation was detected in the presence or absence of p38 MAPK-specific inhibitors. B) Hydrogen peroxide fluxes were mediated by glucose oxidase treatment and eNOS phosphorylation was detected in the presence or absence of p38 MAPK inhibitors.*

To further confirm the importance of p38 MAPK in the upstream signaling of eNOS, we studied the effect of the overexpression of a constitutively active or a dominant negative p38 MAPK-specific upstream activator, MKK6 (Dolado et al., 2007), on eNOS activation. We transfected the endothelial cells with both plasmids, and 24 hours later we treated cells with H_2O_2. As shown in ***Figure 18***, while MKK6 overexpression induced an increase in the phosphorylation levels of eNOS, apart from the expected increase in p38 MAPK activation, the dominant negative MKK6 overexpression abrogated it.

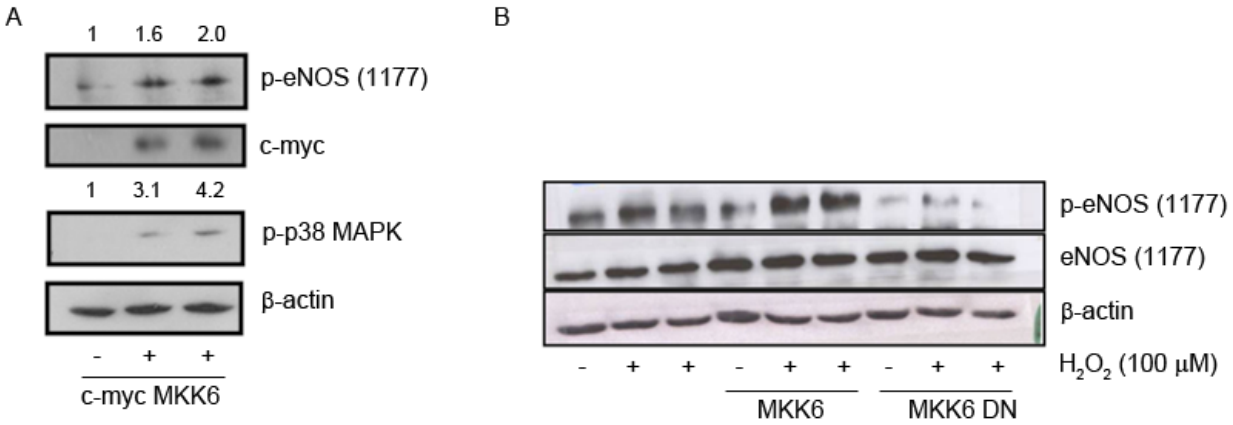

Figure 18. MKK6, p38 MAPK upstream activator, induces eNOS activation. *A) BAECs were transfected with the constitutively active p38 MAPK-specific upstream activator MKK6 and eNOS and p38 MAPK activation was detected. B) BAECs were transfected both with MKK6 contitutively active and MKK6 dominant negative for 24 hours and eNOS activation induced by H_2O_2 was studied.*

Finally, the role of p38 MAPK was evaluated by a loss-of function approach. We used murine embryonic fibroblast (MEFs) from both wild-type and p38α MAPK-deficient mice, and we exposed them to 100 µM of H_2O_2 and studied eNOS phosphorylation. As shown in ***Figure 19***, the induction of eNOS phosphorylation related to H_2O_2 was significantly diminished in MEFs from p38α MAPK null mice.

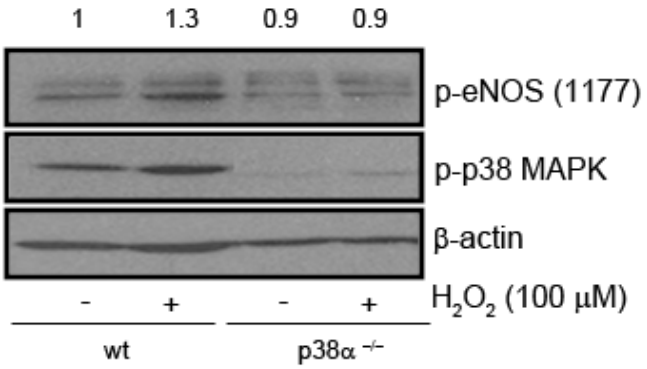

Figure 19. eNOS activation by H_2O_2 is abolished in p38α-knockout MEFs. *Murine embryonic fibroblast (MEFs) from both wild-type and p38α MAPK-deficient mice were exposed to 100µM of H_2O_2 and eNOS phosphorylation was detected.*

Taken together, this set of results confirms the importance of p38 MAPK in the redox-dependent activation of eNOS.

4.1.6 p38α MAPK-MEDIATED eNOS ACTIVATION IS AKT INDEPENDENT

The activation of eNOS at residue Ser1177 by phosphorylation has been widely described in the literature to be catalyzed by numerous kinases including Akt (protein kinase B), AMP-dependent protein kinase (PKA), AMP-activated protein kinase (AMPK), PKG and calcium/calmodulin dependent protein kinase II (CaM kinase II) (Fulton et al., 2001, Michell et al., 2001, Chen et al., 1999b, Dudzinski and Michel, 2007, Fulton et al., 1999). Among them, Akt was described to regulate shear-dependent production of NO. by directly phosphorylating endothelial eNOS at the Ser 1177 residue (Dimmeler et al., 1999a, Fisslthaler et al., 2000), although some further investigations suggested it could be Akt-independent (Boo et al., 2002). Additionally, Akt has been also documented to

mediate eNOS activation by hydrogen peroxide (Hu et al., 2008). We decided to investigate at this point Akt was involved in p38 MAPK action on eNOS mediated by LSS/redox. Neither wortmannin nor LY294002 (both PI3K/Akt inhibitors) blocked H_2O_2 -induced p38 MAPK phosphorylation (***Figure 20***), even more, p38α MAPK knockdown by siRNA did not modify LSS-induced Akt activation (***Figure 21***).

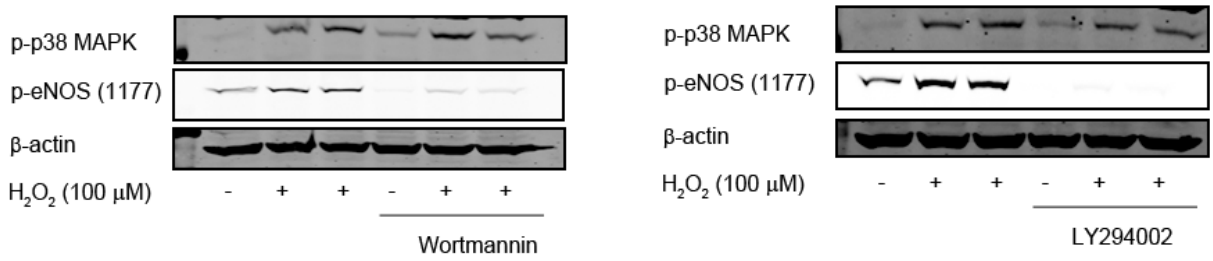

Figure 20. H_2O_2-induced p38 MAPK phosphorylation is not dependent on the PI3K-Akt pathway. *Immunoblot analyses of p38 MAPK activation by H_2O_2 in BAEC incubated with two different PI3-kinase inhibitors (Wortmannin 4 µM or LY294002 30 µM, 2h). Blots are representative of at least 3 independent experiments.*

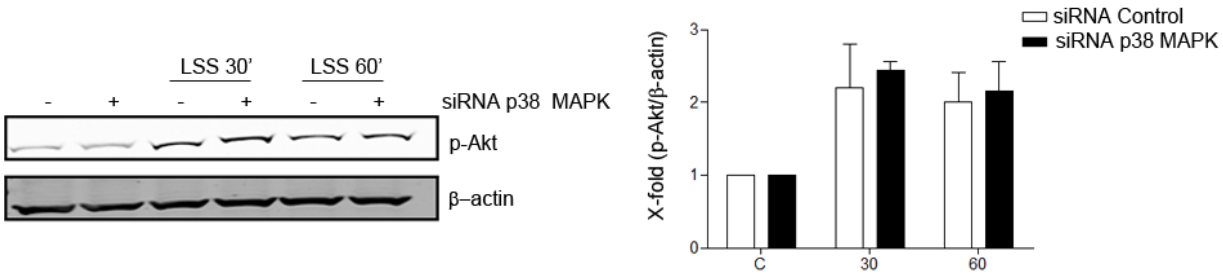

Figure 21.. LSS-dependent Akt phosphorylation is not mediated by p38 MAPK*. BAEC were transfected with the p38αMAPK specific siRNA and activation of Akt induced by LSS was detected by a phospho-specific antibody. The graph represents the mean ± SEM derived from three independent experiments.*

In addition, we performed LSS experiments in siRNA-mediated knockdown endothelial cells, and as it is shown in ***Figure 22***, NOX4 absence does not alter Akt activation during laminar flow.

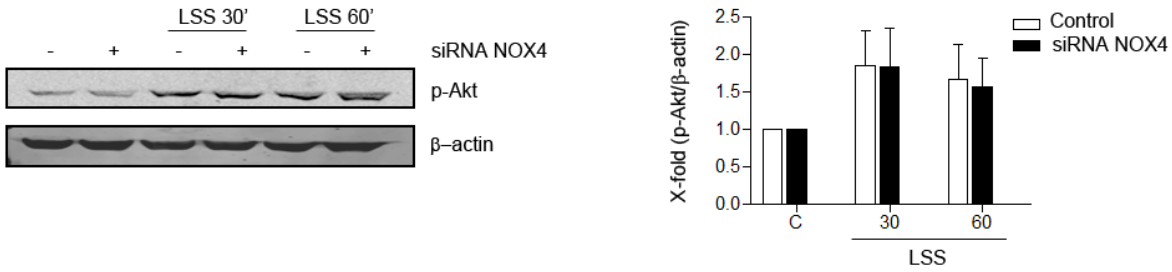

Figure 22.. NOX4 is dispensable for Akt activation by LSS. *Akt activation by LSS was determined using a phospho-specific antibody in BAEC subjected or not to siRNA-mediated NOX4-knockdown. Blot is representative of at least 3 experiments and each bar in the graphs represents the mean ± SEM of independent experiments that yielded similar results.*

These results support that PI3K/Akt does not mediate peroxide-induced p38 MAPK phosphorylation and that p38 MAPK mediated eNOS activation by LSS/redox is independent from the PI3K/Akt pathway.

Taken together these results are consistent with a model in which LSS-NOX4-peroxide induce a sequence of events whereby p38 MAPK activation lies upstream of eNOS phosphorylation, activation, and subsequent nitric oxide generation (Breton-Romero et al., 2012).

4.2 MITOCHONDRIAL MECHANOSENSING DURING LAMINAR FLOW

Although we have described hydrogen peroxide as an intracellular second messenger capable of eliciting the sequential activation of p38MAPK and eNOS during laminar shear stress, a major question remains unanswered: which are the real hydrogen peroxide sensors modified by signaling levels of ROS and targets of mechanotransdution during laminar flow?. Hydrogen peroxide is a mild oxidant that can oxidize cysteine to cysteine sulfenic-acid. However very few proteins are susceptible to be oxidized by hydrogen peroxide. Among these, most of them bear a low-pKa cysteine residue in the form of a thiolate at neutral pH. Different kinetic studies have identified peroxiredoxins as the most favored hydrogen peroxide targets because of their high rate constants and high abundance in mammalian cells (Winterbourn and Hampton, 2008).

4.2.1 PEROXIREDOXINS AS THE HYDROGEN PEROXIDE EARLY SENSORS OF LAMINAR FLOW.

Peroxiredoxins (PRXs) are primary candidates as regulators of local hydrogen peroxide signaling in endothelial cells. PRXs are a ubiquitous family of enzymes which mediate signal transduction in mammalian cells. They are broadly distributed in different subcellular compartments thus sensing regional ROS production (Wood et al., 2003, Kang et al., 2005). PRXs are expressed at high levels in cells, being one of the most abundant protein in erythrocytes (Moore et al., 1991), and composing 0.1-0.8% of the soluble proteins in other mammalian cells (Chae et al., 1999) They are thiol specific-, nonselenium containing enzymes that use redox-active cysteines to reduce peroxides. The six isoforms of mammalian PRXs (1-6) are classified into three different subfamilies based on the conserved cysteine residues. Structural and functional data divide PRXs into three different categories: 2-Cys typical PRX (PRX1-4), 2-Cys atypical PRX (PRX5) and 1-Cys PRX (PRX6). The peroxide sensing is composed of one reaction with two different steps centered around a redox active cysteine called peroxidatic cysteine. The three different types of PRXs have the first step in common, in which the *peroxidatic cysteine*

attacks the peroxide substrate becoming oxidized to a cysteine sulfenic acid (Cys-SOH) (Ellis and Poole, 1997). PRX1-4 form a homodimer in the second step as the peroxidatic cysteine sulfenic acid from one subunit is attacked by the *resolving cysteine* located in the C-terminus of another subunit. This reaction results in the formation of a *stable intermediate disulfide bond*. In PRX5 (2-Cys atypical PRX) both the peroxidatic and the resolving cysteine are contained within the same molecule, so the disulfide bond is an intramolecular one. PRX6 just contains the peroxidatic cysteine and the reaction is completed presumably by a thiol-containing electron donor not completely identified.

To check if PRXs were in fact our hypothetical early hydrogen peroxide sensors during laminar flow, we studied the reactivity of the different PRXs by monitoring dimer formation during laminar shear stress. As explained above, *dimerization* implies an *activation* of these proteins. To do that, we maintained their free thiol groups blocked with an alkylating reagent (present only in the lysis buffer) that reacts with sulfhydryls (N-ethyl maleimide), and then ran the samples in SDS-PAGE gels in reducing and non-reducing conditions (in the presence or absence of the reducing agent Beta-mercaptoethanol respectively). First, we determined if we were able to detect these disulfide bonds, by producing low fluxes of H_2O_2 endogenously. To generate a continuous flux of H_2O_2 we added different quantities of glucose oxidase, the rate of hydrogen peroxide production being previously calculated spectrophotometrically by a coupled reaction with HRP and ABTS as a substrate. As shown in ***Figure 23***, we detected dimerization in PRX2, PRX3 and PRX4. The PRX3 dimerization pattern surprised us, as we detected dimer formation at very low hydrogen peroxide concentrations while disappearing with higher ones. Peroxiredoxins are very sensitive enzymes, responding to very low hydrogen peroxide concentrations. Nevertheless, in the presence of relatively high levels of peroxide substrates, PRXs become hyperoxidized. When an excess of peroxide is produced, a second molecule of peroxide substrate attacks the sulfenic cysteine forming a sulfinic or even a sulfonic acid leading to overoxidation (Cys-$SO_{2/3}$) and inactivation of the PRX. Employment of the specific antibody which recognizes these sulfinic/sulfonic forms of PRX allowed to prove that high concentrations of H_2O_2 result in inactivation of the antioxidant enzyme. We next studied the laminar shear stress effect on the PRXs catalytic cycle.

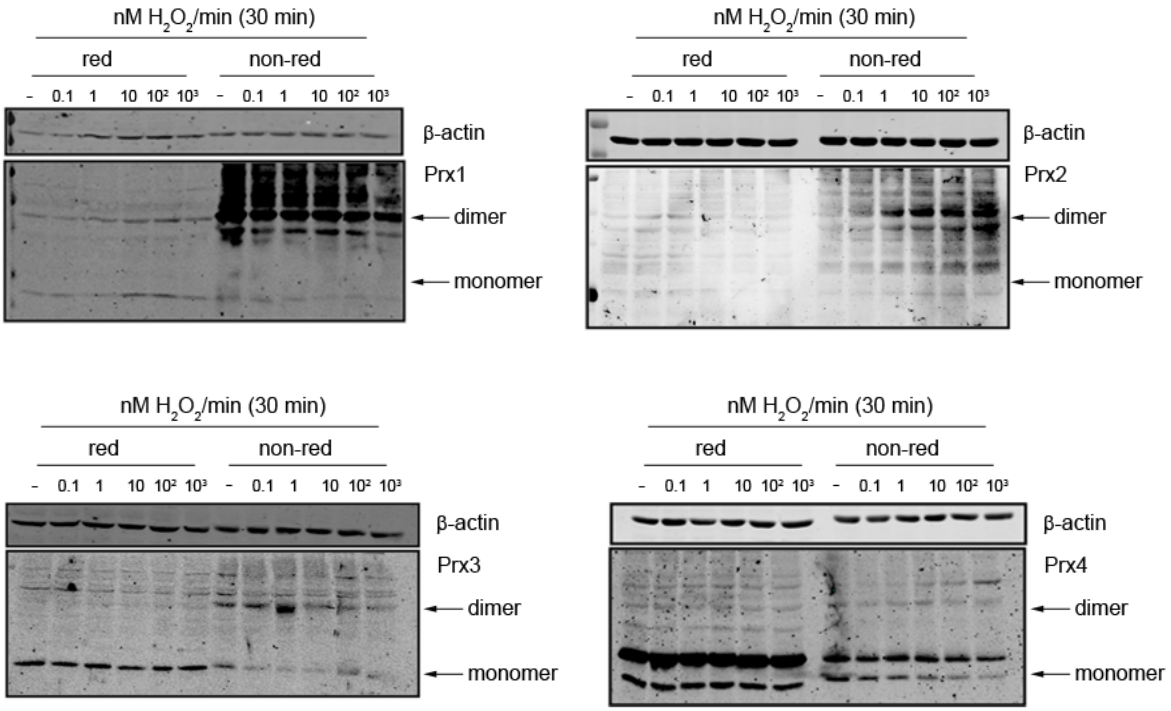

Figure 23. Low fluxes of hydrogen peroxide induce 2-Cys PRXs dimerization. *HUVECs were treated with glucose oxidase to generate fluxes of hydrogen peroxide and dimerization of PRXs was detected in non reducing conditions (SDS-PAGE). Blots probed with specific antibodies are representative of at least three independent experiments.*

As shown in ***Figure 24***, LSS was unable to promote dimerization of PRX 1, 2, 4 or 5. In contrast, LSS was associated with evident dimerization of PRX3 from early time points, suggesting a specific activation of this isoform. We proceeded to test this effect in different endothelial cell types.

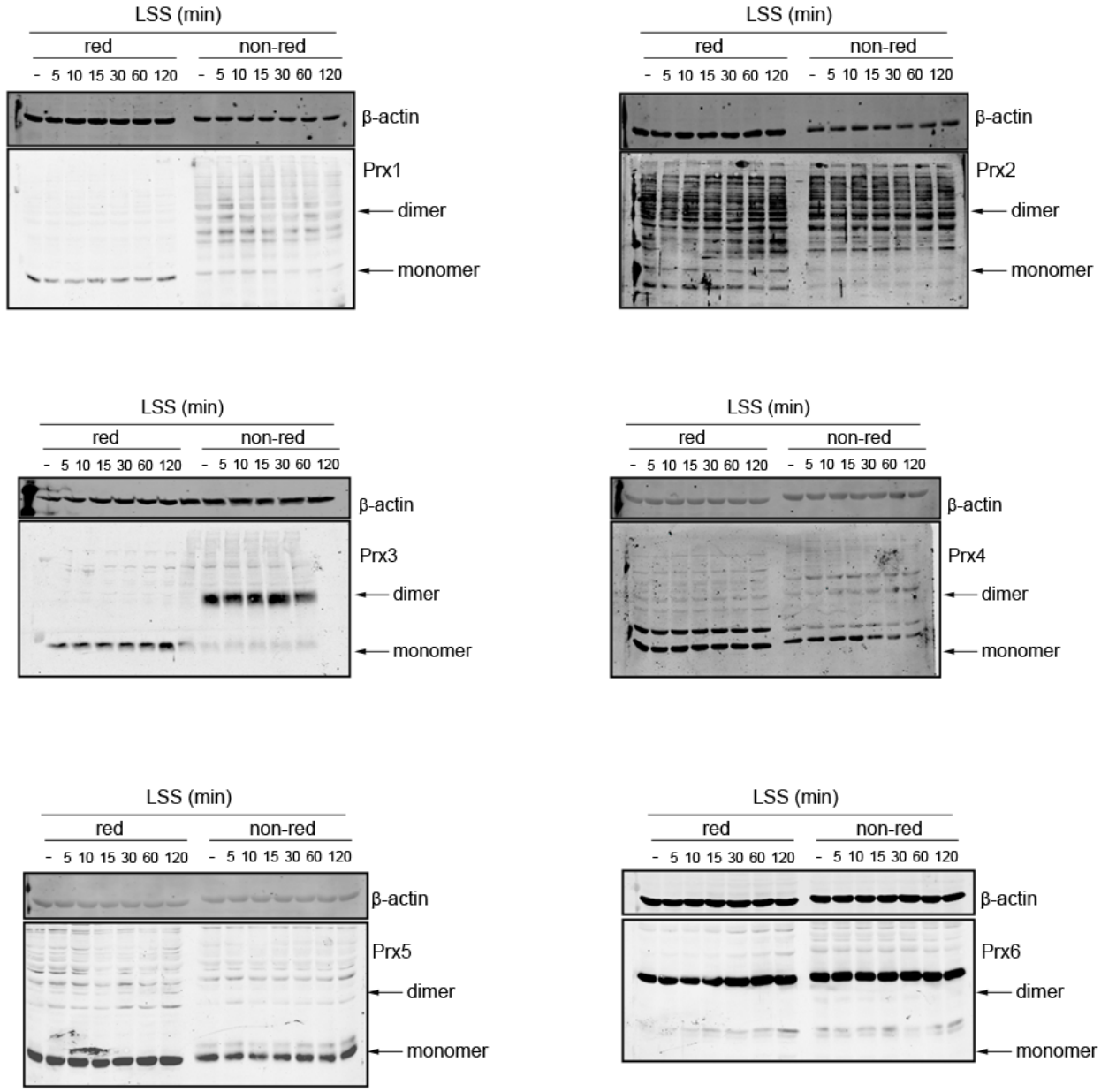

Figure 24. LSS induces PRX3 dimerization. *HUVEC were exposed to LSS and were lysed in the presence of the alkylating reagent N-ethyl maleimide (NEM). Lysates were analyzed by SDS-PAGE in reducing and non-reducing conditions and probed with specific antibodies as shown. Immunoblots are representative of at least three independent experiments.*

As shown in ***Figure 25***, this result was corroborated in bovine aortic and murine lung endothelial cells. We next examined if laminar shear stress could induce PRX overoxidation, interfering in this way with the normal catalytic cycle.

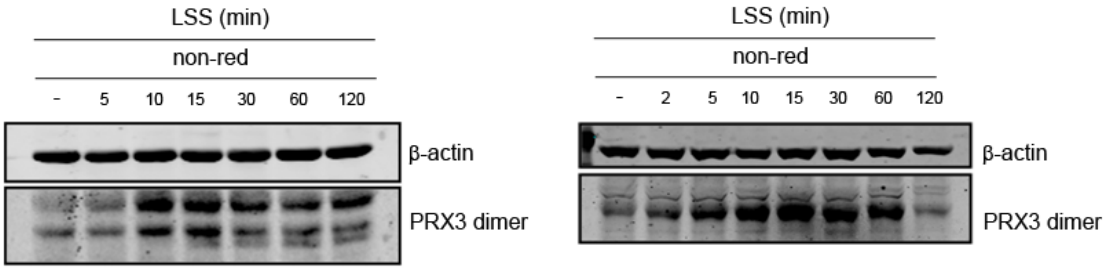

Figure 25. LSS induces PRX3 dimerization in different endothelial cells. *PRX3 dimerization induced by LSS was studied in MLEC (left panel) and BAEC (right panel). Endothelial cells exposed to LSS were lysed in the presence of the alkylating reagent N-ethyl maleimide (NEM) and analyzed by SDS-PAGE in non-reducing conditions. Immunoblots are representative of at least three independent experiments.*

By using exogenous H_2O_2 as a positive control, we confirmed that laminar flow was not able to induce PRX inactivation (***Figure 26***).

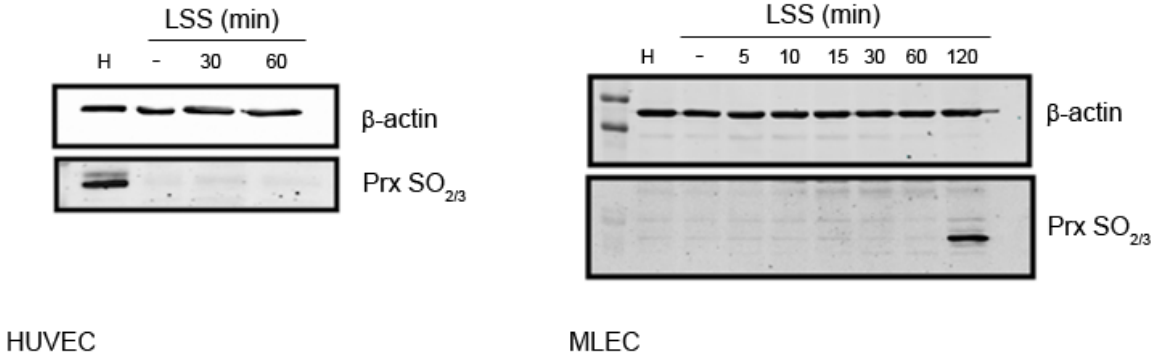

Figure 26. LSS does not induce PRX overoxidation. *Endothelial cells (HUVEC in the left panel and MLEC in the right panel) were exposed to laminar flow and PRX overoxidation was detected by the use of an specific antibody against PRX $SO_{2/3}$. 100 µM H_2O_2 (H) for 30 minutes was used as positive control.*

The generation of controlled glucose oxidase-mediated hydrogen peroxide fluxes demonstrated that overoxidation of PRX3 occurs only under high concentrations PRX3 dimerization is no longer present (***Figure 27***).

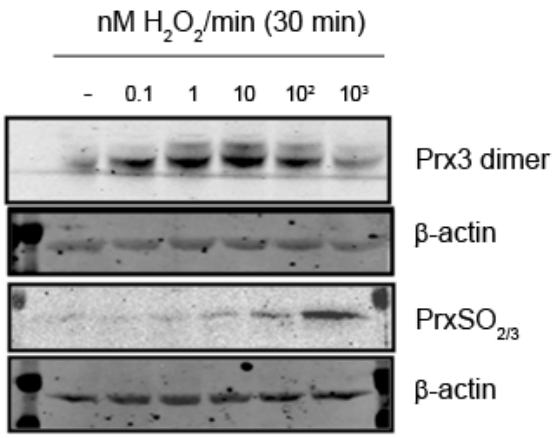

Figure 27. High fluxes of H_2O_2 generated by glucose oxidase induce a decrease in PRX3 dimerization and a notorious PRX overoxidation*. HUVEC were treated with different amounts of glucose oxidase to generate continuous H_2O_2 fluxes. Lysates were analyzed by immunoblots with specific antibodies as indicated.*

This set of results is consistent with the notion that PRX3 is an exquisitely sensitive enzyme responding to concentrations of hydrogen peroxide within the signaling range and hence suggesting a potential role for this redox sensor during laminar flow.

4.2.2 DISULFIDE BOND FORMATION BY LSS IS NOT ASSOCIATED WITH CHANGES IN THE OLIGOMERIC CONFORMATION OF PRX3

Like in other 2-Cys PRXs, the monomeric subunit of PRX3 is a compact globular structure consisting of seven-stranded twisted β sheets surrounded by four α-helices with the peroxidatic cysteine situated in the first turn of the N-terminal section of helix α2 (Cox et al., 2010). PRX3 is an obligate homodimer, which uses the intermolecular redox active disulfide center for its action as an antioxidant enzyme (Wood et al., 2002). For PRX3, different oligomeric states have been described, ranging from individual dimers to complex quaternary structures including doughnut-shaped toroids made up to 12 monomers (dodecamer) with internal and external diameters of 70 Å and 150 Å

respectively (Wood et al., 2003, Gourlay et al., 2003). Although the physiological significance of PRXs oligomerization is not fully understood, it has been reported that AhpC (bacterial peroxiredoxin) mutants that cannot form toroids exhibit a 100-fold decrease in their catalytic efficiency (Parsonage et al., 2005). To test if LSS could modify the oligomerization state of PRX3 we used blue-native PAGE gels. As shown in ***Figure 28***, PRX3 toroids are not disassembled by flow suggesting that perhaps the activation of PRX3 is associated with the formation of "i*ntratoroid*" disulfide bonds.

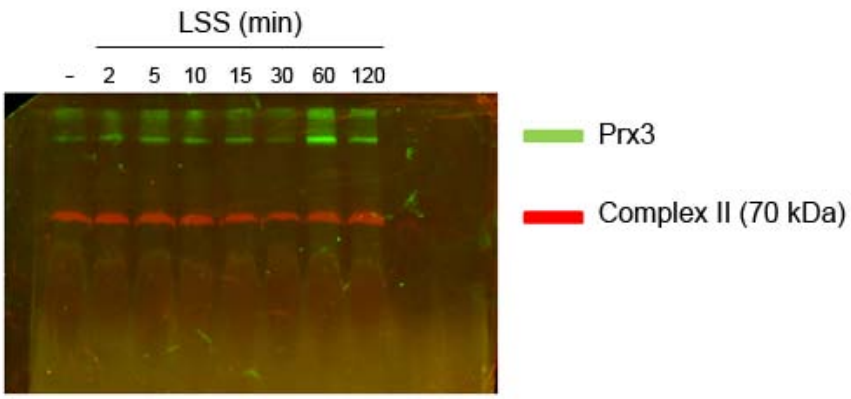

Figure 28. PRX3 oligomeric conformation is not modified by flow induction. *Lysates from BAEC subjected to different periods of LSS were resolved in a 8-16% Bis-Tris Blue Native polyacrilamide gel and analyzed by western blotting using specific antibodies against PRX3 and mitochondrial complex II as control.*

4.2.3 LSS INDUCES MITOCHONDRIAL ROS PRODUCTION

PRX3 has been described to be located exclusively in the mitochondria (Fujii and Ikeda, 2002). We have previously detected ROS production after shear stress in the cytosol. However, mitochondrial involvement had not been directly addressed. To do that, we used a specific mitochondrial ROS probe derived from ethidium bromide (Mitosox). This is a fluorogenic cell-permeant dye selectively targeted to mitochondriae. After LSS exposure, we incubated stressed and static cells with 5 µM Mitosox probe in HBSS for 20 minutes at 37ºC. Cells were trypsinized, resuspended in PBS and analyzed by flow cytometry.

Laminar shear stress increased mitochondrial ROS production as detected by an increase in Mitosox fluorescence in the FL3 channel (***Figure 29***). This result is consistent with the activation of PRX3 within mitochondriae.

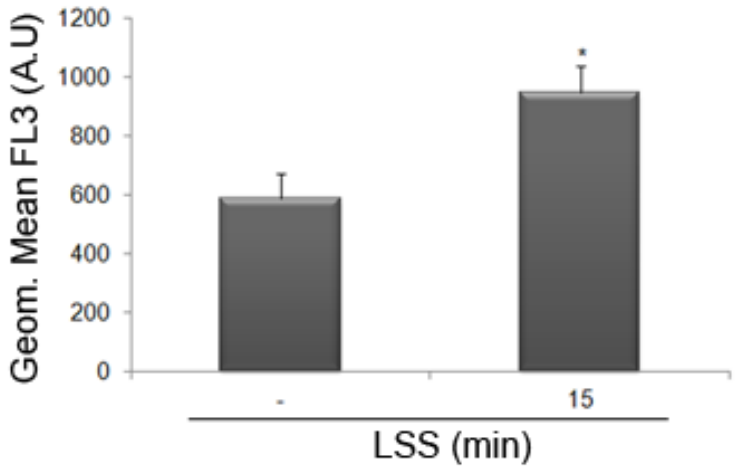

Figure 29. Laminar shear stress increases mitochondrial ROS production. *BAECs were exposed to LSS and mitochondrial superoxide radical anion production was analyzed by flow cytometry in the FL3 channel with the Mitosox probe. Bar graph represent means ± SEM of n=3 experiments. *p<0.05 vs control*

4.2.4 PRX3 DIMERIZATION IS SPATIALLY DEPENDENT

Since PRX3 activation is due to ROS generation, we tried to reduce ROS content in cells priorly to the exposure to LSS, in an attempt to prevent PRX3 dimerization. Preincubation of endothelial cells with PEG-catalase (an enzyme that catalyzes the decomposition of H_2O_2 to water and oxygen) failed to abrogate PRX3 activation. Similar results were obtained when treating the cells with the general antioxidant reagent N-acetyl cysteine (NAC) (***Figure 30***).

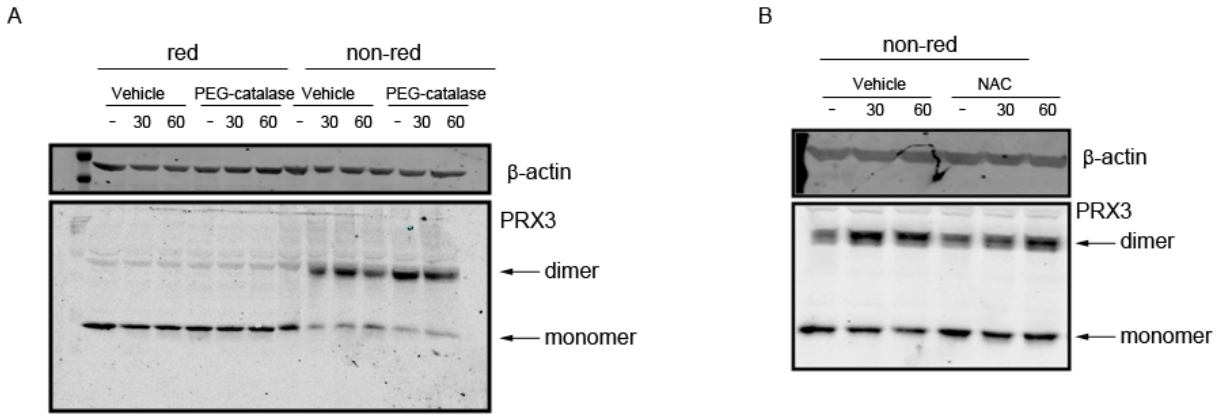

Figure 30. General antioxidants do not prevent PRX3 dimerization induced by LSS. *A) BAEC were exposed to LSS for the indicated time points in the presence or absence of PEG-catalase (100 units/ml overnight) and PRX3 dimerization was detected as described above in Experimental Procedures section. B) Effects of N-acetyl cysteine (NAC, 1 mM overnight) on LSS-induced PRX3 dimerization. Each immunoblot is a representative one from three independent experiments.*

As none of these two antioxidant were able to abolish mitochondrial ROS production by LSS tested Mitosox oxidation (***Figure 31***), although we cannot exclude that more selective mitochondrial antioxidants would be capable of preventing PRX3 dimerization.

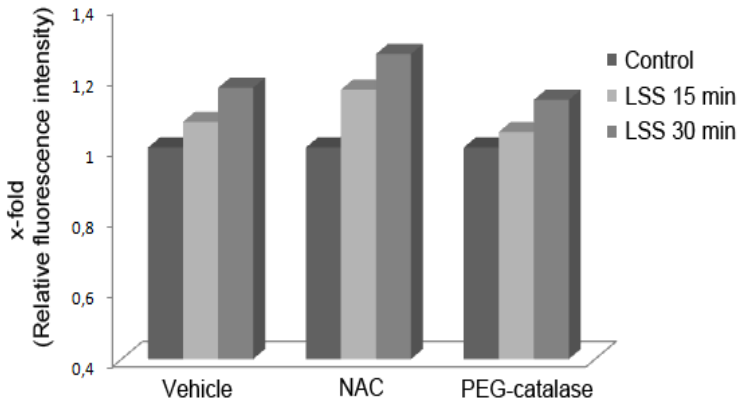

Figure 31. Treatment with NAC or PEG-catalase does not affect mitochondrial ROS production induced by LSS. *BAEC were exposed to LSS for the indicated time points in the presence or absence of PEG-catalase (100 units/ml overnight) or NAC (1 mM overnight). After LSS exposure endothelial cells were incubated for 20 minutes with 5 μM Mitosox and mitochondrial superoxide radical production was analyzed by flow cytometry in the FL3 channel.*

However, in spite of being a highly diffusible molecule, it is likely H_2O_2 preferentially reacts with proteins present in the same organelle where it is produced. In our studies (Breton-Romero et al., 2012), we described the importance of NOX4 in signal transduction during LSS. As some reports have ascribed NOX4 to mitochondriae at least in myocardiocytes (Kuroda et al., 2010); we tested if the genetic deletion of NOX4 could influence LSS-induced PRX3 dimerization. Studies in murine lung endothelial cells from NOX4-deficient mice did not confirm NOX4 dependence of PRX3 activation by laminar flow (***Figure 32***).

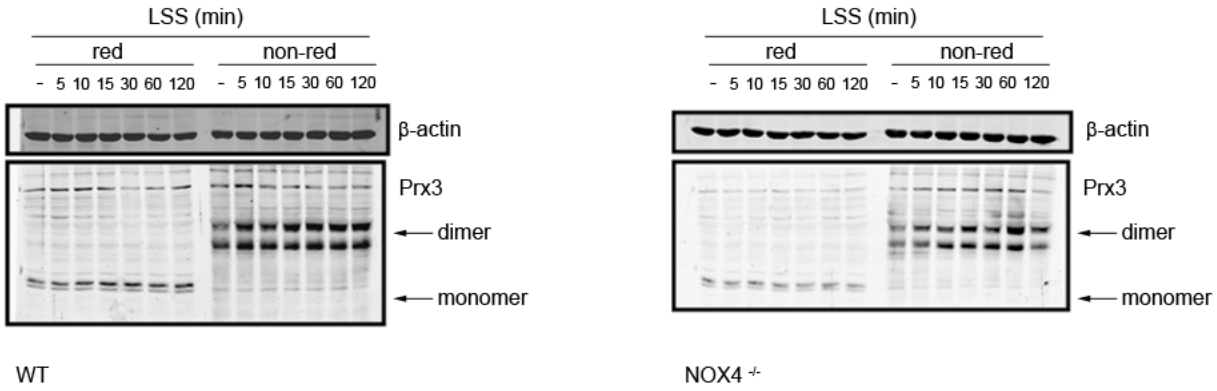

Figure 32. Nox4 deficiency does not prevent PRX3 dimerization. *MLECs isolated form wild-type and NOX4-knockout mice were exposed to LSS and PRX3 dimerization was analyzed by immunobloting. A representative western blot from at least three different experimenst with similar results is shown.*

To investigate the potential regulatory role of organelle topological confinement of H_2O_2 generation in PRX3 activation, we specifically induced ROS production within the mitochondriae by using inhibitions of mitochondrial ETC complexes known to actively participate in superoxide anion radical generation. Both rotenone (complex I inhibitor) and myxothiazol (complex III inhibitor) induced an increase in ROS production (***Figure 33***).

Consistently, these inhibitors promoted an activation of the enzyme evidenced by its dimerization (***Figure 34***).

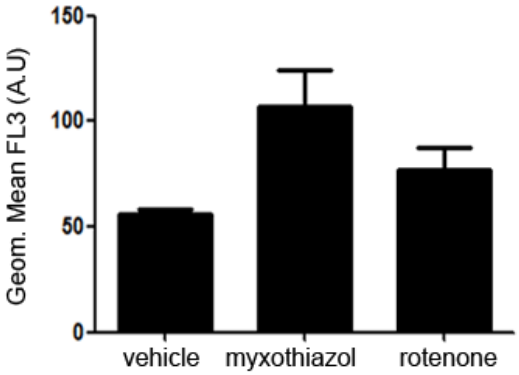

Figure 33. Inhibition of complexes I and III of the electron transport chain is associated with an increase in mitochondrial ROS production. *BAEC were treated with myxothiazol or rotenone 10 μM and 2 μM respectively) and mitochondrial generation of superoxide radical was detected with the Mitosox fluorescent probe by flow cytometry in FL3 channel.*

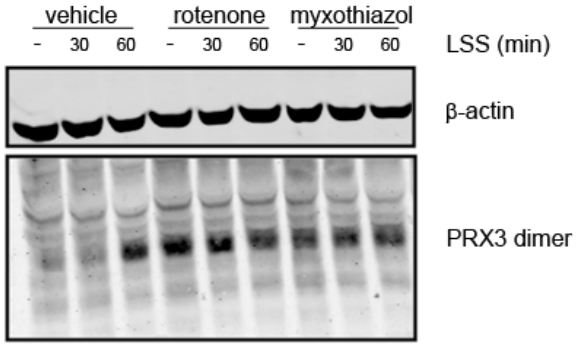

Figure 34. Mitochondrial generation of ROS is sufficient for PRX3 dimerization. *BAEC were treated with myxothiazol or rotenone 10 μM and 2 μM respectively) for 30 minutes before LSS induction and Prx3 dimerization was detected by immunoblot.*

Taken together these results suggest that PRX3 activation by laminar shear stress depends very significantly on the increase of mitochondrial ROS levels.

4.2.6 LAMINAR SHEAR TRESS CAUSES MITOCHONDRIAL FRAGMENTATION.

To confirm the intracellular distribution of PRX3 in our model, we performed confocal immunofluorescence staining studies. Confluent endothelial cells were stained in static conditions using the specific antibody against PRX3 and typical mitochondrial network morphology was observed (***Figure 35***).

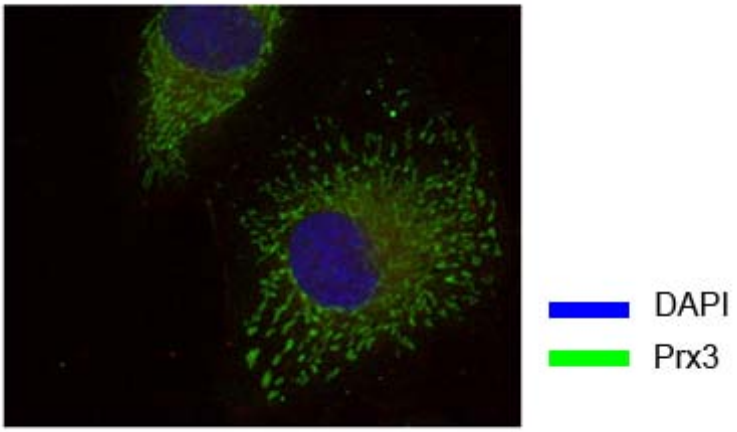

Figure 35. PRX3 is exclusively located in mitochondria. *Confluent BAEC were stained using antibodies specific for PRX3 and a secondary antibody conjugated to Alexa Fluor 488 (green). Images were taken by confocal microscopy. Nuclei were stained with DAPI (blue).*

Keeping in mind that shear stress was able to induce PRX3 activation as shown by its dimerization we decided to investigate if it could alter its subcellular localization. We exposed to LSS BAEC to LSS, and after incubating against PRX3 specific antibody we observed an interesting and unexpected staining pattern completely different from the one obtained in static conditions and compatible with profound changes in mitochondrial morphology (***Figure 36***).

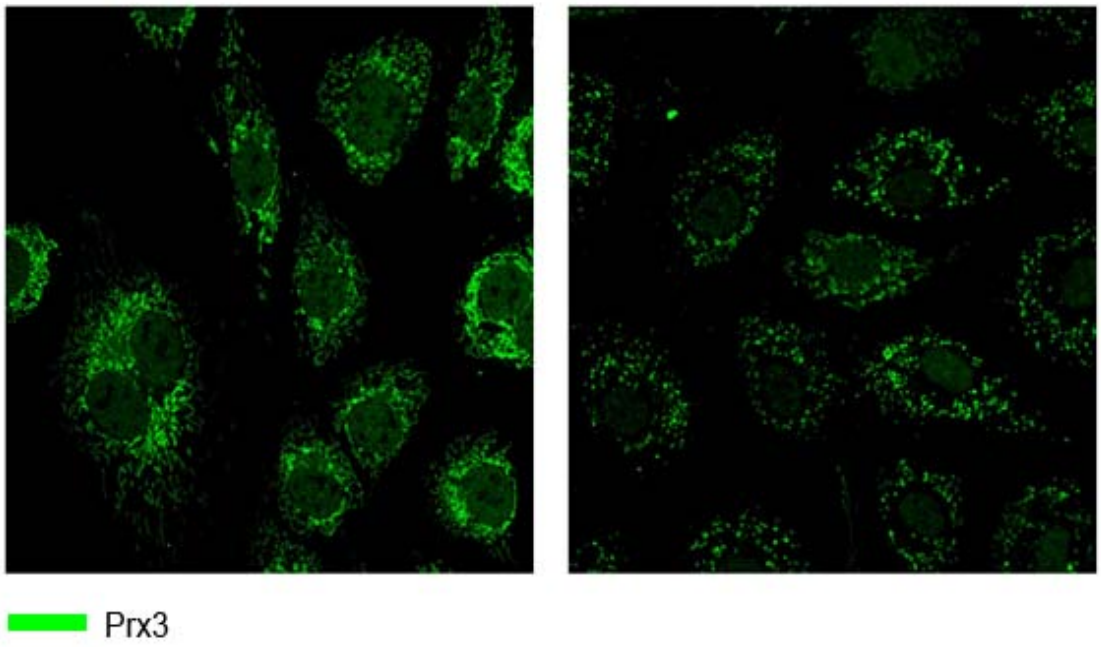

Figure 36.. LSS is associated with a different pattern of PRX3 staining in endothelial cells suggesting changes in mitochondrial dynamics. *Confluent BAEC were exposed to LSS for 15 minutes. Cells were stained using the specific Prx3 antibody, conjugated with a secondary antibody conjugated to Alexa Fluor 488 (green) and imaged by confocal microscopy.*

Taken together, these results indicate that PRX3 is activated at early time points of shear stress. Even when its subcellular location is apparently unaffected significant changes in mitochondrial morphology were detected, an observation which prompted us to investigate these changes in more detail.

To further study potential changes in mitochondrial dynamics during laminar shear stress we used the commercially available mitochondrial-specific marker Mitotracker. We incubated the cells with this reagent before LSS exposure.

As shown in ***Figure 37***, LSS causes a disruption of the tubular mitochondrial network and mitochondriae acquire a fragmented phenotype as compared with static conditions

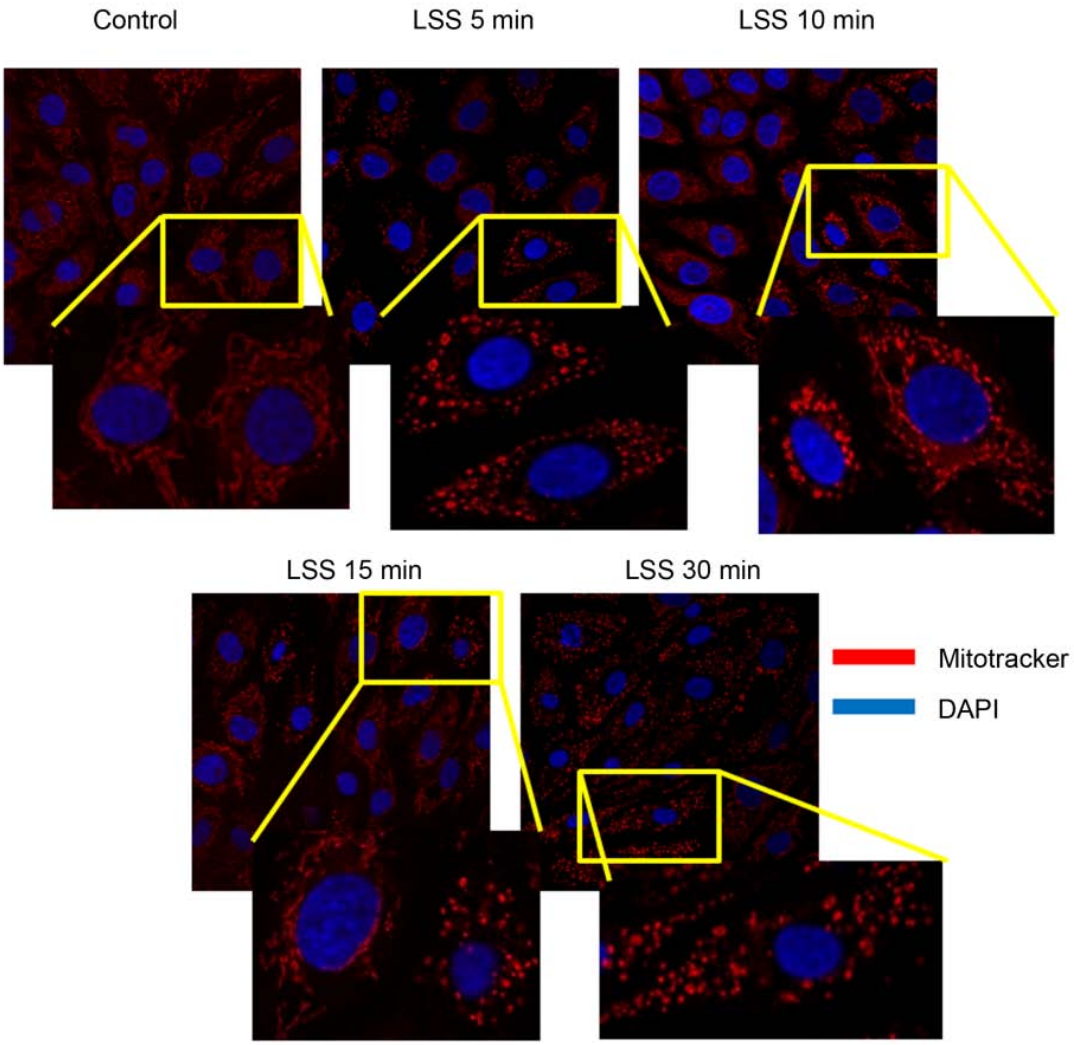

Figure 37. LSS causes a disruption of the tubular mitochondrial network. *Confluent BAEC were incubated for 30 minutes with 500 mM Mitotracker DeepRed before LSS induction. Cells were fixed with 2% paraformaldehyde and permeabilized with 0,25% Triton X-100. Nuclei were labeled with DAPI in 3% bovine serum albumin for 5 minutes at room temperature.*

Samples were also processed by transmission electron microscopy (TEM). For quantification, at least 150 mitochondriae corresponding to a discrete value of sizes for each condition was analyzed from TEM pictures. Data obtained from EM cross-sections of endothelial monolayers revealed a smaller average size in mitochondriae after shear

stress induction compared with static conditions (***Figure 38***). Together these data strongly suggested that during laminar shear stress mitochondrial networks are visibly re-organized from long filamentous interconnected tubules into small punctate spheres.

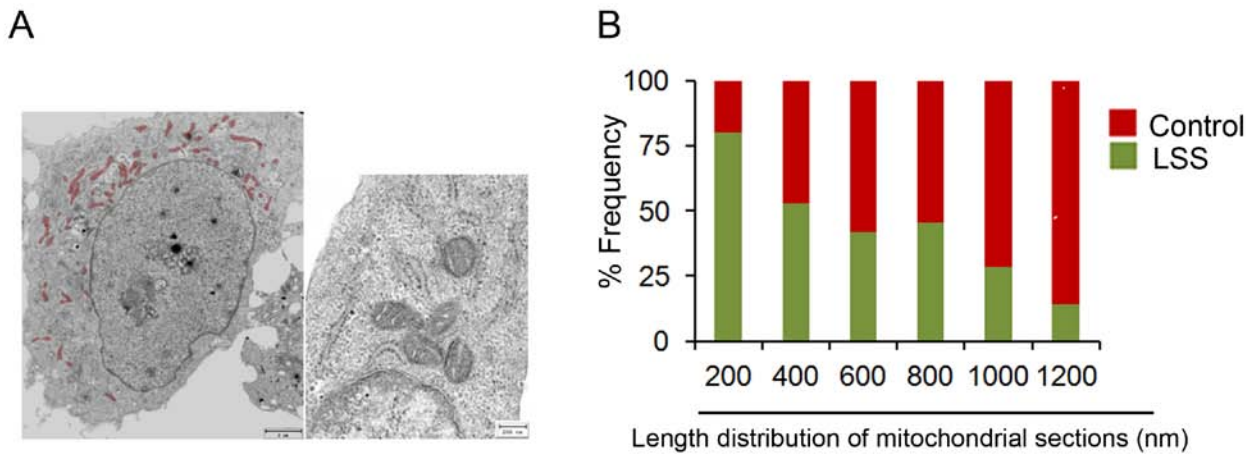

Figure 38. LSS induces changes in mitochondrial size. *Confluent BAEC were exposed for 15 minutes to LSS. Cells were fixed with 2% paraformaldehyde 2% glutaraldehyde and analyzed by electron microscopy (EM). A) Representative image obtained from EM cross-sections in BAECs monolayer (mitochondriae shown in red). Images shown in more detail in the right. B) Bar graph represents quantification of mitochondrial lengths from different 2D EM sections randomly selected (n>150 mitochondriae).*

4.2.7 MITOCHONDRIAL FISSION INDUCED BY LAMINAR SHEAR STRESS IS DRIVEN BY THE DYNAMIN-RELATED PROTEIN 1 (DRP1)

Mitochondria are dynamic organelles that are constantly elongating and dividing to form a network that spans the entire area of the cell (Detmer and Chan, 2007). They are able to shuttle their morphology between two distinct arrangements by undergoing the processes of mitochondrial fusion and fission to generate an elongated interconnected mitochondrial network or a discretely fragmented phenotype respectively (Liesa et al., 2009). The ability of mitochondriae to move and fuse is required by the cell, whereas mitochondrial division or fission allows the correct redistribution of mitochondrial DNA during cell division (Ong and Hausenloy, 2010). Changes in mitochondrial morphology are regulated by the

mitochondrial fusion proteins mitofusins 1 (MFN1), mitofusin 2 (MFN2) and optic atrophy type 1 (OPA1) and the mitochondrial fission proteins dynamin-related peptide 1 (Drp1) and mitochondrial fission protein 1 (Fis1). As mitochondrial fragmentation observed during laminar flow could reflect impaired fusion, enhanced fission or both, we focused our attention on mitochondrial fission dynamics. In mammals, fission is driven by the dynamin-related protein 1 (Drp1). Drp1 is mostly a cytoplasmic protein, with only approximately 3% associated with the mitochondrial outer membrane under basal conditions. To mediate mitochondrial division Drp1 is self-assembled into large multimeric structures and it is recruited to the outer mitochondrial membrane by a mechanism that is not fully understood but may involve Fis1 in some species (Smirnova et al., 2001, Sheridan and Martin, 2010). Once recruited to the outer mitochondrial membrane of the mitochondrial tubules, Drp1 forms spirals around mitochondrial tubules, constricts them, wraps more tightly around the constriction part and ultimately induces fission (Hoppins et al., 2007). In order to study if Drp1 could be involved in laminar shear stress-mediated mitochondrial fragmentation, we induced shear stress experiments and studied Drp1 location in mitochondrial or cytoplasmic fractions. We permeabilized plasmatic membranes with digitonine (50 µg/µl final concentration), centrifugated mitochondrial fractions and lysed them with RIPA buffer. The integrity and purity of the mitochondrial fraction were corroborated by using specific antibodies against abundant known proteins. The presence of CuZnSOD was used as the control for cytosolic fractions detection, while MnSOD was used to confirm mitochondrial purity. As shown in ***Figure 39***, 2-10 minutes after initiating flow experiments, we were able to detect a small fraction of Drp1 in mitochondrial enriched fractions, suggesting a correlation with the early fission process.

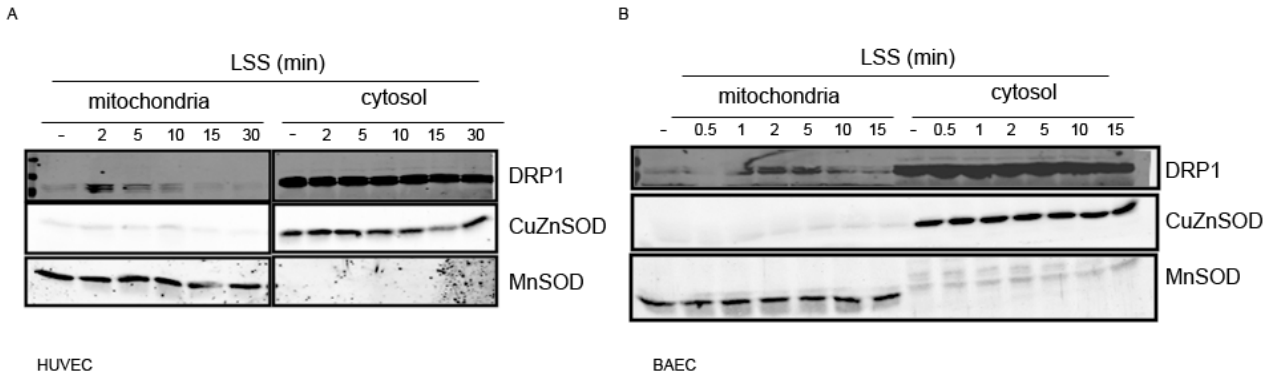

Figure 39. The mitochondrial fission-related protein Drp1 is recruited from the cytosol to the mitochondriae upon LSS exposure*. . Confluent HUVEC and BAEC were exposed to LSS for the indicated times, trypsinized and resuspend in buffer A (150mM KCl, 25mM Tris-HCl, 2mM EDTA, 0.1% BSA, 10mM K-phosphate, 0.1mM $MgCl_2$) and 16mg/ml of digitonine. Mitochondriae were collected by centrifugation and the cytosolic fraction was recovered from the supernatant.*

4.2.8 LAMINAR SHEAR STRESS PROMOTES DRP1 PHOSPHORYATION AT ITS ACTIVATING SITE.

Drp1 activity is regulated by a variety of posttranslational modifications including phosphorylation, sumoylation, ubiquitination, and S-nitrosylation (Soubannier and McBride, 2009, Lackner and Nunnari, 2009, Santel and Frank, 2008). With respect to phosphorylation Drp1 can be phosphorylated at different serine residues leading to changes in its fission activity. While phosphorylation at Ser616 by Cdk1/cyclin B leads to Drp1 activation and the consequent fission stimulation, phosphorylation at Ser637 by PKA inhibits mitochondrial division though an inhibition of Drp1 translocation to mitochondria (Chang and Blackstone, 2007, Cribbs and Strack, 2007). We studied if laminar shear stress could alter Drp1 activity and promote its translocation to the outer mitochondrial membrane by inducing Drp1 phosphorylation. As shown in ***Figure 40***, Drp1 is phosphorylated at its activating residue Ser616 by laminar flow.

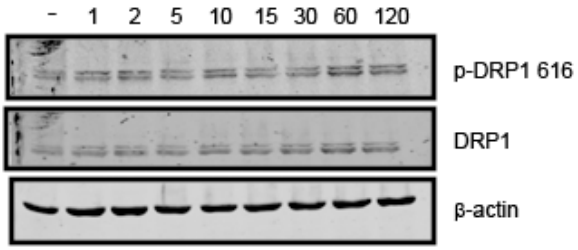

Figure 40. Laminar shear stress induces the phosphorylation (activation) of Drp1 in endothelial cells. *BAEC were subjected to LSS for the indicated times (min), and phosphorylation of Drp1 at its activating site was determined using phospho-specific antibodies.*

These results suggested an important role for Drp1 in laminar shear stress-induced mitochondrial fragmentation.

4.2.9 LAMINAR SHEAR STRESS ALTERS MITOCHONDRIAL BIOENERGETIC.

Mitochondiral dynamics have important bioenergetic consequences (Westermann, 2012, Jezek and Plecita-Hlavata, 2009). Since there is growing evidence of a close relationship between mitochondrial network organization and energy production we studied the effect of laminar shear stress on it. In 2012, Westermann et al proposed a model in which small and fragmented mitochondriae are more prevalent in quiescent and respiration-inactive cells. We determined respiration rates after laminar flow exposure compared with static conditions by two different methodologies. Oxygraphic studies of oxygen consumption were performed by the well established method based on the Clark electrode where the rate of oxygen diffusion to the cathode of the monitoring electrode depends on the oxygen concentration in the incubation chamber where the sample was added. The basal oxygen consumption in the samples was monitored, and then, the uncoupler FCCP was injected within the sample to achive the highest rate of respiration. The absence of effect of an exogenous uncoupler in static conditions in contrast with the effect presented after shear stress induction, suggested that endothelial cells were already under the maximal rate of respiration, and that only after a decrease induced by laminar flow, FCCP was able to increase the respiration rate (data not shown).

Results obtained from oxygraphic studies showed a significantly lower rate of endogenous respiration in cells exposed to laminar shear stress as compared to non-induced cells (***Figure 41***). To gain insight into LSS regulation of mitochondrial function we assessed oxygen consumption in attached instead of suspension cells. After LSS, cells were trypsinazed and rapidly attached by Cell-Tack onto plates specifically designed for the Seahorse Bioscience XF24-3 Analyzer. Plates were equilibrated at 37ºC for 40 min. All wells were injected sequentially with 1 µM oligomycin, 0,6 µM FCCP, 0,4 µM FCCP and 1 µM antimycin A plus 1 µM rotenone to induce different respiratory states. FCCP stimulates respiration in mitochondria by uncoupling ATP synthesis from electron transport, while oligomycin inhibit respiration by inhibiting ATP synthase, and rotenone and antimycin both completely suppress mitochondrial respiration by inhibiting Complex I and Complex III respectively, in the electron transport chain (see experimental procedures for details). As shown in ***Figure 41***, cells subjected to LSS showed lower basal respiration rates normalized by protein content (nmol/min/mg) as compared to static cells. Data obtained with two procedures support that LSS induces a decrease in mitochondrial respiration suggesting that there is a reduced rate of mitochondrial ATP synthesis in vascular endothelial cells after laminar flow induction.

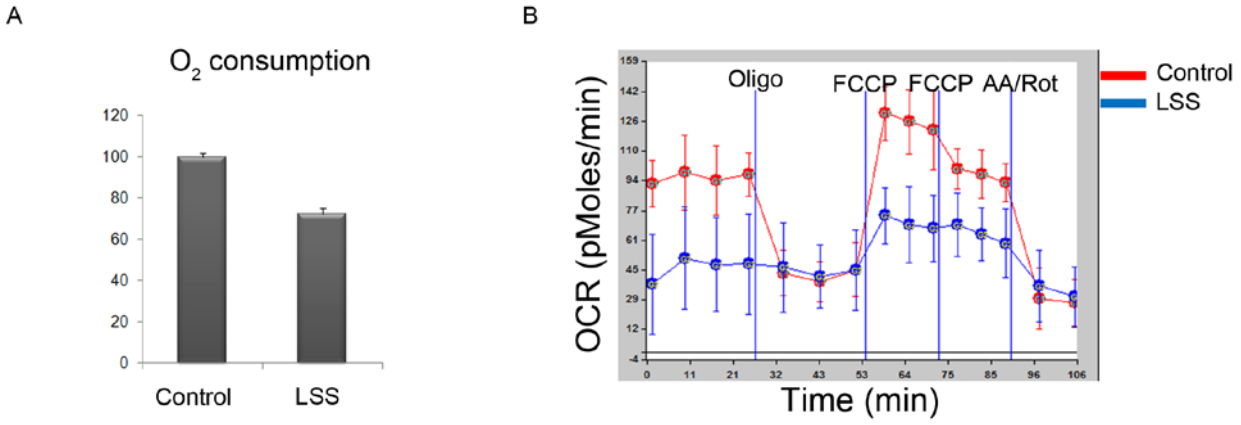

Figure 41. Laminar shear stress is associated with a decrease in endothelial oxygen consumption*. A) HUVECs were exposed to shear stress for 15 minutes, trypsinazed and resuspended in EBM medium. A Clark-type oxygen electrode was used to monitor oxygen consumption. B) Serum starved HUVEC were stimulated for 15 minutes to LSS, trypsinazed and split in Cell-Tak coated SeaHorse Bioscence plate and respiratory rates were measured. (A: 2 µM oligomycin; B: 0.6 µM FCCP; C: 0.4 µM FCCP; D: 1 µM Rotenone and 1 µM Antimycin A.*

We next studied the effect of LSS on mitochondrial membrane potential (ΔΨm). ΔΨm (negative inside and positive outside) determines the electrochemical proton gradient across the mitochondrial inner membrane and constitutes an important indicator of mitochondrial energetic state and cell viability, as well as of mitochondria function and integrity (Chen, 1988). We previously had detected an increase of mitochondrial ROS production after LSS. As the formation of mitochondrial ROS is dependent on ΔΨm, and ROS levels increases exponentially as ΔΨm is hyperpolarized (Lee et al., 2002a), we studied ΔΨm by flow cytometry using the cationic dye Tetramethylrhodamine, methyl ester (TMRM). The quenching of TMRM fluorescence is proportional to ΔΨm (Nicholls and Ward, 2000). In static cells, as expected, the ionophore uncoupler FCCP dissipated ΔΨm (fails to sequester TMRM). In contrast LSS was associated with membrane hyperpolarization (***Figure 42***).

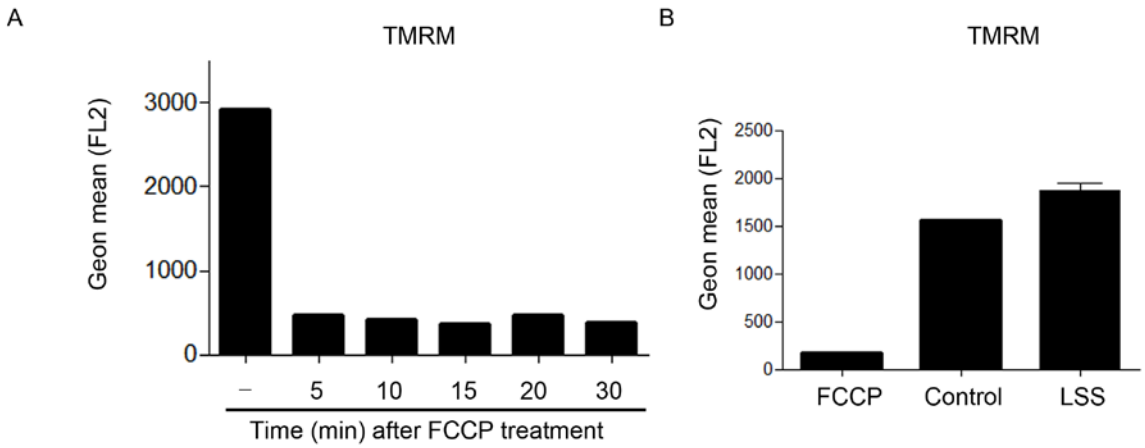

Figure 42. LSS promotes mitochondrial membrane hyperpolarization*. A) BAEC were treated with the uncoupler compound FCCP 5 μM for the indicated time points and incubated with TMRM for 10 minutes (0,5 μM). Mitochondrial polarization was determined by flow cytometry. B) After LSS (15 min) or FCCP (5 μM for 30 minutes) mitochondrial potential was studied by measuring TMRM fluorescence by flow cytometry.*

All this set of results pointed to the mitochondria as an important organelle able to detect and respond to the mechanical force induced by laminar flow and transduce it into biological signals. We hereby propose a model in which Drp1 is an effector of laminar flow, becomes activated and translocates to the outer mitochondrial membrane. Drp1

forms spirals around mitochondrial tubules, constricts them and induces mitochondrial fission which correlates with an increase in ΔΨm and a decrease in mitochondrial respiration. This could lead to an increase in proton leakage and the consequent increment of ROS and PRX3 dimerization.

Several steps in this model remain to be formally proven (see Discussion). An obvious one is the mechanism by which LSS may phosphorylate and activate Drp1.

Changes during conditions of SS have been described to de detected by plasma invaginations that are characterized by the high concentration of specific membrane structures known as caveolae (Razani and Lisanti, 2001). Caveolae play an important role in the regulation of different signaling pathways. In particular, the abundance of caveola is markedly increased in endothelial cells under LSS conditions (Isshiki et al., 2002, Boyd et al., 2003). Yu et al (Yu et al., 2006) have suggested that caveolae are involved in some of the earliest steps associated with the detection of SS in blood vessels. To investigate the role of caveolae in the signaling pathway of our interest, we isolated MLECs from Cav1-deficient mice and counterpart wild-type controls, and studied Prx3 dimerization. As shown in ***Figure 43***, we did not detect significant differences between MLEC from Cav1 knockout animals and those form wild-type.

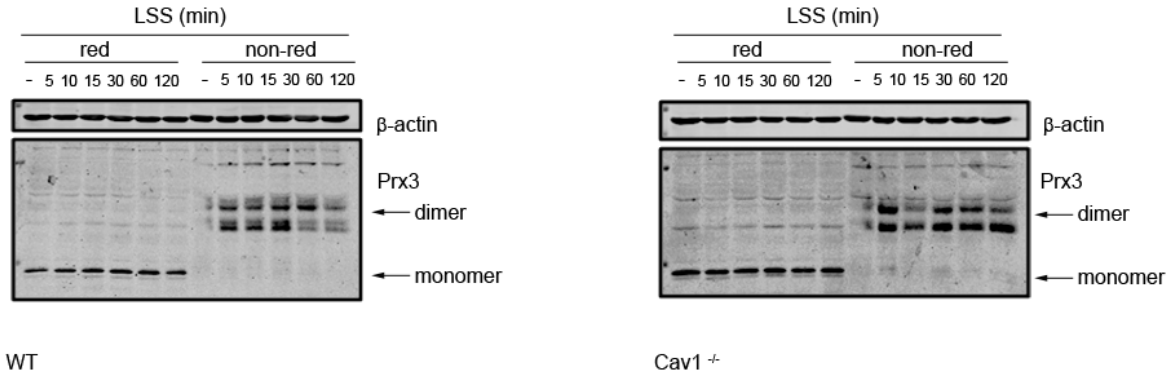

Figure 43. Cav1 deficiency does not prevent PRX3 dimerization. *MLEC isolated from wild-type and Cav1-knockout mice were exposed to LSS and PRX3 dimerization was analyzed by immunobloting. A representative western blot from at least three different experiments with similar results is shown.*

Given the importance of the cytoskeleton in endothelial cell response to SS and the fact that mitochondriae are anchored to it via actin binding complexes in the outer membrane (Boldogh et al., 1998), it was tempting to explore if the cytoskeleton could provide the necessary framework to transmit the signal from the plasma membrane to the mitochondriae. As shown in ***Figure 44***, we detected cytoskeleton rearrangements during LSS. We observed a rapid polymerization of F-actin at very early time points of SS, but a dephosphorylation of myosin light chain 2, thus altering stress fibers formation.

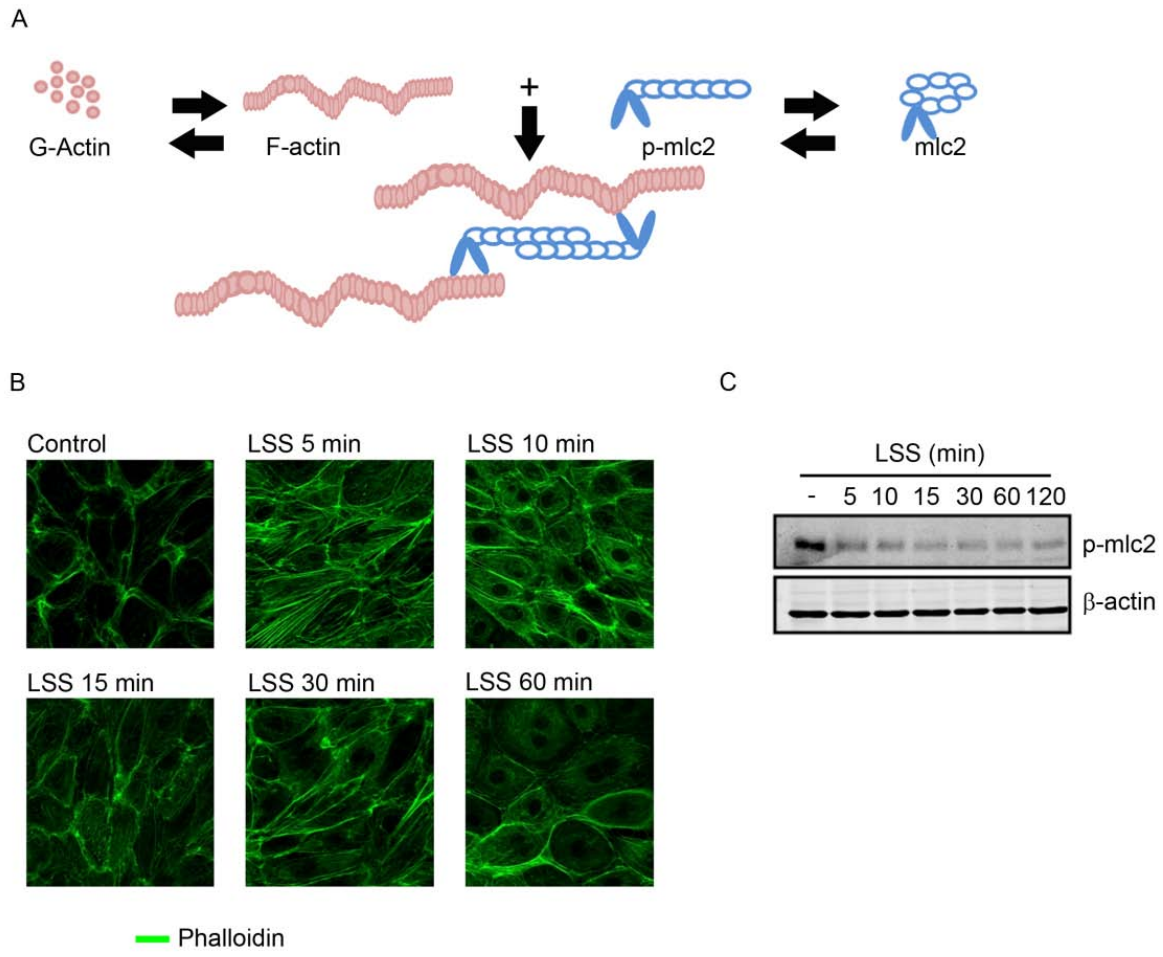

Figure 44. LSS induces cytoskeletal rearrangements. *A) Schematic depicting stress fibers and their components: filaments of F-actin cross linked with active myosin light chain 2 (mlc2). B) Serum starved BAEC were exposed to LSS for the indicated time points and phalloidin was detected by immunofluorescence. C) HUVEC were exposed to LSS for the indicated time points and lysates were analyzed by immunoblotting with of specific antibodies.*

4.3 p38 MAPK CONTROLS eNOS ACTIVATION IN A INDEPENDENT ROS MANNER: ROLE OF PTEN IN THE MODULATION OF ADP-DEPENDENT SIGNALING PATHWAYS

Laminar shear stress has been described to directly activate platelets inducing the release of different agonists which interact with endothelial receptors (Kroll et al., 1996, Anderson et al., 1978). Among these factors, extracellular nucleotides have been defined as vasoactive substances able to interact through endothelial receptors. It has been demonstrated that platelets store ADP at concentrations as high as 653 mM (Holmsen and Weiss, 1979), and upon stimulation, activated platelets release ADP which binds to P2Y1 receptors.

Despite the well established role of the purine nucleotide ADP in platelet biology, relatively little is known about the role of ADP receptors in the vascular endothelium. ADP regulates vascular homeostasis through the activation of selective cell surface receptors located not only on platelets, but also in vascular smooth muscle and endothelial cells (Burnstock, 2007). ADP receptors include the G protein-coupled P2Y and the ligand-gated P2X ion channel receptors. In particular, studies in bovine aortic endothelial cells (BAECs) showed that P2Y1 is the principal purinergic receptor subtype which mediates ADP signaling responses in endothelial cells (Hess et al., 2009). In cardiovascular tissues and cells, the purine nucleotide ADP has been extensively studied, and ADP receptor antagonists have become widely used in cardiovascular therapeutics (Erlinge and Burnstock, 2008, Ralevic and Burnstock, 2003). However, several important aspects regarding the signaling pathways elicited by ADP in the vascular endothelium remain incompletely understood. Previous studies showed that ADP activated eNOS in BAEC. Although eNOS activity was stimulated by ADP, studies using chemical inhibitors or siRNA mediated specific knockdown of the main known upstream modulators of eNOS, did not alter either ADP-dependent eNOS phosphorylation at Ser1177 or nitric oxide production. Pathways analyzed included phosphoinositide 3-kinase/AKt, Erk ½, Src, and calcium/calmodulin-dependent kinase kinase β (CaMKKβ) and AMP-activated protein kinase (AMPK) (Hess et al., 2009).

Given the role of p38 MAPK on eNOS activation, we wondered if this MAPK could play a role in ADP-dependent stimulation of NO pathway.

4.3.1 p38 MAPK INHIBITION BLOCKS ADP-DEPENDENT eNOS ACTIVATION

To this end, we first treated endothelial cells with ADP and checked p38 MAPK activation. As shown in ***Figure 45***, physiological concentrations of ADP promote a robust phosphorylation of p38 MAPK. Panel A and B, show a time course and a dose response experiment for ADP-stimulated p38 MAPK phosphorylation at its activating residues.

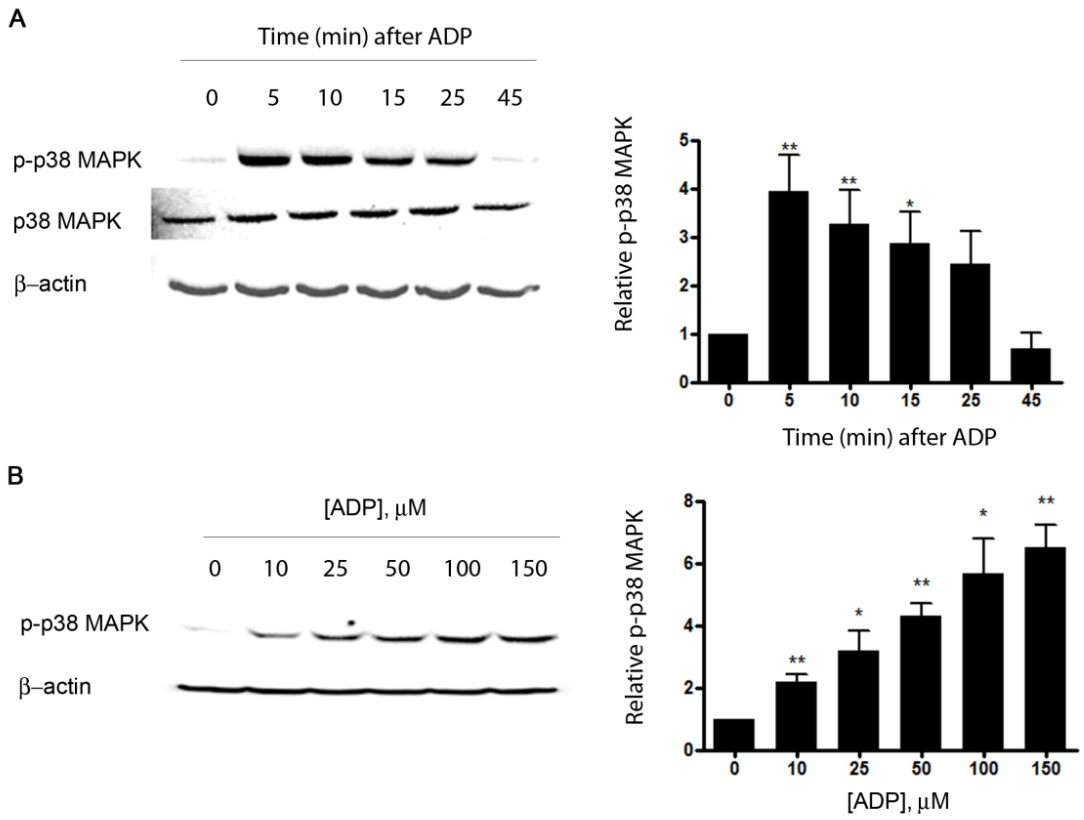

Figure 45. ADP stimulates p38 MAPK phosphorylation. *Lysates prepared from ADP-treated endothelial cells were analyzed in immunoblots probed with antibodies as shown. A) time course of p38 MAPK phosphorylation in endothelial cells treated with ADP (25 μM); B) dose response (determined at t = 20min) for ADP-stimulated p38 MAPK phosphorylation. The blots shown are representative of at least three independent experiments with similar results; the graphs next to each blot represent quantification of pooled data.*

We transfected the endothelial cells with a duplex siRNA targeting construct to knockdown specifically p38 MAPK and studied eNOS activity by measuring nitric oxide production after ADP stimulation. eNOS activity was quantified by measuring the formation of L-[3H]citrulline from L-[3H]arginine. The eNOS activity reaction was initiated in cultured BAEC by adding L-[3H]arginine (10 µCi/ml, diluted with unlabeled L-arginine to give a final concentration of 10 µM). As shown in ***Figure 46***, siRNA-mediated p38 MAPK-knockdown markedly suppressed ADP-induced eNOS activity. To confirm the role of p38 MAPK, we incubated the endothelial cells with a specific p38 MAPK chemical inhibitor (PD169316) before ADP treatment, and evaluated eNOS activity. As expected, similar results were obtained with the cell permeable, competitive and selective p38 MAPK inhibitor.

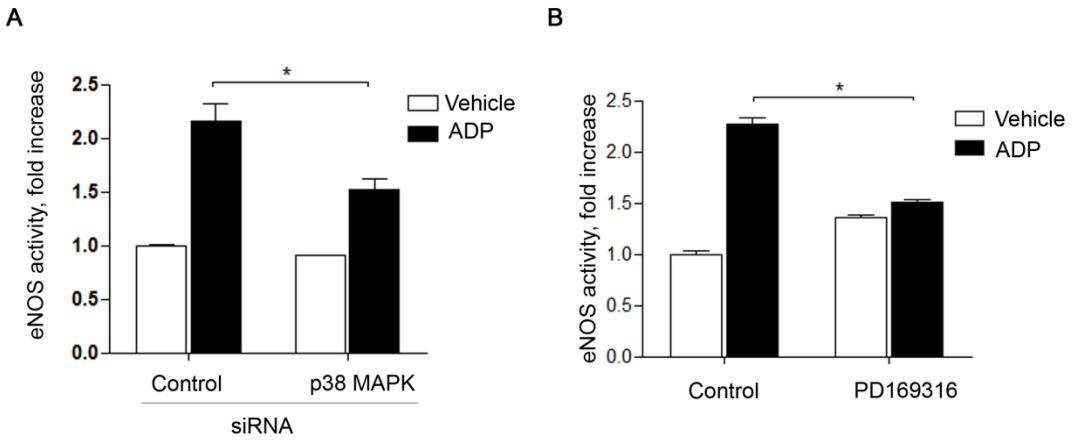

Figure 46. Effects of siRNA-mediated knockdown or pharmacological inhibition of p38 MAPK on eNOS activity. *A) Endothelial cells transfected with control or p38 MAPK siRNA targeting constructs were treated with ADP (25 µM) for 20 minutes and eNOS activity was measured using the [3H]-arginine-[3H]-citrulline assay. B) shows the pooled results of eNOS.*

These concordant effects of siRNA-mediated p38 MAPK knockdown and a p38 MAPK inhibitor established p38 MAPK as an upstream kinase critically involved in ADP-mediated eNOS activation. In our search for signaling pathways that might dynamically connect p38 MAPK and eNOS by ADP, we focused our attention on one phosphatase widely described in the literature to be related to both of our proteins of interest. PTEN (phosphatase and tensin homolog on chromosome 10), is a phosphatase that catalyzes the phosphorylation

of phospholipid as well as phosphoproteins (Li et al., 1997, Steck et al., 1997). The principal PTEN substrate is the phospholipid second messenger phosphatitylinositol 3,4,5-triphosphate (PIP_3), which is dephosphorylated by PTEN to yield phosphatidylinositol 4,5 biphosphate (PIP_2), antagonizing in this way PI3K/Akt pathway (Jiang et al., 2000, Silva et al., 2008) which in turn plays a role in eNOS regulation (Morello et al., 2009, Fulton et al., 1999, Dimmeler et al., 1999a). On the other hand PTEN substrates include diverse protein kinases, among them p38 MAPK (Aikawa et al., 2002).

4.3.2 ADP PROMOTES A TRANSIENT INHIBITION OF PTEN

First we studied if ADP could affect PTEN activation. PTEN is widely distributed in mammalian tissues, and its enzymatic activity has been described to be regulated by different post-translational modifications such as oxidation or phosphorylation. As a member of the tyrosine phosphatase family with redox sensitivity it contains an essential cysteine residue in its active site that is present as a thiolate anion at neutral pH and is the target of specific oxidation. In 2002, Seung-Rock Lee et al described that H_2O_2 was able to induce a reversible inactivation of PTEN through the oxidation of the essential Cys124 and the formation of a disulfide bond between that Cys and Cys 71 (Lee et al., 2002b). On the other hand, PTEN enzymatic activity can be also be controlled by phosphorylation events. PTEN phosphorylation occurs on several theronine and serine residues located in the polybasic domain in the protein's C-terminus domain. Phosphorylation at the C-terminus is associated with inactivation of its lipid phosphatase activity as it blocks membrane binding by recruiting PTEN into the cytosol (Downes et al., 2004) hence contributing to mask positively charged residues (Das et al., 2003). We tested if ADP treatment promoted any post-translational modifications in PTEN. First, we checked if PTEN could become oxidized in non reducing conditions.

As shown in ***Figure 47*** we used H_2O_2 as a positive control and studied PTEN oxidation by detecting the formation of intermolecular disulfid bonds either in time course or dose-response experiments by non reducing SDS-PAGE gels. However, ADP treatment did not induce PTEN oxidation.

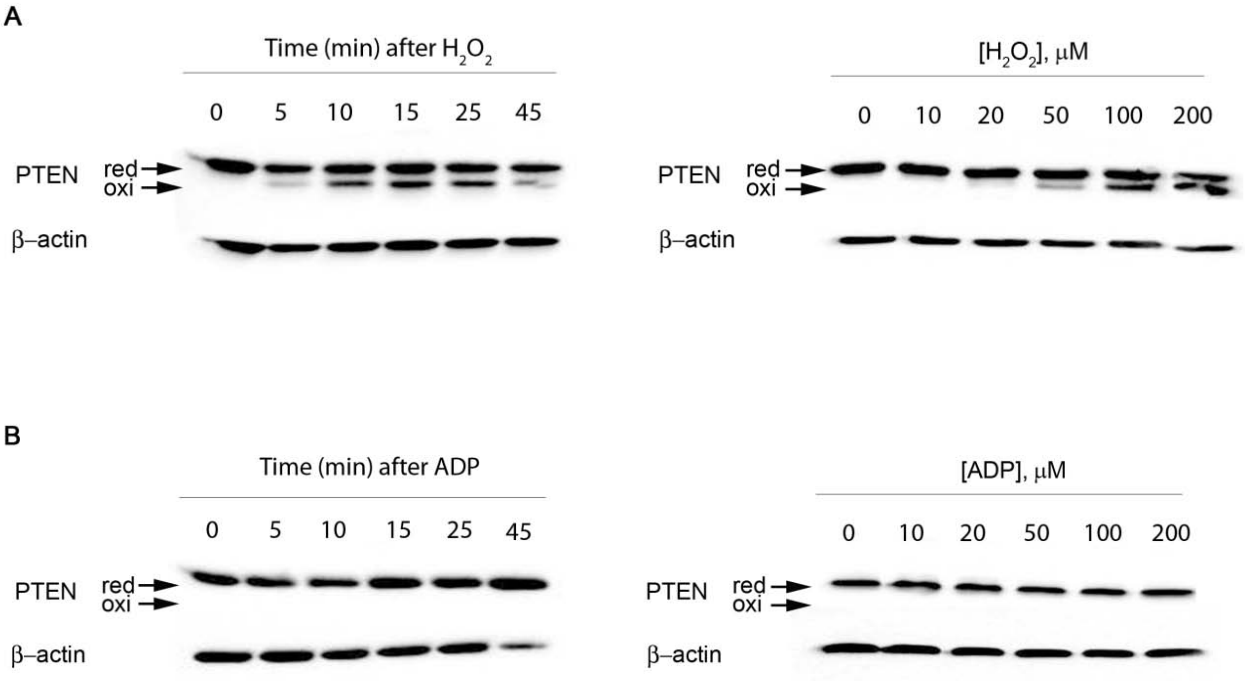

Figure 47. ADP does not produce a reversible oxidation of PTEN as H_2O_2 does*. BAEC were treated with H_2O_2 or ADP and lysates were analyzed in immunoblots probed with antibodies as shown. A) Time course of PTEN oxidation in endothelial cells treated with H_2O_2 (200 μM) and detected by the use of non reducing gels (left panel). The right panel depicts a dose response (determined at t = 30 min) for H_2O_2 -stimulated PTEN oxidation. B) Time course and dose response experiments in endothelial cells treated with ADP (25 μM) for 2 minutes respectively. The blots shown are representative of at least three independent experiments with similar results.*

As described above, PTEN activity has been described to be regulated by phosphorylation, so we decided to check if ADP could phosphorylate PTEN. As it is shown in ***Figure 48***, ADP promoted a reversible phosphorylation of PTEN as detected by the use of specific antibodies which recognize PTEN phosphorylation at the C-terminal domain. This result suggests ADP is able to promote a transient inhibition of PTEN by inducing the phosphorylation of the C-terminal domain of the phosphatase.

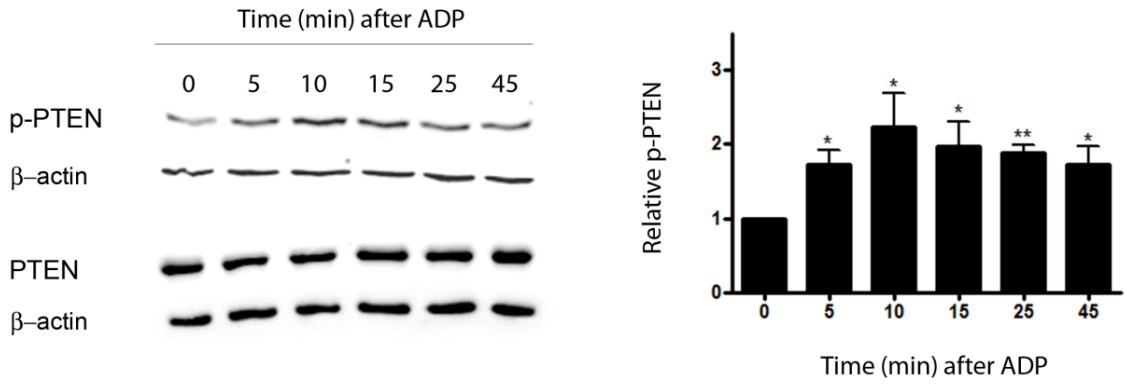

Figure 48. ADP induces a reversible phosphorylation of PTEN*. BAECs were treated with ADP ((25 μM) for the indicated times and lysates were analyzed in immunoblots probed with antibodies as shown. The blots are representative of at least three independent experiments that yielded equivalent results; the graphs next to each blot represent quantification of pooled data.*

4.3.3 PTEN KNOCKDOWN BLOCKS ADP-MEDIATED PIP_3 GENERATION

We designed and validated highly specific and potent duplex siRNA targeting constructs for PTEN that yielded 90% PTEN knockdown (***Figure 49***). Since PTEN is the main phosphoinositide phosphatase that metabolizes PIP_3, we transfected endothelial cells with either control or PTEN siRNA, and determined PIP_3 content using a biochemical assay to isolate lipid rafts, small subcellular plasma membrane structures that contain high levels of sphingolipids (Pike et al., 2002).

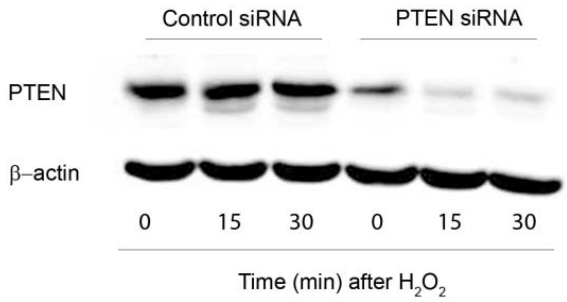

Figure 49. Specific and potent duplex siRNA targeting constructs for PTEN. *BAEC were transfected with a siRNA construct designed specifically to knockdown PTEN. Endothelial cells were treated 48 hours later with 200 μM of H_2O_2 and PTEN expression was detected by using a specific antibody against our protein of interest.*

Different methods to extract lipid rafts have been described in the literature including the extraction of cells with nonionic detergents or detergent-free purification (Song et al., 1996). In this work we have chosen the sodium carbonate extraction based on pH and carbonate resistance which is a non-detergent methodology to isolate PIP_3. As expected; siRNA-mediated PTEN knockdown led a significant increase in cellular PIP_3 levels (***Figure 50***), consistent with the established role of PTEN in PIP_3 metabolism.

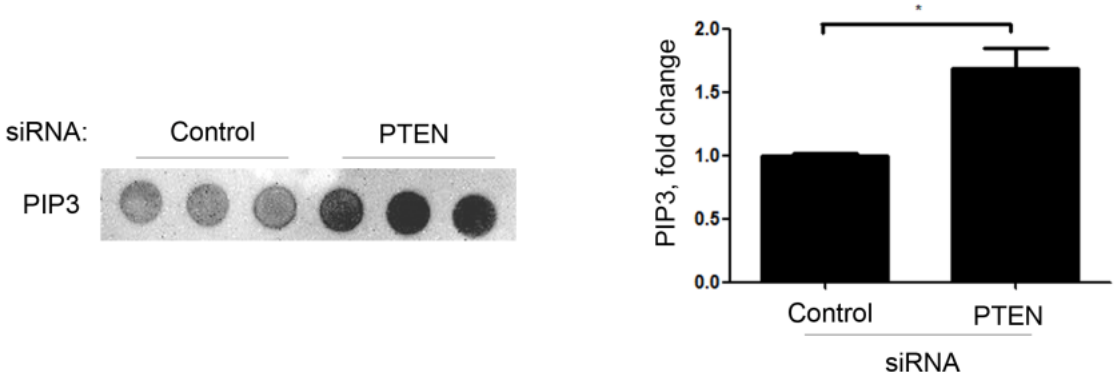

Figure 50. siRNA-mediated PTEN knockdown leads to a significant increase in cellular PIP3 levels. *Endothelial cells transfected with control or PTEN siRNA were harvested and lysed, and total cellular PIP_3 levels were measured in a dot-blot assay that was probed with a GST-tagged PIP_3-Grip construct, which was then developed with an anti-GST antibody, as described in the text. A representative dot-blot is shown, as well as a bar graph showing pooled data from three experiments, each performed in triplicate. * indicates $p < 0.05$.*

To study the inhibitory effect of ADP in PTEN activity, we perfomed live cell imaging experiments. We used a highly specific FRET biosensor for PIP_3 that consists of CFP, the PH domain of GRP (the PIP_3 binding domain), the hinge region, YFP and the membrane anchor from the amino-terminus. In the absence of PIP_3 on the plasma membrane, the hinge region is flexible resulting in a large distance between CFP and YFP which does not allow FRET between the fluorophores. When PIP_3 accumulates in the plasma membrane, GRP PH domain binds tightly to the plasma membrane via PIP_3. This binding results in a conformational change that leads to an increase in FRET efficiency (Aoki et al., 2008). We transfected the endothelial cells with duplex siRNA targeting constructs along with PIP_3 biosensor and 48 hours after the transfection, living cells were imaged by a fluorescence microscope. ADP or vehicle were added and fluorescence images were captured every minute for 1 hour analyzing FRET responses.

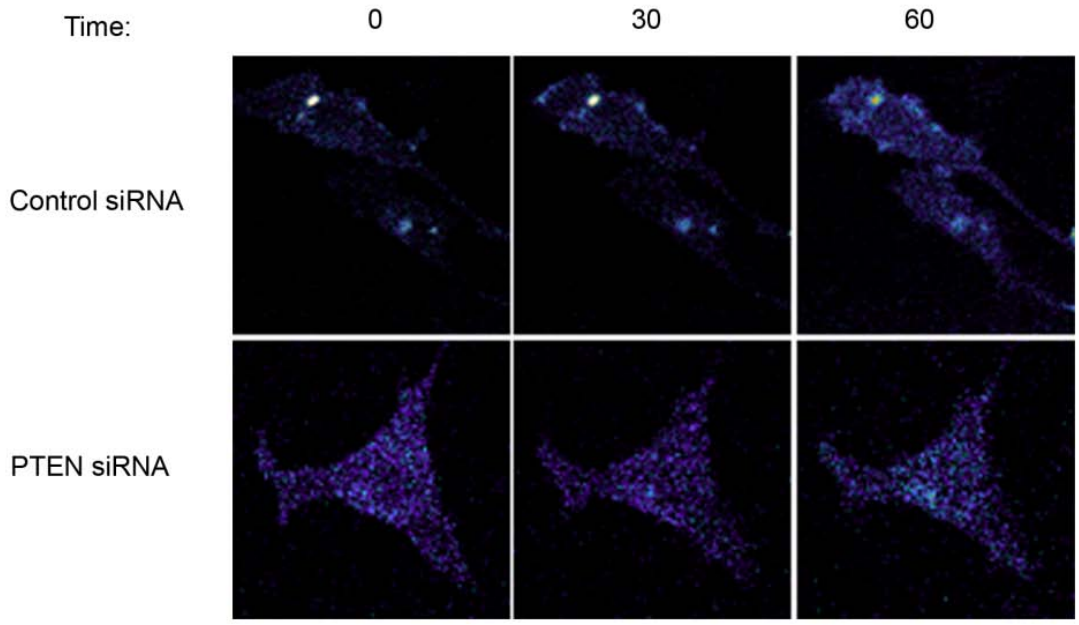

Figure 51. Analyses of PIP_3 metabolism in endothelial cells following siRNA-mediated PTEN knockdown*. Representative images of endothelial cells transfected with PIP_3 biosensor into control or PTEN siRNA-transfected cells. Cells were then treated with ADP (50 µM) and followed for PIP_3-accumulation by FRET microscopy in live cells for 60 min.*

As shown in ***Figure 51***, ADP treatment stimulated a marked rise in the FRET signal from the PIP_3 biosensor, reflecting a dynamic increase in PIP_3 levels along the endothelial cells plasmatic membranes following agonist treatment in control cells. By contrast, following siRNA-mediated PTEN knockdown, the ADP-promoted increase in FRET from the PIP_3 biosensor was no longer observed. FRET biosensor can only detect changes in PIP_3 abundance but not the absolute levels of intracellular PIP_3, so FRET data were normalized to the basal CFP/YFP ratio in each condition (***Figure 52***), indicating that PTEN knockdown effectively suppresses any further increase in PIP_3 after addition of ADP. These analyses in living cells are consistent with our finding that ADP had an inhibitory effect upon PTEN, such that when PTEN is knocked down, further ADP-stimulated PTEN-mediated PIP_3 responses are no longer observed.

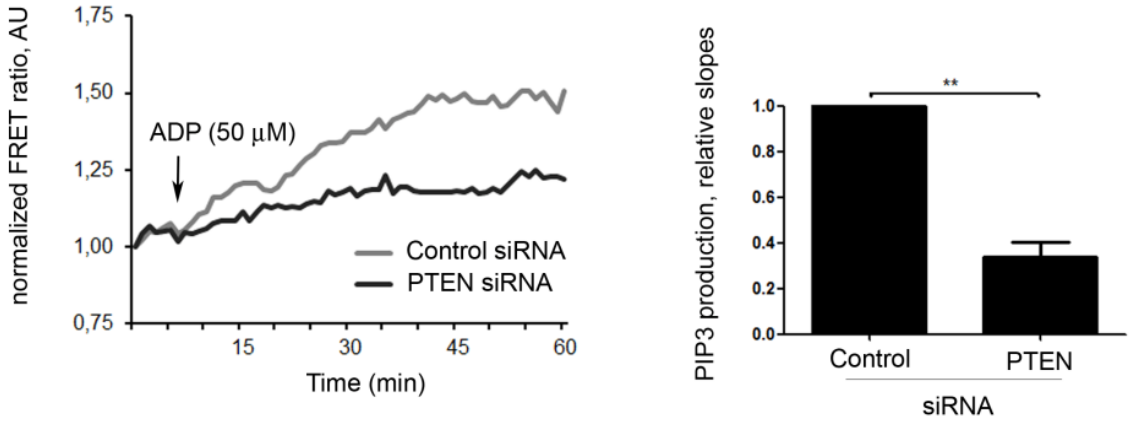

Figure 52. PTEN knockdown suppresses any further increase in PIP3 after addition of ADP*. Tracings shown are representative of three independent experiments. FRET data were normalized to the basal CFP/YFP ratio at t = 0 min. The bar graph represents the mean values ± s.e.m. of three independent experiments analyzing the relative slope of ADP-stimulated PIP3 accumulation at the plasma membrane in control vs. PTEN siRNA-transfected cells. ** indicates p<0.01.*

Once ADP-mediated PTEN inactivation was confirmed, we attempted to evaluate the consequences of PTEN absence on p38 MAPK and eNOS activation.

4.3.4 ADP-MEDIATED eNOS AND p38MAPK ACTIVATION ARE MODULATED BY PTEN

As described above, PTEN antagonizes PI3K action and hence Akt activation. As expected, siRNA-mediated PTEN knockdown markedly increased basal as well as ADP-stimulated Akt phosphorylation and eNOS phosphorylation at serine 1177, which led to an increase in basal and ADP-stimulated eNOS activity (***Figure 53***).

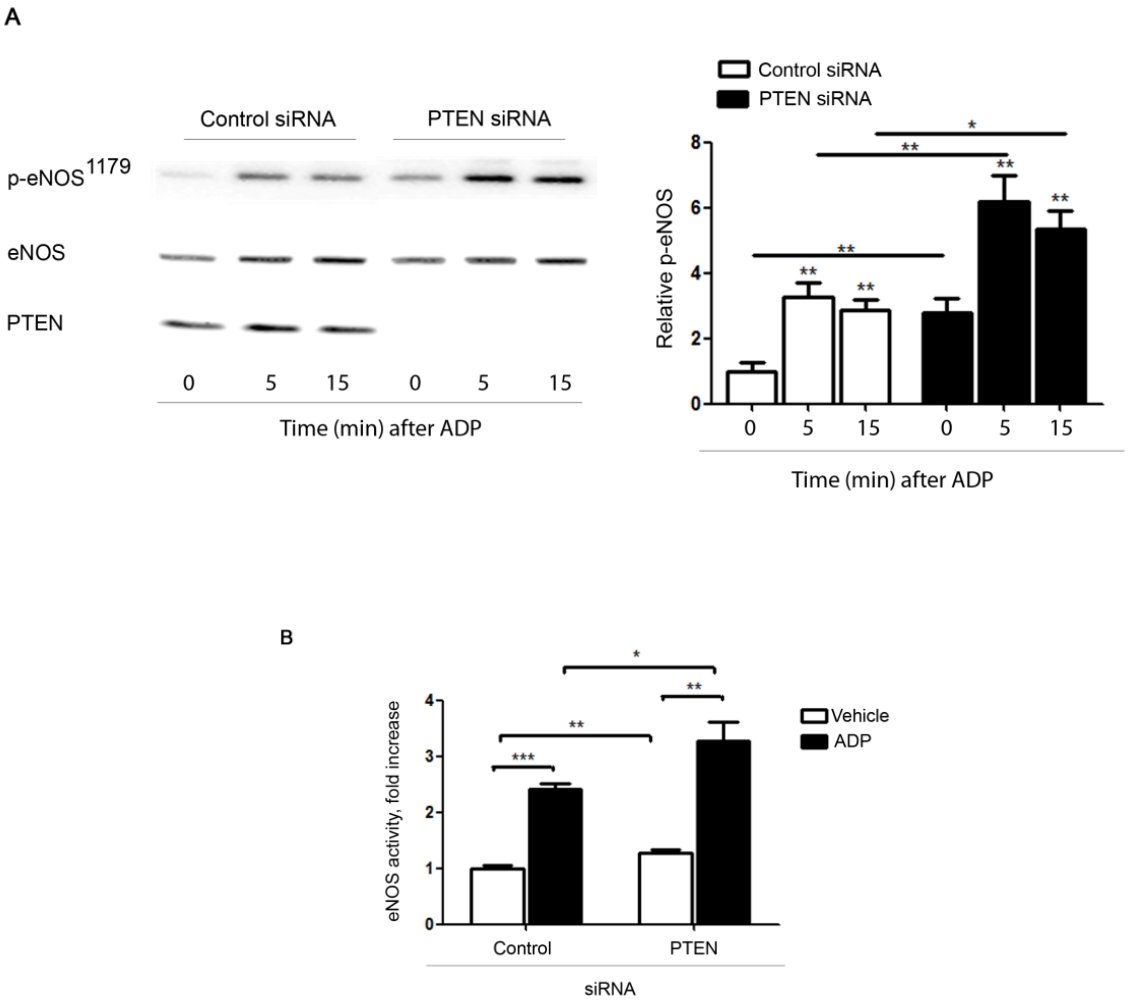

Figure 53. PTEN knockdown promotes an increase in eNOS phosphorylation and enzyme activity. *A) Endothelial lysates were prepared from control or PTEN siRNA-transfected cells that were treated with ADP (25 μM) for the indicated times, and then probed with antibodies in immunoblots as shown. Immunoblot shows a representative time course experiment and bar graph (right panel) shows the mean ± SEM of four independent experiments. B) Pooled data from four experiments measuring eNOS activity using the [3H]-arginine-[3H]-citrulline assay as analyzed in transfected endothelial cells with either PTEN or control siRNA and treated with ADP or vehicle for 20 min. Since basal eNOS activity varied slightly from experiment to experiment, the data are normalized to the enzyme activity observed in control siRNA-transfected cells in the absence of ADP. The graph shows the mean ± s.e.m. of four independent experiments. * indicates p<0.05, ** indicates p<0.01, and *** indicates p<0.001.*

We found that siRNA-mediated PTEN knockdown also led to a marked increase in basal and ADP-stimulated p38 MAPK phosphorylation (***Figure 54*****).** Together these results suggest that ADP activation of both eNOS and p38 MAPK are modulated by PTEN. Based on previous results supporting that p38 MAPK is an upstream regulator of eNOS

activity, we tested if there might exist specific interactions of among these proteins in endothelial responses to ADP.

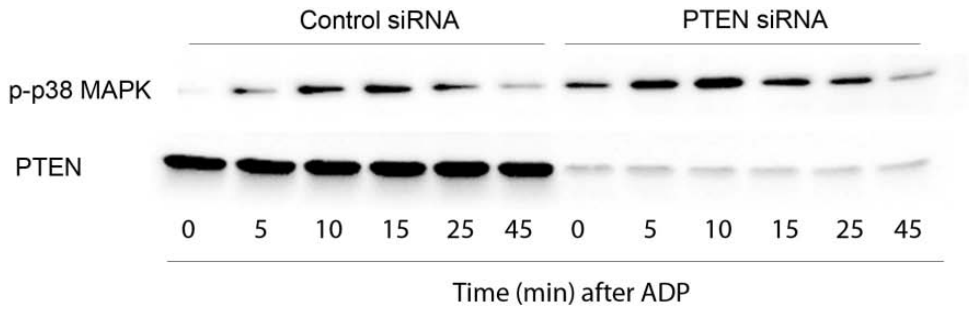

Figure 54. PTEN absence induces p38 MAPK activation. *BAEC were transfected with control or PTEN siRNA and treated with ADP (25 μM) for the indicated times. Lysates were probed with antibodies in immunoblots as shown. Immunoblot shows a representative time course experiment.*

In order to explore the interplay between PTEN and p38 MAPK in eNOS regulation, we performed "double knockdown" experiments using siRNA targeting constructs. First we studied if a specific siRNA construct designed against p38 MAPK had an effect on eNOS or on PTEN expression (***Figure 55***).

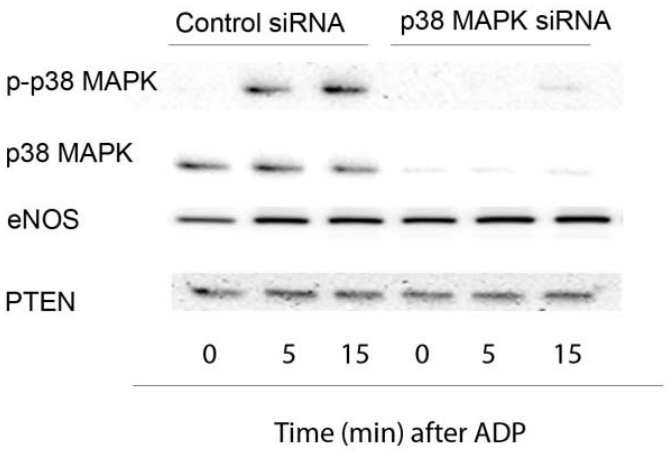

Figure 55.. siRNA-mediated p38 MAPK knockdown has no effect on eNOS and PTEN expression*. Endothelial cells transfected with control or p38 MAPK siRNA targeting constructs were treated with ADP (25 μM) for the indicated times. Equal loading was assessed by immunoblotting with antibodies directed against total eNOS, p38 MAPK and PTEN.*

We transfected BAEC with two separate siRNA constructs to target PTEN and p38 MAPK and tested eNOS activation. As shown in ***Figure 56***, siRNA mediated p38 MAPK knockdown attenuated the increase in eNOS enzyme activity and eNOS phosphorylation that was observed following PTEN knockdown.

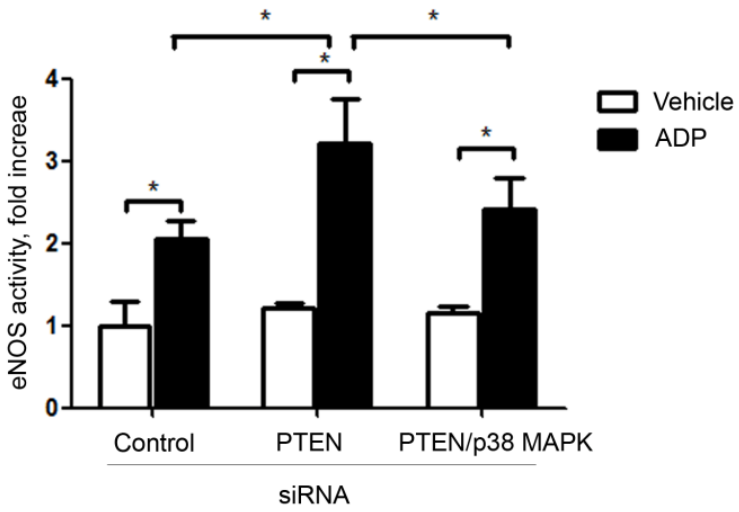

Figure 56. siRNA mediated p38 MAPK knockdown attenuated the increase in eNOS activation following PTEN knockdown. *Endothelial cells were transfected at a final siRNA concentration of 60 nM, comprised of 30 nM PTEN and/or p38 MAPK targeting constructs as indicated; for each experiment the balance was made up by control siRNA to yield a final concentration of 60 nM for all experiments. 48 hours following transfection, endothelial cells were treated with ADP (25 μM) and eNOS activity was analyzed.*

Due to Akt involvement on eNOS activation, and given the fact that PTEN absence has been described to activate Akt, we next studied Akt activation in our signaling pathway. Interestingly, the increase in Akt phosphorylation that was seen after PTEN knockdown was further enhanced by also knocking down p38 MAPK indicating possible interactions between these two kinase pathways (**Figure 57**).

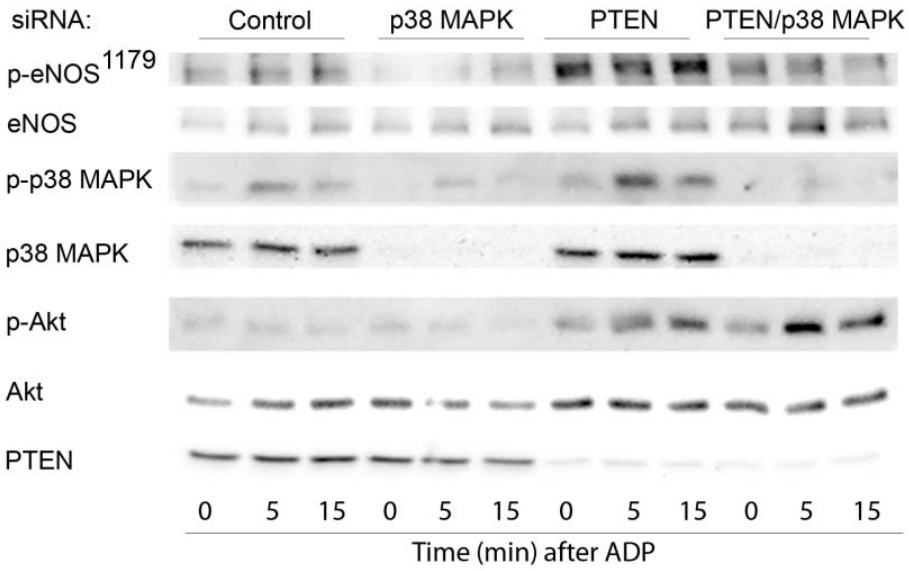

Figure 57. Akt phosphorylation increased after PTEN knockdown was further enhanced by additionally knocking down p38 MAPK. Endothelial cells were transfected at a final siRNA concentration of 60 nM (control siRNA and/or specific siRNAs were mixed to yield a final concentration of 60 nM for all experiments). 48 hours following transfection, endothelial cells were treated with ADP (25 μM) and analyzed by immunoblots probed with antibodies as shown.

We next performed double knockdown experiments with targeting constructs for both PTEN and Akt to study Akt involvement in eNOS activity modulation by ADP. As shown in ***Figure 58***, siRNA-mediated Akt knockdown partially blocked ADP-stimulated eNOS activity, yet additional siRNA-mediated knockdown of PTEN partially recovered the eNOS response to ADP. Taken together, these findings suggest that ADP-stimulated $NO^{\cdot}$ production is enhanced by PTEN phosphorylation and inactivation, which then facilitates the sequential activation of p38 MAPK and eNOS in endothelial cells.

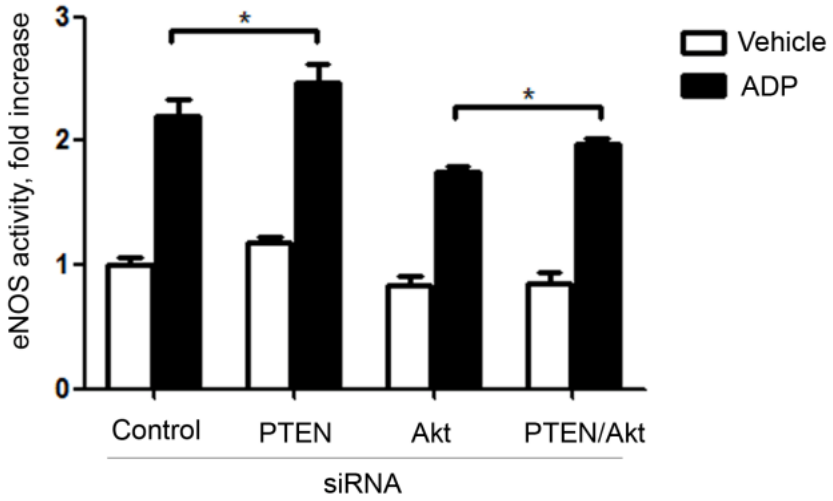

Figure 58. siRNA-mediated knockdown of PTEN partially recovered the eNOS response to ADP in the absence of Akt. *Effect on eNOS activity of the siRNA mediated double knockdown of Akt and PTEN. For each condition siRNA final concentration of 60 nM was used. The results shown for the activity assays represent data pooled from 3 experiments, each performed in duplicate. The immunoblot shown is representative of three independent experiments with similar results. * indicates $p < 0.05$.*

4.3.5 PTEN KNOCKDOWN INHIBITS ENDOTHELIAL CELL MIGRATION

Changes in the levels of the inositol lipids PIP_2 and PIP_3 have important consequences on diverse cellular pathways including cell growth, differentiation, apoptosis, metabolism, and motility in a wide variety of cells. These responses are initiated by the binding of phosphoinositide-binding pleckstrin homology domains that selectively bind PIP_3, PIP_2 and other structurally related bioactive complex lipids (Ferguson et al., 2000). In particular PIP_3 is involved in cell migration, leading to cytoskeleton reorganization (Franca-Koh et al., 2007, Insall and Weiner, 2001). We therefore tested whether PTEN would regulate endothelial cell migration by using the well established “cell wound” or scratch assay. As shown in **Figure 59**, siRNA-mediated PTEN knockdown markedly suppressed directional migration of endothelial cells.

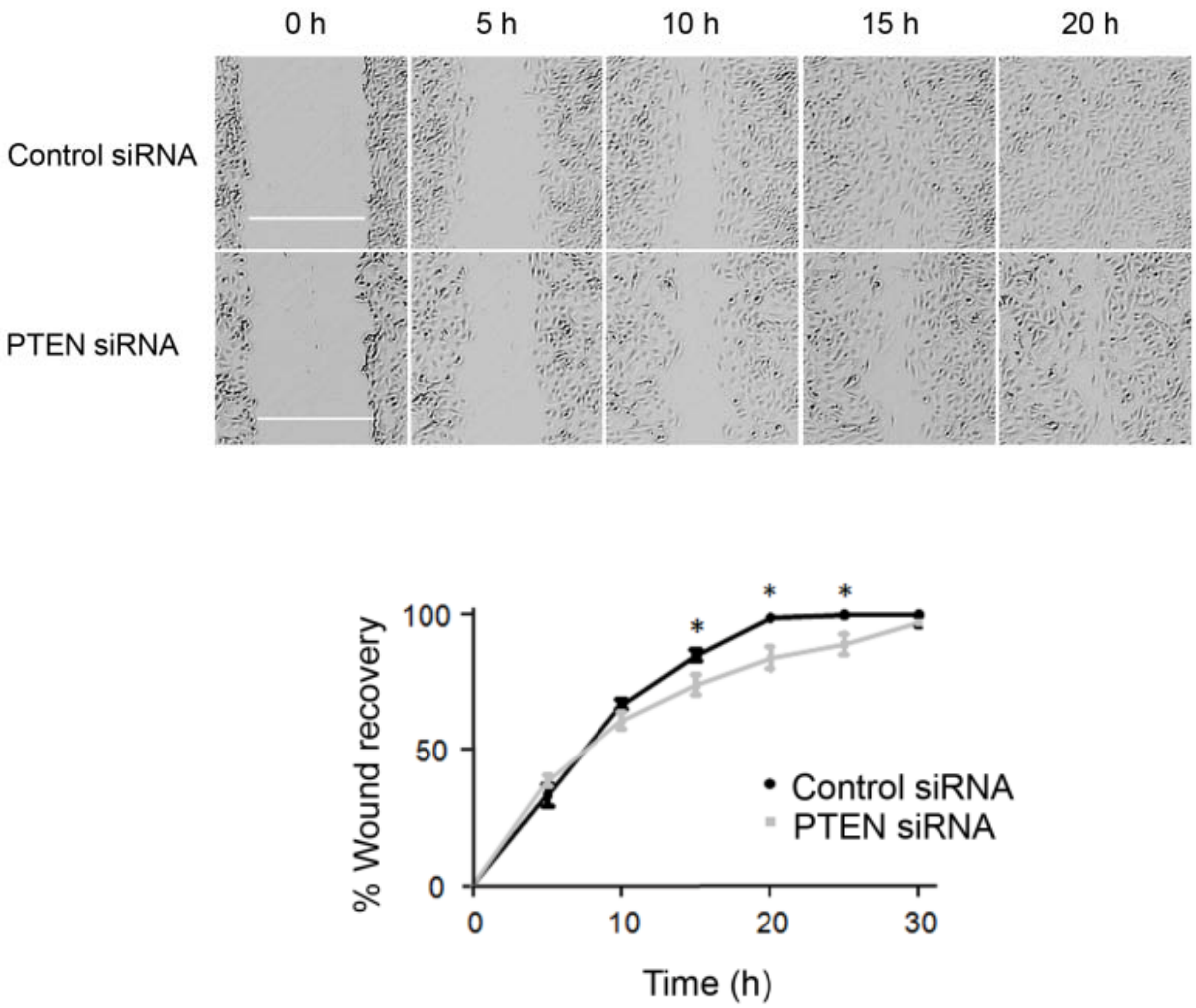

Figure 59. PTEN modulates endothelial cell migration. Scratch assay cell migration was recorded by phase contrast microscopy over a 20h time course after wound scratch in endothelial cells transfected with either control or PTEN siRNA. Pooled data of the scratch assay from three independent experiments is quantified as a function of wound recovery time (right graph).

4.3.6 PTEN MODULATES ACTIN ORGANIZATION AND RAC1 ACTIVATION

PIP_3 is an important regulator of actin polymerization dynamics both spatially and temporally. Although Rho family GTP-ases Cdc42 and Rac have been related to this process, how PIP3 generation is coupled to actin polymerization is not completely understood (Insall and Weiner, 2001). To understand this regulation in endothelial cells we tested whether PTEN knockdown would affect actin polymerization. We used cellular imaging approaches to analyze the effects of siRNA-mediated PTEN knockdown on actin cytoskeleton structure, using phalloidin to label F actin in BAEC. As shown in ***Figure 60***, siRNA mediated PTEN knockdown led to a marked increase in actin polymerization compared with cells transfected with control siRNA.

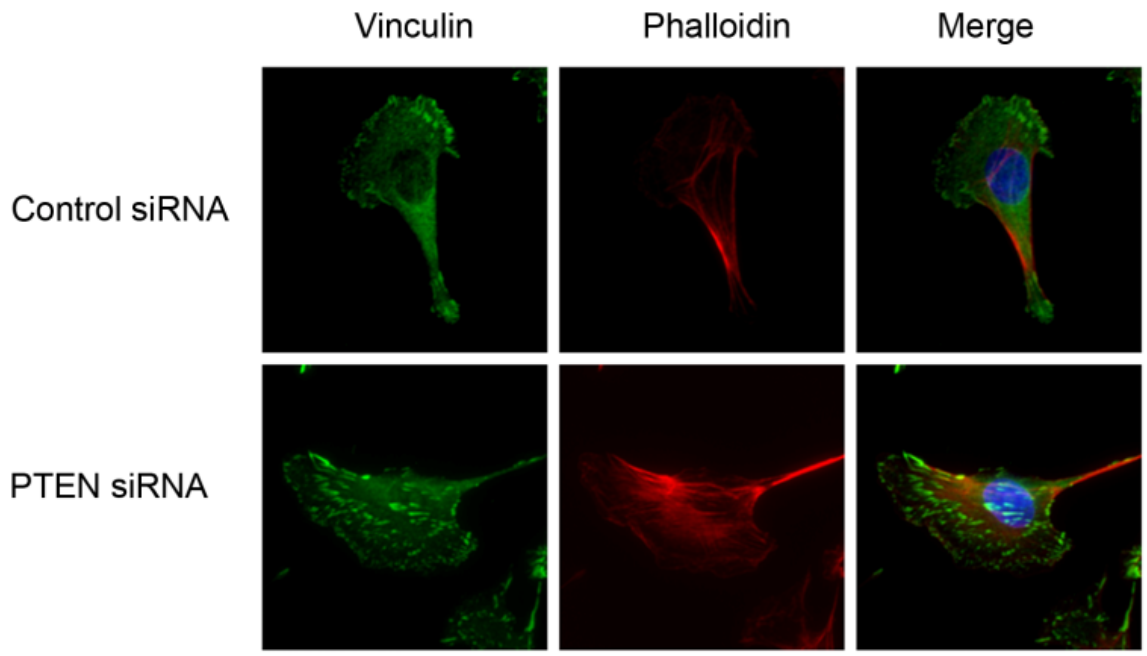

Figure 60. PTEN absence modulates actin re-organization in endothelial cells. Endothelial *cells were transfected with control or PTEN siRNA, and then fixed and stained with phalloidin to reveal polymerized actin (red) in the middle panels or with vinculin antibodies to show focal adhesion contacts (green) in the left panels; the merged images in the right-hand panels show the overlap between actin and vinculin staining in yellow.*

We next studied the effects of PTEN knockdown on the activation of the small GTPase Rac1. Rac1 is a member of the Rho GTPase family that presents a pleckstrin homology (PH) domain in its amino-terminal region which selectively binds phosphoinositides (Konishi et al., 1994). It has been implicated in cortical actin filament reorganization (Bishop and Hall, 2000, Takenawa and Miki, 2001) and Akt phosphorylation (Gonzalez et al., 2004) as well as in ADP-stimulated eNOS activation (Hess et al., 2009). Rac1 activity was analyzed in live cells using a Rac1 FRET biosensor (Aoki et al., 2008). Once Rac1 is activated, a conformational change takes place in the biosensor so that CFP and YFP fluorophores become closer, allowing an increase in the FRET signal. We transfected BAEC with both siRNA targeting constructs and Rac1 biosensor and 48 hours after and studied ADP-mediated Rac1 activation by recording living cell images with a fluorescence microscope. Five minutes after ADP treatment we could detect an increase in the FRET signal which correlated with enhanced Rac1 activity. However ADP-stimulated Rac1 activity was completely blocked following siRNA-mediated PTEN knockdown (***Figure 61***). These results suggest that PTEN is able to modulate actin re-organization and implicate PTEN activation in the pathway between ADP receptor stimulation and activation of Rac1.

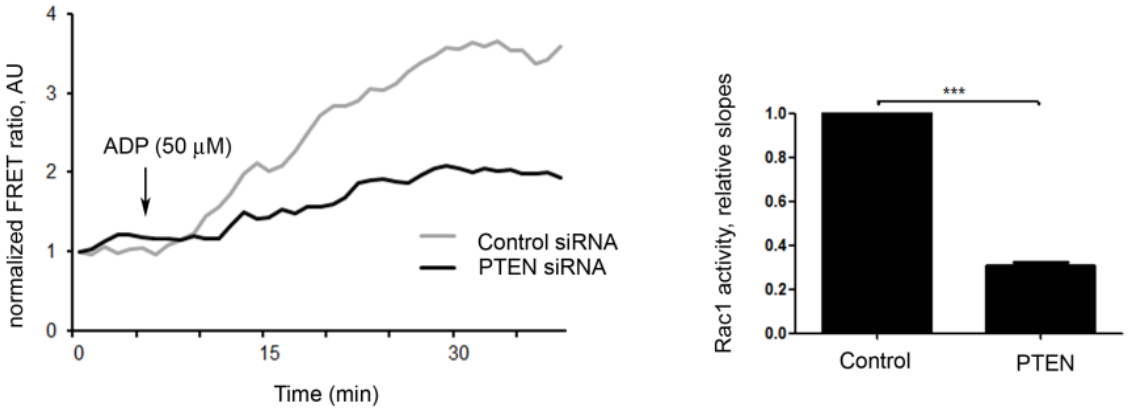

Figure 61. ADP-stimulated Rac1 activity is completely blocked following PTEN knockdown. *Cells transfected with control or PTEN siRNA were co-transfected with a FRET-based active Rac1 biosensor, and then treated with ADP or vehicle. Tracings shown are representative of three independent experiments in which FRET data were normalized to the basal CFP/YFP ratio at 0 min. The bar graph represents the mean values ± SEM of three independent experiments analyzing Rac1 activity slopes in control vs. PTEN siRNA-transfected cells after stimulation with ADP for 40 min. *** indicates p<0.0001.*

Overall, these data support a key role for PTEN in ADP receptor-dependent eNOS activation. This is summarized in a model in which ADP promotes the transient phosphorylation and inactivation of PTEN, leading to an increase in PIP_3 levels. This may result in the activation of PI3K/Akt, Rac1 and p38 MAPK leading to enhanced eNOS activity. These studies provide new insights into the pathway of ADP-mediated signaling to eNOS and may identify new points for pharmacological regulation of NO signaling in the vascular wall.

5. DISCUSSION

ç

5. DISCUSSION

Vascular vessels are constantly exposed to different hemodynamic forces induced by blood flow and constitute important mediators in vascular homeostasis (Lehoux, 2006), but fluid shear stress (SS) seems to be the main determinant in endothelial physiology and cell function (Hahn and Schwartz, 2009). Among different signaling pathways induced by SS, reactive oxygen species (ROS) produced by vascular cells has received increasing attention (Birukov, 2009). In 1994 Laurindo et al observed ROS generation after flow changes using paramagnetic resonance spectroscopy (Laurindo et al., 1994), contributing to explain vascular free radical generation in physiological or pathological circumstances. A couple of years later the oxidative stress concept was redefined by considering not only oxidative damage but also its role in signaling pathways, the so called *signaling face of ROS*. Both laminar shear stress (LSS) and disturbed flow are associated with the generation of ROS (Lehoux, 2006), however only LSS is believed to generate low levels of ROS capable of eliciting redox-sensitive physiological signaling pathways and antioxidant responses. By contrast, disturbed flow increases prolonged ROS generation enhancing the expression of inflammatory mediators that participate in the atherosclerotic lesion formation (De Keulenaer et al., 1998).

Based on their chemical properties and mechanism of production different ROS, but specifically H_2O_2, have been considered to act as cellular second messengers in both prokaryotes and eukaryotes. We found that LSS induces rapidly increased ROS generation in vascular endothelial cells. Although the effects were moderate from the quantitative perspective, the high reproducibility and the fact that the ROS detected were within the physiological signaling range add significance to this observation. Although the establishment of H_2O_2 intracellular levels considered to be physiological is a delicate issue to study, in mammals the physiologic H_2O_2 concentration may reach as low as 0.001 µM, and the maximal intracellular H_2O_2 concentration that can be generated for signaling purposes would be 0.5-0.7 µM (Stone and Yang, 2006). It is likely that steady-state levels above 1 µM start to be toxic and thus lie in the realm of moderate or severe stress rather than of signal transduction conciliable levels (Antunes and Cadenas, 2001). In our

experiments we were able to detect an extracellular release of approximately 0.004 µM of H_2O_2 from LSS-induced compared with controls cells using the specific peroxide reagent Amplex red. Upon exposure to LSS, initiation of intracellular signal transduction is an important molecular event in endothelial cells that modulates the activity and vascular function. This leads to protein and gene expression that acts against the development of atherosclerosis attending to the protective role of the laminar flow (Cai and Harrison, 2000, Dekker et al., 2005, Parmar et al., 2006, Tsao et al., 1996). Endothelial cells must express specific mechanotranducers that are able to convert the mechanical stress into biochemical signals. Although many endothelial proteins or structures have been proposed as potential shear stress *mechano sensors/receptors or transducers,* including integrins (Schwartz and Ginsberg, 2002), cell-cell junction molecules (Kano et al., 2000), adherens junctions (Dejana et al., 1999), ion chanels (Barakat, 2001), tyrosine kinase receptors (Chen et al., 1999a), G-proteins (Gudi et al., 1996) or even the endothelial cytoskeleton (Ali and Schumacker, 2002), the identification of mechanotransducer molecules is still nowadays a matter of active research. In the last decade, a role of signaling by ROS clearly attracts increasing attention as they come into play as possible mediators of shear stress-induced responses (Matlung et al., 2009, Paravicini and Touyz, 2006, Rojas et al., 2006, Waters, 2004). We observed that low-micromolar concentrations and nanomolar fluxes of H_2O_2 induced a fast and visible activation of some LSS targets described in the literature such as p38 MAPK (Sumpio et al., 2005, Surapisitchat et al., 2001) and eNOS (Dimmeler et al., 1999b, Fisslthaler et al., 2000). In addition, shear-induced ROS and $NO^{\cdot}$ both have been described to influence vascular function, lending us to investigate a casual response between both events and the activation of the MAPK previously aforementioned. LSS is also an important stimulus for the upregulation of eNOS expression. Given the short-term activation of eNOS in our model this is not likely the case (Cai et al., 2004). It is estimated that when exogenous H_2O_2 is added to cells, an equilibrium is reached by which the intracellular concentration of H_2O_2 becomes 7- 10-fold less than the one originally added extracellularly (Antunes and Cadenas, 2000). Hence, it is quite likely that the concentrations of H_2O_2 reached during LSS experiments are not far from those obtained when low concentrations of exogenous H_2O_2 are added to the extracellular medium of endothelial cells, or produced endogenously by the generation of fluxes with glucose oxidase treatment. Our data support the fact that p38 MAPK and

eNOS activation by LSS are dependent on ROS production since general antioxidant treatment partially abolishes both responses in endothelial cells. Intracellular ROS generation in endothelial cells may arise from different sources, such as the electron transport chain in the mitochondria, uncoupled eNOS, xanthine oxidase oxidoreductase enzyme, cytochrome P450 and NADPH oxidases (NOXs) among others (Birukov, 2009). Endothelial NOX activity has been described to be increased by the mechanical force of SS (Li and Shah, 2004, Sorescu et al., 2004) and is considered the most relevant source of ROS upon exposure to laminar flow (De Keulenaer et al., 1998, Chatzizisis et al., 2007). Our data support a key role for the major NADPH isoform, NOX4 isoform, in the LSS-mediated generation of peroxide, since abrogation of NOX4 by the use of chemical inhibitors or by siRNA technology impaired LSS-mediated p38 MAPK activation. Experiments conducted in NOX4-/- knockout mice yielded similar results, whereas the deficiency of other NADPH oxidase isoforms present in the vasculature did not modify the activation of our protein of interest. Hence, according to our data it is tempting to speculate that LSS-related mechanotransducing signals can result in NOX4 generation of peroxide at specific subcellular compartments leading to the subsequent activation of p38 MAPK. This may be the result of the inactivation of one or more redox sensitive phosphatases (Tonks, 2005).

It has been pointed out that $NO^{\cdot}$ may promote the activation of p38 MAPK by inducing its phosphorylation (Browning et al., 2000). By contrast, other studies in the context of LSS showed a modest effect of $NO^{\cdot}$ donors on the p38 MAPK pathway. Thus, it was important to clarify the sequential activation of the LSS targets addressed in this study in our model of endothelial cells. Our experiments clearly support eNOS lies downstream of p38 MAPK since: 1) $NO^{\cdot}$ donors were unable to induce p38 MAPK phosphorylation; 2) endothelial cells devoid of eNOS were still able to respond to LSS with p38 phosphorylation; 3) pharmacological inhibition and silencing of p38 MAPK significantly reduced LSS-induced eNOS phosphorylation and $NO^{\cdot}$ synthesis. These events were not just demonstrated in the context of LSS but also by peroxide activation of eNOS supporting the existence of sequential events by which p38 MAPK and its upstream modulators are sufficient to promote eNOS phosphorylation. In addition, data obtained in MEFs from p38α MAPK knockout mice are consistent with the notion that the presence of p38 MAPK is necessary

for H_2O_2-induced eNOS activation. However it is important to point out that hydrogen peroxide has been shown to activate eNOS by several mechanisms, including PI3K/Akt and AMPK (Hu et al., 2008, Thomas et al., 2002) and that some reports support that its vasodilatory action may be $NO^{\cdot}$-independent (Ray et al., 2011, Burgoyne et al., 2007, Matoba et al., 2000). Our data do not fully elucidate the mechanism by which p38 MAPK induces eNOS phosphorylation. The eNOS phosphorylated residue targeted by the antibody in this work is Ser 1177 (human sequence), which has been shown to be specifically modified by several kinases and mainly by stimuli converging at the PI3K/Akt pathway, including LSS (Dudzinski and Michel, 2007, Fleming, 2010). However it is possible that LSS may activate eNOS through other residues, such as Ser 633, also sensitive to hydrogen peroxide as recently shown in myocardiocytes (Sartoretto et al., 2011). Our data do not support a significant participation of the PI3K/Akt pathway because 1) knockdown of NOX4 or p38 MAPK did not modify LSS-mediated phosphorylation of Akt and 2) PI3K inhibitors did not block peroxide-mediated activation of p38 MAPK. However, previous reports have shown that both p38 MAPK and H_2O_2 may activate this pathway (Anter et al., 2004, Chen et al., 2008, Thomas et al., 2002, Cai et al., 2003), suggesting that eNOS activation may be the consequence of multiple convergent mechanisms that are stimuli specific and that may not operate simultaneously.

The major and novel finding of this study is the identification of H_2O_2 as a physiological signaling second messenger produced by LSS and implicated in the activation of a sequential pathway that converges in the activation of eNOS and production of vasoactive molecules which explain the protective role of laminar flow in the vasculature (***Figure 62***).

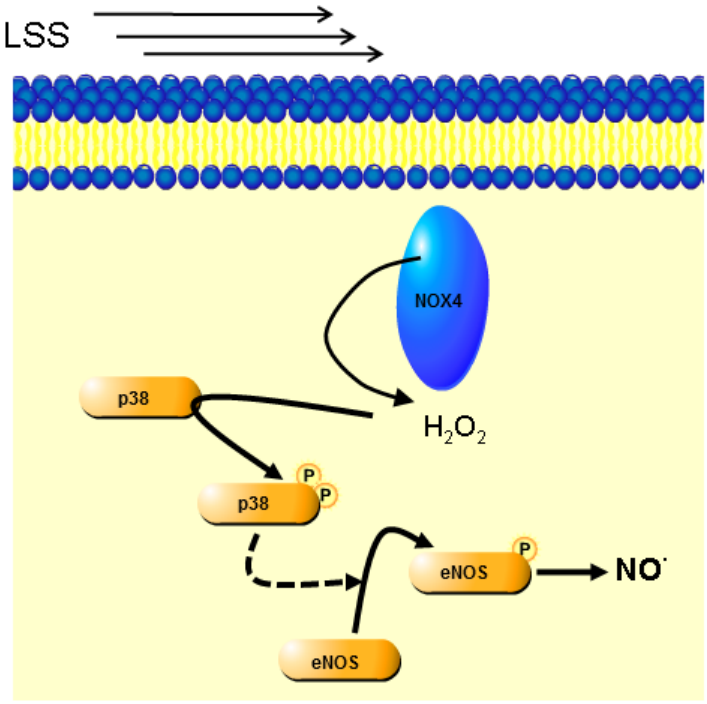

Figure 62. Critical role of hydrogen peroxide signaling in the sequential activation of p38 MAPK and eNOS in laminar shear stress. *We propose a model in which LSS promotes the formation of signaling levels of H_2O_2, which in turn activate p38α MAPK and then stimulate eNOS, leading to increased ·NO generation and protection of endothelial function.*

Our results also support the existence of specific targets for H_2O_2-mediated activation that may account for the LSS-induced protective response in the vascular wall. Since H_2O_2 is a mild oxidant, very few proteins might be expected to be direct targets of its oxidation. Specifically, only proteins with a low-pKa cysteine residue are susceptible to the specific oxidation induced by H_2O_2 (Kim et al., 2000). At neutral pH, they will exist as thiolate anion because of a nearby positively charged amino acid residues in the quaternary structure of the protein. This Cys –thiol deprotonation accounts itself for an enhancement in the rate of reaction with H_2O_2 of 10-100 fold compared with protonated Cys-thiols (Winterbourn and Metodiewa, 1999). It is precisely the oxidation and reduction of thiol proteins the major mechanism by which ROS integrate into cellular signal transduction pathways. Proteins with low-pKa cysteine residues include a broad spectrum of functionalities, from glycolitic enzymes, and structural proteins to regulatory enzymes (Saurin et al., 2004, Cumming et

al., 2004, Baty et al., 2005). Nevertheless, a low pKa of a protein is not the sole determinant of H_2O_2 reactivity. Because of their high rate constant (more than five orders of magnitude higher than other thiol proteins) and their high abundance, peroxiredoxins (prx) are overwhelmingly favored as H_2O_2 targets (Winterbourn and Hampton, 2008). PRXs are a ubiquitous class of cysteine-dependent peroxidases that reduce H_2O_2 and alkylhydroperoxides with the use of reducing equivalents provided from thioredoxins (Trxs) (Rhee et al., 2001, Chae et al., 1994). In mammals there are 6 different PRXs isoforms (PRX1-6) and all of them have a conserved cysteine residue, known as the *"peroxidatic Cys"* which is H_2O_2-sensitive (Rhee and Woo, 2011). In these thiolate dependent peroxidases, the active Cys residue has a reduced pKa of around 4.5 and 5.9 is present as a thiolate anion at neutral pH. The peroxidatic Cys reacts directly with H_2O_2 forming a sulfenic acid (R-SOH) (Claiborne et al., 1999). This group is itself highly unstable and its chemical fate is dictated by the type of PRX. While in 1-Cys PRX, it is presumably reduced by a thiol containing electron donor, in 2-Cys PRX the sulfenic acid suffers a nucleophilic attack by a second Cys thiol, *"the resolving cysteine"* forming a disulfide bond. In addition, the sulfenic acid on the peroxidatic Cys can undergo further oxidation (hyperoxidation) to form a sulfinic acid, initially considered irreversible until the discovery of the tightly regulated enzyme sulfinic acid reductase sulfiredoxin (Srx) (Biteau et al., 2003). We found that LSS did not induce an overoxidation of any of the PRX isoforms, but caused a rapid transition of the monomer to the dimer conformation of PRX3 suggesting an activation of the enzyme during laminar flow. Several members of the PRX family are known to exist in different oligomeric states including dimers, decamers or even dodecamers although the physiological relevance of these high-order oligomeric conformations is not fully understood. The first reports of PRX oligomerization appeared in the late 1960s, when *torin* was described as an abundant protein isolated from human erythrocytes by transmission electron microscopy with an apparent tenfold symmetry (Harris, 1969). However it was not until 2001, when this doughnut-shaped *torin* was identified as mammalian PRX2 (Harris et al., 2001). PRX3 has even been described to form higher order multimers such as two-ring catenanes of two interlocked dodecamers (Cao et al., 2005). However this conformation represents only 3-5% of the population, with most molecules bring present as single toroids. Our data suggest that PRX3 exists in the form of stable oligomeric toroids maintained during laminar flow. Disulfide bonds might be

formed in the "*intratoroid*" without disassembling into dimers despite the activation of the enzyme.

H_2O_2 is thought to be permeable across biological membranes, and thus, it might react with several intra and extracellular targets, however, in spite of being a highly diffusible molecule H_2O_2 seems to preferably react with proteins located in the same organelle where it is produced (Branco et al., 2004, Chen et al., 2008). PRX3 is the only member of the PRX family confined exclusively to the mitochondria, since PRX5 is also found in the cytosol, peroxisomes and nucleus (Seo et al., 2000). An important feature of PRX3 is its significant preference to scavenge H_2O_2 over other peroxides or alkylhydroperoxides. Thus according to our data it was enticing to speculate that PRX3 might be sensing the specific production of H_2O_2 inside mitochondriae. Mitochondriae represent the main intracellular source of ROS under physiological conditions, however mitochondrial ROS production can also be enhanced by several intracellular stimuli. The generation of mitochondrial ROS is a consequence of oxidative phosphorylation linked to aerobic respiration occurring within the mitochondrial electron transport chain (ETC). Electron leakage from the ETC causes partial reduction of molecular oxygen to $O_2^{-\cdot}$ instead of reduction to H_2O. There have been described eight sites in mitochondriae that possess the ability to produce $O_2^{-\cdot}$(Brand, 2010), thus 1-2% of the O_2 consumed is converted into ROS (Chance et al., 1979). Mitochondrial ROS have long been reported as toxic bioproducts of the electron transport system (Shigenaga et al., 1994); however, recent studies indicate that ROS appear to be induced in response to stress and function as a signaling intermediate to facilitate cellular adaptation to challenge (Sena and Chandel, 2012). We found that LSS increased mitochondrial ROS production and decreased respiration rate, changes that are associated to a slowdown of electron transport and a suppression of proton pumping activity by complex I, correlating with an hyperpolarization of the mitochondrial membrane. Mitochondrial ROS are implicated in a variety of diseases such as cancer, inflammatory disorders, and neurodegeneration (Chandel et al., 2001, Kirkinezos and Moraes, 2001) Since these diseases exhibit alterations in the physiological cellular redox system (Sena and Chandel, 2012), we believe our data contribute to establish Prx3 as a plausible pharmacological target.

Mitochondrial function is reflected in their structure and morphology and consequently, mitochondrial morphology is determined by mitochondrial energetics (Yoon, 2004,

Hackenbrock, 1966, Riva et al., 2005). In mammalian cells mitochondriae form reticular networks composed of filamentous tubules which constantly move and change shape through fission and fusion dynamics (Bereiter-Hahn, 1990). In this study we found that under LSS induction, a dynamic change of mitochondrial morphology occurs, and mitochondriae become rapidly fragmented.

Mitochondrial division is induced mainly by cytosolic dynamin-related large GTP-ase. Drp1. After being activated, Drp1 is recruited to the outer-mitochondrial membrane to induce mitochondrial fission, constrict the tubules, wrap tightly around the constricted part and induce fission (Youle and van der Bliek, 2012).

Our study provides insight into the importance of mitochondrial mechanosensing during LSS as a regulator of ROS signaling in the vascular endothelium. Our results do not fully elucidate the mechanism by which the mechanical force of LSS is sensed by Drp1 inducing mitochondrial fission and changes in mitochondrial bioenergetics (***Figure 63*****).**

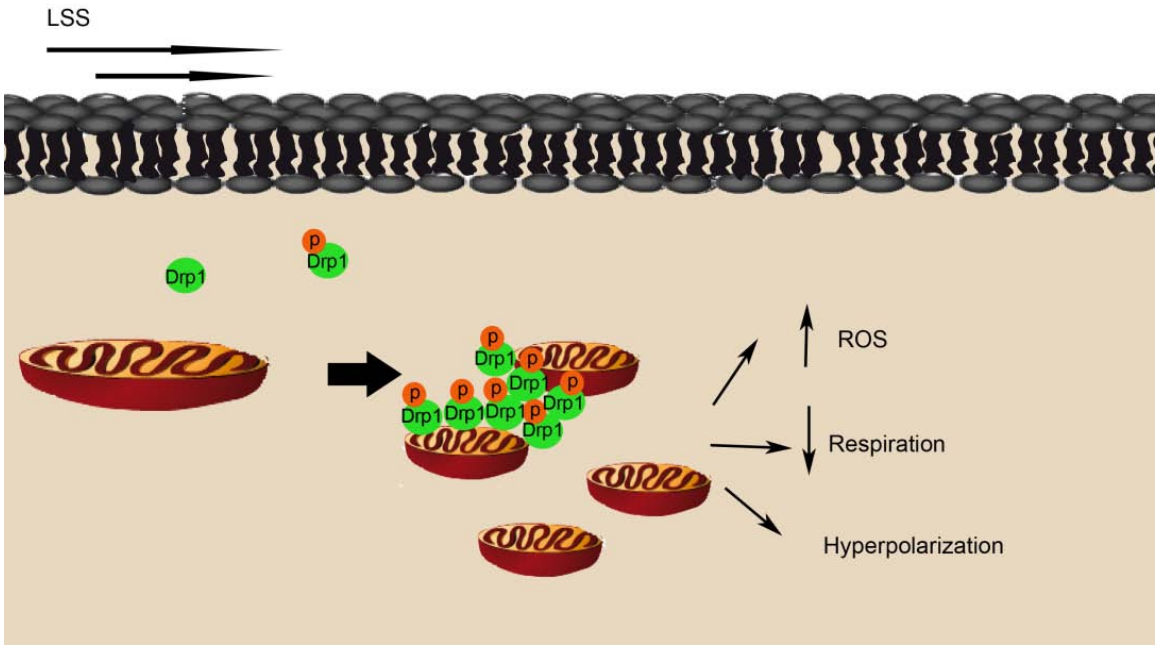

Figure 63. Mitohondriae act as mechanosesor organelles during LSS. *We propose a model in which Drp1 senses laminar flow, becomes activated and translocates to the outer mitochondrial membrane where it forms spirals around mitochondrial tubules inducing mitochondrial fission. This effect correlated with an increase in ROS production, a decrease in mitochondrial respiration rate and an increase in mitochondrial membrane potential.*

Of note, Drp1 activity is regulated by different post-translational modifications: phosphorylation, SUMOylation, S-Nitrosylation and ubiquitination (Chang and Blackstone, 2010). According to our data, Drp1 is phosphorylated at its activating site Ser616 inducing mitochondrial fragmentation, however, we do not discard alternative mechanisms able to transduce the mechanical shear stress to biochemical signaling and mitochondrial function. Given that mitochondriae anchor to the cytoskeleton via actin binding complexes in the outer membrane (Boldogh et al., 1998), it is tempting to venture that it is precisely the cytoskeleton which may provide the necessary framework to transmit the signal from the plasma membrane to mitochondriae. Moreover, the cytoskeleton has as an important role in endothelial cell responses to SS as microtubules, actin and intermediate filaments connect different regions of the cells transmitting mechanical forces from the apical domain (Hahn and Schwartz, 2009).

We are aware that several questions remain unresolved. In particular and as part of the immediate future we would like to investigate:

a) Which are the pathways upstream of Drp1 leading to its activation and directly regulated by shear stress. Good candidates are several MAPKs as well as AMPK and phosphatases such as calcineurin.
b) What is the importance of Drp1 activation and mitochondrial fission for ETC generation of ROS and PRX3 activation/oxidation. Knockdown experiments for Drp1 could provide preliminary answers.
c) Does PRX3 have a critical role in mitochondrial fission? Intuitively we situate PRX3 downstream of Drp1 activation and fission but this has not been formally tested.
d) Does PRX3 oxidation protect from critical changes in mitochondrial bioenergetics. PRX3 knockdown experiments may result of importance in this regard.
e) How intact need mitochondriae need to be for the oxidation of PRX3 to occur? Experiments with dysfunctional mitochondriae, in for example Rho0 endothelial cells may be appropriate approaches to tackle this issue.

Apart from its role in mechanotransduction directly upon endothelial cells, LSS has been described to promote platelet activation inducing the release of different agonists which are able to interact with endothelial receptors modifying endothelial function (Kroll et al., 1996, Anderson et al., 1978). Among these factors, extracellular nucleotides are vasoactive substances able to promote the activation of different signaling pathways. Platelets store the purine nucleotide ADP at concentrations as high as 653 mM (Holmsen and Weiss, 1979), and upon stimulation, activated platelets release ADP which binds to the purinergic receptor subtype P2Y1 expressed on the endothelial cell surface and mediates ADP signaling responses (Hess et al., 2009). Despite ADP has been extensively studied in cardiovascular tissues and cells, and ADP receptor antagonists have become widely used in cardiovascular therapeutics (Ralevic and Burnstock, 2003, Erlinge and Burnstock, 2008), many critical details of the signaling pathways elicited by ADP in the vascular endothelium remain incompletely characterized. eNOS activity has been described to be stimulated by extracellular ADP in endothelial cells. Nevertheless, specific knockdown of known upstream eNOS modulators, such as phophoinositide 3-kinase/AKt, Erk ½, Src, and calcium/calmodulin-dependent kinase kinase β (CaMKKβ) or AMP-activated protein kinase (AMPK), do not modify ADP-mediated activation (Hess et al., 2009).

PTEN (phosphatase and tensin homolog on chromosome 10), is a widely distributed phosphatase in mammalian tissues that catalyzes the dephosphorylation of the phospholipid second messenger phosphatitylinositol 3,4,5-triphosphate (PIP_3) forming the phosphoinositol-4,5-biphosphate (PIP_2). Changes in the levels of these complex lipids influence diverse cellular pathways, including alterations in cell growth, differentiation, apoptosis, metabolism and motility (Downes et al., 2004, Waite and Eng, 2002). These responses are initiated by the binding of phosphoinositides to proteins that possess highly specific phosphoinositide-binding pleckstrin homology domains that selectively bind PIP_3 or PIP_2 (Ferguson et al., 2000). PTEN enzymatic activity results in a depletion of PIP_3 levels and thereby attenuates PI3K/Akt pathway (Jiang et al., 2000, Silva et al., 2008) which in turn plays a role in eNOS regulation (Morello et al., 2009, Fulton et al., 1999, Dimmeler et al., 1999a). PTEN activity is tightly regulated by different post-translational modifications such as oxidation of the essential cysteine residue in its active site of

phosphorylation. According to our data, ADP promotes a dynamic phosphorylation of PTEN in vascular endothelial cells. Phosphorylation of PTEN is associated with inactivation of its lipid phosphatase activity as a consequence of the phosphoenzyme translocation away from the plasma membrane, where the enzyme's hydrophobic lipid substrate are sequestered (Waite and Eng, 2002). We found that PTEN knockdown led to a marked increase in both basal and ADP-dependent eNOS phosphorylation at its Ser1177 activation site implicating PTEN in a broad range of endothelial cell signaling responses involving eNOS. Ser1177 is the most thoroughly studied eNOS phosphorylation site, and has been shown to become phosphorylated by several kinases such as Akt, AMPK, PKG, PKA, or p38 MAPK among others (Dudzinski and Michel, 2007, Breton-Romero et al., 2012). Despite a central role for PTEN in modulating PI3K/Akt signaling pathway in several cell lines (Jiang et al., 2000, Stiles et al., 2004, Keyes et al., 2010, Shen et al., 2006b), we have previously shown that chemical inhibition of the PI3K/Akt pathway does not have an effect on ADP-promoted eNOS phosphorylation (Hess et al., 2009). The fact that basal eNOS activity increases following PTEN knockdown may suggest a role for PTEN in the maintenance of basal vascular tone, yet the fact that ADP treatment further augments eNOS phosphorylation and activation suggests that ADP.mediated eNOS activation also is modulated by PTEN. Our studies provide evidence indicating that inhibition of PTEN may be a determinant of eNOS-dependent endothelium relaxation responses (Guns et al., 2005). Since PTEN may modulate a broad range of PI3K/Akt-independent signaling patways, the enhancement of eNOS phosphorylation following PTEN knockdown most plausible reflects the effect of PTEN on protein substrates Although PTEN major targets are phospholipids, it can also catalyze protein dephosphorylation of different MAPKs, such as p38 MAPK (Shen et al., 2006a, Aikawa et al., 2002). Importantly, in our current study, we found that ADP promotes the robust phosphorylation of p38 MAPK, an effect that was significantly increased after PTEN knockdown.

Given the fact that we have previously described a sequential activation of p38 MAPK and eNOS upon shear stress induction, it was important to verify if p38 MAPK could behave as an upstream modulator of ADP-mediated eNOS responses in the endothelium. We have consistently observed that ADP-stimulated eNOS activation is markedly attenuated

by the inhibition of p38 MAPK. These findings support a model in which p38 MAPK acts as a key modulator of ADP signaling to eNOS. Experiments conducted targeting both p38 MAPK and PTEN by siRNA methodology indicated that the increased eNOS activation promoted by PTEN inhibition was blocked by also knocking down p38 MAPK. Taken together, these findings suggest that ADP-promoted $NO^{\cdot}$ production is enhanced by PTEN phosphorylation and inactivation, which then permits the sequential activation of p38 MAPK and eNOS in vascular endothelial cells.

A key enzymatic role of PTEN is to catalyze PIP_3 conversion into PIP_2 (Salmena et al., 2008, Myers et al., 1998). We performed biochemical analysis of cellular phospholipids proving that PTEN knockdown led to a marked increase in PIP_3 levels in endothelial cells. PTEN modulates not only the abundance of PIP_3, but also the temporal and spatial distribution of this lipid and related biologically active phosphoinositides (Leslie et al., 2008). Analysis in living cells revealed that ADP-dependent increases in PIP_3 were no longer seen following PTEN knockdown, consistent with our finding that ADP promotes PTEN inhibition, such that when PTEN is already knocked down, a further ADP-stimulated PTEN-mediated PIP_3 increase is no longer observed. PTEN has been described to be implicated in cell polarity and migration, leading to cytoskeletal reorganization (Franca-Koh et al., 2007, Insall and Weiner, 2001). According to our data, PTEN knockdown notably suppressed directional migration of endothelial cells, while PIP_3 increase into the cells is enough to stimulate polarized accumulation of cortical actin.

Increasing evidences support that upon PTEN inhibition, PIP_3 accumulates and promotes the activation of distinct proteins involved in actin remodeling and cell motility such as Rac1 by binding to the specific phosphoinositide-binding pleckstrin homology domain (Leslie et al., 2008, Hall, 1998, Nobes and Hall, 1995). We analyzed Rac1 activation in living cells and found that Rac1 activation in response to ADP was decreased following PTEN knockdown. These results implicate PTEN inactivation in the pathway leading from ADP receptor stimulation to activation of Rac1.

The present study demonstrates a role for PTEN in ADP receptor-dependent eNOS activation. Our data support a model in which ADP promotes the transient phosphorylation and inactivation of PTEN, leading to an increase in PIP3 levels, which then triggers the

activation of PI3K /Akt, Rac1 and p38 MAPK, leading to enhanced eNOS activity (***Figure 64*****).**

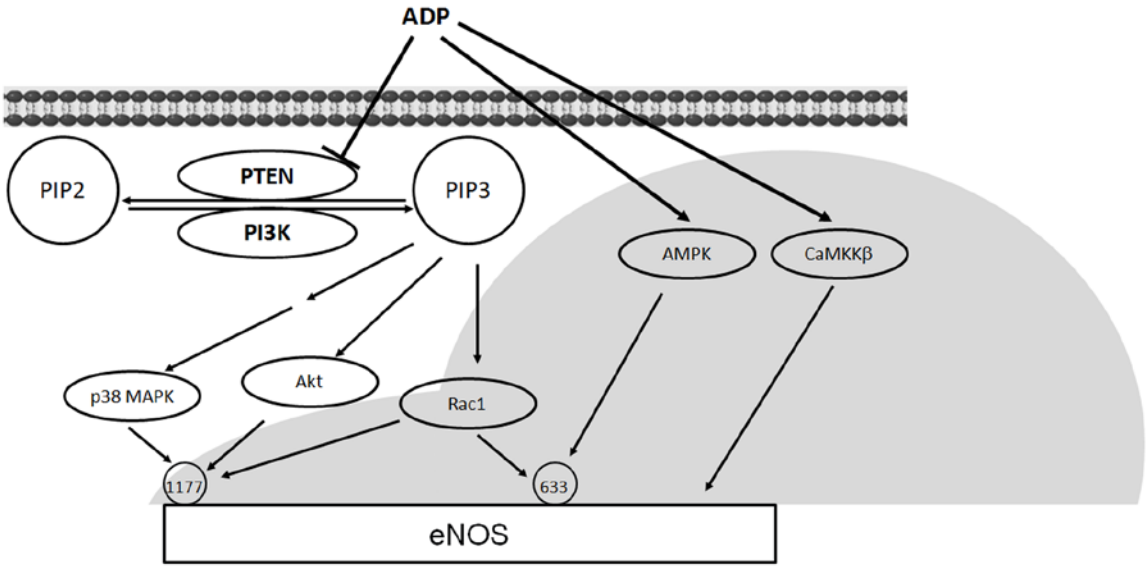

Figure 64. Role of PTEN in modulation of ADP-dependent signaling pathways in vascular endothelial cells. *We propose a model in which activation of the P2Y1 ADP receptor leads to PTEN phosphorylation and inactivation, which in turn attenuates PTEN-catalyzed PIP3 hydrolysis and thereby increases intracellular PIP3. Increased PIP3 leads to activation of kinases Akt and p38 and promotes eNOS and Rac1 activation. In contrast, siRNA-mediated PTEN knockdown impedes further ADP-dependent activation of the small GTPase Rac1, indicating that PTEN is a critical determinant of ADP-dependent signaling pathways leading to Rac1. These studies provide new insights into ADP-mediated eNOS activation with respect to those previously described by Hess et al (grey background) (Hess et al., 2009).*

This thesis adds new insights into the response of the endothelium to the mechanical and biochemical response of the endothelium to fluid flow providing novel targets for pharmacological regulation of $NO^{\cdot}$ signaling and conceptually implicating mitochondrial function in the response to LSS in the vascular endothelium.

6. CONCLUSIONS

6. CONCLUSIONS

In conclusion, in this work we have provided strong evidences for ROS involvement in the response to flow. Our data contribute to establish H_2O_2 as a physiological signaling mediator of mechanotransduction in vascular endothelial cells. More specifically we have described:

1. LSS (12dyn/cm^2) rapidly promotes endothelial intracellular increase in $O_2^{\cdot-}$ and H_2O_2, which in turn trigger the activation of p38 MAPK and eNOS in the endothelium.

2. Whereas the absence of eNOS did not modify p38 MAPK activation by laminar flow, pharmacological inhibition and knockdown of p38 MAPK α isoform present in the vasculature abrogated H_2O_2- and LSS-induced eNOS phosphorylation and reduced vasoactive $NO^{\cdot}$ levels. These effects are independent of Akt activation by LSS.

3. NOX4 is quantitatively the most abundant NADPH oxidase isoform in the endothelium, and its specific knockdown decreased p38 MAPK activation induced by laminar flow.

4. Upon shear stress induction, DRP1 is phosphorylated on its activation site and recruited from the cytosol to the outer mitochondrial membrane promoting mitochondrial constriction and fission.

5. LSS induced a decrease in oxygen consumption which correlates with a transient increase in the inner membrane potential and an increment of mitochondrial ROS.

6. Mitochondrial H_2O_2 produced after LSS induction is rapidly detoxified by the activation of the antioxidant enzyme PRX3 located inside the mitochondria.

7. LSS has an effect on mitochondrial function and thus these organelles should be considered part of the cellular machinery participating in mechanical biosensing.

8. The purine nucleotide ADP promotes the reversible phosphorylation and inactivation of PTEN in vascular endothelial cells.

9. PTEN knockdown led to a marked increase in both basal and ADP-dependent eNOS and p38 MAPK phosphorylation, establishing that p38 MAPK activation lies upstream of eNOS phosphorylation and $NO^{\cdot}$ production induced by the purine nucleotide.

10. PTEN inhibition results in an increase of its main phosphoinositide substrate PIP_3, contributing to inhibit endothelial cell migration and leading to a visible increase in actin polymerization.

7. REFERENCES

7. REFERENCES

AGO, T., KITAZONO, T., OOBOSHI, H., IYAMA, T., HAN, Y. H., TAKADA, J., WAKISAKA, M., IBAYASHI, S., UTSUMI, H. & IIDA, M. 2004. Nox4 as the major catalytic component of an endothelial NAD(P)H oxidase. *Circulation,* 109**,** 227-33.

AIKAWA, R., NAGAI, T., KUDOH, S., ZOU, Y., TANAKA, M., TAMURA, M., AKAZAWA, H., TAKANO, H., NAGAI, R. & KOMURO, I. 2002. Integrins play a critical role in mechanical stress-induced p38 MAPK activation. *Hypertension,* 39**,** 233-8.

ALI, M. H. & SCHUMACKER, P. T. 2002. Endothelial responses to mechanical stress: where is the mechanosensor? *Crit Care Med,* 30**,** S198-206.

ALTENHOFER, S., KLEIKERS, P. W., RADERMACHER, K. A., SCHEURER, P., ROB HERMANS, J. J., SCHIFFERS, P., HO, H., WINGLER, K. & SCHMIDT, H. H. 2012. The NOX toolbox: validating the role of NADPH oxidases in physiology and disease. *Cell Mol Life Sci,* 69**,** 2327-43.

ANDERSEN, J. K. 2004. Oxidative stress in neurodegeneration: cause or consequence? *Nat Med,* 10 Suppl**,** S18-25.

ANDERSON, G. H., HELLUMS, J. D., MOAKE, J. L. & ALFREY, C. P., JR. 1978. Platelet lysis and aggregation in shear fields. *Blood Cells,* 4**,** 499-511.

ANTER, E., THOMAS, S. R., SCHULZ, E., SHAPIRA, O. M., VITA, J. A. & KEANEY, J. F., JR. 2004. Activation of endothelial nitric-oxide synthase by the p38 MAPK in response to black tea polyphenols. *J Biol Chem,* 279**,** 46637-43.

ANTUNES, F. & CADENAS, E. 2000. Estimation of H2O2 gradients across biomembranes. *FEBS Lett,* 475**,** 121-6.

ANTUNES, F. & CADENAS, E. 2001. Cellular titration of apoptosis with steady state concentrations of H(2)O(2): submicromolar levels of H(2)O(2) induce apoptosis through Fenton chemistry independent of the cellular thiol state. *Free Radic Biol Med,* 30**,** 1008-18.

AOKI, K., KIYOKAWA, E., NAKAMURA, T. & MATSUDA, M. 2008. Visualization of growth signal transduction cascades in living cells with genetically encoded probes based on Forster resonance energy transfer. *Philos Trans R Soc Lond B Biol Sci,* 363**,** 2143-51.

ARROYO, C. M. & KOHNO, M. 1991. Difficulties encountered in the detection of nitric oxide (NO) by spin trapping techniques. A cautionary note. *Free Radic Res Commun,* 14**,** 145-55.

BABIOR, B. M., LAMBETH, J. D. & NAUSEEF, W. 2002. The neutrophil NADPH oxidase. *Arch Biochem Biophys,* 397**,** 342-4.

BAE, Y. S., KANG, S. W., SEO, M. S., BAINES, I. C., TEKLE, E., CHOCK, P. B. & RHEE, S. G. 1997. Epidermal growth factor (EGF)-induced generation of hydrogen peroxide. Role in EGF receptor-mediated tyrosine phosphorylation. *J Biol Chem,* 272**,** 217-21.

BALABAN, R. S., NEMOTO, S. & FINKEL, T. 2005. Mitochondria, oxidants, and aging. *Cell,* 120**,** 483-95.

BALLIGAND, J. L., FERON, O. & DESSY, C. 2009. eNOS activation by physical forces: from short-term regulation of contraction to chronic remodeling of cardiovascular tissues. *Physiol Rev,* 89**,** 481-534.

BARAKAT, A. I. 2001. A model for shear stress-induced deformation of a flow sensor on the surface of vascular endothelial cells. *J Theor Biol,* 210**,** 221-36.

BARBEE, K. A., MUNDEL, T., LAL, R. & DAVIES, P. F. 1995. Subcellular distribution of shear stress at the surface of flow-aligned and nonaligned endothelial monolayers. *Am J Physiol,* 268**,** H1765-72.

BATY, J. W., HAMPTON, M. B. & WINTERBOURN, C. C. 2005. Proteomic detection of hydrogen peroxide-sensitive thiol proteins in Jurkat cells. *Biochem J,* 389**,** 785-95.

BEDARD, K. & KRAUSE, K. H. 2007. The NOX family of ROS-generating NADPH oxidases: physiology and pathophysiology. *Physiol Rev,* 87**,** 245-313.

BELOUSOV, V. V., FRADKOV, A. F., LUKYANOV, K. A., STAROVEROV, D. B., SHAKHBAZOV, K. S., TERSKIKH, A. V. & LUKYANOV, S. 2006. Genetically encoded fluorescent indicator for intracellular hydrogen peroxide. *Nat Methods,* 3**,** 281-6.

BENOV, L., SZTEJNBERG, L. & FRIDOVICH, I. 1998. Critical evaluation of the use of hydroethidine as a measure of superoxide anion radical. *Free Radic Biol Med,* 25**,** 826-31.

BEREITER-HAHN, J. 1990. Behavior of mitochondria in the living cell. *Int Rev Cytol,* 122**,** 1-63.

BIRUKOV, K. G. 2009. Cyclic stretch, reactive oxygen species, and vascular remodeling. *Antioxid Redox Signal,* 11**,** 1651-67.

BISHOP, A. L. & HALL, A. 2000. Rho GTPases and their effector proteins. *Biochem J,* 348 Pt 2**,** 241-55.

BITEAU, B., LABARRE, J. & TOLEDANO, M. B. 2003. ATP-dependent reduction of cysteine-sulphinic acid by S. cerevisiae sulphiredoxin. *Nature,* 425**,** 980-4.

BOLDOGH, I., VOJTOV, N., KARMON, S. & PON, L. A. 1998. Interaction between mitochondria and the actin cytoskeleton in budding yeast requires two integral mitochondrial outer membrane proteins, Mmm1p and Mdm10p. *J Cell Biol,* 141**,** 1371-81.

BOO, Y. C., SORESCU, G., BOYD, N., SHIOJIMA, I., WALSH, K., DU, J. & JO, H. 2002. Shear stress stimulates phosphorylation of endothelial nitric-oxide synthase at Ser1179 by Akt-independent mechanisms: role of protein kinase A. *J Biol Chem,* 277**,** 3388-96.

BOYD, N. L., PARK, H., YI, H., BOO, Y. C., SORESCU, G. P., SYKES, M. & JO, H. 2003. Chronic shear induces caveolae formation and alters ERK and Akt responses in endothelial cells. *Am J Physiol Heart Circ Physiol,* 285**,** H1113-22.

BRANCO, M. R., MARINHO, H. S., CYRNE, L. & ANTUNES, F. 2004. Decrease of H2O2 plasma membrane permeability during adaptation to H2O2 in Saccharomyces cerevisiae. *J Biol Chem,* 279**,** 6501-6.

BRAND, M. D. 2010. The sites and topology of mitochondrial superoxide production. *Exp Gerontol,* 45**,** 466-72.

BRETON-ROMERO, R., GONZALEZ DE ORDUNA, C., ROMERO, N., SANCHEZ-GOMEZ, F. J., DE ALVARO, C., PORRAS, A., RODRIGUEZ-PASCUAL, F., LARANJINHA, J., RADI, R. & LAMAS, S. 2012. Critical role of

hydrogen peroxide signaling in the sequential activation of p38 MAPK and eNOS in laminar shear stress. *Free Radic Biol Med,* 52**,** 1093-100.

BRIEGER, K., SCHIAVONE, S., MILLER, F. J., JR. & KRAUSE, K. H. 2012. Reactive oxygen species: from health to disease. *Swiss Med Wkly,* 142**,** w13659.

BROWNING, D. D., MCSHANE, M. P., MARTY, C. & YE, R. D. 2000. Nitric oxide activation of p38 mitogen-activated protein kinase in 293T fibroblasts requires cGMP-dependent protein kinase. *J Biol Chem,* 275**,** 2811-6.

BURGOYNE, J. R., MADHANI, M., CUELLO, F., CHARLES, R. L., BRENNAN, J. P., SCHRODER, E., BROWNING, D. D. & EATON, P. 2007. Cysteine redox sensor in PKGIa enables oxidant-induced activation. *Science,* 317**,** 1393-7.

BURGOYNE, J. R., MONGUE-DIN, H., EATON, P. & SHAH, A. M. 2012. Redox signaling in cardiac physiology and pathology. *Circ Res,* 111**,** 1091-106.

BURNSTOCK, G. 2007. Purine and pyrimidine receptors. *Cell Mol Life Sci,* 64**,** 1471-83.

CAI, H. & HARRISON, D. G. 2000. Endothelial dysfunction in cardiovascular diseases: the role of oxidant stress. *Circ Res,* 87**,** 840-4.

CAI, H., LI, Z., DAVIS, M. E., KANNER, W., HARRISON, D. G. & DUDLEY, S. C., JR. 2003. Akt-dependent phosphorylation of serine 1179 and mitogen-activated protein kinase kinase/extracellular signal-regulated kinase 1/2 cooperatively mediate activation of the endothelial nitric-oxide synthase by hydrogen peroxide. *Mol Pharmacol,* 63**,** 325-31.

CAI, H., MCNALLY, J. S., WEBER, M. & HARRISON, D. G. 2004. Oscillatory shear stress upregulation of endothelial nitric oxide synthase requires intracellular hydrogen peroxide and CaMKII. *J Mol Cell Cardiol,* 37**,** 121-5.

CAO, Z., ROSZAK, A. W., GOURLAY, L. J., LINDSAY, J. G. & ISAACS, N. W. 2005. Bovine mitochondrial peroxiredoxin III forms a two-ring catenane. *Structure,* 13**,** 1661-4.

CLAIBORNE, A., MILLER, H., PARSONAGE, D. & ROSS, R. P. 1993. Protein-sulfenic acid stabilization and function in enzyme catalysis and gene regulation. *FASEB J,* 7**,** 1483-90.

CLAIBORNE, A., YEH, J. I., MALLETT, T. C., LUBA, J., CRANE, E. J., 3RD, CHARRIER, V. & PARSONAGE, D. 1999. Protein-sulfenic acids: diverse roles for an unlikely player in enzyme catalysis and redox regulation. *Biochemistry,* 38**,** 15407-16.

CORSON, M. A., JAMES, N. L., LATTA, S. E., NEREM, R. M., BERK, B. C. & HARRISON, D. G. 1996. Phosphorylation of endothelial nitric oxide synthase in response to fluid shear stress. *Circ Res,* 79**,** 984-91.

COX, A. G., WINTERBOURN, C. C. & HAMPTON, M. B. 2010. Mitochondrial peroxiredoxin involvement in antioxidant defence and redox signalling. *Biochem J,* 425**,** 313-25.

CRIBBS, J. T. & STRACK, S. 2007. Reversible phosphorylation of Drp1 by cyclic AMP-dependent protein kinase and calcineurin regulates mitochondrial fission and cell death. *EMBO Rep,* 8**,** 939-44.

CUMMING, R. C., ANDON, N. L., HAYNES, P. A., PARK, M., FISCHER, W. H. & SCHUBERT, D. 2004. Protein disulfide bond formation in the cytoplasm during oxidative stress. *J Biol Chem,* 279**,** 21749-58.

CHAE, H. Z., KIM, H. J., KANG, S. W. & RHEE, S. G. 1999. Characterization of three isoforms of mammalian peroxiredoxin that reduce peroxides in the presence of thioredoxin. *Diabetes Res Clin Pract,* 45**,** 101-12.

CHAE, H. Z., ROBISON, K., POOLE, L. B., CHURCH, G., STORZ, G. & RHEE, S. G. 1994. Cloning and sequencing of thiol-specific antioxidant from mammalian brain: alkyl hydroperoxide reductase and thiol-specific antioxidant define a large family of antioxidant enzymes. *Proc Natl Acad Sci U S A,* 91**,** 7017-21.

CHANCE, B., SIES, H. & BOVERIS, A. 1979. Hydroperoxide metabolism in mammalian organs. *Physiol Rev,* 59**,** 527-605.

CHANDEL, N. S., SCHUMACKER, P. T. & ARCH, R. H. 2001. Reactive oxygen species are downstream products of TRAF-mediated signal transduction. *J Biol Chem,* 276**,** 42728-36.

CHANG, C. R. & BLACKSTONE, C. 2007. Cyclic AMP-dependent protein kinase phosphorylation of Drp1 regulates its GTPase activity and mitochondrial morphology. *J Biol Chem,* 282**,** 21583-7.

CHANG, C. R. & BLACKSTONE, C. 2010. Dynamic regulation of mitochondrial fission through modification of the dynamin-related protein Drp1. *Ann N Y Acad Sci,* 1201**,** 34-9.

CHATZIZISIS, Y. S., COSKUN, A. U., JONAS, M., EDELMAN, E. R., FELDMAN, C. L. & STONE, P. H. 2007. Role of endothelial shear stress in the natural history of coronary atherosclerosis and vascular remodeling: molecular, cellular, and vascular behavior. *J Am Coll Cardiol,* 49**,** 2379-93.

CHEN, C. A., WANG, T. Y., VARADHARAJ, S., REYES, L. A., HEMANN, C., TALUKDER, M. A., CHEN, Y. R., DRUHAN, L. J. & ZWEIER, J. L. 2010. S-glutathionylation uncouples eNOS and regulates its cellular and vascular function. *Nature,* 468**,** 1115-8.

CHEN, K., KIRBER, M. T., XIAO, H., YANG, Y. & KEANEY, J. F., JR. 2008. Regulation of ROS signal transduction by NADPH oxidase 4 localization. *J Cell Biol,* 181**,** 1129-39.

CHEN, K. D., LI, Y. S., KIM, M., LI, S., YUAN, S., CHIEN, S. & SHYY, J. Y. 1999a. Mechanotransduction in response to shear stress. Roles of receptor tyrosine kinases, integrins, and Shc. *J Biol Chem,* 274**,** 18393-400.

CHEN, L. B. 1988. Mitochondrial membrane potential in living cells. *Annu Rev Cell Biol,* 4**,** 155-81.

CHEN, Z. P., MITCHELHILL, K. I., MICHELL, B. J., STAPLETON, D., RODRIGUEZ-CRESPO, I., WITTERS, L. A., POWER, D. A., ORTIZ DE MONTELLANO, P. R. & KEMP, B. E. 1999b. AMP-activated protein kinase phosphorylation of endothelial NO synthase. *FEBS Lett,* 443**,** 285-9.

CHENG, G., CAO, Z., XU, X., VAN MEIR, E. G. & LAMBETH, J. D. 2001. Homologs of gp91phox: cloning and tissue expression of Nox3, Nox4, and Nox5. *Gene,* 269**,** 131-40.

D'AUTREAUX, B. & TOLEDANO, M. B. 2007. ROS as signalling molecules: mechanisms that generate specificity in ROS homeostasis. *Nat Rev Mol Cell Biol,* 8**,** 813-24.

DAS, S., DIXON, J. E. & CHO, W. 2003. Membrane-binding and activation mechanism of PTEN. *Proc Natl Acad Sci U S A,* 100**,** 7491-6.

DAVIES, P. F. 1995. Flow-mediated endothelial mechanotransduction. *Physiol Rev,* 75**,** 519-60.

DE KEULENAER, G. W., CHAPPELL, D. C., ISHIZAKA, N., NEREM, R. M., ALEXANDER, R. W. & GRIENDLING, K. K. 1998. Oscillatory and steady laminar shear stress differentially affect human endothelial redox state: role of a superoxide-producing NADH oxidase. *Circ Res,* 82**,** 1094-101.

DEJANA, E., BAZZONI, G. & LAMPUGNANI, M. G. 1999. Vascular endothelial (VE)-cadherin: only an intercellular glue? *Exp Cell Res,* 252**,** 13-9.

DEKKER, R. J., VAN THIENEN, J. V., ROHLENA, J., DE JAGER, S. C., ELDERKAMP, Y. W., SEPPEN, J., DE VRIES, C. J., BIESSEN, E. A., VAN BERKEL, T. J., PANNEKOEK, H. & HORREVOETS, A. J. 2005. Endothelial KLF2 links local arterial shear stress levels to the expression of vascular tone-regulating genes. *Am J Pathol,* 167**,** 609-18.

DENISE MARTIN, E., DE NICOLA, G. F. & MARBER, M. S. 2012. New therapeutic targets in cardiology: p38 alpha mitogen-activated protein kinase for ischemic heart disease. *Circulation,* 126**,** 357-68.

DENU, J. M. & DIXON, J. E. 1998. Protein tyrosine phosphatases: mechanisms of catalysis and regulation. *Curr Opin Chem Biol,* 2**,** 633-41.

DENU, J. M. & TANNER, K. G. 1998. Specific and reversible inactivation of protein tyrosine phosphatases by hydrogen peroxide: evidence for a sulfenic acid intermediate and implications for redox regulation. *Biochemistry,* 37**,** 5633-42.

DETMER, S. A. & CHAN, D. C. 2007. Functions and dysfunctions of mitochondrial dynamics. *Nat Rev Mol Cell Biol,* 8**,** 870-9.

DEWEY, C. F., JR., BUSSOLARI, S. R., GIMBRONE, M. A., JR. & DAVIES, P. F. 1981. The dynamic response of vascular endothelial cells to fluid shear stress. *J Biomech Eng,* 103**,** 177-85.

DIAZ-LATOUD, C., BUACHE, E., JAVOUHEY, E. & ARRIGO, A. P. 2005. Substitution of the unique cysteine residue of murine Hsp25 interferes with the protective activity of this stress protein through inhibition of dimer formation. *Antioxid Redox Signal,* 7**,** 436-45.

DIMMELER, S., FLEMING, I., FISSLTHALER, B., HERMANN, C., BUSSE, R. & ZEIHER, A. M. 1999a. Activation of nitric oxide synthase in endothelial cells by Akt-dependent phosphorylation. *Nature,* 399**,** 601-5.

DIMMELER, S., HERMANN, C., GALLE, J. & ZEIHER, A. M. 1999b. Upregulation of superoxide dismutase and nitric oxide synthase mediates the apoptosis-suppressive effects of shear stress on endothelial cells. *Arterioscler Thromb Vasc Biol,* 19**,** 656-64.

DOLADO, I., SWAT, A., AJENJO, N., DE VITA, G., CUADRADO, A. & NEBREDA, A. R. 2007. p38alpha MAP kinase as a sensor of reactive oxygen species in tumorigenesis. *Cancer Cell,* 11**,** 191-205.

DOWNES, C. P., WALKER, S., MCCONNACHIE, G., LINDSAY, Y., BATTY, I. H. & LESLIE, N. R. 2004. Acute regulation of the tumour suppressor phosphatase, PTEN, by anionic lipids and reactive oxygen species. *Biochem Soc Trans,* 32**,** 338-42.

DRUMMOND, G. R., SELEMIDIS, S., GRIENDLING, K. K. & SOBEY, C. G. 2011. Combating oxidative stress in vascular disease: NADPH oxidases as therapeutic targets. *Nat Rev Drug Discov,* 10**,** 453-71.

DUAN, J. & NILSSON, L. 2006. Effect of Zn2+ on DNA recognition and stability of the p53 DNA-binding domain. *Biochemistry,* 45**,** 7483-92.

DUDZINSKI, D. M. & MICHEL, T. 2007. Life history of eNOS: partners and pathways. *Cardiovasc Res,* 75**,** 247-60.

ELLIS, H. R. & POOLE, L. B. 1997. Roles for the two cysteine residues of AhpC in catalysis of peroxide reduction by alkyl hydroperoxide reductase from Salmonella typhimurium. *Biochemistry,* 36**,** 13349-56.

ERLINGE, D. & BURNSTOCK, G. 2008. P2 receptors in cardiovascular regulation and disease. *Purinergic Signal,* 4**,** 1-20.

FERGUSON, K. M., KAVRAN, J. M., SANKARAN, V. G., FOURNIER, E., ISAKOFF, S. J., SKOLNIK, E. Y. & LEMMON, M. A. 2000. Structural basis for discrimination of 3-phosphoinositides by pleckstrin homology domains. *Mol Cell,* 6**,** 373-84.

FINK, B., LAUDE, K., MCCANN, L., DOUGHAN, A., HARRISON, D. G. & DIKALOV, S. 2004. Detection of intracellular superoxide formation in endothelial cells and intact tissues using dihydroethidium and an HPLC-based assay. *Am J Physiol Cell Physiol,* 287**,** C895-902.

FINKEL, T. & HOLBROOK, N. J. 2000. Oxidants, oxidative stress and the biology of ageing. *Nature,* 408**,** 239-47.

FISSLTHALER, B., DIMMELER, S., HERMANN, C., BUSSE, R. & FLEMING, I. 2000. Phosphorylation and activation of the endothelial nitric oxide synthase by fluid shear stress. *Acta Physiol Scand,* 168**,** 81-8.

FLAHERTY, J. T., PIERCE, J. E., FERRANS, V. J., PATEL, D. J., TUCKER, W. K. & FRY, D. L. 1972. Endothelial nuclear patterns in the canine arterial tree with particular reference to hemodynamic events. *Circ Res,* 30**,** 23-33.

FLEMING, I. 2010. Molecular mechanisms underlying the activation of eNOS. *Pflugers Arch,* 459**,** 793-806.

FRANCA-KOH, J., KAMIMURA, Y. & DEVREOTES, P. N. 2007. Leading-edge research: PtdIns(3,4,5)P3 and directed migration. *Nat Cell Biol,* 9**,** 15-7.

FUJII, J. & IKEDA, Y. 2002. Advances in our understanding of peroxiredoxin, a multifunctional, mammalian redox protein. *Redox Rep,* 7**,** 123-30.

FULTON, D., GRATTON, J. P., MCCABE, T. J., FONTANA, J., FUJIO, Y., WALSH, K., FRANKE, T. F., PAPAPETROPOULOS, A. & SESSA, W. C. 1999. Regulation of endothelium-derived nitric oxide production by the protein kinase Akt. *Nature,* 399**,** 597-601.

FULTON, D., GRATTON, J. P. & SESSA, W. C. 2001. Post-translational control of endothelial nitric oxide synthase: why isn't calcium/calmodulin enough? *J Pharmacol Exp Ther,* 299**,** 818-24.

GALLEY, H. F. & WEBSTER, N. R. 2004. Physiology of the endothelium. *Br J Anaesth,* 93**,** 105-13.

GARDNER, P. R., RAINERI, I., EPSTEIN, L. B. & WHITE, C. W. 1995. Superoxide radical and iron modulate aconitase activity in mammalian cells. *J Biol Chem,* 270**,** 13399-405.

GARTHWAITE, J. 1991. Glutamate, nitric oxide and cell-cell signalling in the nervous system. *Trends Neurosci,* 14**,** 60-7.

GODBER, B. L., DOEL, J. J., SAPKOTA, G. P., BLAKE, D. R., STEVENS, C. R., EISENTHAL, R. & HARRISON, R. 2000. Reduction of nitrite to nitric oxide catalyzed by xanthine oxidoreductase. *J Biol Chem,* 275**,** 7757-63.

GONZALEZ, E., NAGIEL, A., LIN, A. J., GOLAN, D. E. & MICHEL, T. 2004. Small interfering RNA-mediated down-regulation of caveolin-1 differentially modulates signaling pathways in endothelial cells. *J Biol Chem,* 279**,** 40659-69.

GOURLAY, L. J., BHELLA, D., KELLY, S. M., PRICE, N. C. & LINDSAY, J. G. 2003. Structure-function analysis of recombinant substrate protein 22 kDa (SP-22). A mitochondrial 2-CYS peroxiredoxin organized as a decameric toroid. *J Biol Chem,* 278**,** 32631-7.

GRANGER, D. N. 1988. Role of xanthine oxidase and granulocytes in ischemia-reperfusion injury. *Am J Physiol,* 255**,** H1269-75.

GRAUMANN, J., LILIE, H., TANG, X., TUCKER, K. A., HOFFMANN, J. H., VIJAYALAKSHMI, J., SAPER, M., BARDWELL, J. C. & JAKOB, U. 2001. Activation of the redox-regulated molecular chaperone Hsp33--a two-step mechanism. *Structure,* 9**,** 377-87.

GREENE, E. L., VELARDE, V. & JAFFA, A. A. 2000. Role of reactive oxygen species in bradykinin-induced mitogen-activated protein kinase and c-fos induction in vascular cells. *Hypertension,* 35**,** 942-7.

GRUBER, C. W., CEMAZAR, M., HERAS, B., MARTIN, J. L. & CRAIK, D. J. 2006. Protein disulfide isomerase: the structure of oxidative folding. *Trends Biochem Sci,* 31**,** 455-64.

GUDI, S. R., CLARK, C. B. & FRANGOS, J. A. 1996. Fluid flow rapidly activates G proteins in human endothelial cells. Involvement of G proteins in mechanochemical signal transduction. *Circ Res,* 79**,** 834-9.

GUNS, P. J., KORDA, A., CRAUWELS, H. M., VAN ASSCHE, T., ROBAYE, B., BOEYNAEMS, J. M. & BULT, H. 2005. Pharmacological characterization of nucleotide P2Y receptors on endothelial cells of the mouse aorta. *Br J Pharmacol,* 146**,** 288-95.

GUZIK, T. J., SADOWSKI, J., GUZIK, B., JOPEK, A., KAPELAK, B., PRZYBYLOWSKI, P., WIERZBICKI, K., KORBUT, R., HARRISON, D. G. & CHANNON, K. M. 2006. Coronary artery superoxide production and nox isoform expression in human coronary artery disease. *Arterioscler Thromb Vasc Biol,* 26**,** 333-9.

HACKENBROCK, C. R. 1966. Ultrastructural bases for metabolically linked mechanical activity in mitochondria. I. Reversible ultrastructural changes with change in metabolic steady state in isolated liver mitochondria. *J Cell Biol,* 30**,** 269-97.

HADDAD, J. J. & LAND, S. C. 2000. O(2)-evoked regulation of HIF-1alpha and NF-kappaB in perinatal lung epithelium requires glutathione biosynthesis. *Am J Physiol Lung Cell Mol Physiol,* 278**,** L492-503.

HAHN, C. & SCHWARTZ, M. A. 2009. Mechanotransduction in vascular physiology and atherogenesis. *Nat Rev Mol Cell Biol,* 10**,** 53-62.

HAIGIS, M. C. & YANKNER, B. A. 2010. The aging stress response. *Mol Cell,* 40**,** 333-44.

HALL, A. 1998. Rho GTPases and the actin cytoskeleton. *Science,* 279**,** 509-14.

HANCOCK, J. T. 2008. The role of redox in signal transduction. *Methods Mol Biol,* 476**,** 1-9.

HARRIS, J. R. 1969. Some negative contrast staining features of a protein from erythrocyte ghosts. *J Mol Biol,* 46**,** 329-35.

HARRIS, J. R., SCHRODER, E., ISUPOV, M. N., SCHEFFLER, D., KRISTENSEN, P., LITTLECHILD, J. A., VAGIN, A. A. & MEISSNER, U. 2001. Comparison of the decameric structure of peroxiredoxin-II by transmission electron microscopy and X-ray crystallography. *Biochim Biophys Acta,* 1547**,** 221-34.

HARRISON, D., GRIENDLING, K. K., LANDMESSER, U., HORNIG, B. & DREXLER, H. 2003. Role of oxidative stress in atherosclerosis. *Am J Cardiol,* 91**,** 7A-11A.

HARRISON, R. 2002. Structure and function of xanthine oxidoreductase: where are we now? *Free Radic Biol Med,* 33**,** 774-97.

HART, C. M., KLEINHENZ, D. J., DIKALOV, S. I., BOULDEN, B. M. & DUDLEY, S. C., JR. 2005. The measurement of nitric oxide production by cultured endothelial cells. *Methods Enzymol,* 396**,** 502-14.

HECKER, M., MITCHELL, J. A., HARRIS, H. J., KATSURA, M., THIEMERMANN, C. & VANE, J. R. 1990. Endothelial cells metabolize NG-monomethyl-L-arginine to L-citrulline and subsequently to L-arginine. *Biochem Biophys Res Commun,* 167**,** 1037-43.

HEITZER, T., KROHN, K., ALBERS, S. & MEINERTZ, T. 2000. Tetrahydrobiopterin improves endothelium-dependent vasodilation by increasing nitric oxide activity in patients with Type II diabetes mellitus. *Diabetologia,* 43**,** 1435-8.

HELMLINGER, G., GEIGER, R. V., SCHRECK, S. & NEREM, R. M. 1991. Effects of pulsatile flow on cultured vascular endothelial cell morphology. *J Biomech Eng,* 113**,** 123-31.

HESS, C. N., KOU, R., JOHNSON, R. P., LI, G. K. & MICHEL, T. 2009. ADP signaling in vascular endothelial cells: ADP-dependent activation of the endothelial isoform of nitric-oxide synthase requires the expression but not the kinase activity of AMP-activated protein kinase. *J Biol Chem,* 284**,** 32209-24.

HESS, D. T., MATSUMOTO, A., KIM, S. O., MARSHALL, H. E. & STAMLER, J. S. 2005. Protein S-nitrosylation: purview and parameters. *Nat Rev Mol Cell Biol,* 6**,** 150-66.

HEUMULLER, S., WIND, S., BARBOSA-SICARD, E., SCHMIDT, H. H., BUSSE, R., SCHRODER, K. & BRANDES, R. P. 2008. Apocynin is not an inhibitor of vascular NADPH oxidases but an antioxidant. *Hypertension,* 51**,** 211-7.

HIGASHI, Y., SASAKI, S., NAKAGAWA, K., FUKUDA, Y., MATSUURA, H., OSHIMA, T. & CHAYAMA, K. 2002. Tetrahydrobiopterin enhances forearm vascular response to acetylcholine in both normotensive and hypertensive individuals. *Am J Hypertens,* 15**,** 326-32.

HOLMGREN, A., JOHANSSON, C., BERNDT, C., LONN, M. E., HUDEMANN, C. & LILLIG, C. H. 2005. Thiol redox control via thioredoxin and glutaredoxin systems. *Biochem Soc Trans,* 33**,** 1375-7.

HOLMSEN, H. & WEISS, H. J. 1979. Secretable storage pools in platelets. *Annu Rev Med,* 30**,** 119-34.

HOLLAND, J. A., MEYER, J. W., CHANG, M. M., O'DONNELL, R. W., JOHNSON, D. K. & ZIEGLER, L. M. 1998. Thrombin stimulated reactive oxygen species production in cultured human endothelial cells. *Endothelium,* 6**,** 113-21.

HOPPE, G., CHAI, Y. C., CRABB, J. W. & SEARS, J. 2004. Protein s-glutathionylation in retinal pigment epithelium converts heat shock protein 70 to an active chaperone. *Exp Eye Res,* 78**,** 1085-92.

HOPPINS, S., LACKNER, L. & NUNNARI, J. 2007. The machines that divide and fuse mitochondria. *Annu Rev Biochem,* 76**,** 751-80.

HU, Z., CHEN, J., WEI, Q. & XIA, Y. 2008. Bidirectional actions of hydrogen peroxide on endothelial nitric-oxide synthase phosphorylation and function: co-commitment and interplay of Akt and AMPK. *J Biol Chem,* 283**,** 25256-63.

IGNARRO, L. J., BUGA, G. M., WOOD, K. S., BYRNS, R. E. & CHAUDHURI, G. 1987. Endothelium-derived relaxing factor produced and released from artery and vein is nitric oxide. *Proc Natl Acad Sci U S A,* 84**,** 9265-9.

INSALL, R. H. & WEINER, O. D. 2001. PIP3, PIP2, and cell movement--similar messages, different meanings? *Dev Cell,* 1**,** 743-7.

ISSHIKI, M., ANDO, J., YAMAMOTO, K., FUJITA, T., YING, Y. & ANDERSON, R. G. 2002. Sites of Ca(2+) wave initiation move with caveolae to the trailing edge of migrating cells. *J Cell Sci,* 115**,** 475-84.

JAKOB, U., MUSE, W., ESER, M. & BARDWELL, J. C. 1999. Chaperone activity with a redox switch. *Cell,* 96**,** 341-52.

JANSSEN-HEININGER, Y. M., MOSSMAN, B. T., HEINTZ, N. H., FORMAN, H. J., KALYANARAMAN, B., FINKEL, T., STAMLER, J. S., RHEE, S. G. & VAN DER VLIET, A. 2008. Redox-based regulation of signal transduction: principles, pitfalls, and promises. *Free Radic Biol Med,* 45**,** 1-17.

JARASCH, E. D., GRUND, C., BRUDER, G., HEID, H. W., KEENAN, T. W. & FRANKE, W. W. 1981. Localization of xanthine oxidase in mammary-gland epithelium and capillary endothelium. *Cell,* 25**,** 67-82.

JEZEK, P. & PLECITA-HLAVATA, L. 2009. Mitochondrial reticulum network dynamics in relation to oxidative stress, redox regulation, and hypoxia. *Int J Biochem Cell Biol,* 41**,** 1790-804.

JIANG, B. H., ZHENG, J. Z., AOKI, M. & VOGT, P. K. 2000. Phosphatidylinositol 3-kinase signaling mediates angiogenesis and expression of vascular endothelial growth factor in endothelial cells. *Proc Natl Acad Sci U S A,* 97**,** 1749-53.

JONES, D. P. 2006. Redefining oxidative stress. *Antioxid Redox Signal,* 8**,** 1865-79.

KAMATA, H., HONDA, S., MAEDA, S., CHANG, L., HIRATA, H. & KARIN, M. 2005. Reactive oxygen species promote TNFalpha-induced death and sustained JNK activation by inhibiting MAP kinase phosphatases. *Cell,* 120**,** 649-61.

KANG, S. W., RHEE, S. G., CHANG, T. S., JEONG, W. & CHOI, M. H. 2005. 2-Cys peroxiredoxin function in intracellular signal transduction: therapeutic implications. *Trends Mol Med,* 11**,** 571-8.

KANO, Y., KATOH, K. & FUJIWARA, K. 2000. Lateral zone of cell-cell adhesion as the major fluid shear stress-related signal transduction site. *Circ Res,* 86**,** 425-33.

KEYES, K. T., XU, J., LONG, B., ZHANG, C., HU, Z. & YE, Y. 2010. Pharmacological inhibition of PTEN limits myocardial infarct size and improves left ventricular function postinfarction. *Am J Physiol Heart Circ Physiol,* 298**,** H1198-208.

KHAZAEI, M., MOIEN-AFSHARI, F. & LAHER, I. 2008. Vascular endothelial function in health and diseases. *Pathophysiology,* 15**,** 49-67.

KIM, J. R., YOON, H. W., KWON, K. S., LEE, S. R. & RHEE, S. G. 2000. Identification of proteins containing cysteine residues that are sensitive to oxidation by hydrogen peroxide at neutral pH. *Anal Biochem,* 283**,** 214-21.

KIRKINEZOS, I. G. & MORAES, C. T. 2001. Reactive oxygen species and mitochondrial diseases. *Semin Cell Dev Biol,* 12**,** 449-57.

KNOOPS, B., CLIPPE, A., BOGARD, C., ARSALANE, K., WATTIEZ, R., HERMANS, C., DUCONSEILLE, E., FALMAGNE, P. & BERNARD, A. 1999. Cloning and characterization of AOEB166, a novel mammalian antioxidant enzyme of the peroxiredoxin family. *J Biol Chem,* 274**,** 30451-8.

KONISHI, H., KURODA, S. & KIKKAWA, U. 1994. The pleckstrin homology domain of RAC protein kinase associates with the regulatory domain of protein kinase C zeta. *Biochem Biophys Res Commun,* 205**,** 1770-5.

KRIEGER-BRAUER, H. I. & KATHER, H. 1995. The stimulus-sensitive H2O2-generating system present in human fat-cell plasma membranes is multireceptor-linked and under antagonistic control by hormones and cytokines. *Biochem J,* 307 (Pt 2)**,** 543-8.

KROLL, M. H., HELLUMS, J. D., MCINTIRE, L. V., SCHAFER, A. I. & MOAKE, J. L. 1996. Platelets and shear stress. *Blood,* 88**,** 1525-41.

KU, D. N. 1997. BLOOD FLOW IN ARTERIES. *Annual Review of Fluid Mechanics,* 29**,** 399-434.

KUMPHUNE, S., BASSI, R., JACQUET, S., SICARD, P., CLARK, J. E., VERMA, S., AVKIRAN, M., O'KEEFE, S. J. & MARBER, M. S. 2010. A chemical genetic approach reveals that p38alpha MAPK activation by diphosphorylation aggravates myocardial infarction and is prevented by the direct binding of SB203580. *J Biol Chem,* 285**,** 2968-75.

KURODA, J., AGO, T., MATSUSHIMA, S., ZHAI, P., SCHNEIDER, M. D. & SADOSHIMA, J. 2010. NADPH oxidase 4 (Nox4) is a major source of oxidative stress in the failing heart. *Proc Natl Acad Sci U S A,* 107**,** 15565-70.

KWON, J., LEE, S. R., YANG, K. S., AHN, Y., KIM, Y. J., STADTMAN, E. R. & RHEE, S. G. 2004. Reversible oxidation and inactivation of the tumor suppressor PTEN in cells stimulated with peptide growth factors. *Proc Natl Acad Sci U S A,* 101**,** 16419-24.

LACKNER, L. L. & NUNNARI, J. M. 2009. The molecular mechanism and cellular functions of mitochondrial division. *Biochim Biophys Acta,* 1792**,** 1138-44.

LANDMESSER, U., DIKALOV, S., PRICE, S. R., MCCANN, L., FUKAI, T., HOLLAND, S. M., MITCH, W. E. & HARRISON, D. G. 2003. Oxidation of tetrahydrobiopterin leads to uncoupling of endothelial cell nitric oxide synthase in hypertension. *J Clin Invest,* 111**,** 1201-9.

LANGREHR, J. M., HOFFMAN, R. A., LANCASTER, J. R., JR. & SIMMONS, R. L. 1993. Nitric oxide--a new endogenous immunomodulator. *Transplantation,* 55**,** 1205-12.

LAURINDO, F. R., PEDRO MDE, A., BARBEIRO, H. V., PILEGGI, F., CARVALHO, M. H., AUGUSTO, O. & DA LUZ, P. L. 1994. Vascular free radical release. Ex vivo and in vivo evidence for a flow-dependent endothelial mechanism. *Circ Res,* 74**,** 700-9.

LEE, I., BENDER, E. & KADENBACH, B. 2002a. Control of mitochondrial membrane potential and ROS formation by reversible phosphorylation of cytochrome c oxidase. *Mol Cell Biochem,* 234-235**,** 63-70.

LEE, S. R., YANG, K. S., KWON, J., LEE, C., JEONG, W. & RHEE, S. G. 2002b. Reversible inactivation of the tumor suppressor PTEN by H2O2. *J Biol Chem,* 277**,** 20336-42.

LEE, Y. J. & SHACTER, E. 2000. Hydrogen peroxide inhibits activation, not activity, of cellular caspase-3 in vivo. *Free Radic Biol Med,* 29**,** 684-92.

LEHOUX, S. 2006. Redox signalling in vascular responses to shear and stretch. *Cardiovasc Res,* 71**,** 269-79.

LESLIE, N. R., BATTY, I. H., MACCARIO, H., DAVIDSON, L. & DOWNES, C. P. 2008. Understanding PTEN regulation: PIP2, polarity and protein stability. *Oncogene,* 27**,** 5464-76.

LEVESQUE, M. J. & NEREM, R. M. 1985. The elongation and orientation of cultured endothelial cells in response to shear stress. *J Biomech Eng,* 107**,** 341-7.

LI, H., SAMOUILOV, A., LIU, X. & ZWEIER, J. L. 2001. Characterization of the magnitude and kinetics of xanthine oxidase-catalyzed nitrite reduction. Evaluation of its role in nitric oxide generation in anoxic tissues. *J Biol Chem,* 276**,** 24482-9.

LI, J., YEN, C., LIAW, D., PODSYPANINA, K., BOSE, S., WANG, S. I., PUC, J., MILIARESIS, C., RODGERS, L., MCCOMBIE, R., BIGNER, S. H., GIOVANELLA, B. C., ITTMANN, M., TYCKO, B., HIBSHOOSH, H., WIGLER, M. H. & PARSONS, R. 1997. PTEN, a putative protein tyrosine phosphatase gene mutated in human brain, breast, and prostate cancer. *Science,* 275**,** 1943-7.

LI, J. M. & SHAH, A. M. 2004. Endothelial cell superoxide generation: regulation and relevance for cardiovascular pathophysiology. *Am J Physiol Regul Integr Comp Physiol,* 287**,** R1014-30.

LI, Y. S., HAGA, J. H. & CHIEN, S. 2005. Molecular basis of the effects of shear stress on vascular endothelial cells. *J Biomech,* 38**,** 1949-71.

LIESA, M., PALACIN, M. & ZORZANO, A. 2009. Mitochondrial dynamics in mammalian health and disease. *Physiol Rev,* 89**,** 799-845.

LIOCHEV, S. I. & FRIDOVICH, I. 1999. Superoxide and iron: partners in crime. *IUBMB Life,* 48**,** 157-61.

LO, Y. Y. & CRUZ, T. F. 1995. Involvement of reactive oxygen species in cytokine and growth factor induction of c-fos expression in chondrocytes. *J Biol Chem,* 270**,** 11727-30.

MALEK, A. M., ALPER, S. L. & IZUMO, S. 1999. Hemodynamic shear stress and its role in atherosclerosis. *JAMA,* 282**,** 2035-42.

MARTINEZ, M. C. & ANDRIANTSITOHAINA, R. 2009. Reactive nitrogen species: molecular mechanisms and potential significance in health and disease. *Antioxid Redox Signal,* 11**,** 669-702.

MATLUNG, H. L., BAKKER, E. N. & VANBAVEL, E. 2009. Shear stress, reactive oxygen species, and arterial structure and function. *Antioxid Redox Signal,* 11**,** 1699-709.

MATOBA, T., SHIMOKAWA, H., NAKASHIMA, M., HIRAKAWA, Y., MUKAI, Y., HIRANO, K., KANAIDE, H. & TAKESHITA, A. 2000. Hydrogen peroxide is an endothelium-derived hyperpolarizing factor in mice. *J Clin Invest,* 106**,** 1521-30.

MAY, J. M. & DE HAEN, C. 1979. Insulin-stimulated intracellular hydrogen peroxide production in rat epididymal fat cells. *J Biol Chem,* 254**,** 2214-20.

MENG, T. C., FUKADA, T. & TONKS, N. K. 2002. Reversible oxidation and inactivation of protein tyrosine phosphatases in vivo. *Mol Cell,* 9**,** 387-99.

MICHELL, B. J., CHEN, Z., TIGANIS, T., STAPLETON, D., KATSIS, F., POWER, D. A., SIM, A. T. & KEMP, B. E. 2001. Coordinated control of endothelial nitric-oxide synthase phosphorylation by protein kinase C and the cAMP-dependent protein kinase. *J Biol Chem,* 276**,** 17625-8.

MILKIEWICZ, M., KELLAND, C., COLGAN, S. & HAAS, T. L. 2006. Nitric oxide and p38 MAP kinase mediate shear stress-dependent inhibition of MMP-2 production in microvascular endothelial cells. *J Cell Physiol,* 208**,** 229-37.

MONCADA, S., PALMER, R. M. & HIGGS, E. A. 1989. Biosynthesis of nitric oxide from L-arginine. A pathway for the regulation of cell function and communication. *Biochem Pharmacol,* 38**,** 1709-15.

MONCADA, S., PALMER, R. M. & HIGGS, E. A. 1991. Nitric oxide: physiology, pathophysiology, and pharmacology. *Pharmacol Rev,* 43**,** 109-42.

MOORE, R. B., MANKAD, M. V., SHRIVER, S. K., MANKAD, V. N. & PLISHKER, G. A. 1991. Reconstitution of Ca(2+)-dependent K+ transport in erythrocyte membrane vesicles requires a cytoplasmic protein. *J Biol Chem,* 266**,** 18964-8.

MORELLO, F., PERINO, A. & HIRSCH, E. 2009. Phosphoinositide 3-kinase signalling in the vascular system. *Cardiovasc Res,* 82**,** 261-71.

MYERS, M. P., PASS, I., BATTY, I. H., VAN DER KAAY, J., STOLAROV, J. P., HEMMINGS, B. A., WIGLER, M. H., DOWNES, C. P. & TONKS, N. K. 1998. The lipid phosphatase activity of PTEN is critical for its tumor supressor function. *Proc Natl Acad Sci U S A,* 95**,** 13513-8.

NA, H. K. & SURH, Y. J. 2006. Transcriptional regulation via cysteine thiol modification: a novel molecular strategy for chemoprevention and cytoprotection. *Mol Carcinog,* 45**,** 368-80.

NARDAI, G., SASS, B., EBER, J., OROSZ, G. & CSERMELY, P. 2000. Reactive cysteines of the 90-kDa heat shock protein, Hsp90. *Arch Biochem Biophys,* 384**,** 59-67.

NATHAN, C. 2003. Specificity of a third kind: reactive oxygen and nitrogen intermediates in cell signaling. *J Clin Invest,* 111**,** 769-78.

NAVARRO-ANTOLIN, J., LOPEZ-MUNOZ, M. J., KLATT, P., SORIA, J., MICHEL, T. & LAMAS, S. 2001. Formation of peroxynitrite in vascular endothelial cells exposed to cyclosporine A. *FASEB J,* 15**,** 1291-3.

NEMOTO, S., TAKEDA, K., YU, Z. X., FERRANS, V. J. & FINKEL, T. 2000. Role for mitochondrial oxidants as regulators of cellular metabolism. *Mol Cell Biol,* 20**,** 7311-8.

NEREM, R. M., ALEXANDER, R. W., CHAPPELL, D. C., MEDFORD, R. M., VARNER, S. E. & TAYLOR, W. R. 1998. The study of the influence of flow on vascular endothelial biology. *Am J Med Sci,* 316**,** 169-75.

NICHOLS, W. W., O'ROURKE, M. F. E. & KENNEY, W. L. 1991. McDonald's Blood Flow in Arteries: Theoretical, Experimental and Clinical Principles, ed. 3. *Journal of Cardiopulmonary Rehabilitation and Prevention,* 11**,** 407.

NICHOLS WW, O. R. M. M. S. 2005. Blood Flow in Arteries: Theoretical, Experimental and Clincal Principles. *Hodder Arnold Publication,*.

NICHOLLS, D. G. & WARD, M. W. 2000. Mitochondrial membrane potential and neuronal glutamate excitotoxicity: mortality and millivolts. *Trends Neurosci,* 23**,** 166-74.

NOBES, C. D. & HALL, A. 1995. Rho, rac, and cdc42 GTPases regulate the assembly of multimolecular focal complexes associated with actin stress fibers, lamellipodia, and filopodia. *Cell,* 81**,** 53-62.

OGINO, K. & WANG, D. H. 2007. Biomarkers of oxidative/nitrosative stress: an approach to disease prevention. *Acta Med Okayama,* 61**,** 181-9.

OKAMOTO, T., AKUTA, T., TAMURA, F., VAN DER VLIET, A. & AKAIKE, T. 2004. Molecular mechanism for activation and regulation of matrix metalloproteinases during bacterial infections and respiratory inflammation. *Biol Chem,* 385**,** 997-1006.

ONG, S. B. & HAUSENLOY, D. J. 2010. Mitochondrial morphology and cardiovascular disease. *Cardiovasc Res,* 88**,** 16-29.

PAPADAKI, M. & ESKIN, S. G. 1997. Effects of fluid shear stress on gene regulation of vascular cells. *Biotechnol Prog,* 13**,** 209-21.

PAPADAKI, M., ESKIN, S. G., RUEF, J., RUNGE, M. S. & MCINTIRE, L. V. 1999. Fluid shear stress as a regulator of gene expression in vascular cells: possible correlations with diabetic abnormalities. *Diabetes Res Clin Pract,* 45**,** 89-99.

PARAVICINI, T. M. & TOUYZ, R. M. 2006. Redox signaling in hypertension. *Cardiovasc Res,* 71**,** 247-58.

PARMAR, K. M., LARMAN, H. B., DAI, G., ZHANG, Y., WANG, E. T., MOORTHY, S. N., KRATZ, J. R., LIN, Z., JAIN, M. K., GIMBRONE, M. A., JR. & GARCIA-CARDENA, G. 2006. Integration of flow-dependent endothelial phenotypes by Kruppel-like factor 2. *J Clin Invest,* 116**,** 49-58.

PARSONAGE, D., YOUNGBLOOD, D. S., SARMA, G. N., WOOD, Z. A., KARPLUS, P. A. & POOLE, L. B. 2005. Analysis of the link between enzymatic activity and oligomeric state in AhpC, a bacterial peroxiredoxin. *Biochemistry,* 44**,** 10583-92.

PIKE, L. J., HAN, X., CHUNG, K. N. & GROSS, R. W. 2002. Lipid rafts are enriched in arachidonic acid and plasmenylethanolamine and their composition is independent of caveolin-1 expression: a quantitative electrospray ionization/mass spectrometric analysis. *Biochemistry,* 41**,** 2075-88.

PTASINSKA, A., WANG, S., ZHANG, J., WESLEY, R. A. & DANNER, R. L. 2007. Nitric oxide activation of peroxisome proliferator-activated receptor gamma through a p38 MAPK signaling pathway. *FASEB J,* 21**,** 950-61.

RALEVIC, V. & BURNSTOCK, G. 2003. Involvement of purinergic signaling in cardiovascular diseases. *Drug News Perspect,* 16**,** 133-40.

RAY, P. D., HUANG, B. W. & TSUJI, Y. 2012. Reactive oxygen species (ROS) homeostasis and redox regulation in cellular signaling. *Cell Signal,* 24**,** 981-90.

RAY, R., MURDOCH, C. E., WANG, M., SANTOS, C. X., ZHANG, M., ALOM-RUIZ, S., ANILKUMAR, N., OUATTARA, A., CAVE, A. C., WALKER, S. J., GRIEVE, D. J., CHARLES, R. L., EATON, P., BREWER, A. C. & SHAH, A. M. 2011. Endothelial Nox4 NADPH oxidase enhances vasodilatation and reduces blood pressure in vivo. *Arterioscler Thromb Vasc Biol,* 31**,** 1368-76.

RAZANI, B. & LISANTI, M. P. 2001. Caveolin-deficient mice: insights into caveolar function human disease. *J Clin Invest,* 108**,** 1553-61.

RESNICK, N., YAHAV, H., SHAY-SALIT, A., SHUSHY, M., SCHUBERT, S., ZILBERMAN, L. C. & WOFOVITZ, E. 2003. Fluid shear stress and the vascular endothelium: for better and for worse. *Prog Biophys Mol Biol,* 81**,** 177-99.

RHEE, S. G. 2006. Cell signaling. H2O2, a necessary evil for cell signaling. *Science,* 312**,** 1882-3.

RHEE, S. G., BAE, Y. S., LEE, S. R. & KWON, J. 2000. Hydrogen peroxide: a key messenger that modulates protein phosphorylation through cysteine oxidation. *Sci STKE,* 2000**,** pe1.

RHEE, S. G., CHANG, T. S., BAE, Y. S., LEE, S. R. & KANG, S. W. 2003. Cellular regulation by hydrogen peroxide. *J Am Soc Nephrol,* 14**,** S211-5.

RHEE, S. G., KANG, S. W., CHANG, T. S., JEONG, W. & KIM, K. 2001. Peroxiredoxin, a novel family of peroxidases. *IUBMB Life,* 52**,** 35-41.

RHEE, S. G. & WOO, H. A. 2011. Multiple functions of peroxiredoxins: peroxidases, sensors and regulators of the intracellular messenger H(2)O(2), and protein chaperones. *Antioxid Redox Signal,* 15**,** 781-94.

RIVA, A., TANDLER, B., LOFFREDO, F., VAZQUEZ, E. & HOPPEL, C. 2005. Structural differences in two biochemically defined populations of cardiac mitochondria. *Am J Physiol Heart Circ Physiol,* 289**,** H868-72.

ROJAS, A., FIGUEROA, H., RE, L. & MORALES, M. A. 2006. Oxidative stress at the vascular wall. Mechanistic and pharmacological aspects. *Arch Med Res,* 37**,** 436-48.

ROS, J., JIMENEZ, W., LAMAS, S., CLARIA, J., ARROYO, V., RIVERA, F. & RODES, J. 1995. Nitric oxide production in arterial vessels of cirrhotic rats. *Hepatology,* 21**,** 554-60.

ROSSI, F. & ZATTI, M. 1964. Biochemical aspects of phagocytosis in polymorphonuclear leucocytes. NADH and NADPH oxidation by the granules of resting and phagocytizing cells. *Experientia,* 20**,** 21-3.

SALMENA, L., CARRACEDO, A. & PANDOLFI, P. P. 2008. Tenets of PTEN tumor suppression. *Cell,* 133**,** 403-14.

SANTEL, A. & FRANK, S. 2008. Shaping mitochondria: The complex posttranslational regulation of the mitochondrial fission protein DRP1. *IUBMB Life,* 60**,** 448-55.

SARTORETTO, J. L., KALWA, H., PLUTH, M. D., LIPPARD, S. J. & MICHEL, T. 2011. Hydrogen peroxide differentially modulates cardiac myocyte nitric oxide synthesis. *Proc Natl Acad Sci U S A,* 108**,** 15792-7.

SATTLER, M., WINKLER, T., VERMA, S., BYRNE, C. H., SHRIKHANDE, G., SALGIA, R. & GRIFFIN, J. D. 1999. Hematopoietic growth factors signal through the formation of reactive oxygen species. *Blood,* 93**,** 2928-35.

SAURIN, A. T., NEUBERT, H., BRENNAN, J. P. & EATON, P. 2004. Widespread sulfenic acid formation in tissues in response to hydrogen peroxide. *Proc Natl Acad Sci U S A,* 101**,** 17982-7.

SCHRECK, R., RIEBER, P. & BAEUERLE, P. A. 1991. Reactive oxygen intermediates as apparently widely used messengers in the activation of the NF-kappa B transcription factor and HIV-1. *Embo J,* 10**,** 2247-58.

SCHRODER, K., ZHANG, M., BENKHOFF, S., MIETH, A., PLIQUETT, R., KOSOWSKI, J., KRUSE, C., LUEDIKE, P., MICHAELIS, U. R., WEISSMANN, N., DIMMELER, S., SHAH, A. M. & BRANDES, R. P. 2012. Nox4 is a protective reactive oxygen species generating vascular NADPH oxidase. *Circ Res,* 110**,** 1217-25.

SCHWARTZ, M. A. & GINSBERG, M. H. 2002. Networks and crosstalk: integrin signalling spreads. *Nat Cell Biol,* 4**,** E65-8.

SEMENZA, G. L. 2001. HIF-1 and mechanisms of hypoxia sensing. *Curr Opin Cell Biol,* 13**,** 167-71.

SENA, L. A. & CHANDEL, N. S. 2012. Physiological roles of mitochondrial reactive oxygen species. *Mol Cell,* 48**,** 158-67.

SEO, M. S., KANG, S. W., KIM, K., BAINES, I. C., LEE, T. H. & RHEE, S. G. 2000. Identification of a new type of mammalian peroxiredoxin that forms an intramolecular disulfide as a reaction intermediate. *J Biol Chem,* 275**,** 20346-54.

SERGEY DIKALOV, K. K. G., AND DAVID G. HARRISON 2007. Measurement of Reactive Oxygen Species in Cardiovascular Studies. *Hypertension,* 49**,** 717–727.

SETH, D. & RUDOLPH, J. 2006. Redox regulation of MAP kinase phosphatase 3. *Biochemistry,* 45**,** 8476-87.

SHEN, Y. H., ZHANG, L., GAN, Y., WANG, X., WANG, J., LEMAIRE, S. A., COSELLI, J. S. & WANG, X. L. 2006a. Up-regulation of PTEN (phosphatase and tensin homolog deleted on chromosome ten) mediates p38 MAPK stress signal-induced inhibition of insulin signaling. A cross-talk between stress signaling and insulin signaling in resistin-treated human endothelial cells. *J Biol Chem,* 281**,** 7727-36.

SHEN, Y. H., ZHANG, L., UTAMA, B., WANG, J., GAN, Y., WANG, X., CHEN, L., VERCELLOTTI, G. M., COSELLI, J. S., MEHTA, J. L. & WANG, X. L. 2006b. Human cytomegalovirus inhibits Akt-mediated eNOS activation through upregulating PTEN (phosphatase and tensin homolog deleted on chromosome 10). *Cardiovasc Res,* 69**,** 502-11.

SHERIDAN, C. & MARTIN, S. J. 2010. Mitochondrial fission/fusion dynamics and apoptosis. *Mitochondrion,* 10**,** 640-8.

SHIGENAGA, M. K., HAGEN, T. M. & AMES, B. N. 1994. Oxidative damage and mitochondrial decay in aging. *Proc Natl Acad Sci U S A,* 91**,** 10771-8.

SICARD, P., CLARK, J. E., JACQUET, S., MOHAMMADI, S., ARTHUR, J. S., O'KEEFE, S. J. & MARBER, M. S. 2010. The activation of p38 alpha, and not p38 beta, mitogen-activated protein kinase is required for ischemic preconditioning. *J Mol Cell Cardiol,* 48**,** 1324-8.

SILVA, A., YUNES, J. A., CARDOSO, B. A., MARTINS, L. R., JOTTA, P. Y., ABECASIS, M., NOWILL, A. E., LESLIE, N. R., CARDOSO, A. A. & BARATA, J. T. 2008. PTEN posttranslational inactivation and hyperactivation of the PI3K/Akt pathway sustain primary T cell leukemia viability. *J Clin Invest,* 118**,** 3762-74.

SIMONS, J. M., HART, B. A., IP VAI CHING, T. R., VAN DIJK, H. & LABADIE, R. P. 1990. Metabolic activation of natural phenols into selective oxidative burst agonists by activated human neutrophils. *Free Radic Biol Med,* 8**,** 251-8.

SITIA, R. & MOLTENI, S. N. 2004. Stress, protein (mis)folding, and signaling: the redox connection. *Sci STKE,* 2004**,** pe27.

SMIRNOVA, E., GRIPARIC, L., SHURLAND, D. L. & VAN DER BLIEK, A. M. 2001. Dynamin-related protein Drp1 is required for mitochondrial division in mammalian cells. *Mol Biol Cell,* 12**,** 2245-56.

SONG, K. S., LI, S., OKAMOTO, T., QUILLIAM, L. A., SARGIACOMO, M. & LISANTI, M. P. 1996. Co-purification and direct interaction of Ras with caveolin, an integral membrane protein of caveolae microdomains. Detergent-free purification of caveolae microdomains. *J Biol Chem,* 271**,** 9690-7.

SORESCU, G. P., SONG, H., TRESSEL, S. L., HWANG, J., DIKALOV, S., SMITH, D. A., BOYD, N. L., PLATT, M. O., LASSEGUE, B., GRIENDLING, K. K. & JO, H. 2004. Bone morphogenic protein 4 produced in endothelial cells by oscillatory shear stress induces monocyte adhesion by stimulating reactive oxygen species production from a nox1-based NADPH oxidase. *Circ Res,* 95**,** 773-9.

SOUBANNIER, V. & MCBRIDE, H. M. 2009. Positioning mitochondrial plasticity within cellular signaling cascades. *Biochim Biophys Acta,* 1793**,** 154-70.

SPIEKERMANN, S., LANDMESSER, U., DIKALOV, S., BREDT, M., GAMEZ, G., TATGE, H., REEPSCHLAGER, N., HORNIG, B., DREXLER, H. & HARRISON, D. G. 2003. Electron spin resonance characterization of vascular xanthine and NAD(P)H oxidase activity in patients with coronary artery disease: relation to endothelium-dependent vasodilation. *Circulation,* 107**,** 1383-9.

SRIKUN, D., ALBERS, A. E., NAM, C. I., IAVARONE, A. T. & CHANG, C. J. 2010. Organelle-targetable fluorescent probes for imaging hydrogen peroxide in living cells via SNAP-Tag protein labeling. *J Am Chem Soc,* 132**,** 4455-65.

STECK, P. A., PERSHOUSE, M. A., JASSER, S. A., YUNG, W. K., LIN, H., LIGON, A. H., LANGFORD, L. A., BAUMGARD, M. L., HATTIER, T., DAVIS, T., FRYE, C., HU, R., SWEDLUND, B., TENG, D. H. & TAVTIGIAN, S. V. 1997. Identification of a candidate tumour suppressor gene, MMAC1, at chromosome 10q23.3 that is mutated in multiple advanced cancers. *Nat Genet,* 15**,** 356-62.

STILES, B., GROSZER, M., WANG, S., JIAO, J. & WU, H. 2004. PTENless means more. *Dev Biol,* 273**,** 175-84.

STOCKER, R. & KEANEY, J. F., JR. 2004. Role of oxidative modifications in atherosclerosis. *Physiol Rev,* 84**,** 1381-478.

STONE, J. R. & YANG, S. 2006. Hydrogen peroxide: a signaling messenger. *Antioxid Redox Signal,* 8**,** 243-70.

STROES, E., KASTELEIN, J., COSENTINO, F., ERKELENS, W., WEVER, R., KOOMANS, H., LUSCHER, T. & RABELINK, T. 1997. Tetrahydrobiopterin restores endothelial function in hypercholesterolemia. *J Clin Invest,* 99**,** 41-6.

SUMPIO, B. E., YUN, S., CORDOVA, A. C., HAGA, M., ZHANG, J., KOH, Y. & MADRI, J. A. 2005. MAPKs (ERK1/2, p38) and AKT can be phosphorylated by shear stress independently of platelet endothelial cell adhesion molecule-1 (CD31) in vascular endothelial cells. *J Biol Chem,* 280**,** 11185-91.

SUNDARESAN, M., YU, Z. X., FERRANS, V. J., IRANI, K. & FINKEL, T. 1995. Requirement for generation of H2O2 for platelet-derived growth factor signal transduction. *Science,* 270**,** 296-9.

SURAPISITCHAT, J., HOEFEN, R. J., PI, X., YOSHIZUMI, M., YAN, C. & BERK, B. C. 2001. Fluid shear stress inhibits TNF-alpha activation of JNK but not ERK1/2 or p38 in human umbilical vein endothelial cells: Inhibitory crosstalk among MAPK family members. *Proc Natl Acad Sci U S A,* 98**,** 6476-81.

TAKAC, I., SCHRODER, K., ZHANG, L., LARDY, B., ANILKUMAR, N., LAMBETH, J. D., SHAH, A. M., MOREL, F. & BRANDES, R. P. 2011. The E-loop is involved in hydrogen peroxide formation by the NADPH oxidase Nox4. *J Biol Chem,* 286**,** 13304-13.

TAKENAWA, T. & MIKI, H. 2001. WASP and WAVE family proteins: key molecules for rapid rearrangement of cortical actin filaments and cell movement. *J Cell Sci,* 114**,** 1801-9.

TARPEY, M. M., WINK, D. A. & GRISHAM, M. B. 2004. Methods for detection of reactive metabolites of oxygen and nitrogen: in vitro and in vivo considerations. *Am J Physiol Regul Integr Comp Physiol,* 286**,** R431-44.

THANNICKAL, V. J., ALDWEIB, K. D. & FANBURG, B. L. 1998. Tyrosine phosphorylation regulates H2O2 production in lung fibroblasts stimulated by transforming growth factor beta1. *J Biol Chem,* 273**,** 23611-5.

THOMAS, S. R., CHEN, K. & KEANEY, J. F., JR. 2002. Hydrogen peroxide activates endothelial nitric-oxide synthase through coordinated phosphorylation and dephosphorylation via a phosphoinositide 3-kinase-dependent signaling pathway. *J Biol Chem,* 277**,** 6017-24.

THOMAS, S. R., WITTING, P. K. & DRUMMOND, G. R. 2008. Redox control of endothelial function and dysfunction: molecular mechanisms and therapeutic opportunities. *Antioxid Redox Signal,* 10**,** 1713-65.

TONKS, N. K. 2005. Redox redux: revisiting PTPs and the control of cell signaling. *Cell,* 121**,** 667-70.

TRAUB, O. & BERK, B. C. 1998. Laminar shear stress: mechanisms by which endothelial cells transduce an atheroprotective force. *Arterioscler Thromb Vasc Biol,* 18**,** 677-85.

TSAI, B., RODIGHIERO, C., LENCER, W. I. & RAPOPORT, T. A. 2001. Protein disulfide isomerase acts as a redox-dependent chaperone to unfold cholera toxin. *Cell,* 104**,** 937-48.

TSAO, P. S., BUITRAGO, R., CHAN, J. R. & COOKE, J. P. 1996. Fluid flow inhibits endothelial adhesiveness. Nitric oxide and transcriptional regulation of VCAM-1. *Circulation,* 94**,** 1682-9.

TZIMA, E., IRANI-TEHRANI, M., KIOSSES, W. B., DEJANA, E., SCHULTZ, D. A., ENGELHARDT, B., CAO, G., DELISSER, H. & SCHWARTZ, M. A. 2005. A mechanosensory complex that mediates the endothelial cell response to fluid shear stress. *Nature,* 437**,** 426-31.

USHIO-FUKAI, M., ALEXANDER, R. W., AKERS, M., YIN, Q., FUJIO, Y., WALSH, K. & GRIENDLING, K. K. 1999. Reactive oxygen species mediate the activation of Akt/protein kinase B by angiotensin II in vascular smooth muscle cells. *J Biol Chem,* 274**,** 22699-704.

VAN DER WIJK, T., OVERVOORDE, J. & DEN HERTOG, J. 2004. H2O2-induced intermolecular disulfide bond formation between receptor protein-tyrosine phosphatases. *J Biol Chem,* 279**,** 44355-61.

VASQUEZ-VIVAR, J., KALYANARAMAN, B., MARTASEK, P., HOGG, N., MASTERS, B. S., KAROUI, H., TORDO, P. & PRITCHARD, K. A., JR. 1998. Superoxide generation by endothelial nitric oxide synthase: the influence of cofactors. *Proc Natl Acad Sci U S A,* 95**,** 9220-5.

WAITE, K. A. & ENG, C. 2002. Protean PTEN: form and function. *Am J Hum Genet,* 70**,** 829-44.

WATERS, C. M. 2004. Reactive oxygen species in mechanotransduction. *Am J Physiol Lung Cell Mol Physiol,* 287**,** L484-5.

WERNER, E. & WERB, Z. 2002. Integrins engage mitochondrial function for signal transduction by a mechanism dependent on Rho GTPases. *J Cell Biol,* 158**,** 357-68.

WESTERMANN, B. 2012. Bioenergetic role of mitochondrial fusion and fission. *Biochim Biophys Acta,* 1817**,** 1833-8.

WIND, S., BEUERLEIN, K., ARMITAGE, M. E., TAYE, A., KUMAR, A. H., JANOWITZ, D., NEFF, C., SHAH, A. M., WINGLER, K. & SCHMIDT, H. H. 2010. Oxidative stress and endothelial dysfunction in aortas of aged spontaneously hypertensive rats by NOX1/2 is reversed by NADPH oxidase inhibition. *Hypertension,* 56**,** 490-7.

WINTER, J. & JAKOB, U. 2004. Beyond transcription--new mechanisms for the regulation of molecular chaperones. *Crit Rev Biochem Mol Biol,* 39**,** 297-317.

WINTERBOURN, C. C. & HAMPTON, M. B. 2008. Thiol chemistry and specificity in redox signaling. *Free Radic Biol Med,* 45**,** 549-61.

WINTERBOURN, C. C. & METODIEWA, D. 1999. Reactivity of biologically important thiol compounds with superoxide and hydrogen peroxide. *Free Radic Biol Med,* 27**,** 322-8.

WOOD, Z. A., POOLE, L. B., HANTGAN, R. R. & KARPLUS, P. A. 2002. Dimers to doughnuts: redox-sensitive oligomerization of 2-cysteine peroxiredoxins. *Biochemistry,* 41**,** 5493-504.

WOOD, Z. A., SCHRODER, E., ROBIN HARRIS, J. & POOLE, L. B. 2003. Structure, mechanism and regulation of peroxiredoxins. *Trends Biochem Sci,* 28**,** 32-40.

YIANNIS S. CHATZIZISIS, A. U. C., MICHAEL JONAS, ELAZER R. EDELMAN, CHARLES L. FELDMAN, AND PETER H. STONE 2007. Role of Endothelial Shear Stress in the Natural History of Coronary Atherosclerosis and Vascular Remodeling: Molecular, Cellular, and Vascular behavior. *J. Am. Coll. Cardiol.,* 49**,** 2379-2393.

YOON, Y. 2004. Sharpening the scissors: mitochondrial fission with aid. *Cell Biochem Biophys,* 41**,** 193-206.

YOSHIZUMI, M., ABE, J., TSUCHIYA, K., BERK, B. C. & TAMAKI, T. 2003. Stress and vascular responses: atheroprotective effect of laminar fluid shear stress in endothelial cells: possible role of mitogen-activated protein kinases. *J Pharmacol Sci,* 91**,** 172-6.

YOULE, R. J. & VAN DER BLIEK, A. M. 2012. Mitochondrial fission, fusion, and stress. *Science,* 337**,** 1062-5.

YU, J., BERGAYA, S., MURATA, T., ALP, I. F., BAUER, M. P., LIN, M. I., DRAB, M., KURZCHALIA, T. V., STAN, R. V. & SESSA, W. C. 2006. Direct evidence for the role of caveolin-1 and caveolae in mechanotransduction and remodeling of blood vessels. *J Clin Invest,* 116**,** 1284-91.

ZAFARI, A. M., USHIO-FUKAI, M., AKERS, M., YIN, Q., SHAH, A., HARRISON, D. G., TAYLOR, W. R. & GRIENDLING, K. K. 1998. Role of NADH/NADPH oxidase-derived H2O2 in angiotensin II-induced vascular hypertrophy. *Hypertension,* 32**,** 488-95.

ZHANG, Z., OLIVER, P., LANCASTER, J. R., JR., SCHWARZENBERGER, P. O., JOSHI, M. S., CORK, J. & KOLLS, J. K. 2001. Reactive oxygen species mediate tumor necrosis factor alpha-converting, enzyme-dependent ectodomain shedding induced by phorbol myristate acetate. *FASEB J,* 15**,** 303-5.

ZHAO, H., KALIVENDI, S., ZHANG, H., JOSEPH, J., NITHIPATIKOM, K., VASQUEZ-VIVAR, J. & KALYANARAMAN, B. 2003. Superoxide reacts with hydroethidine but forms a fluorescent product that is distinctly different from ethidium: potential implications in intracellular fluorescence detection of superoxide. *Free Radic Biol Med,* 34**,** 1359-68.

ZWEIER, J. L., WANG, P., SAMOUILOV, A. & KUPPUSAMY, P. 1995. Enzyme-independent formation of nitric oxide in biological tissues. *Nat Med,* 1**,** 804-9.

8. ANEXO 1

1. INTRODUCCIÓN

1.1 ENDOTELIO

El endotelio vascular es un órgano estructuralmente formado por una monocapa de células endoteliales, que se encuentra tapizando la superficie interna de los vasos sanguíneos y el corazón. En un adulto el endotelio consta de aproximadamente 10^{13} células, cubre un área de entre 1-7 m^2 y pesa aproximadamente 1 kg (Khazaei et al., 2008) . Debido a su localización, el endotelio actúa como una barrera mecánica entre la sangre y otros órganos y tejidos. Se comporta como una barrera semi-permeable capaz de regular la transferencia de moléculas de diferentes tamaños entre la sangre y el espacio intersticial, siendo la integridad de su estructura imprescindible tanto para el mantenimiento de la pared vascular como para una correcta función circulatoria. Sin embargo, el endotelio no se comporta únicamente como una barrera inerte, sino como un órgano metabólicamente activo e implicado en la regulación de una gran variedad de procesos tanto fisiológicos como patológicos. Por su ubicación, el endotelio detecta tanto cambios en las fuerzas hemodinámicas que actúan sobre la pared vascular (estímulos biomecánicos), como señales químicas (estímulos bioquímicos), respondiendo frente a los mismos a través de rutas bioquímicas relacionadas con la homeostasis vascular (Galley and Webster, 2004). La capacidad de detectar cambios en las fuerzas hemodinámicas de la sangre y responder a ellas fue descrita por primera vez hace más de 150 años por el patólogo Virchow quien demostró que la heterogeneidad morfológica del endotelio a lo largo de la vasculatura correlacionaba con los diferentes patrones de flujo sanguíneo a los cuales las células se veían sometidas. A raíz de estas observaciones, se sucedieron distintos estudios tanto *in vitro* como *in vivo* para intentar caracterizar los efectos del flujo sanguíneo sobre el endotelio (Resnick et al., 2003).

El endotelio presenta una tendencia fisiológica a promover la liberación de sustancias vasoactivas que promueven la vasodilatación, e inhibir tanto la agregación plaquetaria como la adhesión leucocitaria (Galley and Webster, 2004). En aquellas condiciones en las cuales el equilibrio entre estímulos vasodilatadores y antiproliferativos, y los estímulos vasoconstrictores y proliferativos se ve alterado, se produce la llamada *disfunción*

endotelial, que es un claro indicador y predictor de la existencia de una patología vascular y juega un papel crítico tanto en el inicio, como en el desarrollo de enfermedades vasculares como la aterosclerosis, la hipertensión o la diabetes (Khazaei et al., 2008).

1.2 FUERZAS HEMODINÁMICAS EN LA VASCULATURA

El flujo sanguíneo, de carácter pulsátil debido al bombeo del corazón, genera diferentes fuerzas homeostáticas sobre las células endoteliales que se encuentran tapizando los vasos sanguíneos. Las células endoteliales experimentan principalmente tres tipos de fuerzas mecánicas:

- La presión (conocida también como presión hidrostática): está originada por las fuerzas hidrostáticas que ejerce la sangre sobre la pared del vaso sanguíneo.
- Tensión circunferencial: es la fuerza creada longitudinalmente por la existencia de conexiones intercelulares entre células endoteliales. Se origina debido a variaciones en el diámetro de los vasos sanguíneos como consecuencia al carácter pulsátil del flujo sanguíneo.
- Fuerza de rozamiento: (conocida como *shear stress*) es la fuerza de tracción que produce la sangre a su paso sobre la superficie de las células endoteliales. Se define como la fuerza de rozamiento tangencial por unidad de área producida por el movimiento de un fluido viscoso sobre una superficie sólida (Papadaki et al., 1999).

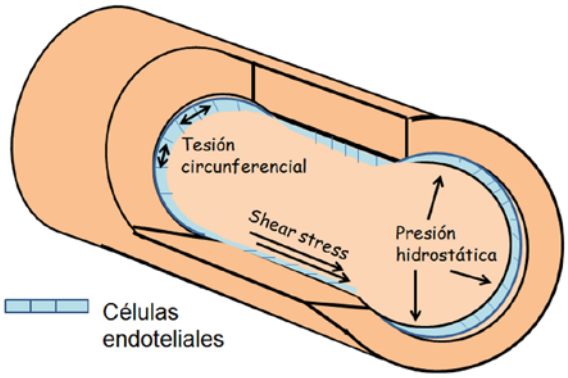

Ilustración 1. ***Fuerzas mecánicas sobre el endotelio.*** *El flujo sanguíneo ejerce principalmente tres tipos de fuerzas hemodinámicas sobre el endotelio: las presión hidrostática, la tensión circunferencial y la fuerza de rozamiento o shear stress (Papadaki and Eskin, 1997)*

Ésta última, la fuerza de rozamiento o shear stress, tiene gran importancia hemodinámica, ya que estimula la liberación de sustancias vasoactivas y cambios en la expresión génica, metabolismo e incluso la morfología celular (Davies, 1995).

La magnitud de la fuerza de rozamiento ocasionada por el flujo sanguíneo puede estimarse en la mayor parte de la vasculatura asumiendo que la sangre se comporta como un fluido newtoniano incompresible que circula por el interior de un tubo circular. Los fluidos newtonianos son aquellos en los que la viscosidad del fluido se considera constante en el tiempo, existe una relación linear entre la tensión y la velocidad de deformación y su flujo se rige por las ecuaciones de Navier-Stokes.

Asi, la fuerza de rozamiento que produce el flujo sanguineo (τ_s) es proporcional a la viscosidad de la sangre (μ), y al gradiente de la velocidad perpendicular a la dirección de la fuerza de rozamiento ($\frac{du}{dy}$) (Nerem et al., 1998):

$$\tau = \mu \frac{du}{dy}$$

El flujo de sangre puede ser modelado como un flujo laminar simple que discurre por un tubo circular, donde el diámetro del vaso es mucho mayor que las células endoteliales de forma individual. Por ello, la fuerza de rozamiento sobre la pared vascular (Ƭ) se puede calcular mediante la fórmula de Poiseuille (Nerem et al., 1998) :

$$\tau_{pared\ vascular} = \frac{32\mu Q}{\pi D^3} = \frac{4\mu Q}{\pi r^3}$$

siendo Q la velocidad del flujo, μ la viscosidad de la sangre, D el diámetro y r el radio interior del vaso sanguíneo (Ku, 1997).

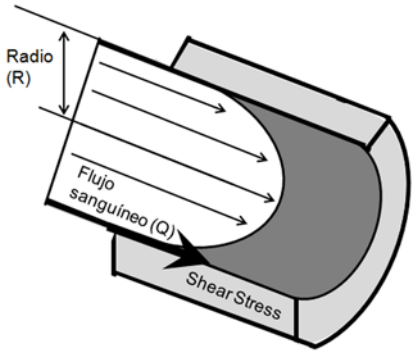

Ilustración 2. Ley de Hagen Poiseuille: Perfil de velocidad en un tubo circular *(Malek et al., 1999). Modelo en el cual se describe la relación entre el flujo, las propiedades de la sangre y el tamaño del vaso sanguíneo en las zonas rectilíneas de la vasculatura.*

La fuerza de rozamiento o shear stress no es constante a lo largo del sistema circulatorio, en la mayoría de las arterias de un adulto su magnitud varía entre 2 y 20 dina/cm^2 (Dewey et al., 1981), mientras que en el sistema venoso lo hace entre 1 y 6 dina/cm^2 (Malek et al., 1999). Las variaciones en el flujo sanguíneo ocasionan alteraciones en las fuerzas hemodinámicas, y son responsables de distintos procesos fisiológicos como el desarrollo de los vasos durante la embriogénesis y la generación y remodelado de los vasos adultos, o la regulación del tono vascular (Resnick et al., 2003).

1.3 BIOLOGÍA DE LA CÉLULA ENDOTELIAL Y SHEAR STRESS

Tal y como hemos descrito previamente, la fuerza de rozamiento o shear stress es la fuerza tangencial producida como consecuencia de la fricción que produce la sangre sobre el endotelio, y concretamente sobre las células endoteliales. Se puede expresar en unidades de fuerza/unidad de área (N/m^2; Pascal [Pa] o bien dinas/cm^2). (1N/m^2 = 1 Pa = 10 dynas/cm^2) (Nichols et al., 1991).

Su intensidad no solo depende de la viscosidad de la sangre y de su velocidad, sino que en el endotelio también depende del contacto con las irregularidades u obstrucciones presentes a lo largo de la pared vascular del sistema circulatorio (Yiannis S. Chatzizisis, 2007). Se pueden diferenciar básicamente dos tipos de flujo sanguíneo: flujo laminar y flujo turbulento (Nichols WW, 2005).

- *Flujo laminar:* se considera el tipo de flujo fisiológico y característico de trayectorias rectilíneas y sanas de la vasculatura. En ellas, la sangre fluye de manera ordenada, unidireccional y paralela a la pared vascular de los vasos por los que discurre, y las células endoteliales están sometidas a una fuerza de rozamiento de carácter pulsátil como consecuencia del propio bombeo cardiaco. Se considera un tipo de flujo con consecuencias protectoras al promover la liberación por parte de las células endoteliales de diferentes factores que favorecen la supervivencia celular y previenen procesos como la coagulación, la migración leucocitaria, y la proliferación de células musculares lisas y por ende la aterogénesis (Yoshizumi et al., 2003, Traub and Berk, 1998). Los datos provenientes de experimentos *in vitro* e *in vivo* apoyan que las células que se ven sometidas a flujo laminar sufren un alargamiento y una reorientación con su eje longitudinal paralelo a la dirección del flujo (Helmlinger et al., 1991, Levesque and Nerem, 1985, Dewey et al., 1981, Flaherty et al., 1972). Esta reorientación produce a su vez una disminución en la resistencia endotelial al shear stress (Barbee et al., 1995).

- *Flujo turbulento:* se conoce también a este tipo de flujo sanguíneo con el nombre de flujo oscilatorio, y se considera fuertemente asociado con la aterogénesis. A diferencia del flujo laminar, el flujo turbulento presenta una magnitud variable a lo largo de su recorrido. Es un flujo irregular, y se observa en las bifurcaciones de los vasos, y en vasos sanguíneos cuyas paredes no son uniformes por alteraciones en su estructura, o por la presencia de obstrucciones en su interior (Chatzizisis et al., 2007). Las células endoteliales expuestas al flujo oscilatorio no son capaces de reorientarse en la dirección del flujo sanguíneo, y están sujetas a un rango amplio de magnitud de shear stress. En las zonas expuestas a flujo turbulento se promueve la secreción de diferentes factores como angiotensina II (Ang II), factor de crecimiento derivado de plaquetas (PDGF), endotelina 1 (ET-1), proteína quimioatrayente de monocitos (MCP-1) o la molélula de adhesión vascular-1 (VCAM-1), que contribuyen al desarrollo de placas de ateroma en estas regiones. La liberación de todas estas sustancias por las células endoteliales, así como la expresión de moléculas de adhesión, promueven señales pro-trombóticas, pro-

migratorias y pro-apoptóticas en el endotelio. Todo ello contribuye al desarrollo de placas de ateroma en estas regiones.

La naturaleza y la magnitud del shear stress, son completamente imprescindibles para el mantenimiento de la estructura y la función vascular, y se considera una de las fuerzas principales de regulación homeostática endotelial

El flujo laminar produce en las células endoteliales una respuesta que da lugar a la activación de toda una serie de cascadas de señalización. En los últimos años se ha perseguido activamente la identificación y el estudio de aquellas moléculas capaces de percibir una señal mecánica en la membrana y transducirla en una señal bioquímica al espacio intracelular. Diferentes componentes situados precisamente en la superficie de las células endoteliales (superficie basal, luminal e incluso aquella en contacto con otras células) como el glicocálix, las integrinas, la molécula de adhesión plaqueto-endotelial-1 (PECAM-1), el cilio primario, las caveolas, o receptores tirosin-kinasas o iónicos se han descrito como potenciales “mecanosensores”. Son capaces de percibir la señal mecánica y traducirla en respuestas químicas que se propagan por medio del citoesqueleto o por la activación de cascadas de señalización al interior celular. Esto conlleva la activación de segundos mensajeros y factores de transcripción que se unen a los elementos de respuesta a flujo (del inglés *shear stress responsive elements SSRE*) en los promotores de distintos genes induciendo o suprimiendo su expresión (Papadaki and Eskin, 1997, Tzima et al., 2005, Davies, 1995). Muchas de las cascadas de señalización activadas por medio del flujo laminar convergen en la activación de diferentes proteínas MAP quinasas, lo cual sugiere un papel importante en la mecanotransducción (Li et al., 2005).

Asimismo, en la última década distintas publicaciones han implicado a las especies reactivas de oxígeno (ROS) en el mantenimiento de la integridad de la pared vascular y en su respuesta activa al flujo sanguíneo. Tanto el flujo laminar, como el turbulento están asociados a un incremento en la generación de ROS; sin embargo solo un incremento puntual y controlado de las ROS generado por efecto del flujo laminar parece tener un papel importante en la señalización celular, y ser necesario para la activación de determinadas rutas intracelulares (Lehoux, 2006, De Keulenaer et al., 1998).

Precisamente, el flujo laminar se caracteriza por su capacidad de regular el efecto de dichas especies reactivas de oxígeno, debido en parte a la estimulación de una respuesta antioxidante en las células endoteliales, previniendo de este modo el desarrollo de enfermedades inflamatorias relacionadas con el riesgo cardiovascular.

1.4 ESPECIES REACTIVAS DE OXÍGENO: NATURALEZA, FUENTES Y DETECCIÓN.

Bajo el término especies reactivas de oxígeno (ROS), se definen todo un conjunto de especies químicas que se forman como consecuencia de una reducción incompleta de la molécula de oxígeno, independientemente que sean radicales libres o no.

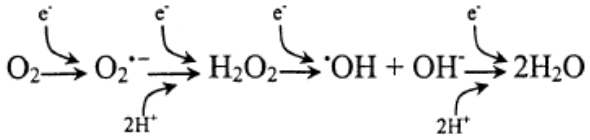

Ilustración 3. Las ROS se forman como consecuencia de una reducción incompleta del oxígeno molecular

La primera ROS que se produce como consecuencia de la reducción por un electrón del oxígeno bimolecular es el anión superóxido ($O_2^{\cdot-}$), especie radicalaria muy reactiva aunque inestable que de forma espontánea o por medio de las enzimas superóxido dismutasas (SOD) dismuta en la segunda especie reactiva, el peróxido de hidrógeno (H_2O_2). En presencia de metales de transición en estado reducido como Fe^{2+}, Cu^{+}, Co^{2+} o Ni^{2+} el H_2O_2 puede aceptar un electrón para producir una especie de oxígeno mucho mas reactiva, el radical hidroxilo ($^{\cdot}OH$) capaz de oxidar gran cantidad de moléculas biológicas. Las principales características de las distintas especies reactivas de oxígeno se detallan a continuación:

ROS	*Principales características*
$O_2^{-\cdot}$	Radical libre
	Altamente reactivo
	Vida media baja
	Baja solubilidad, no difunde a través de las membranas biológicas
	Sistemas enzimáticos capaces de neutralizarlo: superoxido dismutasa (SOD)
H_2O_2	No radical libre
	Donador de dos electrones
	No altamente reactivo
	Vida media larga
	Difunde a través de membranas biológicas
	Origina $HO^{\cdot}$ tras la interacción con metales por reacción no enzimática (R. de Fenton)
	Papel importante como molécula señalizadora (segundo mensajero)
	Sistemas enzimáticos capaces de neutralizarlo: catalasa, glutationperoxidasa tiorredoxinas, peroxirredoxinas
.OH	Radical libre
	Donador de un electrón
	Elevada reactividad frente a biomoléculas

Tabla 1. Principales características de las ROS.

La generación de ROS se produce bajo condiciones tanto fisiológicas como las fisiopatológicas. Muchos tipos celulares, y entre ellos las células endoteliales, son capaces de producir niveles bajos de $O_2^{-\cdot}$ y H_2O_2 en respuesta a diferentes estímulos extracelulares, entre los que se encuentran (Rhee et al., 2000):

- citoquinas tales como factor de crecimiento transformante β-1 (TGF-β1) (Thannickal et al., 1998), interleuquina-1 (Krieger-Brauer and Kather, 1995), interleuquina-3 (Sattler et al., 1999), interferón-γ (Krieger-Brauer and Kather, 1995) o el factor de necrosis tumoral-α (TNF-α) (Lo and Cruz, 1995);
- factores de crecimiento como el factor de crecimiento derivado de plaquetas (PDGF) (Sundaresan et al., 1995), factor de crecimiento epidérmico (EGF) (Bae et al., 1997), factor de crecimiento de fibroblastos (FGF) (Lo and Cruz, 1995) o la insulina (May and de Haen, 1979);

- agonistas de los receptores acoplados a proteínas G como angiotensina II (Zafari et al., 1998, Ushio-Fukai et al., 1999), trombina (Holland et al., 1998), tirotropina (Krieger-Brauer and Kather, 1995), la endotelina y la bradiquinina (Greene et al., 2000);
- shear stress (Rhee et al., 2000).

Debido a sus propiedades citotóxicas y mutagénicas, las ROS han sido consideradas durante mucho tiempo como los productos tóxicos liberados por el propio metabolismo aeróbico. Sus niveles basales en el endotelio se encuentran estrechamente regulados por distintas enzimas antioxidantes como la catalasa, glutatión-peroxidasa (GPx), peroxirredoxinas (PRX), tiorredoxinas (TRX), superóxido dismutasa (MnSOD y CuZnSOD) y hemo-oxigenasa (HO-1) entre otras. Un exceso de ROS en el endotelio se ha asociado con un deterioro de la función endotelial y el desarrollo de distintas enfermedades vasculares como la hipertensión pulmonar, aterosclerosis (Stocker and Keaney, 2004, Harrison et al., 2003), envejecimiento (Haigis and Yankner, 2010), diabetes e incluso diferentes procesos neurodegenerativos (Andersen, 2004) . La consecuencia de un desequilibrio entre la producción de ROS y su neutralización por sistemas antioxidantes da lugar al denominado "*estrés oxidativo*" (Ray et al., 2012). Sin embargo, recientemente se ha reconsiderado la importancia de estas especies, al describirlas como *moléculas señalizadoras* en gran cantidad de procesos tanto fisiológicos, como patológicos (Sergey Dikalov, 2007). Por lo tanto, el concepto de estrés oxidativo ha evolucionado para definirse como una "*alteración en la señalización redox"* (Jones, 2006).

FUENTES DE LAS ROS:

Se han descrito numerosos sistemas biológicos capaces de generar ROS in vivo. La generación intracelular en las células endoteliales tiene su origen en distintas fuentes. Las más importantes son las enzimas NADPH oxidasas, la respiración mitocondrial, las óxido nítrico sintasas y la enzima xantina oxidoreductasa aunque una pequeña cantidad

de especies reactivas de oxígeno provienen de otros sistemas como las ciclooxigenasa, lipooxigenasas o incluso el citocromo P450.

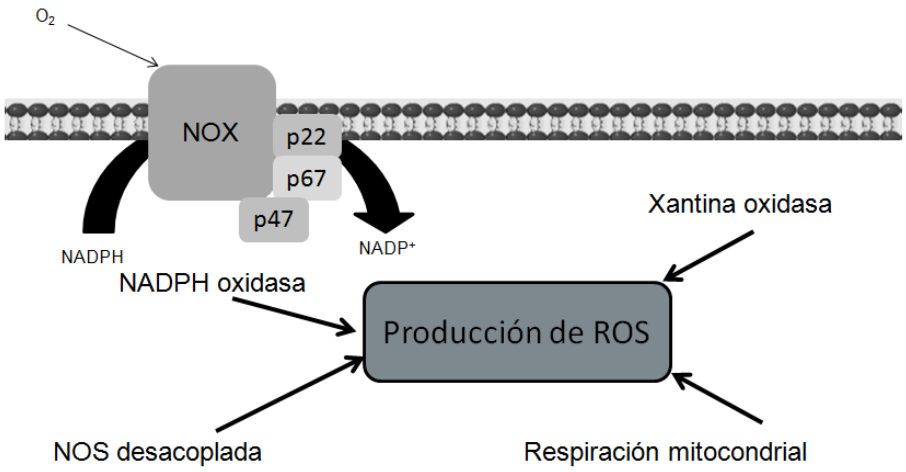

Ilustración 4. Fuentes de ROS en el endotelio vascular. *La generación de ROS en las células endoteliales proviene principalmente de NADPH oxidasas, la respiración mitocondrial, NOS desacopladas y la enzima xantina oxidasa.*

NADPH OXIDASAS:

La NADPH oxidasa es una enzima asociada a la membrana que cataliza la reducción del oxígeno molecular utilizando NADPH como donador de electrones para producir anión superóxido (Bedard and Krause, 2007). A diferencia de otras oxidasas, no tiene otra función biosintética o catabólica conocida a parte de la propia generación de especies reactivas de oxigeno (Brieger et al., 2012, Burgoyne et al., 2012). La primera isoforma caracterizada fue la NADPH oxidasa presente en fagocitos donde tiene un papel fundamental en la actividad bactericida (Rossi and Zatti, 1964, Babior et al., 2002). En la actualidad se conocen hasta 7 miembros de la familia NADPH oxidasas con una amplia distribución tisular (NOX1-5 y Duox 1-2) (Cheng et al., 2001). Todas las isoformas constan de una subunidad de 6 dominios α-hélice trans-membrana cuyos dominios N y C-

terminal se encuentran en el citosol, y la presencia de otras subunidades como la subunidad catalítica p22phox, las citosólicas p47phox y la p67phox o incluso proteínas G de la familia de Rac varía con la isoforma. Además de las diferencias estructurales (esquematizadas en ***Ilustración 5***) y su expresión diferencial en distintos tejidos, las distintas isoformas poseen diferencias en cuanto a la generación de especies reactivas de oxígeno. Por ejemplo, las isofomas NOX1, NOX2 y NOX5 producen principalmente anión radical superóxido, mientras que la producción de peróxido de hidrogeno se ve favorecida en la isoforma NOX4 (Altenhofer et al., 2012, Takac et al., 2011). Las células endoteliales expresan mayoritariamente la isofoma NOX4 (Ago et al., 2004, Schroder et al., 2012) que no requiere ninguna subunidad citosólica como p47phox, p67phox o Rac para ser activa.

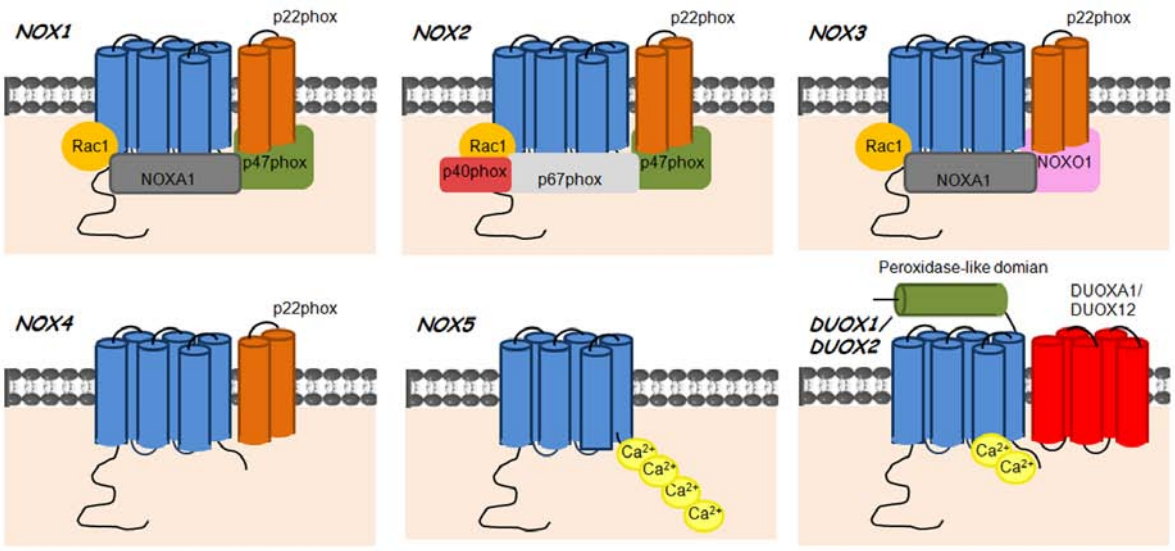

Ilustración 5. Isoformas de NADPH oxidasa. *Los siete miembros de la familia NADPH oxidasa descritos poseen un núcleo catalítico de seis dominios transmembrana y diferentes subunidades en su estructura. Figura adaptada de (Drummond et al., 2011).*

MITOCONDRIAS:

Las mitocondrias representan la principal fuente intracelular de especies reactivas de oxigeno en condiciones fisiológicas. No obstante su producción de ROS puede verse incrementada por diferentes estímulos. La generación de ROS mitocondrial se produce como consecuencia de la fosforilación oxidativa unida a la respiración aeróbica en la cadena de transporte electrónico mitocondrial (ETC). Esta maquinaria de más de 80 péptidos organizados en 4 complejos diferentes se localiza en la membrana interna mitocondrial (Finkel and Holbrook, 2000), y cataliza la transferencia de electrones que conduce en última instancia a la formación de ATP por el complejo V. Sin embargo, a lo largo de la cadena respiratoria, algunos electrones que derivan de moléculas reductoras como NADH o FADH se "fugan" y reaccionan directamente con el oxígeno generando radicales libres. De este modo, se ha descrito que en torno a un 1-2% del oxígeno molecular consumido reacciona con esta "fuga" de electrones, reduciéndose de manera incompleta en forma de anión radical superóxido (Chance et al., 1979). Tras el descubrimiento de la isoforma mitocondrial SOD (MnSOD) en la matriz mitocondrial, se constató no solo la generación de anión superóxido si no también de peróxido de hidrógeno mitocondrial. Recientemente se ha descrito el papel esencial que tiene dicha generación de ROS mitocondrial en la señalización redox (Nemoto et al., 2000, Werner and Werb, 2002).

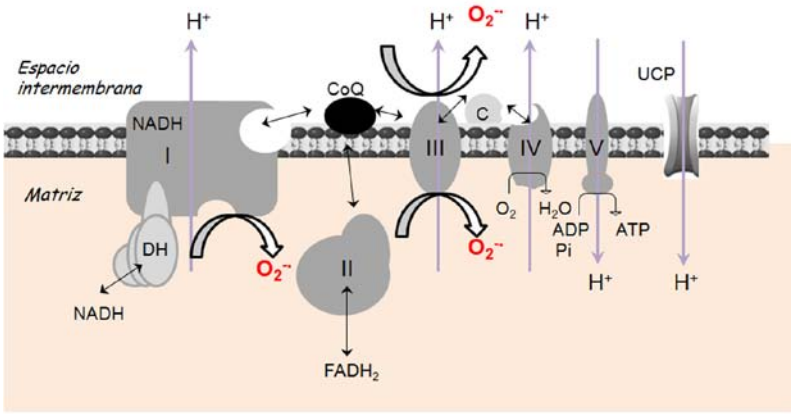

Ilustración 6. Generación de ROS mitocondrial. *El anión superóxido mitocondrial tiene su origen en la fuga de electrones que se produce principalmente en los complejos I y III de la cadena de transporte mitocondrial. Figura adaptada de (Hancock, 2008).*

NITRIC OXIDE SYNTHASE(S):

A mediados de la década de 1980-90, se descubrió que la naturaleza química del hasta entonces llamado *"factor relajante derivado del endotelio (EDRF)"* se correspondía con el monóxido de nitrógeno, más conocido como óxido nítrico ($NO^{\cdot}$) (Hancock, 2008). En mamíferos el $NO^{\cdot}$ se sintetiza por una familia de enzimas denominadas óxido nítrico sintasas (NOS). Existen tres isoformas diferentes, dos de ellas presentes constitutivamente, la oxido nítrico sintasa endotelial (eNOS o NOS3), y la óxido nítrico sintasa neuronal (nNOS o NOS1) y una isoforma inducible (iNOS o NOS2). Todas ellas son flavoproteinas dependientes de calcio, que actúan como homodímeros bombeando electrones desde el donador de electrones NADPH anclado a su dominio C-terminal (dominio reductasa) al dominio N-terminal hemo (dominio oxidasa). Son capaces de reducir el oxígeno molecular, oxidando L-arginina y formando L-citrulina y $NO^{\cdot}$ en una reacción que requiere varios cofactores como son tetrahidrobiopterina (BH4), flavina adenina dinucleótido, flavina adenina mononucleótido (FMN) y el grupo hemo. El monómero de las NOSs consiste genéricamente en un dominio oxigenasa N-terminal asociado al grupo hemo y un dominio reductasa C-terminal asociado a las flavinas, unidos por una región reguladora que contiene el motivo de interacción con la calmodulina (***Ilustración 7***).

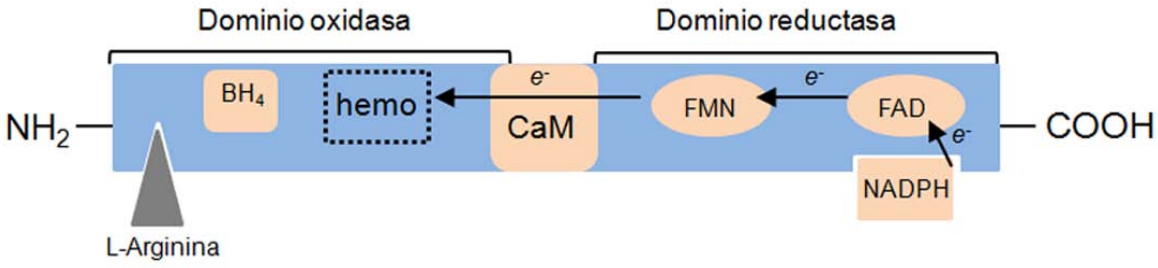

Ilustración 7. Representación de la estructura de NOS. *El dominio reductasa contiene los sitios de unión para flavin adenin dinucleótid (FAD), flavin mononucleótido (FMN) y NADPH. El dominio oxigenasa consiste en un grupo hemo y los sitios de unión a L-arginina y tetrahidrobiopterina (BH4). Entre ambos dominios se encuentra el dominio de unión a calmodulina.*

La dimerización de la NOS es esencial para su actividad al permitir que ocurra la transferencia de electrones desde el dominio reductasa de un monómero al dominio

oxigenasa del otro. Sin embargo estas enzimas también pueden convertirse en una fuente de anión radical superóxido, en aquellas condiciones en las cuales el endotelio se encuentre expuesto a estrés oxidativo, o cuando se limitan las concentraciones tanto de L-arginina como de BH_4 (Vasquez-Vivar et al., 1998). En estas condiciones, eNOS se desacopla a forma monomérica, y produce anión superóxido en vez de sintetizar oxido nítrico (Landmesser et al., 2003). Cuando ocurre esto los electrones durante su transporte entre ambos dominios son desviados hacía el oxígeno molecular, en lugar de hacía la L-arginina, generándose las ROS. En los últimos años, se ha descrito la S-glutationilación como un nuevo mecanismo por el cual se puede producir el desacoplamiento de eNOS (Chen et al., 2010). El desacoplamiento de la eNOS, y la producción de anión superóxido se han implicado en diferentes patologías que cursan con una disfunción endotelial como hipercolesterolemia, diabetes o hipertension (Stroes et al., 1997, Heitzer et al., 2000, Higashi et al., 2002).

El óxido nítrico producido por tejidos biológicos es un regulador esencial de diferentes funciones en la vasculatura, entre las cuales destacamos la regulación de la presión, el tono vascular y la agregación plaquetaria (Zweier et al., 1995, Moncada et al., 1991, Moncada et al., 1989, Garthwaite, 1991, Langrehr et al., 1993). Sin embargo, puede producir daño celular debido a la formación de elevados niveles de especies reactivas de nitrógeno (RNS). Las RNS son compuestos derivados del $NO^{\cdot}$ que juegan un papel fisiológico fundamental en muchos tipos celulares (Martinez and Andriantsitohaina, 2009). Cada uno de estos compuestos presenta diferentes propiedades tales como la reactividad, la vida media, la solubilidad o incluso la actividad biológica (Nathan, 2003). En la ***Tabla 2***, se muestra un listado de las principales RNS descritas. Aunque las RNS pueden reaccionar con distintas ROS, cabe resaltar la alta reactividad del $NO^{\cdot}$ con el anión radical superóxido para producir peroxinitrito ($ONOO^{-}$) (oxidante altamente reactivo que participa en los procesos de nitración de proteínas mediante reacciones no enzimáticas).

RNS	*Fórmula*	*Formación*
Trióxido de dinitrógeno	N_2O_3	De $NO^{\cdot}$ y O_2
Óxido nítrico o monóxido de nitrógeno	$NO^{\cdot}$	De NOS
Nitrito	NO_2^-	De $NO^{\cdot}$
Dióxido de nitrógeno	$NO_2^{\cdot}$	De la descomposición de $ONOO^-$
Catión nitronio	NO_2^+	De la descomposicón de $ONOOCO_2^-$
Catión nitrosonio	NO^+	De $NO^{\cdot}$
Anión nitroso peroxicarbonato	$ONOOCO_2^-$	De $ONOO^-$ y CO_2
Nitroxilo	HNO	De la reducción por un electrón de $NO^{\cdot}$
Cloruro de nitrilo	$Cl\text{-}NO_2$	De NO_2^- y HOCl
Peroxinitrito	$ONOO^-$	De $NO^{\cdot}$ y $O_2^{\cdot -}$
S-Nitrosotiol	RSNOs	De la unión covalente de un tiol al $NO^{\cdot}$

Tabla 2. Principales RNS (Martinez and Andriantsitohaina, 2009).

Las RNS producen principalmente tres tipos de modificaciones post-traduccionales:

- S-nitrosilación: se produce una unión covalente del $NO^{\cdot}$ con un grupo tiol para dar lugar a un derivado S-nitrosotiol (RSNO) (Hess et al., 2005).
- S-glutationilación: adición de una molécula de glutatión (GSH) o de otros tioles de bajo peso molecular, a los residuos sulfhidrilo de las cisteínas de las proteínas formando un disulfuro mixto. Reacción reversible por Trx y Grx (Holmgren et al., 2005).
- Nitración de tirosinas: es un proceso que consta de dos pasos, en la primera reacción se genera un radical tirosilo tras la oxidación de tirosinas por ROS. En la segunda reacción, el radical tirosilo reacciona con NO_2 y da lugar a 3-NO_2-Tyr (3-nitrotirosina).

Tal y como hemos descrito anteriormente para las ROS, cuando se produce una pérdida del equilibrio entre la producción de RNS y la actividad de los sistemas encargados de neutralizarlos se produce el denominado estrés nitroxidativo (Ogino and Wang, 2007) , que puede contribuir al daño y muerte celular.

XANTINA OXIDASA:

La xantina oxidoreductasa (XOR) es una metaloflavoproteina que cataliza los últimos pasos del metabolismo de purinas: la oxidación de la hipoxantina a xantina y de la xantina a ácido úrico utilizando como aceptor al oxígeno y generando anión radical superóxido o peróxido de hidrógeno como productos de la reacción (Jarasch et al., 1981). Se puede encontrar en dos formas, como xantina dehidrogenasa (XDH) y como xantina oxidasa (XO) (Harrison, 2002) siendo la relación entre XO y XDH en las células un parámetro crítico para determinar la cantidad de ROS producida por estas enzymas (Granger, 1988). La XO se expresa en niveles altos en la superficie luminal del endotelio de muchos órganos, y un incremento de su expresión y actividad se ha relacionado con distintas patologías vasculares (Guzik et al., 2006, Spiekermann et al., 2003). En la última década se ha descrito un nuevo papel esencial en la vasculatura para esta enzima al descubrirse su capacidad de producir $NO^{\cdot}$ (Godber et al., 2000, Li et al., 2001, Harrison, 2002).

A continuación se resumen las principales fuentes de generación de cada una de las ROS en el endotelio.

ROS	*Principales fuentes*
$O_2^{-\cdot}$	"Fuga" de electrones de la cadena respiratoria NADPH oxidasa Xantina oxidasa eNOS desacoplada
H_2O_2	Dismutación espontánea o catalizada por SOD del $O_2^{-\cdot}$ NADPH oxidasa Glucosa oxidasa Xantina oxidasa
$OH^{\cdot}$	Del $O_2^{-\cdot}$ via SOD y H_2O_2 via metales de transición (Cu, Fe)

Tabla 3. Principales fuentes de ROS.

La relevancia fisiológica que tienen las especies reactivas de oxigeno en la señalización celular, así como la naturaleza y el origen de las mismas no son completamente

conocidas. Esto es debido en parte a la gran dificultad que supone el estudio tanto de la generación como de su detección por la escasez y limitada especificidad de las técnicas empleadas. A continuación se describen las principales técnicas empleadas en la detección y cuantificación de las distintas especies reactivas de oxígeno (ROS) y nitrógeno (RNS), enumerando las principales ventajas e inconvenientes de las mismas.

DETECCIÓN DE ROS Y RNS:

$O_2^{\cdot -}$ (ANIÓN RADICAL SUPERÓXIDO):

- REDUCCIÓN DEL CITOCROMO C:

$$Fe^{3+} + \text{cit}\,c + O_2^{\cdot -} \rightarrow Fe^{2+} + \text{cit}\,c + O_2$$

PRINCIPIOS DE LA DETECCIÓN: en presencia del $O_2^{\cdot -}$ se produce la reducción del ferricitocromo c a ferrocitocromo c con la liberación de una molécula de oxígeno. La reducción del citocromo se cuantifica espectrofotométricamente a 550 nm, utilizando el coeficiente de extinción molar para el ferricitocromo de 0.89×10^4 M^{-1}/cm^{-1}.

- **VENTAJAS:**
  - Se puede medir la producción de $O_2^{\cdot -}$ in vitro por numerosas enzimas, o incluso en células o tejidos
- **INCONVENIENTES:**
  - La medida no es específica de $O_2^{\cdot -}$. Para demostrar específicamente su generación es necesario abolir la señal mediante la adición exógena de SOD
  - La permeabilidad intracelular del citocromo c es limitada
  - Baja sensibilidad de la técnica para detectar pequeñas cantidades del $O_2^{\cdot -}$.
  - Pueden interferir gran cantidad de antioxidantes endógenos en la medida

- ACONITASA:

PRINCIPIOS DE LA DETECCIÓN: La aconitasa es una enzima que cataliza la isomerización reversible de citrato a isocitrato a través de la formación de cis-aconitato en el ciclo de Krebs. Como miembro de la familia de las hidratasas contiene en su sitio activo un grupo prostético [4Fe-4S] altamente susceptible de ser inactivado por anión radical superóxido, el cual reacciona selectivamente con el grupo hierro-azufre inactivando el enzima. Para evaluar la actividad aconitasa se lleva a cabo un ensayo acoplado con isocitrato dehidrogenasa siguiendo el aumento de absobancia a 340 nm en el tiempo.

- **VENTAJAS:**
  - Puede emplearse para la detección de la generación de $O_2^{-\cdot}$ citosólico y mitocondrial
  - Técnica altamente selectiva para $O_2^{-\cdot}$
- **INCONVENIENTES:**
  - Una fracción de la enzima aconitasa se encuentra basalmente inactiva
  - La aconitasa puede ser inactivada también por $ONOO^-$.

- HIDROETIDINA:

PRINCIPIOS DE LA DETECCIÓN:

La hidroetidina (dihidroetidina, HE) es un compuesto permeable a través de la membrana plasmática que pueden transferir dos electrones al anión radical superóxido provocando su oxidación.

- **VENTAJAS:**
  - Compuesto permeable
  - Los derivados de la HE detectan específicamente ROS generados a nivel mitocondrial (sonda Mitosox)
  - La oxidación intracelular de la HE por el anión $O_2^{-\cdot}$ puede analizarse por citometría de flujo o microscopía de fluorescencia
- **INCONVENIENTES:**
  - Su oxidación no se produce exclusivamente por $O_2^{-\cdot}$, sino que reacciona con muchos oxidantes diferentes

- Se puede considerar a esta sonda como un indicador general del estado redox
- Altamente susceptible de oxidación por la luz y de *photobleaching*
- El empleo de altas concentraciones de la sonda puede dar lugar a falsos positivos

➢ ENSAYO DE LUCIGENINA:

PRINCIPIOS DE LA DETECCIÓN: el anión radical superóxido puede ser detectado mediante el empleo de técnicas quimioluminiscentes, siendo la lucigenina el compuesto más empleado para ello.

0 **VENTAJAS:**

- Permeable a través de las membranas lipídicas celulares
- Alta especificidad
- Alta sensibilidad
- Toxicidad celular reducida

0 **INCONVENIENTES:**

- Posible generación artefactual de anion radical superóxido debido al reciclado oxidativo de la propia lucigenina
- Técnica no cuantitativa

➢ RESONANCIA DE ESPÍN ELECTRÓNICO Y ATRAPAMIENTO DE ESPÍN:

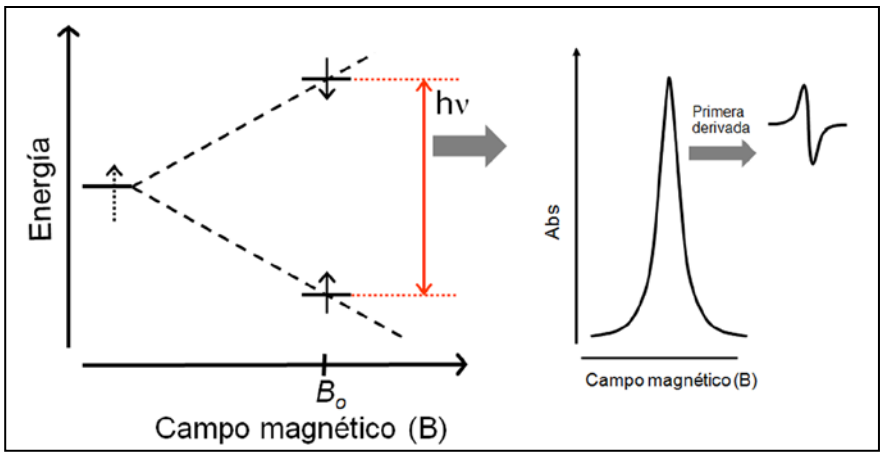

Ilustración 8. Principio del EPR

PRINCIPIOS DE DETECCIÓN: esta técnica también se denomina *Resonancia Electrónica Paramagnética (EPR*). Es una técnica espectroscópica sensible a electrones desapareados basada en sus propiedades magnéticas. Los electrones desapareados pueden existir en dos orientaciones diferentes, paralela y antiparalela con respecto al campo magnético aplicado. La diferencia de energía de estos estados corresponde a la región de microondas del espectro electromagnético. Esta técnica permite la detección de radicales libres en sistemas biológicos a pesar de su baja concentración y su corta vida media al utilizar "*atrapadores de espin*" *(spin traps)* específicos para las especies radicalarias y formar así aductos más estables.

- **VENTAJAS:**
  - Detección directa de radicales libres
  - Estabilización de ROS para su evaluación por la formación de aductos estables
- **INCONVENIENTES:**
  - Los aductos activos pueden reducirse en presencia de antioxidantes endógenos
  - Alta sensibilidad a la luz

H_2O_2(PERÓXIDO DE HIDRÓGENO):

- AMPLEX RED:

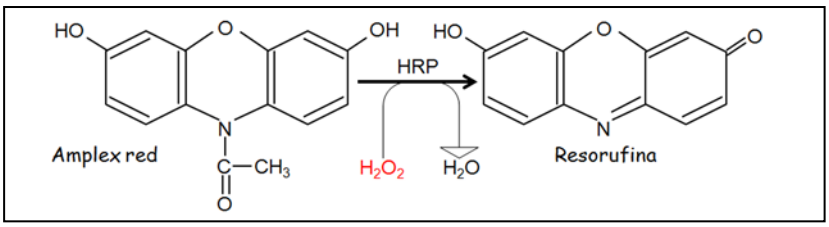

Ilustración 9. Detección de H_2O_2 por Amplex red

PRINCIPIOS DE LA DETECCIÓN: El H_2O_2 reacciona con el reactivo Amplex Red [N-acetyl-3,7,dihydroxyphenoxazine] en una reacción catalizada por la enzima peroxidasa de

rábano dando lugar a la resorufina. La resorufina es un producto fluorescente cuya formación puede seguirse espectrofotométricamente al presentar un máximo de fluorescencia de emisión y excitación de 587 y 563 nm respectivamente.

- **VENTAJAS:**
  - Técnica muy sensible que permite la medida de pequeñas concentraciones de H_2O_2 (límite de detección 50 nM)
  - La peroxidasa de rábano es activa en un rango amplio de pH
- **INCONVENIENTES:**
  - El reactivo Amplex red es altamente susceptible de ser oxidado por la luz
  - Distintos tampones pueden interferir produciendo falsos positivos en las medidas. Es necesario comprobar la reacción previamente en el tampón de interés

➢ DCFH-DA [5-(AND 6-)CLOROMETIL-2′,7′-DIACETATO DE DICLOROFLUORESCEINA] (CMDCFH-DA):

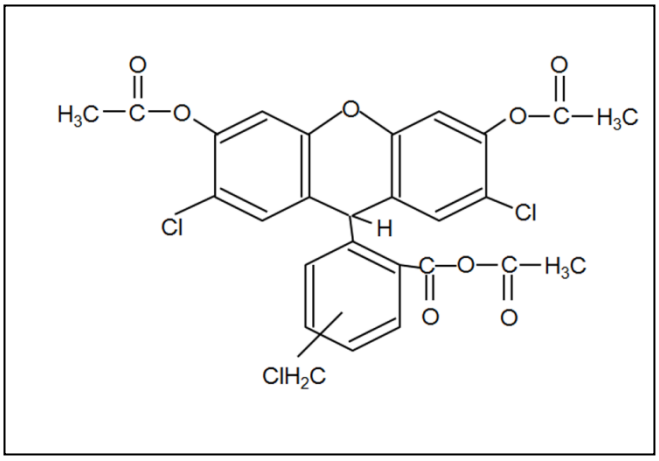

Ilustración 10. CMDCFH-DA

PRINCIPIOS DE LA DETECCIÓN*:* El carboximetilo derivado de la fluoresceína (CMDCFH-DA) es un compuesto que difunde libremente a través de la membrana plasmática. En el interior celular, el CMDCFH-DA es desacetilado por las esterasas, dejando de ser permeable y evitando de ese modo su salida a través de la bicapa lipídica. Su oxidación por agentes como el H_2O_2 lo transforma en un compuesto flurorescente, CMDCFH. La acumulación de esta sonda en las células puede ser medida después de excitar a una longitud de onda de 488 nm, como un aumento de la intensidad de fluorescencia recogida a 530 nm La fluorescencia es proporcional a la concentración de ROS en el interior celular.

- **VENTAJAS:**
  - Permeable a través de la membrana plasmática
  - Muy sensible a cambios en el estado oxidativo celular
  - Técnica adecuada para la monitorización de la generación de especies reactivas en el tiempo
  - La fluorescencia de la sonda puede detectarse por medio de citometría de flujo o microscopia de fluorescencia
- **INCONVENIENTES:**
  - No es una sonda específica para H_2O_2 ya que puede reaccionar con otros muchos oxidantes. Se puede considerar, al igual que la dihidroetidina como un indicador de estado redox
  - La sonda se oxida en solución, por ello se requiere su uso inmediatamente tras su preparación
  - Presenta una alta citotoxicidad que puede originar oxidaciones artefactuales con el riesgo de atribuirse las medidas a la generación de ROS
  - Alta susceptibilidad a ser oxidada por la luz y a *photobleaching*

➢ VECTORES HYPER:

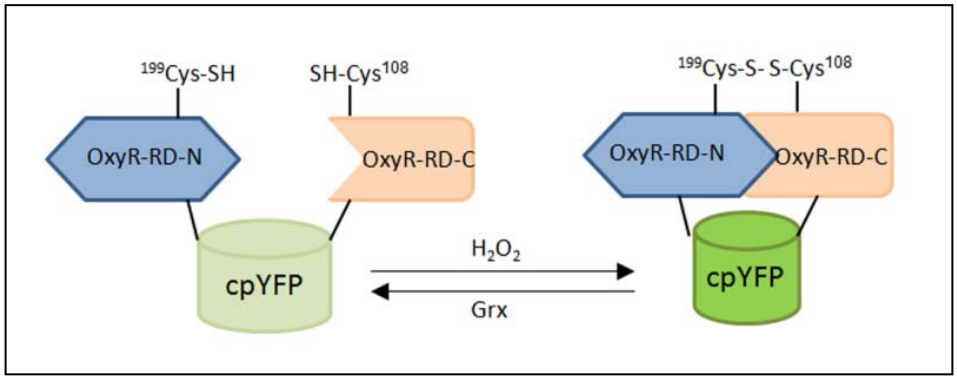

Ilustración 11. Estructura del vector HyPer

PRINCIPIOS DE LA DETECCIÓN: El vector Hyper (cuyo espectro de fluorescencia presenta dos máximos de excitación a 420 y 500 nm y una fluorescencia de emisión máxima a 516 nm) consiste en la proteína fluorescente amarilla circular permutada (cpYFP) insertada en el dominio de regulación de la proteína procariota sensora de H_2O_2 denominada OxyR. El

H_2O_2 induce la formación de un puente disulfuro entre las cisteinas 199 y 208 situadas en los extremos N y C terminal de la proteína OxyR respectivamente. Este cambio conformacional origina un cambio ratiométrico de la fluorescencia de cpYFP.

- **VENTAJAS:**
  - Alta especificidad de esta sonda fluorescente para la detección de H_2O_2 en el interior celular
  - Alta sensibilidad frente a H_2O_2. El anión $O_2^{-\cdot}$, glutatión oxidado, $ONNO^-$ o el propio $NO^\cdot$ no interfieren en su medida
  - Consiste en un sensor ratiométrico. Ante exposición a H_2O_2, se produce un incremento en la fluorescencia excitada a 420 mn mientras que disminuye aquella a 500 nm
  - La fluorescencia puede medirse mediante citometría de flujo, lectores de placa o microscopía de fluorescencia
- **INCONVENIENTES:**
  - Reacción reversible por glutarredoxinas (Grx)
  - Altamente dependiente de la eficiencia de la transfección
  - Susceptible de *photobleaching*

➢ ENSAYO ESPECTOFOTOMÉTRICO CON 3,5,3' 5' TETRAMETILBENZIDINA (TMB):

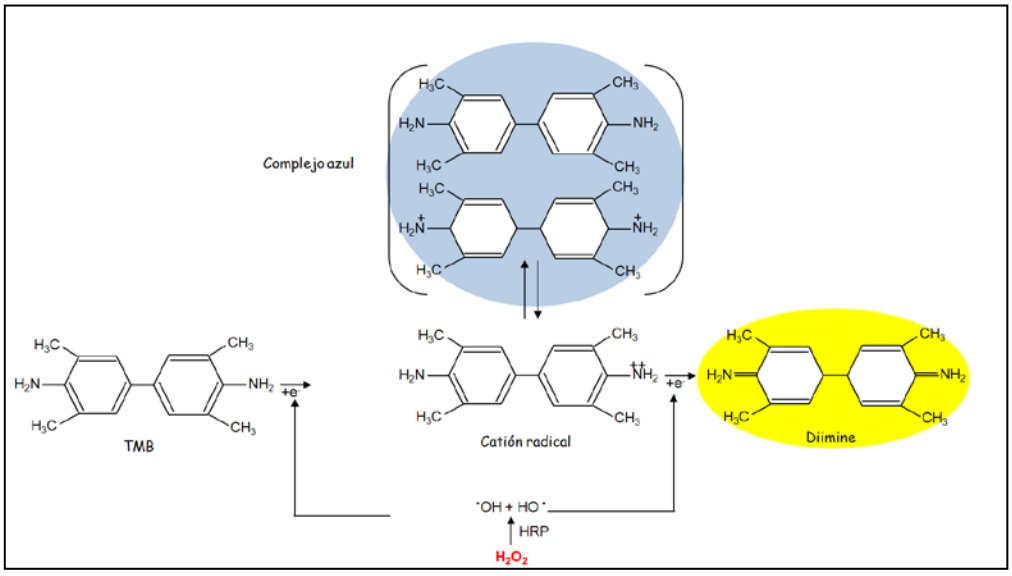

Ilustración 12. Estructura química del TMB y sus productos de oxidación

PRINCIPIOS DE LA DETECCION: El H_2O_2 reacciona con el reactivo TMB en una reacción catalizada por la enzima peroxidasa de rábano dando lugar a la formación de un producto intermedio en equilibro con un complejo responsable del color azul de la reacción (Abs 653 nm). La oxidación de este producto intermedio da lugar a un producto amarillo, la diimina (Abs 450 nm)

- **VENTAJAS:**
  - Alta sensibilidad al H_2O_2
  - Alta estabilidad de los productos de oxidación
- **INCONVENIENTES:**
  - Sensibilidad a la luz

➢ PEROXI GREEN Y TECNOLOGÍA SNAP-TAGGED:

PRINCIPIOS DE LA DETECCIÓN: SNAP–tagR es una variante de 20kDa de la proteina de reparación de ADN O^6-alquilguanina-DNA alquiltransferasa (AGT) que reacciona de forma covalente con derivados de bencilguanina y bencilcloropirimidina permitiendo así la unión de ligandos sintéticos. La sonda está sintetizada a partir de la sonda permeable Peroxi-Green (PG-1) que es activada por H_2O_2 tras la desprotección del grupo boronato. A partir de PG-1 se pueden sintetizar, por conjugación con 2-cloro-6-aminopirimidina, análogos que entran selectivamente en el interior de orgánulos específicos (Srikun et al., 2010).

- **VENTAJAS:**
  - Permeable a través de la bicapa lipídica celular
  - Selectividad frente a H_2O_2
  - Alta sensibilidad
  - Permite detectar la producción de H_2O_2 en compartimentos subcelulares concretos al diseñar análogos de la sonda para orgánulos específicos
- **INCONVENIENTES:**
  - Reacción no reversible por el H_2O_2, por lo que esta metodología no puede emplearse para determinar una producción transitoria de H_2O_2

- Pocos datos publicados en la literatura

$NO^{\cdot}$:

➢ REACCIÓN DE GRIESS:

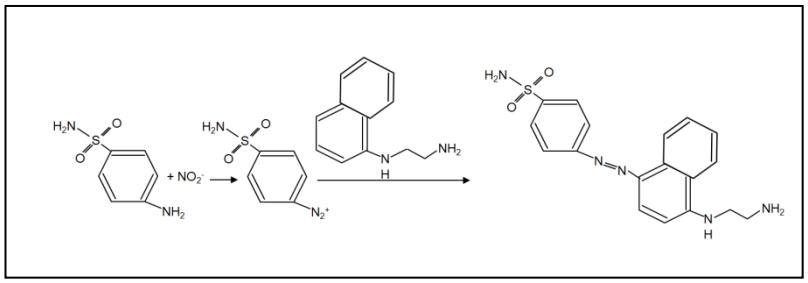

Ilustración 13. Reacción de Griess

PRINCIPIOS DE LA DETECCIÓN: Este método se basa en la reacción de nitritos y nitratos en medio ácido con el reactivo de Griess. La detección se inicia con la reacción de la muestra con sulfanilamina dando lugar a un derivado diazonio que reacciona a su vez con una amina aromática (N-1 naftil-etilendiamina). La presencia de nitritos y nitratos en la muestra puede cuantificarse espectofotométricamente por la formación de un complejo de coloración rosada durante la reacción que absorbe a una longitud de onda de 540 nm.

0 **VENTAJAS:**

- Útil para la detección de nitritos en fluidos extracelulares como plasma, orina y linfa
- Ensayo rápido, barato y fácil de llevar a cabo

0 **INCONVENIENTES:**

- Medida indirecta de $NO^{\cdot}$
- Límite de detección: 2-3 µM
- La presencia de heparina en las muestras produce una precipitación del reactivo de Griess

- ESPECTROSCOPÍA DE FLUORESCENCIA:

PRINCIPIO DE LA DETECCIÓN: La detección fluorimétrica de $NO^{\cdot}$ se lleva a cabo mediante el uso de dos sondas diferentes: 2,3-diaminonaftaleno (DAN) o diaminofluoresceín-2-diacetato (DAF).

La reacción de DAN con los nitritos en condiciones ácidas origina un compuesto fluorescente (NAT). DAF-DA difunde al interior de las células donde queda retenido al ser hidrolizado por esterasas perdiéndo así su grupo diacetato. Al reaccionar con $NO^{\cdot}$ da lugar a la formación de un producto fluorescente (DAF-2 T).

- **VENTAJAS:**
  - Alta sensibilidd frente a nitritos y $NO^{\cdot}$
  - Elevada especificidad
  - Técnica empleada en experimentación *in vivo* e *in vitro*
- **INCONVENIENTES:**
  - DAF puede reaccionar con anion nitroxilo
  - Sensible a la luz (puede dar falsos positivos)

- ANALISIS POR TÉCNICAS DE QUIMIOLUMINISCENCIA:

PRINCIPIO DE LA DETECCIÓN*:* el NO. al combinarse con ozono produce NO. en estado excitado (NO_2^*). Este método se basa en la medida de la energía en forma de protones que emite el NO_2^* al decaer. Las emisiones de fotones producidas en la reacción se miden a través de un fotomultiplicador .

- **VENTAJAS:**
  - Detecta $NO^{\cdot}$ y sus productos de oxidación: nitrito (NO_2^-) y nitrato (NO_3^-)
  - Alta sensibilidad (límite de detección 1 pM $NO^{\cdot}$)
  - Se requieren pequeños volúmenes de muestra
  - Muestra pocas interferencias
- **INCONVENIENTES:**
  - Se require muestras líquidas o gaseosas
  - Equipamiento especial
  - Método no válido para analizar la producción de nitritos liberados en pequeños intervalos de tiempo

- RESONANCIA DE ESPÍN ELECTRÓNICO Y ATRAPAMIENTO DE ESPÍN:

  PRINCIPIOS DE LA DETECCIÓN: técnica descrita previamente. Para la detección específica del $NO^{\cdot}$ el "atrapador de spin" de elección es el complejo Fe(II)-dietilditiocarbamato, $Fe(DETC)_2$.

  - **VENTAJAS:**
    - Elevada especificidad
    - No reacciona con nitritos ni nitratos
    - La alta estabilidad de los aductos permite la medida de $NO^{\cdot}$ acumulado en el tiempo
  - **INCONVENIENTES:**
    - $Fe(DETC)_2$ puede oxidarse por H_2O_2 o $O_2^{-\cdot}$
    - Sensible a la luz

.

- DETECCIÓN ELECTROQUÍMICA DE $NO^{\cdot}$:

  PRINCIPIOS DE LA DETECCIÓN: técnica amperométrica que determina la generación de $NO^{\cdot}$ en la superficie del electrodo generalmente de grafito o platino. Los electrodos empleados en la detección electroquímica del $NO^{\cdot}$ generalmente son de carbono o platino.

  - **VENTAJAS:**
    - Sensibilidad apropiada para la detección de $NO^{\cdot}$ en muestras biológicas
    - Metodología cuantitativa

Además, existen diferentes ensayos empleados en la determinación indirecta de NO. Entre ellos destacan:

- Determinación de cGMP: la activación de la enzima guanilato ciclasa por NO conlleva a la producción de cGMP (Ros et al., 1995).
- Determinación de L-citrulina: el NO se produce durante la conversión de L-arginina a L-citrulina (Hecker et al., 1990). Este ensayo detecta la producción de [^{3}H]-L citrulina a partir de [^{3}H]-L-arginina marcada radioactivamente.

- Tratamientos con hemoglobina: el NO produce la oxidación de la hemoglobina para formar methemoglobina que puede ser detectada espectofotométricamente (Ignarro et al., 1987). La unión del NO a hemoglobina puede además ser detectada mediante resonancia paramagnética de spin electrónico (EPR) al detectar los aductos nitroxil-hemoglobina formados (Arroyo and Kohno, 1991).

1.5 SEÑALIZACIÓN REDOX

Durante muchos años se han considerado a las ROS como productos tóxicos del metabolismo celular, asumiendo que lo mejor para las células era su rápida eliminación o neutralización (Rhee, 2006). Sin embargo, desde finales de los años 90 hay cada vez más evidencias de la importancia que tienen las ROS como moléculas señalizadoras en gran cantidad de procesos fisiológicos. Las distintas especies reactivas presentan diferentes propiedades biológicas como la reactividad, su vida media o permeabilidad a través de las membranas entre otras. Mientras que el $^{\cdot}OH$ presenta una elevada reactividad indiscriminada hacia gran cantidad de moléculas biológicas, el anión radical superóxido es una especie altamente inestable con una vida media muy corta lo que le permite reaccionar con muy pocas moléculas (entre ellas, reacciona específicamente con proteínas con grupos hierro-azufre alterando su actividad) (Gardner et al., 1995). Sin embargo, son las características intrínsecas y específicas del H_2O_2 las que le confieren un papel esencial en la señalización desde hace algo más de dos décadas. El H_2O_2 es una molécula pequeña y ubicua capaz de difundir a través de las membranas celulares y alcanzar distintos orgánulos celulares y actuar como un segundo mensajero (D'Autreaux and Toledano, 2007, Rhee et al., 2003). A pesar de ser un oxidante débil y por lo tanto relativamente inerte a la gran mayoría de las moléculas biológicas, induce modificaciones covalentes y reversibles en grupos tioles localizados en diferentes dominios de las proteínas induciendo de ese modo un cambio en su actividad. Concretamente, es capaz de oxidar residuos cisteína originando la aparición de puentes disulfuro (R-S-S-R) mediante la formación de compuestos intermedios altamente inestables denominados

ácidos sulfénicos (R-S-OH) (Claiborne et al., 1993, Denu and Tanner, 1998). Los puentes disulfuro formados puede ser de distinta naturaleza.

- Puentes disulfuro intramoleculares: son el resultado de la unión de dos cisteínas presentes en la misma proteína (Lee et al., 2002b)
- Puentes disulfuro intermoleculares: se producen entre cisteínas localizadas en dos moléculas diferentes dando lugar a la formación homo- o hetero-dímeros (van der Wijk et al., 2004)
- Puentes disulfuro mixtos: se producen entre el glutatión y el tiol de otra proteína (proceso denominado S.glutationilación).

Tras la formación del puente disulfuro, ante un exceso de H_2O_2, los tioles pueden experimentar ulteriores oxidaciones y producir ácido sulfínico ($R\text{-}SO_2H$) o incluso ácido sulfónico ($R\text{-}SO_3H$). No obstante, para que estos grupos tiólicos sean susceptibles de ser oxidados por un oxidante débil como es el H_2O_2, tienen que poseer unas características especiales. La constante de disociación (pKa) de los grupos sulfhidrilos de la gran mayoría de los residuos de cisteína (Cys-SH) es en torno a 8.5 por lo que H_2O_2 no es capaz de inducir su oxidación. Sin embargo, existen algunas proteínas cuyos valores de pKa son inferiores, y existen en forma de tiolatos a pH neutro (Rhee et al., 2003). Esto es debido a las interacciones que se producen entre el residuo tiolato cargado negativamente y otros residuos adyacentes en su estructura cuaternaria con carga opuesta.

Tras la oxidación de las cisteínas susceptibles, los tioles has de ser reducidos de nuevo para poner fin a la señal desencadenada por el H_2O_2. Este proceso lo llevan a cabo gran cantidad de sitemas biológicos mediante procesos enzimáticos o no enzimáticos.

Los disulfuros y ácidos sulfénicos son reducidos por TRX y PRX, mientras que las GRX catalizan la reducción de disulfuros mixtos (la reducción de cisteínas S-glutationiladas (Holmgren et al., 2005)). La reducción de los grupos sulfínicos la llevan a cabo una familia de enzimas dependientes de ATP cuya expresión y actividad está estrechamente controlada, son las llamadas sulfirredoxinas (Srx) (Biteau et al., 2003) y la "sobreoxidación" hasta ácido sulfónico se considera biológicamente irreversible.

La oxidación no es exclusiva de los residuos cisteína, sino que se ha descrito que otros como metionina, triptófano o tirosinas pueden ser también modificados por el estado redox. Sin embargo, aún no se conoce el significado, ni el impacto funcional que tienen dichas oxidaciones (Janssen-Heininger et al., 2008).

Con el fin de identificar y describir la importancia en la función celular que tiene la señalización redox, es imprescindible, en primer lugar, conocer las principales dianas células capaces de detectar y transducir la señalización por H_2O_2.

PRINCIPALES DIANAS MOLECULARES DEL H_2O_2:

- PROTEÍNAS TIROSIN-FOSFATASAS: la actividad de las proteínas de la familia tirosin-fosfatasas (PTP) requiere de la existencia de una cisteína reducida en su centro catalítico. Estas cisteínas esenciales poseen un pKa entre 4.7 y 5.4 (His-Cys-X-X-Gly-X-X-Arg-Ser/Thr, donde X es cualquier aminoácido) y por lo tanto existen en forma de tiolato a pH neutro (Denu and Dixon, 1998). Dicha característica les hace susceptibles de ser inactivados por un estímulo oxidativo, siendo por lo tanto dianas de diferentes oxidantes débiles entre los que se encuentra el H_2O_2.

  La fosforilación de una proteina se produce por el equilibrio entre aquellas proteinas quinasas encargadas de fosforilarla (proteínas tirosin-kinasas, PTKs) y las enzimas fosfatasas que retiran esos grupos fosfato. Por lo tanto una inactivación oxidativa de las tirosin-fosfatasas supone un incremento en la fosforilación, y en muchos casos activación de diferentes MAPK (Kamata et al., 2005, Seth and Rudolph, 2006). La inhibición de las PTP se ha descrito tras la producción endogena de H_2O_2 tras la exposición a factores de crecimiento como EGF con la inhibición concomitante de PTP1B (Bae et al., 1997) o PDGF que induce la oxidación e inhibición de las fosfatasas SHP-2 (Meng et al., 2002) y PTEN (Kwon et al., 2004).

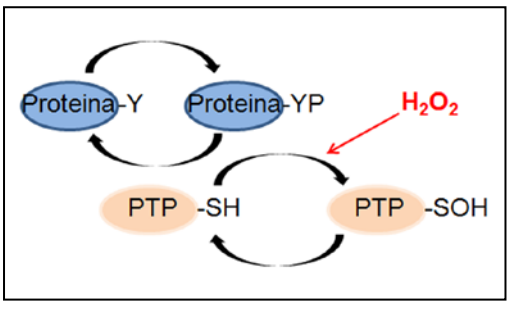

Ilustración 14. Inactivación oxidativa por H_2O_2 de proteínas con un residuo tirosina

- PROTEASAS: proteasas como la caspasa o diferentes metaloproteasas (MMPs) también se regulan por estrés oxidativo. En el caso específico de las caspasas, el H_2O_2 inhibe su activación (Lee and Shacter, 2000), mientras que algunos estudios sugieren que las MMPs pueden ser tanto activadas como inhibidas por ROS (Zhang et al., 2001, Okamoto et al., 2004).
- CHAPERONAS Y PROTEÍNAS IMPLICADAS EN EL PLEGAMIENTO: este grupo de proteínas incluyen a las proteínas de choque térmico (Hsp) y la proteína disulfuro isomerasa (PDI) (Winter and Jakob, 2004). Las proteínas de choque térmico Hsp25, 33, 60, y 90 presentan residuos de cisteínas en sus sitios activos susceptibles de ser modificados por el estado redox, lo cual supone un cambio en su función chaperona (Diaz-Latoud et al., 2005, Hoppe et al., 2004, Nardai et al., 2000). Concretamente la proteína de choque térmico Hsp33 en su estado inactivo tiene cuatro residuos de cisteína en forma de tiolato unidos a un ión Zn^{2+}. La oxidación de estos residuos supone la formación de dos puentes disulfuro intramoleculares y la liberación del átomo de Zn produciéndose la activación de la chaperona (Jakob et al., 1999, Graumann et al., 2001). En el caso de la PDI (miembro multifuncional de la superfamilia de las tiorredoxinas (Janssen-Heininger et al., 2008)), solamente puede unirse a su sustrato en estado reducido, mientras que la oxidación de sus residuos cisteínas produce la liberación del mismo (Sitia and Molteni, 2004, Tsai et al., 2001). Además, la PDI en su estado oxidado con sus tioles activos unidos en forma de puente disulfuro puede actuar como un electrófico induciendo la formación de puentes disulfuro en diferentes proteínas (Gruber et al., 2006).
- FACTORES DE TRANSCRIPCIÓN: la actividad de muchos factores de transcripción puede ser modificada por estrés oxidativo debido tanto a la oxidación de quinasas, fosfatasas o chaperonas (Na and Surh, 2006) como a su propia modificación oxidativa. En 1993, NF-κB fue el primer factor de transcripción descrito como capaz de responder directamente al estado redox celular (Schreck et al., 1991) y desde entonces se han encontrado cisteínas susceptibles en gran cantidad de factores de transcripción incluyendo p53, Hif1 y AP-1 (Semenza, 2001, Haddad and Land, 2000, Duan and Nilsson, 2006).
- ENZIMAS IMPLICADAS EN LA SEÑALIZACIÓN REDOX: en la siguiente tabla se muestra una selección de enzimas antioxidantes cuyas cisteínas del centro activo pueden

ser modificadas por estrés oxidativo, así como la velocidad de reacción con el H_2O_2 de cada una de ellas. De entre todas ellas, cabe destacar la importancia de las PRXs, proteínas con una constante de velocidad 7 órdenes de magnitud superior al resto y por lo tanto con mucha mayor afinidad por H_2O_2 (Winterbourn and Hampton, 2008).

Tioles	*Constante de velocidad (M^{-1} s^{-1})*
GSH	0.89
Cisteína	2.9
N-Acetilcisteína	0.16
Tiorredoxinas	1.05
Peroxirredoxinas	1-4 x 10^7

Tabla 4. Contanstes de velocidad de distintos tioles con H_2O_2.

1.6 PEROXIREDOXINAS

Las PRXs son una familia ubicua de enzimas antioxidantes presentes en todos los organismos, cuya función biológica es la reducción de peróxidos (peróxidos orgánicos y peróxido de hidrógeno). En mamíferos se han descrito 6 tipos de PRXs diferentes que pueden clasificarse en tres clases: 2-Cys PRXs típicas (PRX 1-4); 2-Cys PRXs atípicas (PRX 5), y 1-Cys PRX (PRX 6) (Seo et al., 2000, Knoops et al., 1999). Todas ellas comparten el mismo ciclo catalítico en el que una cisteína denominada peroxidática es susceptible de ser modificada por el peróxido sustrato formándose un ácido sulfénico. Es el reciclaje de este ácido de nuevo a tiol lo que diferencia cada una de las clases de PRX (Wood et al., 2003).

- 2-CYS PRXS TÍPICAS (PRX 1-4): en el segundo paso de la reacción, la segunda cisteína denominada resolutiva y localizada en el dominio C-terminal de otra molécula de

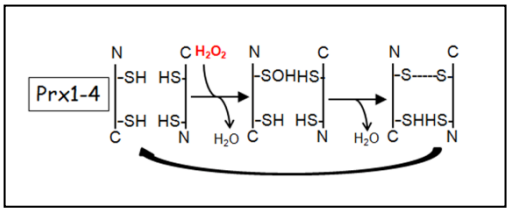

Ilustración 15. Ciclo catalítico de 2-Cys PRX típicas.

PRX ataca al sulfénico formando un puente disulfuro intermolecular. Esta reacción es revertida por la reducción de oxidoreductasas (principalmente las tioredoxinas).

- 2-CYS PRXS ATÍPICAS (PRX5): en este tipo de PRXs las dos cisteínas, tanto la catalítica como la resolutiva se encuentran en la misma molécula. Por ello se forma un puente disulfuro intramolecular que será reciclado por un donador de electrones.

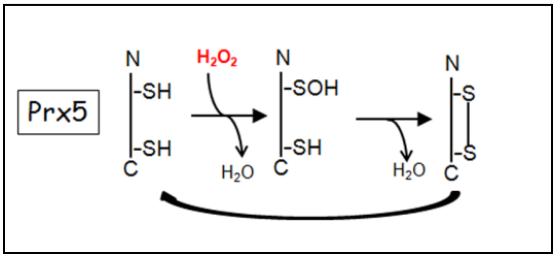

Ilustración 16. Ciclo catalítico de 2-Cys PRX atípicas

- 1-CYS PRXS (PRX6): en el ciclo catalítico de estas PRX no interviene una cisteína resolutiva, sino que la cisteína catalítica es reducida por la acción de un donador de electrones que contiene un grupo tiol.

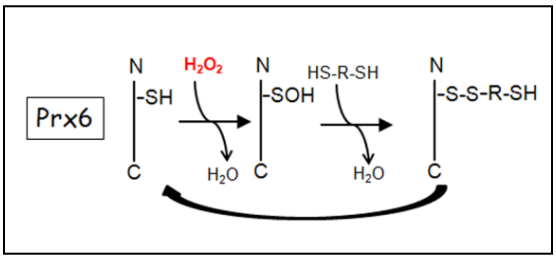

Ilustración 17. Ciclo catalítico de 1-Cys PRX

2. CONCLUSIONES

A lo largo de esta tesis doctoral hemos demostrado el papel protector que tienen las ROS en el endotelio vascular expuesto al flujo sanguíneo. Nuestros datos contribuyen a establecer la función fisiológica que posee el H_2O_2 como molécula señalizadora en el endotelio. Específicamente, hemos demostrado:

1. LSS (12 dina/cm^2) promueve la generación de ROS, $O_2^{\cdot-}$ y H_2O_2, que son necesarios para la activación secuencial de p38 MAPK y eNOS en el endotelio vascular.

2. La ausencia de eNOS en el endotelio no altera la activación de la proteína MAP kinasa p38 por flujo laminar. Sin embargo, una depleción de la proteína MAP kinasa p38 o su inhibición farmacológica impide la fosforilación de eNOS y la producción de $NO^{\cdot}$ inducida tanto por LSS como por el tratamiento con H_2O_2. Los efectos mencionados son independientes de la activación de Akt.

3. La depleción específica de la isoforma de NADPH oxidasa mayoritaria en el endotelio vascular (NOX4), inhibe la activación de la proteína MAP kinasa p38 por flujo laminar.

4. LSS induce la activación de la proteína citosólica Drp1 y su traslocación a la membrana externa mitocondrial. Esto origina cambios en la morfología mitocondrial promoviendo la fragmentación de las redes mitocondriales (fisión).

5. LSS provoca una disminución en el consumo de oxígeno mitocondrial, que se correlaciona con un incremento en el potencial de membrana mitocondrial y un aumento en la producción de ROS.

6. El H_2O_2 producido a nivel mitocondrial como consecuencia del flujo laminar, es neutralizado tras la activación de la enzima antioxidante PRX3.

7. LSS es capaz de modificar la función mitocondrial por lo que estos orgánulos deben ser considerados parte de la maquinaria celular con funciones sensoras de estímulos biomecánicas

8. El nucleótico purínico ADP induce la inactivación transitoria de PTEN en células endoteliales vasculares al promover su fosforilación.

9. La depleción de PTEN supone un incremento en la fosforilación basal e inducida por ADP de la proteína MAP kinasa p38 y de eNOS. La fosforilación de eNOS y la producción de NO. por el nucleótido purínico ADP dependen de la activación de la proteína MAP kinasa p38.

10. La depleción de la fosfatasa PTEN en células endoteliales inhibe la migración celular e induce un incremento en la polimerización de actina cortical. Estos procesos están estrechamente ligados a un incremento en los niveles de su principal sustrato, PIP_3.

9. ANEXO 2